# Accessory Rare Metal Mineralization in the Coldwell Alkaline Complex, Northwest Ontario.

by

Richard Morison McLaughlin ©

A thesis submitted in partial fulfillment of the requirements for the degree of Master of Science

Lakehead University, Thunder Bay, Ontario

April, 1990

## Abstract

Accessory rare metal mineralization has been investigated in seven lithologies in intrusive Centres I and III of the Coldwell alkaline complex. All units contain minerals that are enriched in a suite of granitophile elements, which typically include Nb, REE, Y, Th, U and Zr. Mineral abundances, composition, and mode of occurrence differ between units.

Centre III is characterized by crystallization of subhedral-to-euhedral chevkinite, pyrochlore and monazite from late-stage melts or residual pore fluids in the more-evolved quartz and ferro-edenite syenites. These minerals are invariably altered to fluorocarbonate or recrystallized by later $F^-$ and $CO_3^{2-}$-bearing deuteric fluids. The Centre I, ferroaugite syenite minerals exhibit similar morphological and replacement textures to those present in Centre III. In contrast, the Craddock Cove syenite is mildly K and Fe-metasomatised with incipient replacement of plagioclase and amphibole by K-feldspar, zircon, fluorocarbonate, Nb-rutile (?), allanite, and rare chevkinite. Fe-rich fluids under oxidizing conditions are believed to have precipitated $Fe^{3+}$-bearing fluorocarbonate in which one third of the (REE)F layers are replaced by $Fe^{3+}$ layers.

Most Centre I rare earth minerals are enriched in the HREE relative to those from centre III, in particular pyrochlore, fluorocarbonate, allanite in the eastern contact pegmatites and the quartz syenite dykes. Compositional data for adjacent syntaxial intergrown domains of bastnaesite, synchysite, and parisite indicate that HREE-enrichment may, in part, be influenced by the Ca content of the species.

The highest contents of Ce (4193 ppm), Zr (1613 ppm), Y (650 ppm), Th (223 ppm) and U (428 ppm) were found in the quartz syenite dykes intruding the Craddock Cove syenite and Port Munroe megaxenolith. The emplacement of the quartz syenite dykes and the introduction of the metasomatizing fluids of the Craddock Cove syenite may be temporally related to the differentiation of residual fluids in the apical zone of the Centre I magma chamber. Complexing of $F^-$ and $CO_3^{2-}$ with rare metals may have permitted their concentration, transportation and precipitation in structurally favourable settings. The megaxenoliths have been susceptible to brittle fracturing and should be considered primary targets for further exploration. The Craddock Cove syenites, although intruded by the dykes, may have been hot during dyke emplacement and therefore not as prone to brittle fracturing.

## Acknowledgments

Dr. R. Mitchell is thanked for suggesting this topic and for his helpful advice during the past two years. I am indebted to Anne Hammond and Reino Viitala for sample preparation, to Shelly Moogk for computer assistance, and to Dr. Tom Griffith for his guidance in the Scientific Instrumentation Labratory. Without their help this project could not have been completed. Many thanks to Allan Mackenzie for his instruction on the fundamentals of electron microscopy and for his technical advice. I am grateful to many others including Dr. G. Platt and Dr. S. Kissin for their practical suggestions and to the students and faculty who have made my stay at Lakehead University a memorable experience.

TABLE OF CONTENTS

# 1.0 Introduction

## 1.1 Regional Geology

The Coldwell alkaline complex, located on the north shore of Lake Superior, intrudes the metavolcanic and metasedimentary rocks of the Schreiber-White Lake Archean Belt. It is situated at the bifurcation of two tholeiitic volcanic belts, the Osler volcanics to the west, and the Mamainse-Michipicoten volcanics to the east and is the southern most member of a series of north-south trending alkaline-carbonatite intrusions (Killala Lake, Prairie Lake, Chipman Lake). To the east another belt of alkali intrusives follows the Kapuskasing gravity high (Fig 1.1).

The type of regional igneous activity - intrusion and extrusion of large volumes of basic magma and emplacement of alkaline and carbonatitic melts is believed to reflect mantle plume generated intracratonic rifting. Such tectonic settings, as found in the Gregory- Kavirondo rifts of east Africa and the Kangedlugssuaq area of east Greenland, create triple junctions of failure (Brooks, 1973). The intrusion of the alkaline rocks during the Keweenwan rifting probably occurred along the failed arms of the rift centre with the Coldwell complex being emplaced at the triple junction (Mitchell and Platt, 1978).

## 1.2 The Coldwell Complex

The complex, having a diameter of 25 Km, is the largest alkaline intrusion in North America. The alkaline rocks of Neohelikian age are believed to be products of three intrusive events, each defined by a distinct differentiation trend.The magmatic activity commenced with the intrusion of the border gabbro in Centre I and progressed in a westerly direction. The order of emplacement

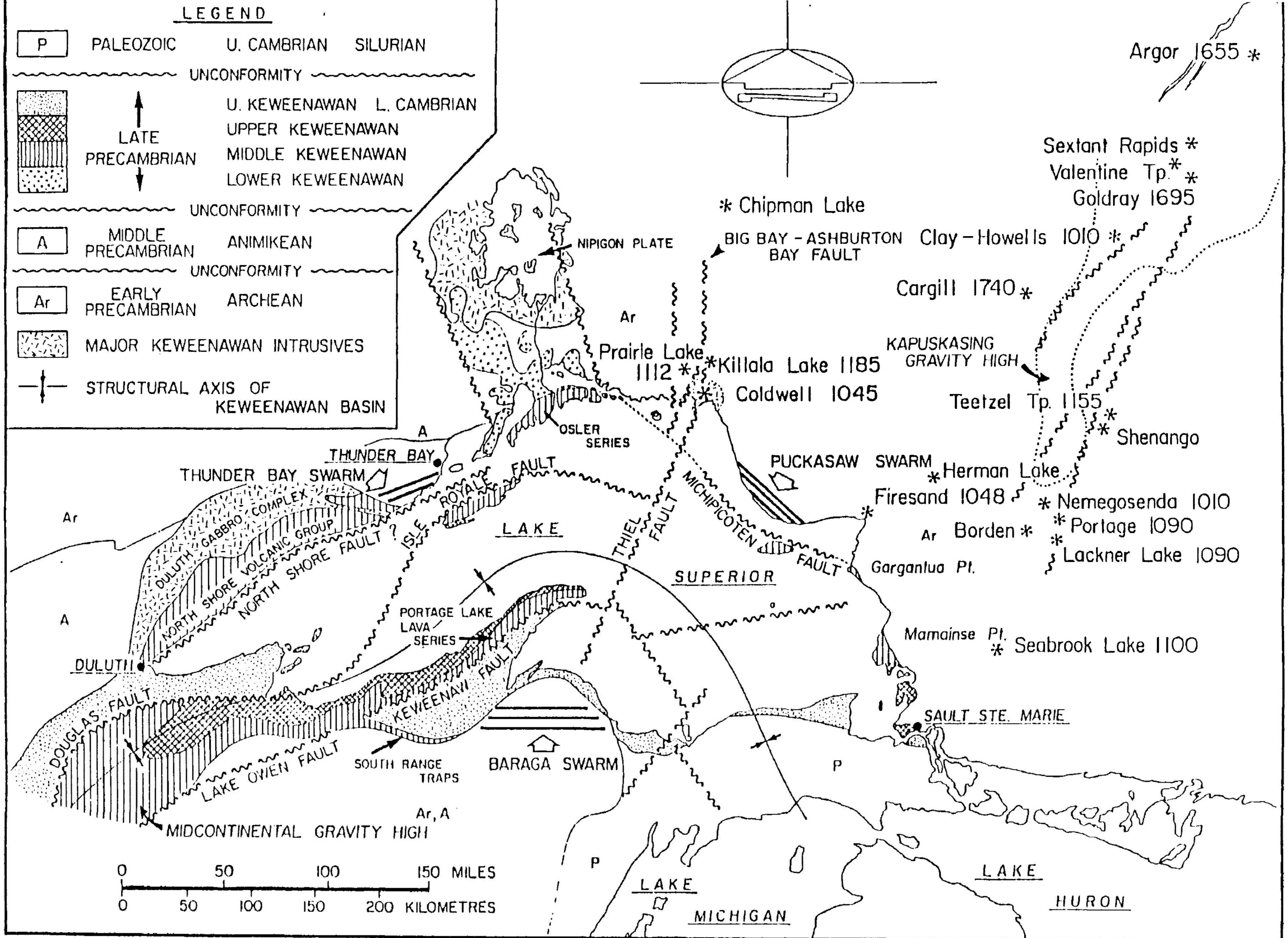


Figure 1.1 - Tectonic setting of the Lake Superior Basin (from Mitchell and Platt, 1978).

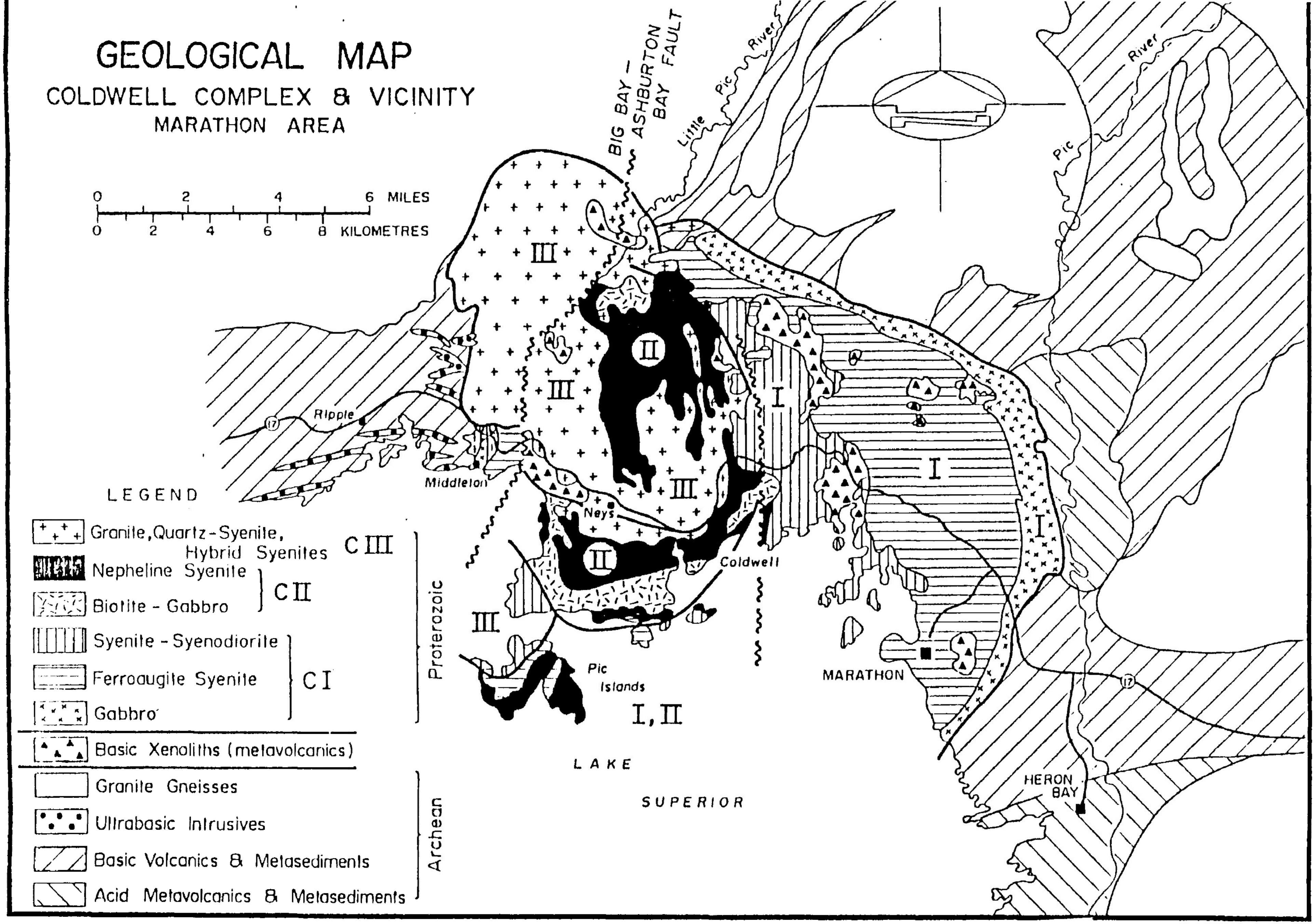


Figure 1.2 - Geological map of the Coldwell Alkaline Complex (from Mitchell and Platt, 1978).

of magmatic centres are as follows.

Centre I: Saturated alkaline rocks with peralkaline oversaturated residua.

Centre II: Miascitic, undersaturated alkaline rocks.

Centre III: Alkaline rocks with oversaturated residua.

It is believed that the magmas were emplaced by cauldron subsidence, as evidenced by the occurence of concentric marginal intrusions and down-faulted , partially-assimilated remnants of the capping lavas. The central portion of the complex, mainly Centre II lithologies, may be a down-faulted block and therefore, may represent a higher stratigraphic level (Mitchell and Platt, 1978, 1982)(Fig 1.2).

1.2.1 Centre I

The original form of the centre I intrusion has been complicated by post-intrusive block faulting, particularly in the western portion of the body. These rocks are characterized by extensive metasomatism, brecciation and the inclusion of basalt xenoliths along brecciated lithologies. K-metasomatism is present in the north western syenites (highway 17 syenites adjacent to the Redsucker Cove breccia zone) and Na-metasomatism and albitization in the south west( Currie, 1980; Kent, 1981). The formation of these rocks is unclear. Currie, (1980) classified the western syenites as fenites formed by the infusion of metasomatising fluids during the emplacement of the adjacent nepheline syenite melt. A second hypothesis suggests that the western syenites of Centre I represent volatile-rich rocks originally close to the roof of the complex (Mitchell and Platt, 1978). This is supported by the presence of complex pegmatites in the region and abundant basaltic enclaves, which may in fact be capping lavas down-faulted into the apex of the magma chamber during cauldron subsidence.

The border gabbro is the oldest unit of the complex and occurs as a ring shaped body forming the eastern and northern margin of the intrusion. Intruding the gabbro is a ferroaugite syenite which forms the bulk of the Centre I rocks. This red to dark green syenite can be massive or layered. Mitchell and Platt, (1978) studied the southeastern ferroaugite syenite and determined that the body crystallized from the base upwards (east to west) with simultaneous crystallization at the roof, trapping residual fluids in the upper portions of the sequence. Distinctive differentiation trends towards iron enrichment is evidenced by the formation of acmite and ferrorichterite and increased peralkalinity by the crystallization of aenigmatite and sodic amphiboles in the trapped intercumulus liquids of the upper syenites. The eastern contact patch pegmatites, containing ferrorichterite, alkali-feldspar, aenigmatite, acmite pyroxene , quartz, zircon, and calcite, are considered final differentiates and are the only rocks which are wholly peralkaline (Mitchell and Platt 1978).

The southwestern syenite in the Craddock Cove - Port Munroe localities is complex. A large , hundred of metres in size, basalt xenolith is exposed west of port Munro. Brittle fracturing has occured within the basalt allowing for the injection of numerous syenite and quartz syenite dykes. Tinquaite, quartz syenite and lamprophyre dykes also cross cut the syenite. Thin veins of epidote and fluorite mineralization fill fractures in the west. The southwestern syenites (red syenites) are intensly Na-metasomatized along the Redsucker Cove breccia zone with the degree of alteration decreasing to the east (Kent, 1981).

Near vertically-dipping syenitoid dykes vein and permeate both the western syenites and basalt xenoliths and are composed of an assemblage of albite, calcite, magnetite, quartz, andradite, and chalcopyrite. Kent,(1981) described staurolite as a common phase in these dykes. Based on semi-quantitative analysis and x-ray diffraction data, it is believed that the mineral referred to as staurolite was mis-identified and that it is in fact anisotropic garnet (andradite).

The mineralogy and petrography of the quartz syenite dykes are similar with the exception of the most easterly dyke C2925. It has, in addition to the assemblage described above, green aegirine-augite and strongly pleochroic dark green amphibole filling thin (< 10 mm) fractures in the dyke.

### 1.2.2 Centre II

Centre II is composed of a biotite-bearing gabbro body exposed on the Coldwell Peninsula which is intruded and metasomatised by a natrolite-bearing nepheline syenite.

Mineral compositions in Centre II nepheline syenite display moderate iron enrichment. Amphiboles in the syenites are aluminous and range from magnesian hastingsitic hornblende to hastingsite, while the pyroxenes exhibit Na and $Fe^{3+}$ trends from aegirine-augite towards acmite (Mitchell and Platt, 1982).The rare metal mineralogy of Centre II rocks was not examined in this study.

### 1.2.3 Centre III

Rocks of this magmatic episode are exposed in three main areas: Pic Island - Guse point, north of the Coldwell Peninsula between Killala Lake road and the Little Pic River, and in the western contact zone. The syenites of centre III are a complex composite group of rocks ranging mineralogically from quartz bearing syenites to granites.The syenites and quartz syenites are characterized by the presence of sodic amphiboles, fluorite , zircon and braid perthites. Earlier syenites are veined and brecciated by later syenites, indicating several episodes of intrusion. Lukosius-Sanders, (1988) has distinquished four separate intrusive phases defined on mineralogical and textural considerations. The chronological order of intrusion is as follows: Magnesio-hornblende syenite, ferro-edenite syenite, contaminated ferro-edenite syenite, and quartz syenite.

Magnesio-hornblende syenites have limited distribution. They are characterized by a synneusis texture and the constituents include patch antiperthite, albite, magnesio-hornblende, aluminous pyroxene, biotite, apatite, quartz, zircon, magnetite, ilmenite, and fluorite.

Multiple intrusions of ferro-edenite syenite constitute the predominant Centre III lithology. Generally it is a porphyritic rock with braid antiperthite, calcic to alkali amphibole, annite, aluminous hedenbergitic pyroxene to acmitic hedenbergite, quartz, zircon, apatite, fluorite, magnetite, and ilmenite.

Alkaline basalts and Archean country rocks were brecciated by, and incorporated into , the ferro-edenite syenites. The repetitious nature of ferro-edenite syenite injection has resulted in brecciation of early syenites by later ones.This suite is hybridized by assimilation of autoliths of ferro-edenite syenite and xenoliths of basalt and metasediments forming a compositionally distinct contaminated ferro-edenite syenite.

The quartz syenites are coarse grained, massive rocks containing braided antiperthite, abundant quartz, calcic to alkali amphibole, hedenbergite, annite, magnetite, ilmenite, fluorite, apatite, sphene.

The majority of Centre III syenites crystallized under relatively dry, hypersolvus conditions. However, rocks situated at the periphery of the exposed centre III intrusions, particularly the Guse Point-Pic Island area have undergone alteration by hydrothermal fluids, introduced along zones of weakness.

## 1.3 Uranium and Niobium Exploration

Uranium and niobium occurrences in the Port Munro area have encouraged sporadic claim staking by prospectors and mining companies since 1932. Exploration activity has focused primarily on 2 structures, the numerous quartz syenite dykes cross cutting the basalt xenoliths and red syenites, and on the xenolith - syenite contacts. Although assays showed significant rare metal abundances in both environments, the highest grades were obtained from quartz syenite dykes. They have been found along the east shore of Port Munro, Mons Point, Ypres Point, and north of highway 17 near Craddock and Johnson lakes (Marathon Columbian Property, Noranda Mines, 1954) and are easily identifiable by exhibiting radioactivity 2 -3 times above background levels. The highest grade dyke, located along the C.P.R. tracks just west of Port Munro, was staked by Tor Gustafson in 1949. Pye (1954, p. 2)described this showing in some detail; " The dyke rock is pink and fine-grained, and contains numerous irregular cracks which are filled by a coarse-grained green pyroxene, and where this pyroxene is most abundant the radioactivity is such as to give readings anywhere from 30 to 60 times above background throughout the length of the dyke. Assays of grab samples indicate up to 1.35 % Nb2O5, 0.08 % UO2, 3.00 % ThO2, and 0.12 % $Ce_2O_3$". Samples coded C2925 in this study were obtained from the Tor Gustafson occurrence.

## 1.4 Study Area

The study has attempted to document and describe rare metal mineralization in specific lithologies and localities in Centre I and Centre III syenites. To prevent confusion, names of lithologies and localites used in past reports, theses, and papers have been retained, while new ones have been added only where necessary. With the exception of the 2900 series (Fig 1.3), rock specimens used in this thesis were collected during previous petrological investigations of the Coldwell complex. In Centre III, samples of magnesio-hornblende, ferro-edenite, contaminated ferro-edenite, and quartz syenites from the western contact, the Ashburton Lookout and Neys Lookout are mainly those collected by Lukosius-Sanders, (1988).

Five separate localities and lithologies have been investigated in the southern part of Centre I. 1) The Craddock Cove (red) syenites are located along highway 17 between the Redsucker Cove breccia zone and Wolf Camp Lake. 2) The southeastern ferroaugite syenite including those samples (C30-C70) obtained approximately 4 km west of Marathon. Sample localities are given in Mitchell and Platt, (1978). 3) The eastern contact pegmatites found at the eastern margin ferroaugite intrusion, along highway 17. 4)The Angler Creek ferroaugite syenite, samples C2905 - C2910, adjacent to the Craddock Cove syenite. 5) The quartz syenite dykes intruding the basalt xenolith and red syenites of the Port Munro and Craddock Cove area (Kent, 1981).

Compositional data for the rare metal minerals were obtained using an Energy Dispersive Spectrometer in conjunction with an Hitachi 570 Scanning Electron Microscope. Analytical precision, accuracy and methods of aquisition are outlined in appendix 1.1.

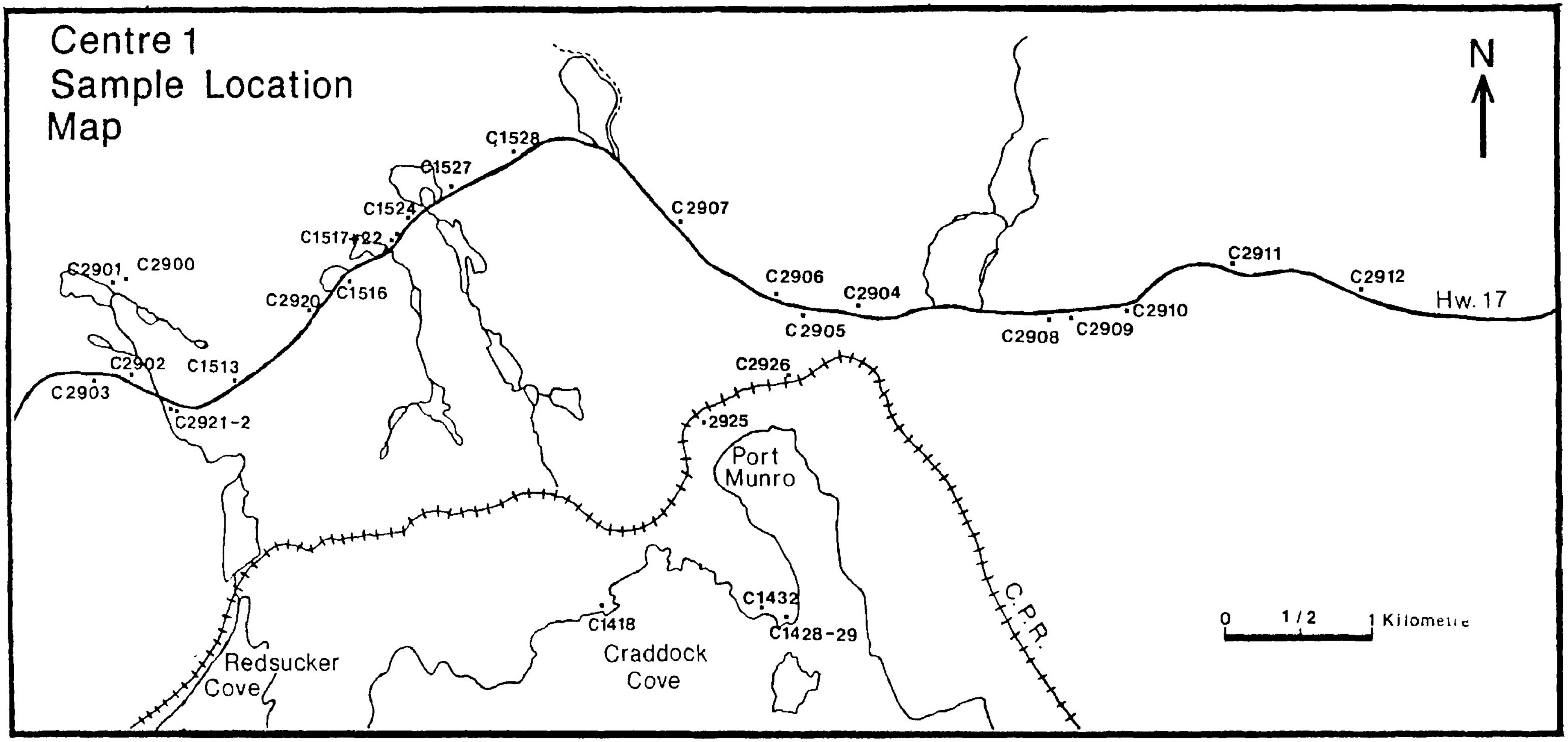


Fig 1.3. Sample location map for Centre I ferroaugite syenite, Craddock Cove syenite, and quartz syenite dykes.

## 2.0 Fluorocarbonates

The bastnaesite group of fluorocarbonates has four main members: bastnaesite (La, Ce, Nd) $(CO_3)F$, parisite ( La, Ce, Nd $)_2Ca(CO_3)_3F_2$, roentgenite (La, Ce, Nd $)_3Ca_2(CO_3)_5F_3$, and synchysite ( La, Ce, Nd $)Ca(CO_3)_2F$. They are strongly LREE-selective with the rare exception of bastnaesite-(Y), bastnaesite-(Nd), and synchysite-(Y). The structure of the family can be described in terms of layers of (REE)F, Ca ions, and $CO_3$ (Van Landuyt et al, 1975) . The composition of the various species is dependant on the periodicity of each layer within a mixed layer compound. In this respect, the intermediate members, parisite and roentgenite can be viewed as being composed of alternating layers of the Ca absent member (bastnaesite), and the Ca-bearing member (synchysite).

Fluorocarbonates are commonly found as deuteric alteration products of other rare earth bearing minerals, such as allanite (Meintzer et al, 1988; Littlejohn, 1981a,1981b; and Cerny et al , 1972) and chevkinite (Segalstad and Larsen, 1978). The replacement minerals are attributed to postmagmatic fluid activity involving F and $CO_3$ enriched hydrothermal solutions. These processes commonly result in the development of intergrowth textures between fluorocarbonate and other rare earth fluorides and oxides (Lahti et al, 1988). The fluorocarbonates may form pseudomorphs, e.g. bastnaesite after okanoganite in the Golden Horn Batholith (Boggs, 1984).

One or more fluorocarbonate species have been identified in all lithologic units studied in the Coldwell complex and are the dominant REE mineral in the Centre I Craddock Cove syenites and eastern contact pegmatities. Occurences are unevenly distributed within units and abundances fluctuate greatly between samples. The flourocarbonates occur as individual crystals and, more commonly, as syntaxial intergrown polycrystals of the type described by Donnay et al (1953), Boggs (1984), de St Jorre (1986). The species positively identifed using x-ray diffraction (Fig 2.1 and Table 2.1) and /or quantitative chemical analysis are :

| | |
|---|---|
| bastnaesite- (Ce) | $(Ce,La)CO_3F$ |
| synchysite- (Ce) | $(Ce,La)Ca(CO_3)_2F$ |
| parisite-(Ce) | $(Ce,La)_2Ca(CO_3)_3F_2$ |

The largest grains of fluorocarbonates are typically intergrowths of bastnaesite-parisite, bastnaesite-synchysite, or more rarely bastnaesite-synchysite-parisite. Though most grains are of micron size and not large enough for macroscopic identification or extraction, aggregates consisting of the three carbonate species and Nb-rutile were obtained from the eastern contact pegmatites. Macroscopically these show a range in colour from grey-to-orange to brick red. Colouration appears to be a function of the species content with grey aggregates being bastnaesite-rich, and the red grains containing synchysite. In thin section, the syntaxial intergrowths are visible as alternating bands of colourless bastnaesite and translucent blood red synchysite and parisite. The bastnaesite shows moderate-to-high birefringence, whereas Ca-fluorocarbonate birefringence is masked by its intense colour. Fluorocarbonates from the other lithologic units were too small for macroscopic or optical study, therefore their morphology and paragenesis were investigated using SEM back-scattered electron imagery.

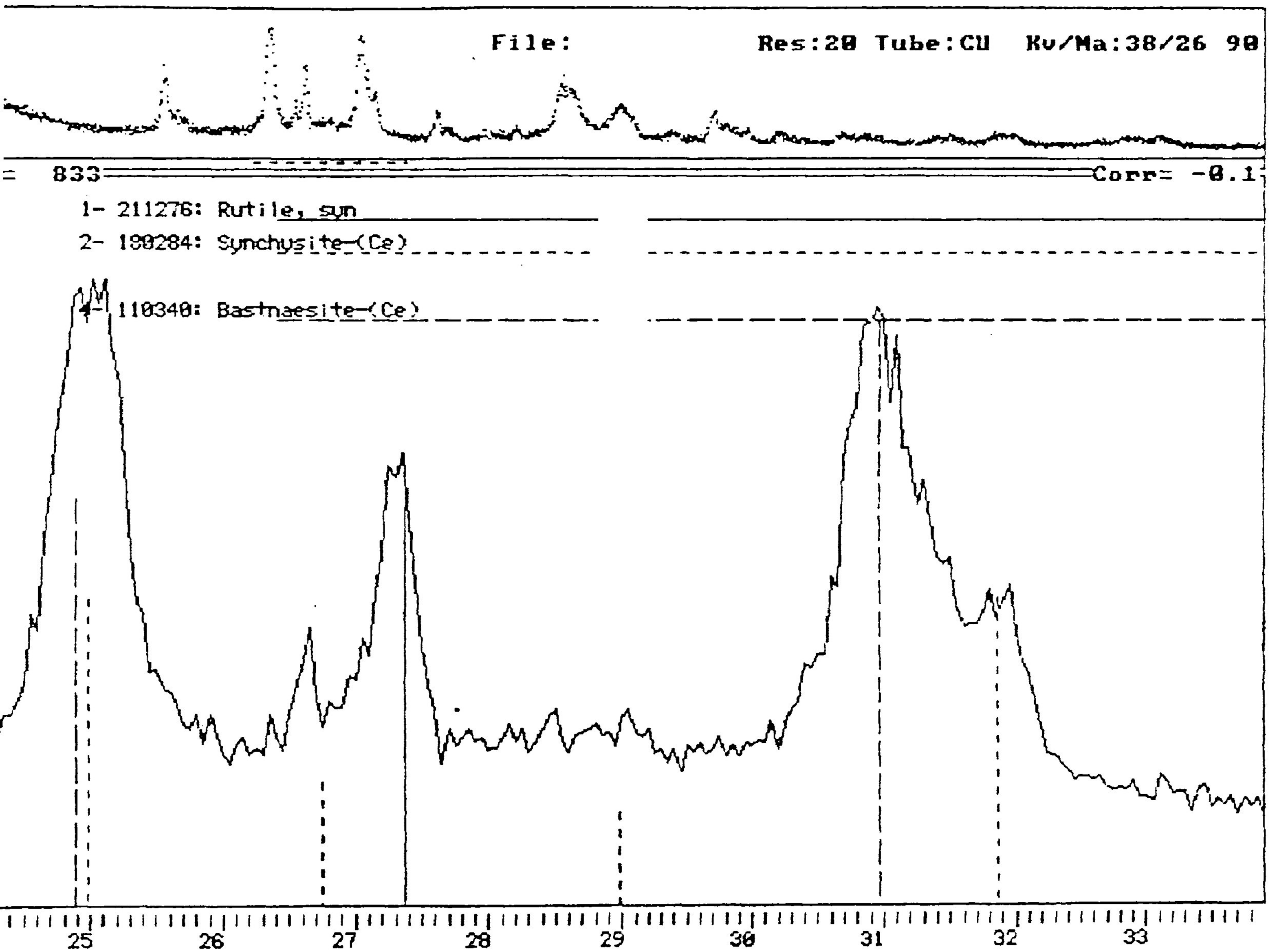


Fig 2.1. X-ray diffractometer scan of fluorocarbonate polycrystal with Nb-rutile over the region from 24-34°. Peaks at 2.877 Å and 2.793 Å signify bastnaesite and synchysite. Intensities are proportional to their relative abundance. Peak at 3.245 Å denotes the presence of Nb-rutile. Sample (C1A) is from the eastern contact pegmatites.

| Rutile | | Synchysite | | Bastnaesite | | C1A Eastern contact pegmatite | |
|---|---|---|---|---|---|---|---|
| d A | Int. | d A | Int. | d A | Int. | d A | Int. |
| | | 9.1 | 60 | | | | |
| | | | | 4.88 | 40 | 4.88 | 72 B |
| | | | | | | 4.66 | 36 |
| | | 4.53 | 50 | | | 4.54 | 31 S |
| | | | | | | 4.43 | 26 |
| | | | | | | 3.56 | 98 |
| | | 3.55 | 100 | 3.564 | 70 | 3.54 | 100 B,S |
| | | | | | | 3.53 | 100 |
| | | 3.32 | 40 | | | 3.33 | 44 S |
| 3.247 | 100 | | | | | 3.245 | 72 R |
| | | | | | | 3.117 | 31 |
| | | 3.07 | 30 | | | 3.059 | 31 S |
| | | | | 2.879 | 100 | 2.877 | 95 B |
| | | | | | | 2.863 | 91 |
| | | 2.80 | 100 | | | 2.793 | 48 S |
| | | | | 2.610 | 1 | | |
| 2.487 | 50 | | | | | 2.489 | 36 R |
| | | | | 2.445 | 9 | 2.449 | 23 B |
| | | | | | | 2.430 | 22 |
| 2.297 | 8 | 2.30 | 20 | | | 2.304 | 20 S, R |
| | | 2.28 | 20 | 2.273 | 3 | 2.274 | 20 B, S |
| | | | | | | 2.249 | 20 |
| | | | | 2.238 | 3 | | |
| 2.188 | 25 | | | | | 2.192 | 23 R |
| 2.054 | 10 | 2.06 | 50 | 2.057 | 40 | 2.047 | 63 B,S |
| | | | | 2.016 | 40 | 2.019 | 53 S |
| | | 2.01 | 20 | | | | |
| | | 1.934 | 50 | 1.898 | 40 | 1.898 | 41 B, S |
| | | 1.873 | 40 | | | 1.866 | 31 S |
| | | 1.821 | 5 | | | | |
| | | 1.777 | 10 | 1.783 | 9 | 1.776 | 21 B, S |
| | | 1.749 | 10 | | | | |
| 1.687 | 60 | 1.704 | 10 | 1.674 | 21 | 1.688 | 36 B, S, R |
| | | 1.661 | 30 | | | 1.664 | 25 S |
| | | | | | | 1.653 | 23 |
| 1.624 | 20 | | | 1.629 | 1 | 1.626 | 22 B, R |
| | | | | 1.573 | 15 | 1.572 | 17 B |
| | | 1.528 | 30 | | | 1.529 | 14 S |
| 1.480 | 10 | | | 1.481 | 9 | 1.482 | 18 B, R |
| 1.453 | 10 | | | | | 1.452 | 14 R |
| 1.424 | 2 | | | 1.439 | 11 | | |
| | | 1.401 | 30 | | | 1.390 | 9 S |
| 1.360 | 20 | | | | | 1.366 | 15 R |
| 1.347 | 12 | 1.345 | 10 | 1.347 | 7 | 1.349 | 16 B, S, R |
| | | 1.329 | 10 | | | | |
| 1.304 | 2 | | | 1.298 | 15 | 1.299 | 19 B,R |
| | | 1.290 | 30 | | | | |
| | | | | 1.277 | 7 | 1.281 | 17 B |
| 1.244 | 4 | 1.230 | 10 | | | | |
| 1.201 | 2 | | | 1.223 | 2 | | |
| 1.170 | 6 | | | 1.204 | 6 | | |
| 1.148 | 4 | 1.189 | 10 | 1.190 | 3 | | |
| 1.114 | 2 | | | | | | |
| 1.094 | 8 | | | 1.180 | 9 | | |
| 1.083 | 4 | 1.160 | 30 | | | | |
| | | | | 1.156 | 11 | | |
| 1.043 | 6 | | | 1.068 | 4 | | |
| 1.036 | 6 | | | | | | |
| 1.027 | 4 | | | | | | |
| 0.970 | 2 | | | | | | |
| 0.964 | 2 | | | | | | |

Table 2.1. X-ray powder data for fluorocarbonates and Nb-rutile. B-bastnaesite, S-synchysite, R- nb-rutile.

## 2.1 Textural Relationships

### 2.1.1 C I, Ferroaugite Syenite

All three members of the fluorocarbonate family are found in the central ferro-augite syenites and usually occur replacing apatite, amphibole and earlier formed REE bearing minerals. Apatite exhibits extensive marginal replacement by assemblages of coarse monazite, fluorocarbonate (70µm) (bastnaesite-to-synchysite) and calcite. The largest fluorocarbonate grains consist of syntaxial intergrowths, while finer grains (<4µm) replace the mafic phases along fractures. In rare cases, small grains of bastnaesite, zircon, chlorite, fergusonite, elpidite, pyrochlore, quartz, and a REE-silicate tentatively identified as britholite form aggregates interstial to feldspar grains.

Fluorocarbonates in the southeastern ferro-augite syenite also replace apatite with syntaxial intergrowths of bastnaesite and parisite or anhedral intergrowths of bastnaesite and monazite.

### 2.1.2 C 1, Eastern Contact Pegmatites

In the eastern contact pegmatites the fluorocarbonates occur as anhedral polycrystalline aggregates intimately intergrown with anhedral-to-acicular Nb-rutile, and rarely Nb-bearing ilmenite, forming complete pseudomorphs after a large primary mineral. The nearly-opaque pseudomorphs can be as large as 4.0 mm but usually do not exceed 1.0 mm, and are euhedral stubby prisms and skeletiform grains. They are commonly found partially-included in K-feldspar and as inclusions in amphibole, suggesting a rather early stage of formation for the precursor mineral. Rutile and columbite are present in concentrations high enough to result in near-complete opacity of the assemblage, leaving only small irregular translucent-to-transparent patches of pure fluorocarbonate. Backscattered electron imagery reveals a complex polycrystalline intergrowth of Nb-rutile and the fluorocarbonates composed of approximately 60% flourocarbonate and 40% fine grained rutile together with traces of columbite (Fig 2.2 & 2.3). Of the fluorocarbonates, bastnaesite is the dominant replacement mineral and parisite is more abundant than synchysite.

The thickness of the fluorocarbonate domains in syntaxial intergrowths may range from 1μm to 30μm. The syntaxy is complex with crystal interfaces being distinct and planar to gradational (Fig 2.2), the latter is probably due to orientation edge effects. Donnay et al (1953) describe similar syntaxial polycrystalline aggregates with planar interfaces parallel to (0001). They suggest that syntaxy of the fluorocarbonate species reflects the lack of solid solution in the (REE)$FCO_3 \cdot CaCO_3$ system and conclude that the periodicity of the phase may be a function of pH fluctuation in the mineralizing fluid.

Because of the similar morphology of the pseudomorph to chevkinite and its replacement phases,found in the Ashburton Lookout syenites, as well as its replacement phases, it is suggested that chevkinite is a probable precursor mineral. However, relict chevkinite is not been found, and therefore other REE minerals cannot be excluded as possible predecessors (allanite ?).

A similar intergrowth of bastnaesite and Fe-Ti minerals has been identified in a peralkaline granite from Mulanje in the Chilwa alkaline province, Malawi. The bastnaesite phase of a monazite, fluocerite, and bastnaesite intergrowth, is itself, intergrown with an unidentified Fe, Ti, Nb-oxide (Platt et al, 1987).

Fig 2.2 and 2.3. [Centre I, pegmatite eastern Contact]. 2.2) Backscattered micrograph of a skeletal pseudomorph of bastnaesite, synchysite, Nb-rutile and columbite. 2.3) One aggregate domain of bastnaesite (b) - synchysite (s) shows syntaxial intergrowths and a second domain is composed of acicular and anhedral Nb-rutile (rt) and interstitial columbite (c) (sample - C1A).

Fig 2.4 and 2.5. [Centre I, Craddock Cove syenite]. 2.4) Backscattered micrograph of acicular synchysite, ilmenite, magnetite, biotite and quartz assemblage. 2.5)Acicular synchysite (s) and bastnaesite (b) show syntaxial as well as irregular intergrowths. Other minerals include ilmenite (il) and magnetite (m) (sample - C1A).


001104 20KV
.75mmC

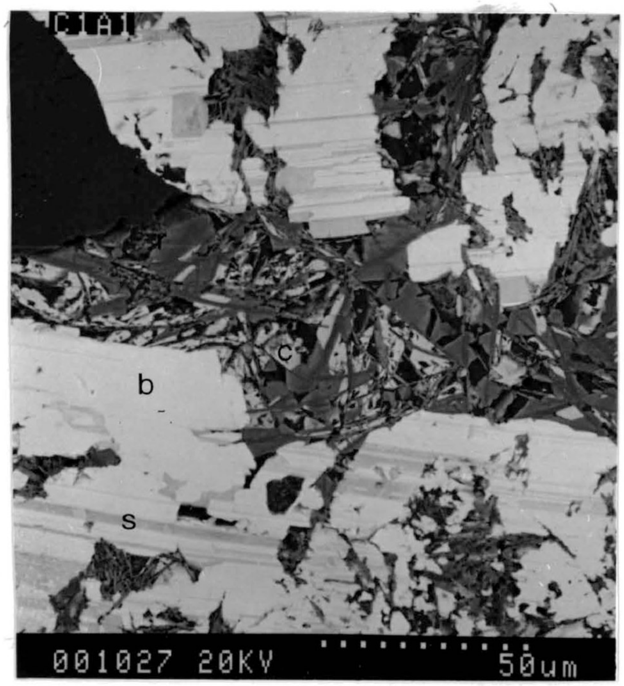
C1A1
c
b
s
001027 20KV
50um


001010 20KV
150umB

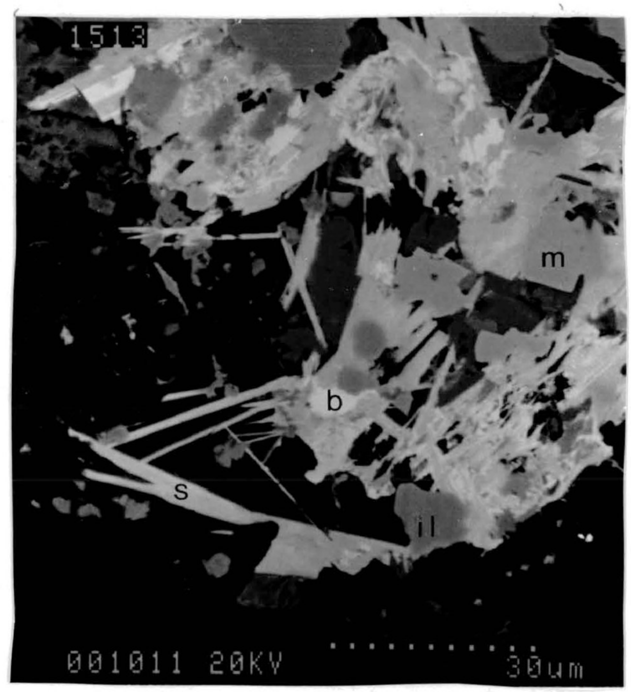
1513
m
b
s
il
001011 20KV
30um

## 2.1.3 C I. Craddock Cove Syenites

The Craddock cove syenites include the southern syenites located between Redsucker Cove and Port Munroe as defined by Kent, (1981.) together with the red syenites found along highway 17 between the Redsucker breccia zone and the ferro-augite syenite contact. Most samples obtained from this region contained minor amounts of fluorocarbonates, with the exception of the synchysite-rich sample C1513.

The southern Craddock Cove syenites are characterized by extensive Na-Metasomatism, in which the degree of albitization increases towards the west. Secondary albite ($An_{0-5}$) is the dominant alkali feldspar and forms up to 80 % of the mode in altered specimens. In highly-altered samples near Redsucker Cove, albite is the only feldspar in the rock and is stained and pseudomorphed by hematite (Kent ,1981). In these western samples bastnaesite occurs as small anhedral blebs (<4 µm ) in the secondary albite. Samples obtained near Craddock Cove show little fluorocarbonate mineralization.

The northern Craddock Cove rocks encompass syenites and syenitic pegmatites composed mainly of large subhedral perthite and minor amounts of fluorite. These rocks are characterized by low grade K-metasomatism, as K-feldspar replaces early euhedral and interstial amphibole. Western syenite samples C1513-C1524 show an apparent trend of decreasing fluorocarbonate mineralization and K-metasomatism towards the east. The eastern syenitic pegmatites have little fluorocarbonate mineralization.

Western mineralization is dominated by synchysite, to a lesser extent bastnaesite, and rarely parisite. The fluorocarbonate phases exhibit two morphological types of intergrowths.

1) tabular crystals of synchysite or bastnaesite-synchysite syntaxial intergrowths.
2) intimate, non-syntaxial intergrowths of synchysite and bastnaesite with Nb-rutile (?).

Both intergrowths replace mafic phases and form partial replacement aggregates with K-feldspar, zircon, quartz, calcite, and niobium rutile. The textural relationships and the close association with K-feldspar indiate that the fluorocarbonate precipitation may be contemporaneous with the K-metasomatism.

Tabular grains replace amphibole along their rims and form mixtures of K-feldspar, quartz, calcite, magnetite or, less commonly, zircon, and Nb-rutile. Coarse fluorocarbonates are commonly present as syntaxial intergrowths or isolated tabular-to-acicular synchysite (Fig 2.4 and 2.5). Associated with the coarser fluorocarbonate is a chaotic intimately intergrown fluorocarbonate, that is possibly a dissolution of the coarser fluorocarbonate. Unusual textures consisting of synchysite, bastnaesite, and Nb-rutile occur as replacements of an early euhedral mineral. Intergrowths of synchysite bastnaesite and Nb-rutile form ovoids (upto 20μm) in the longitudinal direction of the pseudomorph. Ovoids are typically rimmed by a thin bastnaesite coating which in turn is enclosed in homogeneous synchysite (Fig 2.6). The origin of this morphology is unknown.

The Nb-rutile and fluorocarbonate mixture also completely pseudomorph euhedral minerals (chevkinite ?). Due to the fine grained nature of the intergrowths it proved impossible to obtain accurate compositional data for

Fig 2.6. [Centre I, Craddock Cove syenite]. BSE image of an unusual texture showing replacement "ovoids" of Nb-rutile (?) and fluorocarbonate coated with thin bastnaesite rims and encapsulated in homogeneous synchysite (sample C1513).

Fig 2.7 and 2.8. [Centre I, quartz syenite dyke - C1432]. BSE micrograph of tabular fluorocarbonate species (parisite, synchysite, and bastnaesite) with clusters of anhedral zircon inclusions. Both rare metal minerals are embedded in chlorite and quartz.

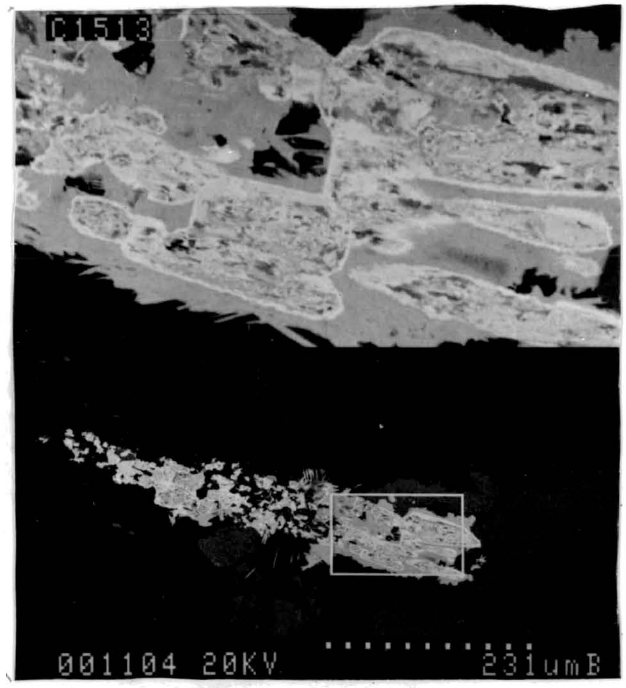
C1513
001104 20KV
231umB


C1432
001101 20KV
.60mmC


z
b
p
001102 20KV
60um

the fluorocarbonate phases present.

## 2.1.4 C I, Quartz Syenite Dykes

Only one quartz syenite dyke (C1432) contains significant quantites of fluorocarbonate. In this dyke large (100μ) tabular fluorocarbonate grains occur as discrete one species grains or as syntaxial intergrowths of two or more species. The dominant member is parisite, followed by bastnaesite and then synchysite. The intergrowths are usually broad, with grains rarely composed of more than 3 syntaxial domains. They are interstial to the k-feldspar grains and commonly embedded in quartz and chlorite together with other rare-metal minerals, i.e. pyrochlore, columbite, allanite and zircon (Fig 2.7 and 2.8). Inclusions of zircon (upto 15μm) in the fluorocarbonate are common. Samples C1428, C1429, and C1418 contain extremely rare Ca- fluorocarbonate as minute grains ( <3μm) bordering allanite.

## 2.1.5 C III, Ferro-edenite Syenite

In the western contact zone, rare bastnaesite occurs as small (10μm) anhedral isolated grains bordered by interstitial secondary albite and rarely quartz, and may be seen interstially between perthite grains. The bulk of the bastnaesite is associated with albite. Small anhedral grains of monazite and /or ilmenite form aggregates with the fluorocarbonate.

Lukosius-Sanders (1988) suggested that the secondary plagioclase is a product of deformation recrystallization due to the influx of water of possibly meteoric origin. However, due to the strong association of plagioclase and bastnaesite it is likely that REE- bearing carbothermal fluids and not ground water were the source of both the bastnaesite and plagioclase.

The Ferro-edenite syenite from the Ashburton lookout area contains rare

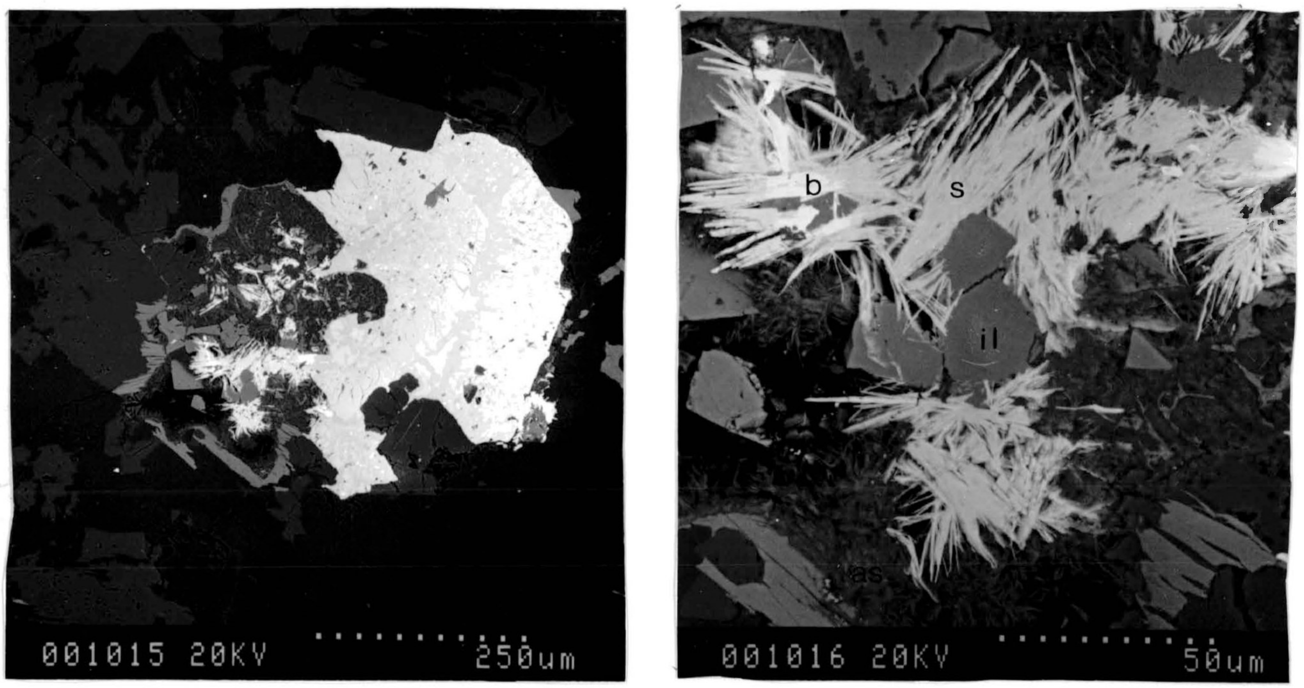


Fig 2.9 and 2.10. [ Centre III, ferro-edenite syenite, Neys - Ashburton Lookout area]. Acicular synchysite (s) surrounding ilmenite (il) replaces alteration silicate (as). Synchysite rarely nucleates on bastnaesite (b) (sample # C2122).

Fig 2.11 and 2.12. [Centre III, quartz syenite]. BSE image of a pyrochlore (?) altered to fluorocarbonate, thorite and a Nb-Ti-bearing mineral. Stringers of Nb-REE mineraloid penetrate into surrounding phases. 2.12) X-ray maps of Th, Nb, Ce (REE), and Ti defining replacement phases. High Th and Ce concentrations denote thorite (thorogummite ?) and fluorocarbonate replacement respectively (sample # C2155).

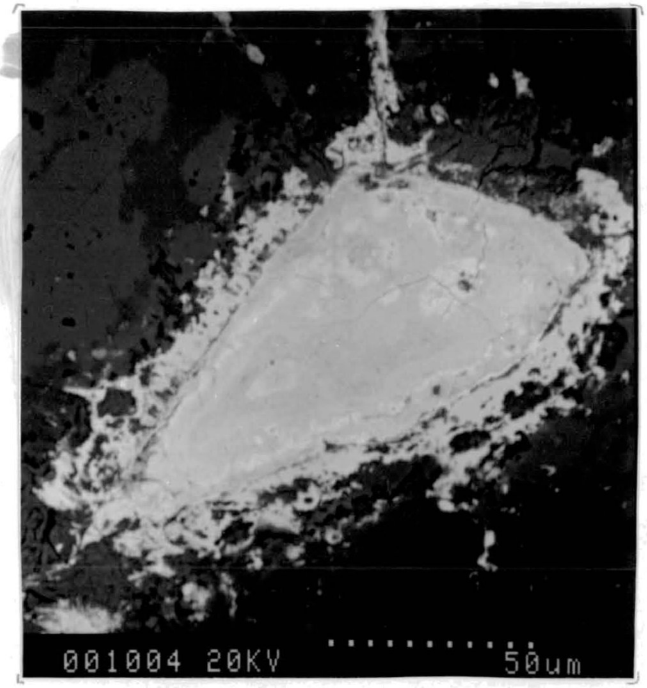
001004 20KV
50um

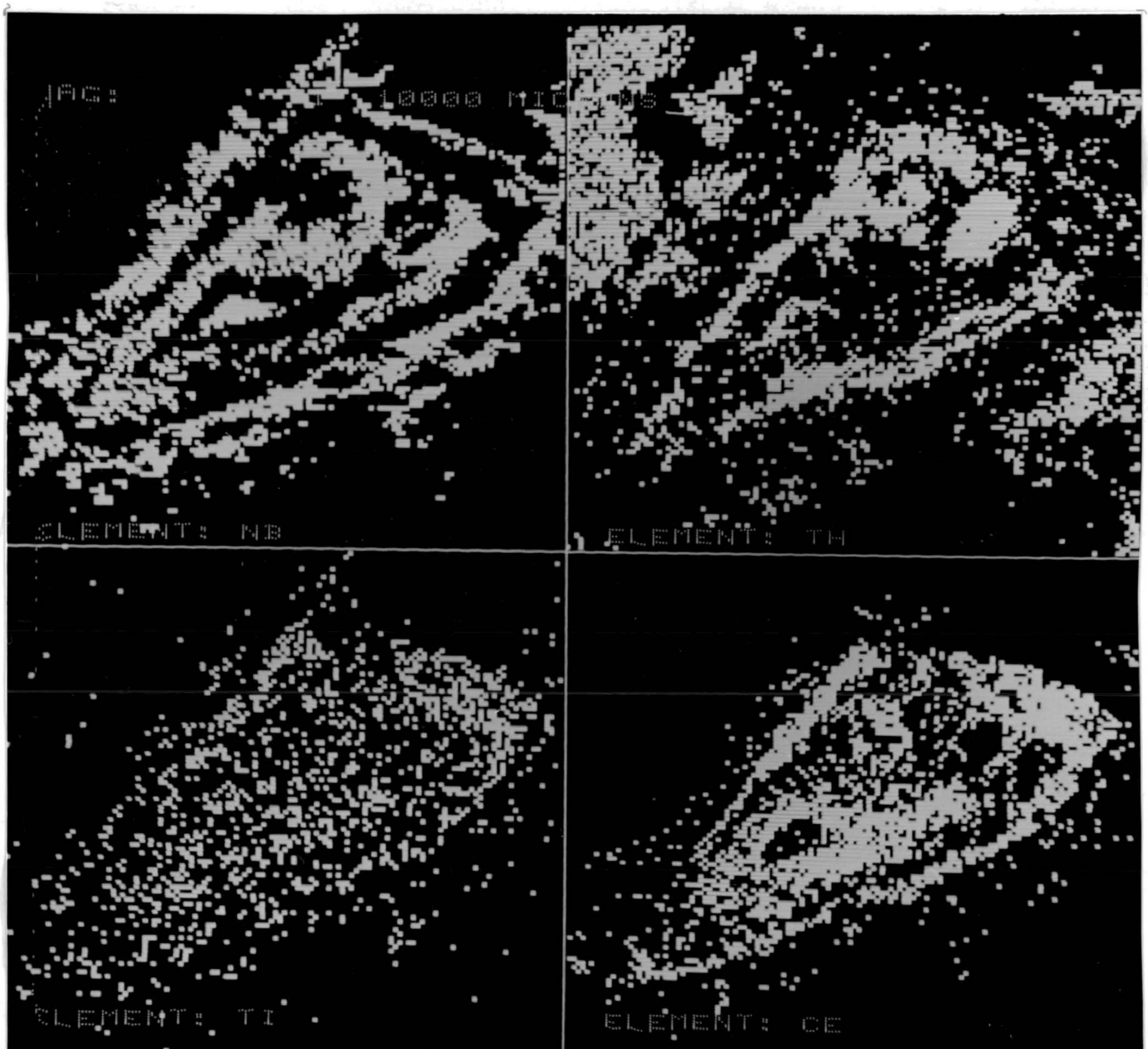
ELEMENT: NB
ELEMENT: TH
ELEMENT: TI
ELEMENT: CE

small acicular crystals intergrown with secondary chlorite. Bastnaesite may or may not occur as nucleation points for the Ca-bearing fluorocarbonates (Fig 2.9 and 2.10). Ca-fluorocarbonate rarely occurs with anhedral ilmenite and monazite. The monazite and fluorocarbonate boundary is usually distinct, but in some cases monazite and bastnaesite may be intimately intergrown .

Samples examined from ferro-edenite syenites have rare fluorocarbonate as small anhedral grains of bastnaesite or synchysite bordering large LREE bearing apatites.

## 2.1.6 C III, Quartz Syenite

The quartz syenite from the western contact zone contains rare acicular Ca- fluorocarbonate intergrown with iddingsite-bowlingite, Ti-Nb-bearing oxides and thorite. The small size of the Ti-Nb-mineral precluded identification, but it is possibly Nb-rutile, which is rarely seen partially-rimming other alteration silicates. Fluorocarbonate is present in fractures in amphibole grains, within cleavage traces and along grain boundaries in biotite.

The textural relationships in the quartz syenite from the Ashburton region are similar to those seen in the western contact zone. Rare fluorocarbonate is associated with thorite, Nb-oxides( pyrochlore ?), and secondary silicates. Grains composed of multiple phases of fluorocarbonate, Nb-oxide, and thorite replace a primary precursor - pyrochlore (Fig 2.11 and 2.12). Two chevkinite rich samples taken from Ashburton lookout area show replacement by acicular Nb-bearing ilmenite embedded in anhedral bastnaesite (Fig 2.13).

One quartz syenite sample was examined from the Radio Tower Hill area and showed no fluorocarbonate mineralization.

Fig 2.13. Relatively large chevkinite showing both mottled alteration and partial replacement features. Acicular niobium bearing ilmenite (dark) is embedded in bastnaesite (light) (sample # 2454).

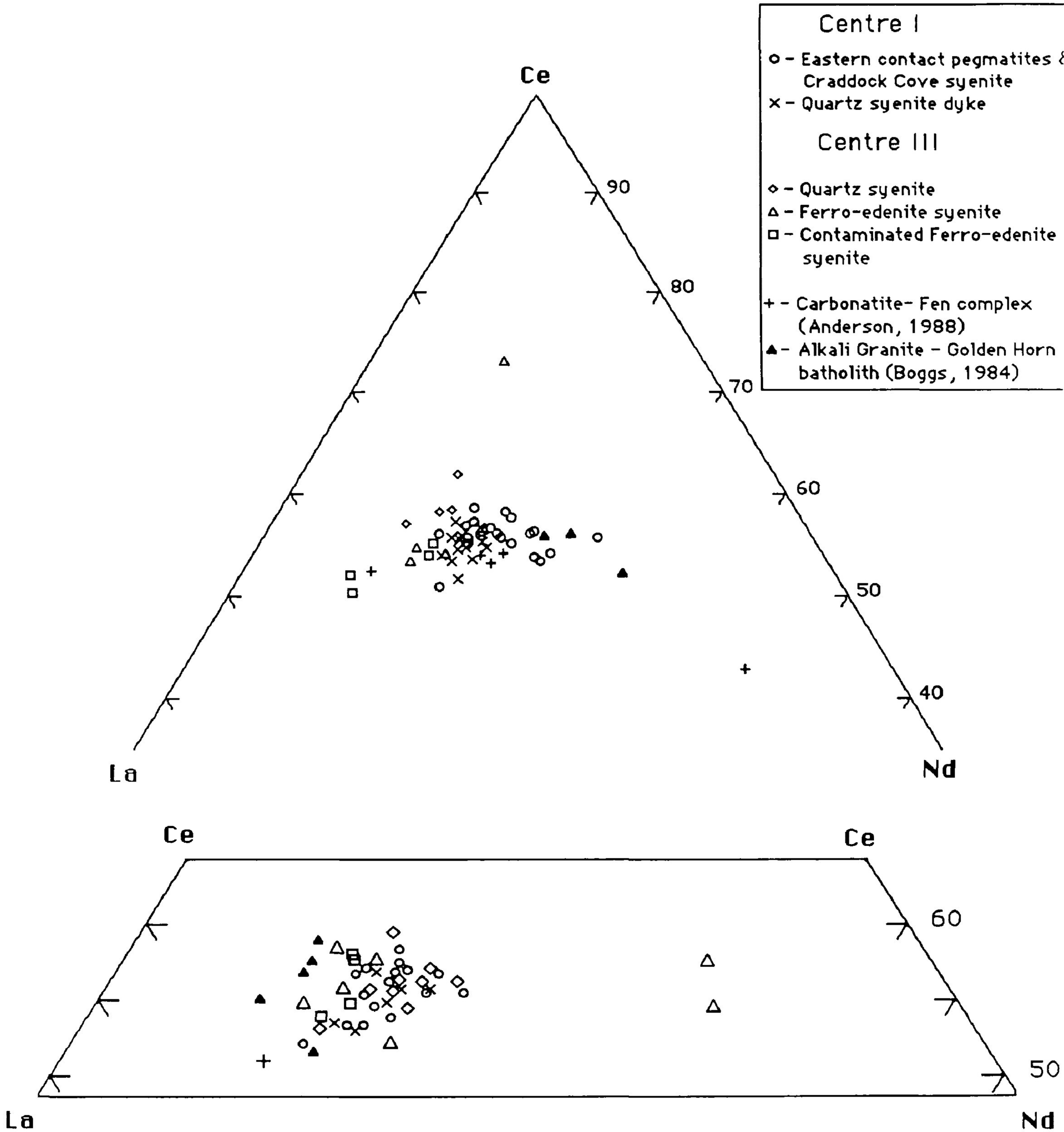


Fig 2.14 La - Ce - Nd plots of Ca-fluorocarbonate ( top ) and bastnaesite ( bottom). The Ca - bearing fluorocarbonates plot in a larger compostional field than the bastnaesites. For both species Centre I compostions are apparently enriched in Nd than Centre III.

## 2.1.7 C III, Magnesio-hornblende Syenite

Fluorocarbonate is rare in the magnesio-hornblende syenites from the Neys-Ashburton lookout area and is present only as small grains along fractures in amphibole.

## 2.2 Fluorocarbonate Compositional Variation

Compositions of fluorocarbonates determined in this work are listed in Appendix 1.1. Analysis of the fluorocarbonates from both centres show the carbonates to be La, Ce and Nd-enriched bastnaesite, parisite and synchysite. Several compositions, especially those from Centre III, have CaO wt % ranging from 1.00 wt% to 4.00 wt %. These samples have Ca and REE proportions intermediate between the ideal stoichiometry of the four fluorocarbonate endmembers. Electron probe studies of fluorocarbonates from an arfvedsonite granite in the Golden Horn Batholith(Boggs, 1984)and from an ankeritic ferro-carbonatite in the Fen complex, SE Norway (Anderson, 1986) also have compositions intermediate to the four endmembers. This could be due to the presence of additional members suggested by Van Landuyt et al,( 1975). However, it is assumed that the intermediate compositional values of the Coldwell complex fluorcarbonates are a result of electron beam overlap of intergrowths of more than one identified species and not due to the presence of intermediate compounds.

Bastnaesite and Ca-fluorocarbonate are plotted on separate La-Ce-Nd ternary diagrams (Fig 2.14). Coldwell bastnaesites, as a group, plot in a narrow range, between 50-60%Ce and 20-30% La with only subtle differences between those from Centre I and Centre III. The Centre I bastnaesite grains are Nd-rich compared to those from Centre III, with the eastern contact pegmatite minerals exhibiting the greatest Nd-enrichment. The bastnaesites from the western contact zone and Ashburton lookout areas of Centre III show no distinct differences in composition.

The Coldwell bastnaesites are relatively more Nd and Ce-rich than the Fen complex bastnaesite (Andersen, 1986) and more Nd-rich than those from the Fjalskar granite, Finland (Lahti et al, 1988).

Because of the variable Ca content and the problem of determining species, all calcium-bearing fluorocarbonates were plotted on a single La-Ce-Nd ternary diagram. Comparisons between the two ternary diagrams indicate that the Ca-fluorocarbonates REE proportions are more diverse and are slightly more Nd-rich and Ce-poor than the bastnaesites.

The centre III minerals show a broader distribution of Ce-La content ranging from 51% Ce (contaminated ferro-edenite syenite) to 74% Ce (ferro-edenite syenite) relative to centre I. With the exception of the one Ce-enriched Ca-fluorocarbonates from the ferro-edenite syenite, those from the quartz syenite are Ce-rich in comparison to Ca-fluorocarbonates from the ferro-edenite and contaminated ferro-edenite syenites. The Ca-fluorocarbonates are, in general, more Ce-rich than fluorocarbonates from the Fen Complex (Fig 2.14).

Fluorocarbonates occurring in various rock types increase in light lanthanide content in the series; granite and granite pegmatite, alkaline rocks, carbonatites. The degree of increase is different for each endmember (Fleischer, 1978). In the same rock type, bastnaesite is LREE-enriched relative to Ca-bearing members, this relative enrichment increasing with Ca-content. The difference in relative enrichment increases from granite and granite pegmatites through to alkaline rocks. Fluorocarbonate data from several centre I samples are plotted on a La/Nd vs. Ca/REE diagram (Fig 2.15). The eastern contact pegmatite and quartz syenite dyke C1432 fluorocarbonates

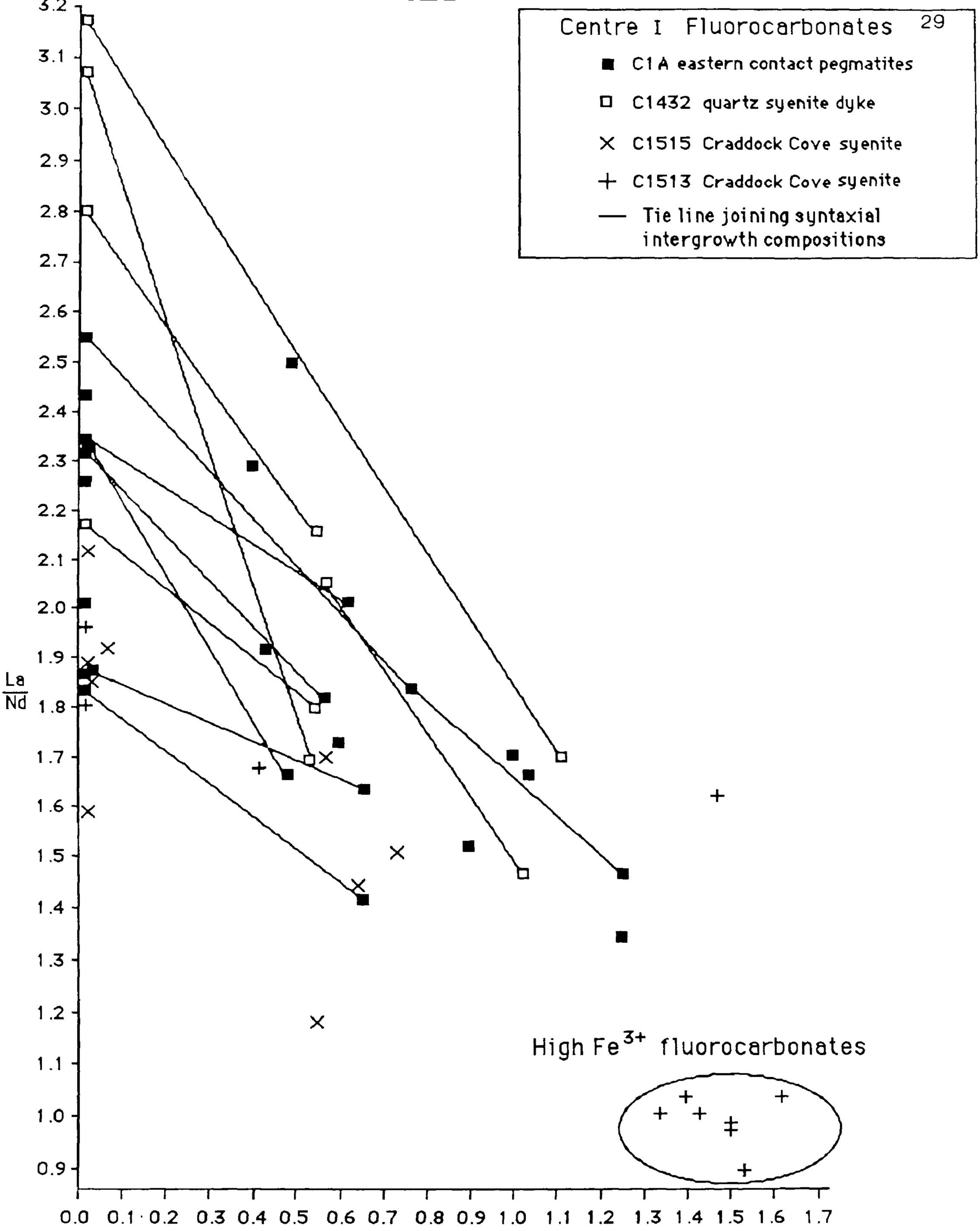


Fig 2.15. La-Nd enrichment vs Ca/REE plot for various compositions of fluorocarbonate from centre I. The ideal Ca/REE for bastnaesite is 0.0, for parisite is 0.5 , and synchysite is 1.0. Adjacent syntaxial domain compositions are signified by tie lines. There is a distinct trend of HREE enrichment for the Ca- bearing members from bastnaesite through synchysite.

polycrystals are the coarsest grained in the complex and show syntaxial intergrowths of bastnaesite and various Ca-fluorocarbonates. On the diagram tie lines join adjacent intergrowths. A similar trend of decreasing La/Nd as well as La/Ce from bastnaesite through the group to synchysite was qualitatively described in the Thor Lake fluorocarbonates (St. de Jorre, 1985). This relationship holds true for fluorocarbonates from the same sample and for adjacent fluorocarbonate intergrowths.

By definition the adjacent intergrowths formed in one precipitory event (Donnay and Donnay, 1953), therefore it can be assumed that major fluctuations in pressure, temperature, and REE proportions would not occur during genesis. It may be concluded that LREE-enrichment of bastnaesite relative to an adjacent Ca-fluorocarbonate is a result of crystal lattice differences between the mixed compounds. One is composed of (REE)F and $CO_3$ layers, the other has additional Ca ion layers. The presence of these extra layers may in some way affect the REE site making it more favourable to the smaller HREE elements. This hypothesis would imply that the Ca-fluorocarbonate trend on the ternary diagram (Fig 2.15) is not only a function of REE proportion in mineralizing fluid, but also a function of the amount of Ca in the species.

The C1513 fluorocarbonates from Craddock Cove syenites contain considerable amounts of Fe (1-12.8 wt%). Most of this iron must be in the trivalent state to satisfy the charge balance and $Fe^{3+}$ incorporated into the REE site results in stoichiometry close to synchysite. There are two possible site models:

1) The $Fe^{3+}$ and REE may occur in solid solution, where $Fe^{3+}$ replaces REE from the (REE)F layers. This would explain the presence of $Fe^{3+}$ content in the Ca- bearing endmembers and not bastnaesite. With increased Ca the smaller

HREE and $Fe^{3+}$, relative to the LREE and $Fe^{2+}$, may be more easily accomodated into the lattice. However, the cation radius of $Fe^{3+}$ of 0.63 (Shannon and Prewitt,1966) is still significantly smaller than that of Nd (1.135) and it is unlikely that significant amounts of $Fe^{3+}$ would substitute.

2) The second possibility is that the $Fe^{3+}$ ions form individual layers that substitute for individual (REE)F layers. In Fig 2.5 many of the Ca-Fe-fluorocarbonate compositions cluster around 1.5 on the Ca/REE axis. If an average of 1.5 is assumed for this compound,deviations from the average being explained by assigning different portions of Fe to the Ca sites as $Fe^{2+}$ and the rest to the REE site as $Fe^{3+}$, it would imply a replacment of one third of the (REE)F layers by $Fe^{3+}$ layers.

In the Centre III lithologies and the Craddock Cove syenite, the fluorocarbonates form secondary minerals replacing primary REE-bearing phases - pyrochlore, chevkinite, apatite, allanite and rarely sphene. Comparable replacement relationships have been found in granites (Littlejohn, 1981; Lahti and Suominer, 1988; Cerny and Cerna, 1972) and have been interpreted as alteration products due to hydrothermal action by late-stage magmatic fluids. Both the Coldwell units are similar in that $F^-$ and $CO_2$ rich solutions have permeated the rocks transporting and/or remobilizing the REE elements, but major compositional and genetic differences exist between fluids from Craddock Cove and Centre III.

In Centre III lithologies, fluorocarbonates are rare and occur as a fine grained replacement for pre-existing REE-minerals and less commonly associated with alumino-silicate alteration. During "bastnaesization" REE may be removed from the precursor mineral and redeposited as a secondary generation of fluorocarbonate and thus, represent a localized redistribution of the rare earth elements. Such a "autometasomatic" origin is implied for all fluorocarbonate mineralization in the samples investigated from Centre III.

The relatively large amounts of fluorocarbonate (C1513) cannot be explained by remobilization of REE from the breakdown of early minerals. Fluorocarbonate mineralization is directly related to K-metasomatism as evidenced by replacement relationships. Therefore, it is postulated K, rare-metals, and Fe - enriched fluids have infiltrated the western red syenites from an "external source". Whether the hydrothermal alteration is a result of residual fluids from the crystalization of the red syenite or related to other magmatic events is uncertain (see section 16.0).

## 3.0 Chevkinite (Perrierite ?)

Chevkinite is a rare earth titanium silicate mineral that readily accommodates elements such as Zr, Nb, Ta, Y, Th, and Sr within its lattice. The ideal stoichiometry is $A_4BC_4Si_4O_{22}$ where A site= REE, Th, Ca, Sr, Na, K; B= $Fe^{2+}$,Mg, Mn, Ca; C= Ti, Mg, Mn, $Fe^{3+}$, $Fe^{2+}$, Al (Segalstad, 1978; Ito et al, 1971; Platt et al, 1987) . A representative EDS spectrum of chevkinite from the Coldwell complex is shown in Fig 3.1.

The identification of chevkinite is complicated by the existence of the dimorph, perrierite, which is almost identical in composition and similar in structure to chevkinite. Therefore, X-ray diffraction is necessary for a conclusive identification of the mineral. Unfortunately the small grain size of the Coldwell chevkinite from the various lithologic units made it impossible to separate concentrates for x-ray diffraction study. In the absence of crystallographic data a method based on the ionic radius is used to determine the mineral species (see below).

### 3.1 Textural Relationships

The chevkinite is found in four distinct lithologic units within the Coldwell complex. In centre I rare grains are found in the ferro-augite syenite (samples C2905,C2909, and C2908) and one sample from the red syenite (C2920). In Centre III , isolated areas in the contaminated ferro-edenite syenite (C2028 and 2036- Western Contact) and the quartz syenites (C2116,C2923, and C2454- Ashburton Lookout area) may contain chevkinite.

#### 3.1.1 C III, Quartz Syenite

The alkaline quartz syenite near Ashburton Lookout contains relatively large amounts, up to 0.5 modal %, chevkinite. The stubby euhedral-to-subhedral

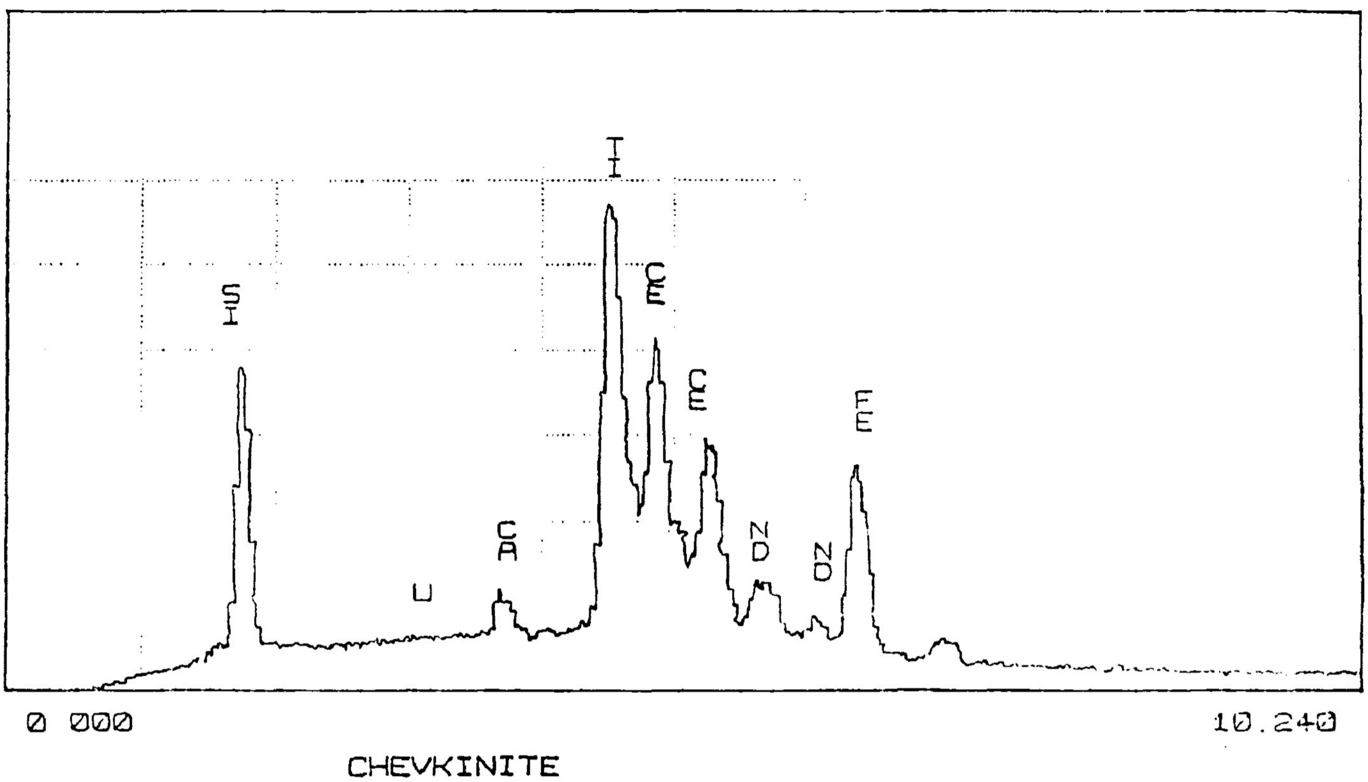


Fig 3.1. EDS spectrum of chevkinite from ferro-augite syenite (C2908).

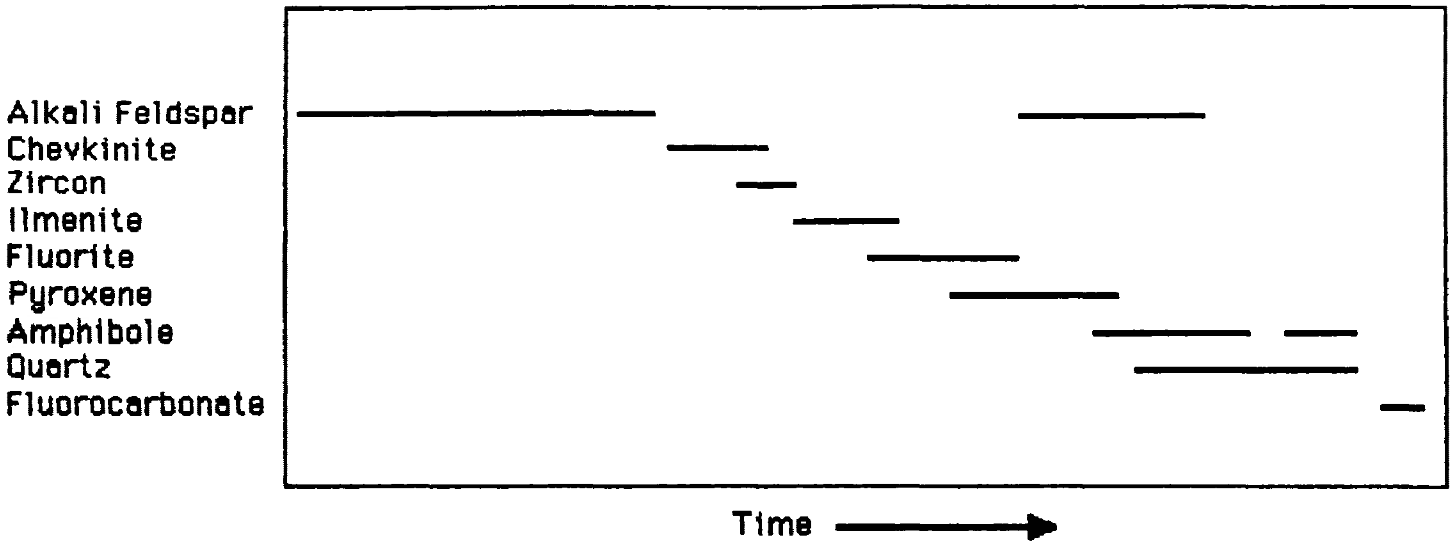


Fig 3.2 Paragenetic sequence in Centre III quartz syenite - Ashburton Lookout

Fig 3.3. SEM backscattered micrograph of chevkinite (CH) and alteration mantles interstial to perthite (P) and partially included in amphibole (AM). The "fresh" core (light) is surrounded by hydrated alteration (dark) (sample # C2454).

Fig 3.4. SEM back scattered micrograph of chevkinite, alkali-feldspar and fluorocarbonate from the ferro-edenite syenite. Fluorocarbonate .has precipitated along fractures and dilated feldspar cleavage planes Alteration occurs around grain margin as 3 distinct compositional domains a,b, and c (see appendix 2.2). Elemental comparisons between domains are graphed in Fig 3.9 (sample # C2036).

Fig 3.5. SEM backscattered micrograph of allanite (al), K-feldspar, calcite (ca), and chevkinite (ch) aggregate replacing amphibole (sample # C2920).

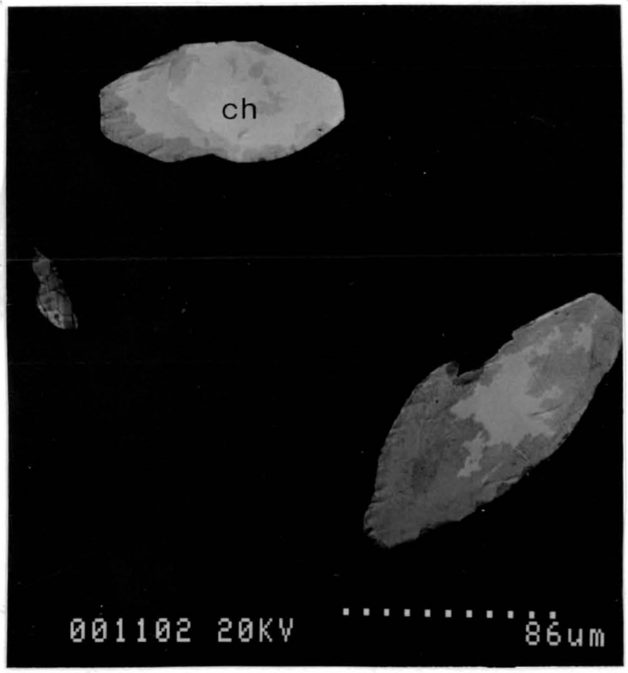
ch
001102 20KV
86um
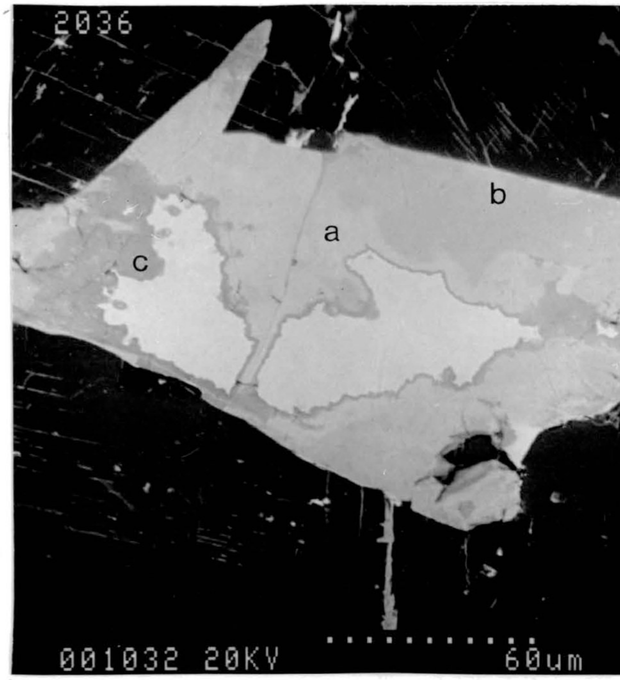
2036
b
a
c
001032 20KV
60um

001106 20KV
200umC
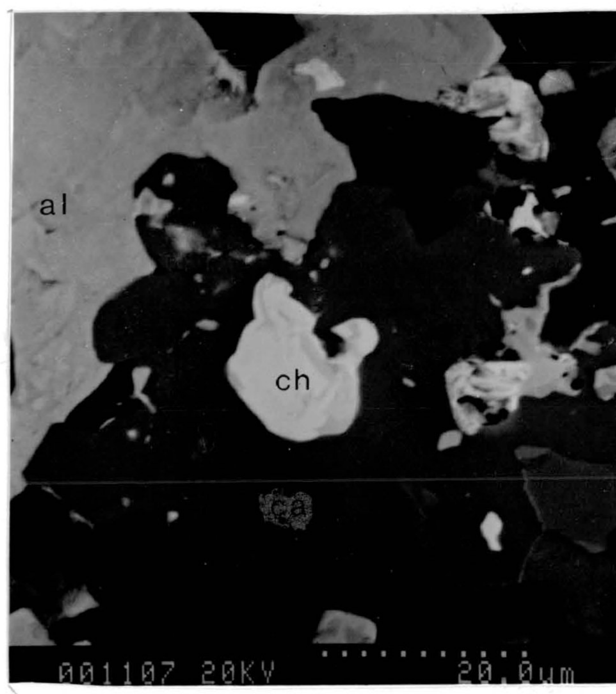
al
ch
ca
001107 20KV
20.0um

grains range in size from 50 μm to 250 μm, and occur as inclusions in interstial quartz between perthite prisms, occasionally included or partially-included in amphibole or perthite and more rarely in zircon, ilmenite and magnetite. The proposed paragenetic sequence is given in Fig 3.2. In thin section dark reddish brown cores are rimmed by light brown-to-pale-orange alteration mantles. The lack of pleochroism and complete opacity of the "fresh" cores and mantles in polarized transmitted light is undoubtedly a result of severe metamictization. Backscattered images of the grains show alteration mantles as mottled rims around a heterogeneous core (Fig 3.3). Complete alteration of the chevkinite is rare.

### 3.1.2 Contaminated Ferro-edenite Syenite

Chevkinite is rare and too small for optical investigation. Back scattered imagery reveals small anhedral-to-subhedral 20μm-40μm in diameter chevkinite as inclusions in perthite with the larger grains exhibiting a similar mottled alteration mantle to that seen in the quartz syenite. One unusually large chevkinite - alteration grain contains three distinct alteration domains (Fig 3.4). Chemical analysis of the zoning is given in appendix 2.2.

### 3.1.1 Ferroaugite Syenite

Chevkinite in the Craddock Cove ferro-augite syenite is found in samples C2905, C2908, C2909, and C2914. Small grains, commonly less than 50μm, are anhedral-to-euhedral and are included in the interstial mafics. Rare large grains of chevkinite show a distinct chemical zoning, reflecting variations in Ti, Nb and Fe. Chevkinite is absent in the southeastern ferro-augite syenite

### 3.1.4 Craddock Cove Red Syenite

Only 2 samples are known to contain chevkinite, C1513 and C2920. In section C2920 chevkinite is found associated with aggregates of allanite, calcite, and potassium feldspar (Fig 3.5). Small (<40 μm) anhedral grains are included in anhedral to subhedral allanite, or calcite. In sample C1513 euhedral chevkinites approximately 50μm in diameter are commonly altered to multiple Nb-bearing phases (tentatively identified as Nb-rutile and pyrochlore) and fluorocarbonate.

## 3.2 Composition

Representative compositions are given in appendix (2.2). Most Coldwell chevkinites exhibit low total oxide percentages as a result of their apparent metamict and hydrated nature. Chevkinites from the different lithologic units show similar compositions with subtle differences occurring in elemental proportions. The centre III contaminated ferro-edenite syenite (C2028 and C2036) and quartz syenite have similar total $(REE)_2O_3$ wt % contents, ranging from (36.03-41.19 wt%) and (36.53-42.28 wt %) respectively. The Centre I minerals appear to have higher $(REE)_2O_3$ wt% contents with the ferro-augite syenite containing 38.16% - 45.79% and the red syenite having 45.06 - 46.21 wt%. The chevkinite of centre III exhibits a general trend which is seen in other REE-bearing minerals from various deposits, namely, a gross enrichment of LREE from granite pegmatites through syenites or quartz syenite to alkaline syenite or syenite pegmatite (Fleischer, 1965). Material in the contaminated ferro-edenite syenite is enriched in the MREE relative to that in the quartz syenite (Fig 3.6). Chevkinites from the ferro-augite syenite also have REE proportions similar to other alkaline quartz syenite rocks.

Differences in CaO (wt %) content are evident between chevkinite from each of the Coldwell centres. In centre III CaO abundances range between 2.9-5.01 wt%, while lower CaO contents (0.95-3.13 wt %) are found in centre I.

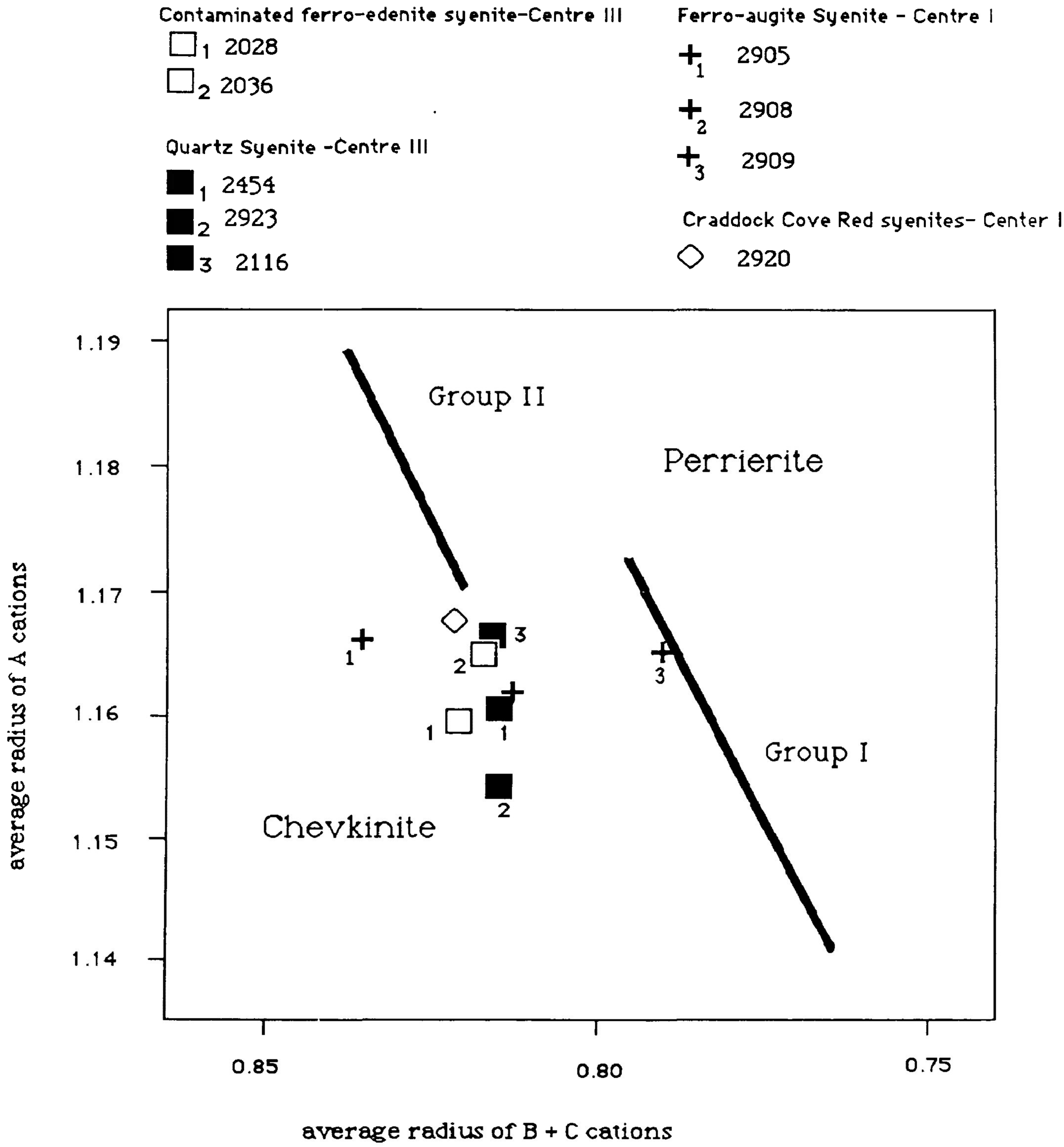


Fig 3.7 Distribution of Coldwell chevkinites as a function of average cation radii of A and B + C sites. Group I and Group II are defined after Segalstad and Larsen (1978) and Platt et al (1987). Fe is calculated as $Fe^{2+}$

Correspondingly the total rare earth contents of the ferro-augite syenite and Craddock Cove syenite chevkinite are higher (41.34-46.21 wt % oxide) than those of centre III (36.03-42.28 wt %).

Thorium is present in most chevkinites and occurs in significant amounts in examples from the contaminated ferro-edenite syenite ($ThO_2$= 0.84-4.23 wt %).

It is interesting to note that chevkinite from the Craddock Cove syenite sample shows unusually high amounts of FeO (13.07-13.39 wt %). High FeO is also characteristic of the fluorocarbonates (see section 2.2) and pyrochlores (see section 4.4) from this area.

## 3.3 Chevkinite vs Perrierite

Although the similar composition of the two minerals suggests a polymorphic relationship between chevkinite and perrierite, crystal-chemical differences exist between the related species. Studies of synthetic members by Ito (1967) showed that the relative cation size between A, B, and C sites determines which structure will form. An excessive difference in the average cation size between the A site and the B, C sites favours the stability of perrierite over chevkinite. This compositional control appears to be stronger than any temperature effect. Pressure and temperature indirectly affect the structure by influencing the A site composition, at least in the 7.5-20 Kbar and 900-1050°C range (Green and Pearson ,1988) . Compositional variation in the B, C sites occurs with changing $fO_2$ conditions. Fe becomes more abundant with increasing $fO_2$ as the $Fe^{3+}$ increases. As suggested by Haggerty and Mariano (1983) and Green and Pearson (1988), it is difficult, especially when pressure effects are not known, to distinguish chevkinite from perrierite solely on the basis of composition and cation radius of elements in specific sites. Therefore, the identification of the Coldwell chevkinites using this method cannot be considered definitive.

Segalstad and Larsen (1978) found that 12 analyses of chevkinite and perrierite formed 2 distinct groups: group I has Ca completely accommodated in the A sites, and group II has most Ca located in the B and C sites.

Average A site cation radius vs. average B+C cation radius for the Coldwell chevkinites are shown in Fig 3.7.The grains from C2920, C2116, C2028, C2036, C2454, and C2923 are plotted as averages of the chevkinite compositions from each sample while the others ( C2905/28, C2909/2, and C2908), due to the scarcity of grains for analysis, are values from single grains. Cation radii, as determined by Shannon and Prewitt (1969), were applied to the chevkinite compositional data and the appropriate cations were assigned to sites A, B, and C of the structural formula presented on p. 33. All $Ca^{2+}$ was assigned to site A. The cation radius values plot well within the chevkinite field of group I reflecting compositions with relatively high Ca abundance ( 2.90 - 5.01 wt % CaO) for centre III chevkinites and 0.95-3.13 wt % CaO for Centre I syenites ) and lower REE abundance (36.03- 42.28 wt % $(REE)_2O_3$ for centre III and 41.34 - 46.21 wt% $(REE)_2O_3$ for the centre I syenites). Cation proportions suggest the accommodation of most Ca in the A site. Sample C2909 is anomalous in its close proximity to the chevkinite/perrierite boundary.

The location of data points on Fig 3.7 is based on calculation of total iron as FeO, however it is probable that a portion of Fe is present in the trivalent state. Significant amounts of ferric iron wil reduce the average cation radius for the B+C cations shifting plots closer to the group I chevkinite-perrierite boundary (Platt et al, 1987). Therefore, the determination of the oxidation state of the iron will have a bearing on the confidence of the species

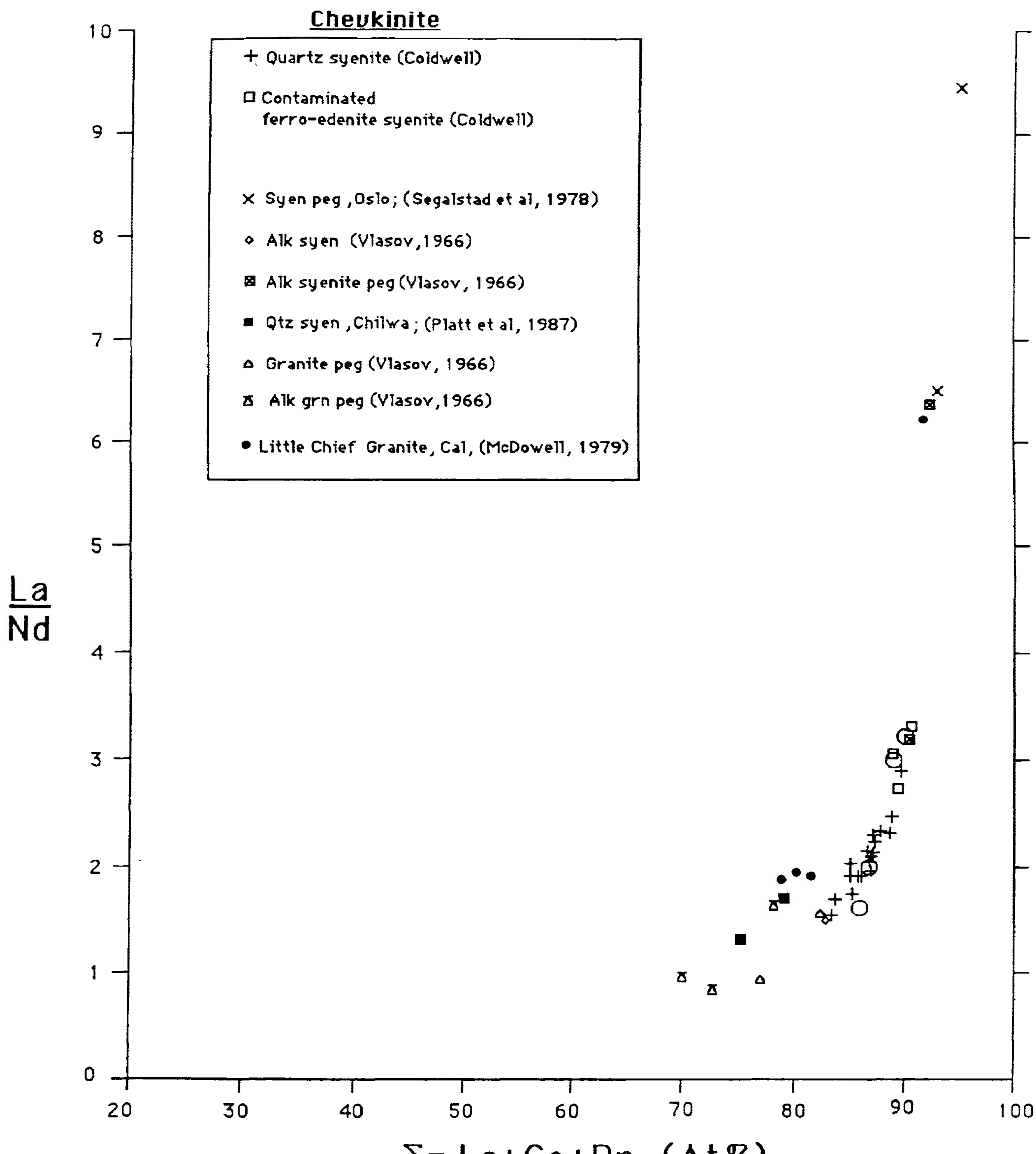


Fig 3.6. Significant LREE enrichment occurs from granite pegmatites through syenites or quartz syenites to alkaline syenite or syenite pegmatite (Fleischer, 1965). A similar trend is seen in the higher La/Nd ratio for the contaminated ferro-edenite syenite chevkinites relative to the quartz syenite. The compositions from the ferroaugite syenite correspond to chevkinite from other alkaline syenites or quartz syenites.

determination. It is assumed that for chevkinites from both centres the dominant state of Fe is divalent. This is based on two independant pieces of evidence.

1) Analysis of chevkinites from other occurrences consistently show divalent Fe to be more abundant than trivalent Fe. Platt et al, (1987) estimated the $Fe^{2+}/Fe^{3+}$ content of an average of 6 chevkinite analysis from a peralkaline quartz syenite to be 1.5 or greater based on the distribution of iron when calculated to 13 cations. Segalstad and Larsen (1978) determined by analysis that chevkinites from a series of syenite pegmatites from the Oslo region in Norway contains iron almost exclusively as FeO. McDowell (1979) obtained ratios $Fe^{3+}/(Fe^{2+} + Fe^{3+})$ ratios that ranged between 0.14 - 0.40.

2) Recalculation of $Fe^{2+}$, $Fe^{3+}$ on a stoichiometric basis (Droop,1987), shows that the $Fe^{3+}/(Fe^{2+} + Fe^{3+})$ ratios of the Coldwell chevkinites range between (0.13-0.30),which is consistent with the values found in the literature.

## 3.4 Alteration of Chevkinite

Quantitative analyses (appendix 2.3) of alteration rims of grains from the Ashburton Lookout quartz syenite and western contact contaminated ferro-edenite syenite were compared to the enclosed "fresh" cores to determine major compositional loss or gain of elements from a deuteric or hydrothermal fluid. To correct for the low analytical totals (80-85 wt %) of the alteration mantles, element proportions are calculated for each particular cation as a percentage of the total amount of cations. In Fig 3.8 the elemental differences in Fe, Nb, Ti, Ca, La, Ce, Pr, Nd, Si, and Th of the mantle relative to the core are shown as percentages.

The 3 grains from the quartz syenite show a strong pattern of Fe, Ca, and

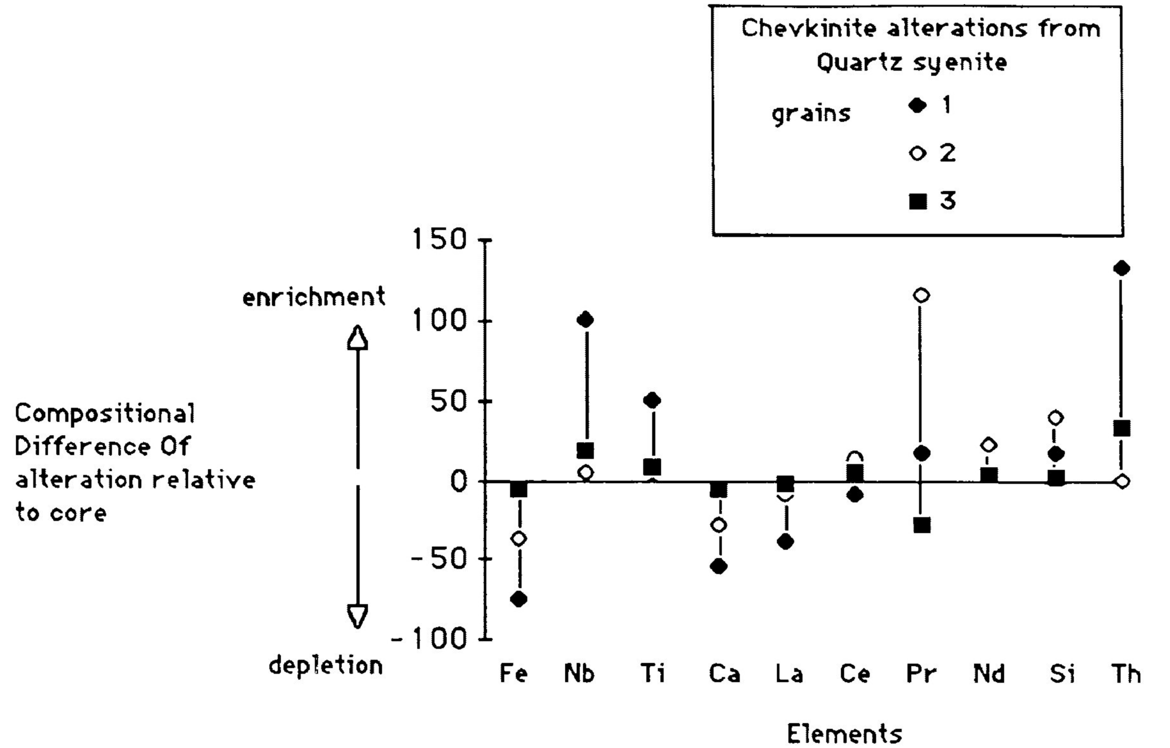


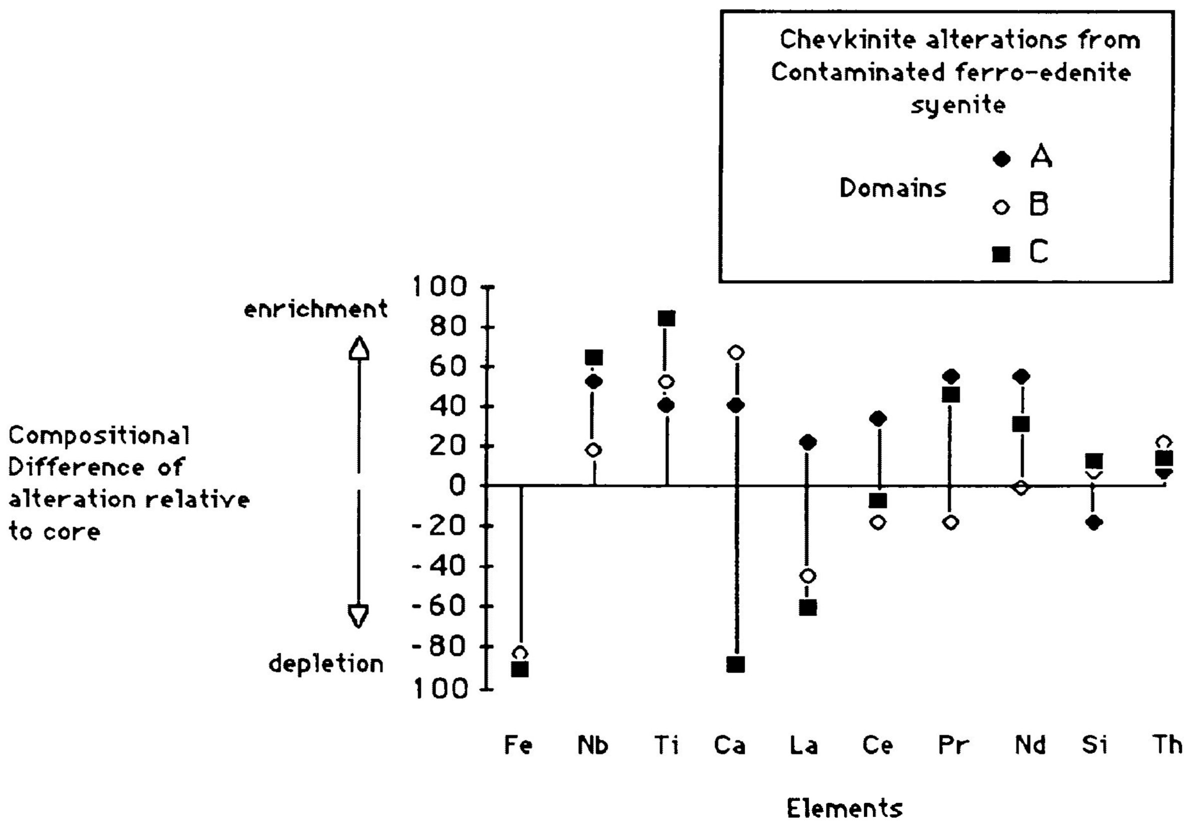


Fig 3.8 Compositional differences between core and alteration mantles are represented as elemental enrichments or depletions in alteration relative to cores for chevkinites in the quartz syenite and a chevkinite from the contaminated ferro-edenite syenite. All grains show strong depletion in Fe, Ca, REE and enrichment in Nb, Ti, Si. Preferential removal of LREE vs. MREE is evident.

rare earth-depletion and a relative enrichment in Ti and Si. Of particular note is the apparent depletion of Nd through La. A similar orange alteration rimming chevkinite in alkaline granites (Payette et al. 1988) is also characterized by a depletion in Fe, Ca, and REE and enrichment in Ti.

A complex alteration pattern observed in the contaminated ferro-edenite syenite chevkinite shows 3 distinct alteration regions (Fig 3.4). Though the altered zones are compositionally distinct, the general patterns of Fe, Ca, and REE depletion and the strong enrichment in the Ti (Fig 3.8 ) are similar to those described above.

The origin and mobility of the REE derived from the chevkinite are confirmed by fluorocarbonate mineralization along feldspar cleavage planes. Hydration of chevkinite resulted in grain expansion, dilation of adjacent feldspar cleavage planes, removal of REE, and precipitation of fluorocarbonate along the opened fractures.

## 3.5 Comparisons

Chevkinite is a rare mineral occassionally found in granites (Harding et al,1982 and Mcdowell, 1979). A significant proportion of identified chevkinites are associated with peralkaline and alkaline syenites and granites. Platt et al, (1987) investigated chevkinite in two peralkaline quartz syenites from the Chilwa alkaline Province, Malawi. Payette et al (1988) identified chevkinite in peralkaline and alkaline granites of the Welsford anorogenic igneous complex. Segalstad and Larsen (1978) reported an occurrence from the Oslo peralkaline granites and chevkinite has been found in metaluminous and mildly peralkaline ryholite tuffs (Novak and Mahood, 1986) .

Major element compositions, Ca, Fe, Ti, and LREE of the Coldwell chevkinites are comparable to those mentioned above (Table 3.1). However, the

Table 3.1. Chemical composition ( weight percent oxides) of chevkinites from various localities

| | a | b | c | d | e | |
|---|---|---|---|---|---|---|
| Si02 | 19.86 | 20.33 | 19.50 | 20.20 | 17.88 | |
| Al203 | 0.07 | 2.79 | 0.16 | 0.12 | 0.47 | |
| Ti02 | 17.07 | 18.76 | 17.50 | 18.30 | 17.71 | |
| Nb205 | nd | 0.02 | 1.60 | 0.64 | 0.23 | |
| Fe0 | 10.06 | 7.27 | 11.20 | 11.30 | 10.50 | |
| Fe203 | ---- | ---- | ---- | ---- | 7.08 | |
| Mn0 | 1.01 | 0.11 | nd | na | 0.02 | |
| Mg0 | 0.05 | 0.85 | nd | na | ---- | |
| Ca0 | 3.20 | 5.67 | 3.31 | 2.82 | 2.66 | |
| Th02 | 1.62 | 0.79 | 0.60 | 0.33 | 3.61 | |
| Y203 | 0.29 | 0.24 | 0.57 | 0.23 | | |
| La203 | 23.76 | 11.44 | 13.00 | 12.10 | | |
| Ce203 | 19.26 | 17.85 | 18.60 | 21.40 | 36.26 | REE203 |
| Pr203 | 2.46 | 2.03 | 2.00 | na | | |
| Nd203 | 2.32 | 5.49 | 10.10 | 6.29 | | |
| Sm203 | nd | 0.88 | 1.38 | 2.67 | | |
| Sum | 101.03 | 94.50 | 97.92 | 97.10 | 96.42 | |

a- Segalstad and Larsen,( 1978); from syenite pegmatite, Oslo, Norway.
b- McDowell, ( 1979); from Little Chief Granite.
c- Platt et al, ( 1987); from quartz syenite, Chilwa, Malawi.
d- Novak and Mahood, ( 1986); from peralkaline tuff, Kane Springs Wash Calderak, Nevada.
e- Zhang et al, ( 1976); from quart syenite dykes, Hubei, China.

minor elements, Nb and Th, are typically more abundant in the Coldwell specimens (eg. maximum $Nb_2O_5$=7.21 wt % in the ferro-augite syenite, and maximum $ThO_2$= 3.28 wt % in the contaminated ferro-edenite). The Craddock Cove chevkinites are unique, relative to Coldwell samples and those from other deposits, in their unusually high Fe content of over 13 wt %. Typical FeO contents range from 8-11 wt % in minerals from granitoid rocks with the exception of iron chevkinite in a quartz syenite from Hubei, China (Zhang et al, 1976). A significant amount of $Fe_2O_3$ (7.08 wt %) in the mineral is attributed to water-transported ferric iron introduced into the mineral lattice through fractures (Zhang et al, 1976). The Craddock Cove chevkinites appear to be a minor part of a replacement assemblage of allanite, K-feldspar, and calcite formed during a metasomatic event. If experimental studies by Green and Pearson, (1988) are applicable to (low ?) temperature and pressure metasomatism, the higher Fe contents may be a result of a raised $fO_2$ and the predicted increase in $Fe^{3+}$ in the mineralizing fluids.

## 4.0 Pyrochlore

The minerals of the pyrochlore subgroup are the commonest niobium minerals in alkaline intrusions and comprise some of the most complex rare-metal bearing species. The general formula is $A_{2-m}B_2O_6(O,OH,F)_{1-n} \cdot pH2O$, where m=0-1, n=0-1, p is variable, and the A site= Ca, Na, REE, U, Th, Sr, and Fe; the B site= Nb, Ti, and Ta (Foord, 1982). The complexity of the substitution has lead to a chemical classification of minerals with the pyrochlore structure by subgroups based on the B site composition. Individual species within each subgroup are defined by the A site constituents (Hogarth , 1977). The Coldwell niobates, with the exception of one composition in the betafite subgroup, are strongly partitioned into the Nb-dominant pyrochlore division of the group triangle (Fig 4.1).

Pyrochlore is the most abundant of the Nb-bearing minerals in the Coldwell rocks. It has been identified on the basis of composition in the centre III quartz syenite, contaminated ferro-edenite syenite, ferro-edenite syenite and in the Centre I ferro-augite syenite, Craddock Cove red syenites, and the quartz syenite dykes. The large grain size of the mineral in the ferro-augite syenite patch pegmatites from the eastern contact allowed separation and confirmation of the identity by X-ray diffraction techniques. Mineral paragenesis varies within the complex from simple primary crystallization from the melt to precipitation and replacement of earlier niobate phases by metasomatic/hydrothermal fluids. Commonly both modes of occurrence appear in the same sample. The size of the grains and complexity of the replacement intergrowths between two or possibly more phases made SEM X-ray mapping essential in determining the multiphase interrelationships.

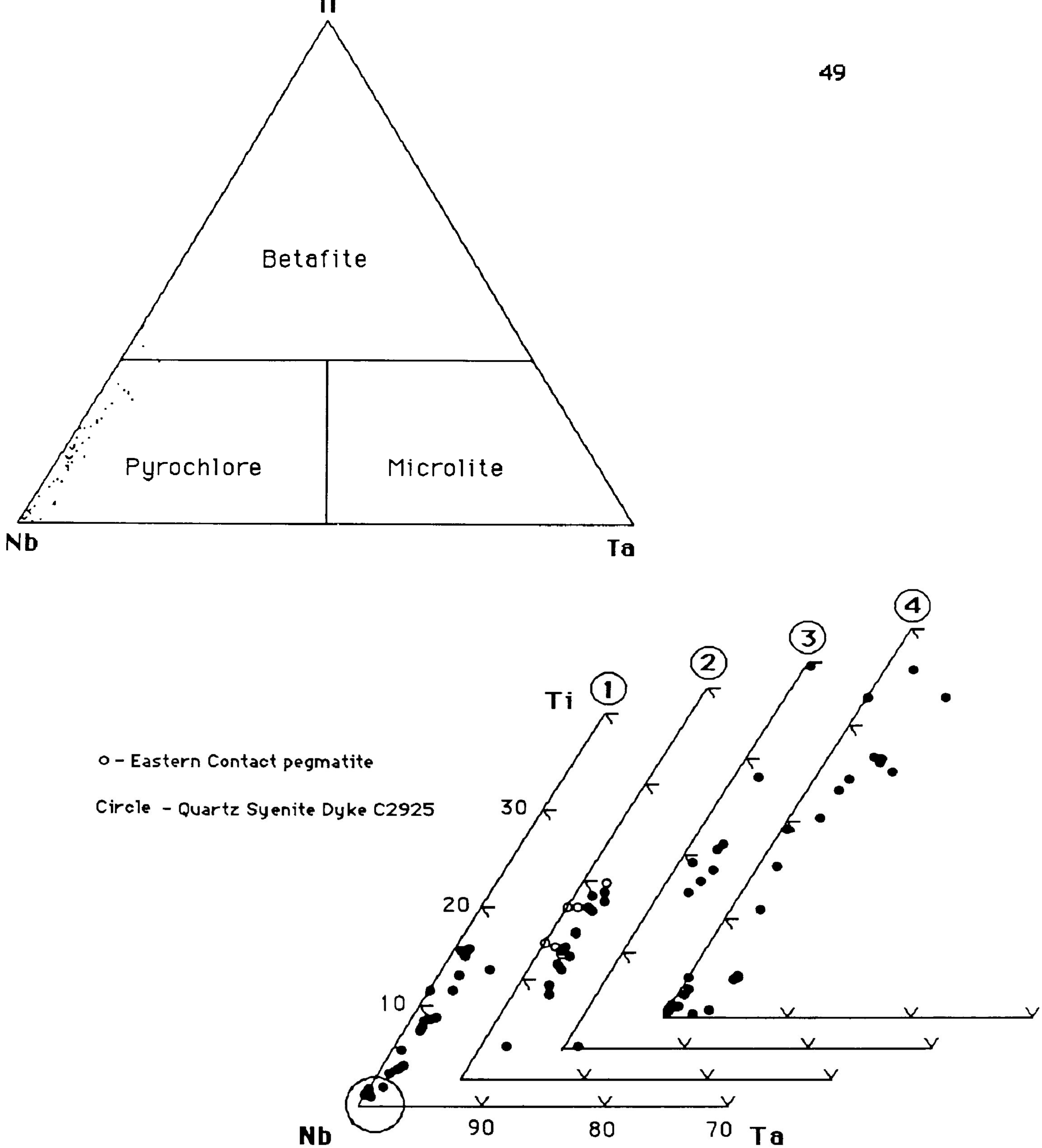


Fig 4.1 Pyrochlore subgroups as defined by Hogarth, (1988). The atomic compositions for the Coldwell pyrochlores are plotted on four Ti-Nb-Ta ternary diagrams. The pyrochlores as a group are Nb-dominant. Compositions of minerals from different lithologic units are viewed in detail in lower diagrams. In Centre I, 1= Quartz syenite dykes, 2=Ferroaugite syenite, 3=Craddock Cove syenites; in Centre III, 4=Ferro-edenite syenite, contaminated ferro-edenite syenite, and quartz syenite.

## 4.1 Textural Relationships

### 4.1.1 C.I. Quartz Syenite Dykes

Pyrochlore is found in four quartz syenite dykes (C1418, C1428, C1432, and C2925) as a replacement phase of the previously formed Nb-bearing minerals, columbite and fersmite (Fig. 4.2 and 4.3). Irregular pyrochlore alteration mantles enclose grain remnants and in some cases, almost completely pseudomorph the original grain. The primary anhedral-to-subhedral minerals seldom exceed 100µm, whereas the pyrochlore alteration seldom exceeds 20µm. Rare small (approximately 70µm) subhedral-to-euhedral pyrochlore grains are found in several of the dykes. Two or more pyrochlore varieties are present in one grain, commonly a core of one composition is mantled by material of distinctly different composition. The genesis of these grains is unclear . They may represent a complete pseudomorph of fersmite or columbite or be a partial replacement of a primary pyrochlore. Grains that are large enough for optical examination are corroded and turbid in appearence. Enclosing and adjacent mafics ( Pyroxene-C2925, Amphibole, biotite-C1418-C1432) show evidence of alpha- radiation damage - halos and radial fractures around the hydrated minerals. The niobates are closely associated with fluorite and the other dominant rare metal minerals, fluorocarbonate, thorite and zircon. In dyke C2925, niobates and thorite-zircon intergrowths rim or occur as inclusions in fluorite. The resulting radiation damage causes a reddish purple colouration around fluorite grain borders or as patches and zones within the fluorite.

### 4.1.2 Ferroaugite Syenite

In the ferroaugite syenite rare subhedral-to-euhedral pyrochlore (<100µm) form inclusions in amphibole and quartz and are partially included in potassium

Fig 4.2. Complex replacement texture of columbite (cb) and pyrochlore (p) is exhibited in back scatter micrograph and X-ray maps. Patches enriched in Ca and REE identifies pyrochlore, Nb and Fe signify columbite domains. X-ray maps: Upper Left - Nb, UR - Ca, LL - Fe, LR - REE (sample # C1432).

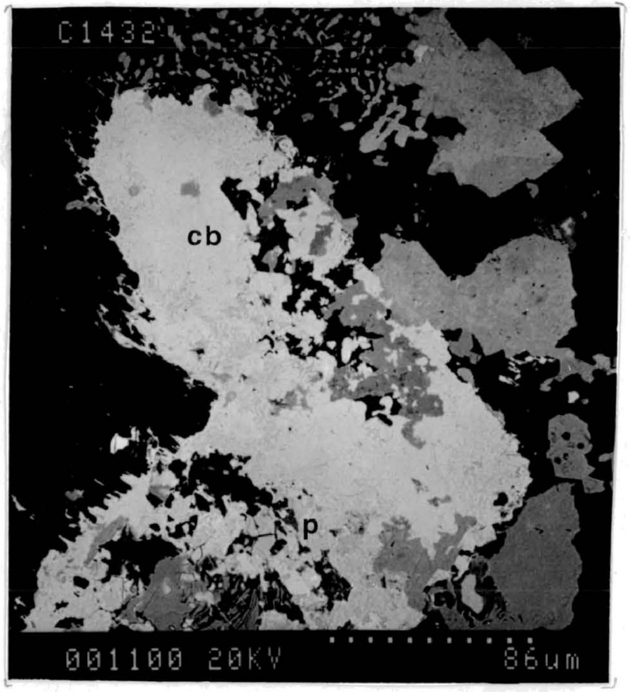
C1432
cb
p
001100 20KV
86um

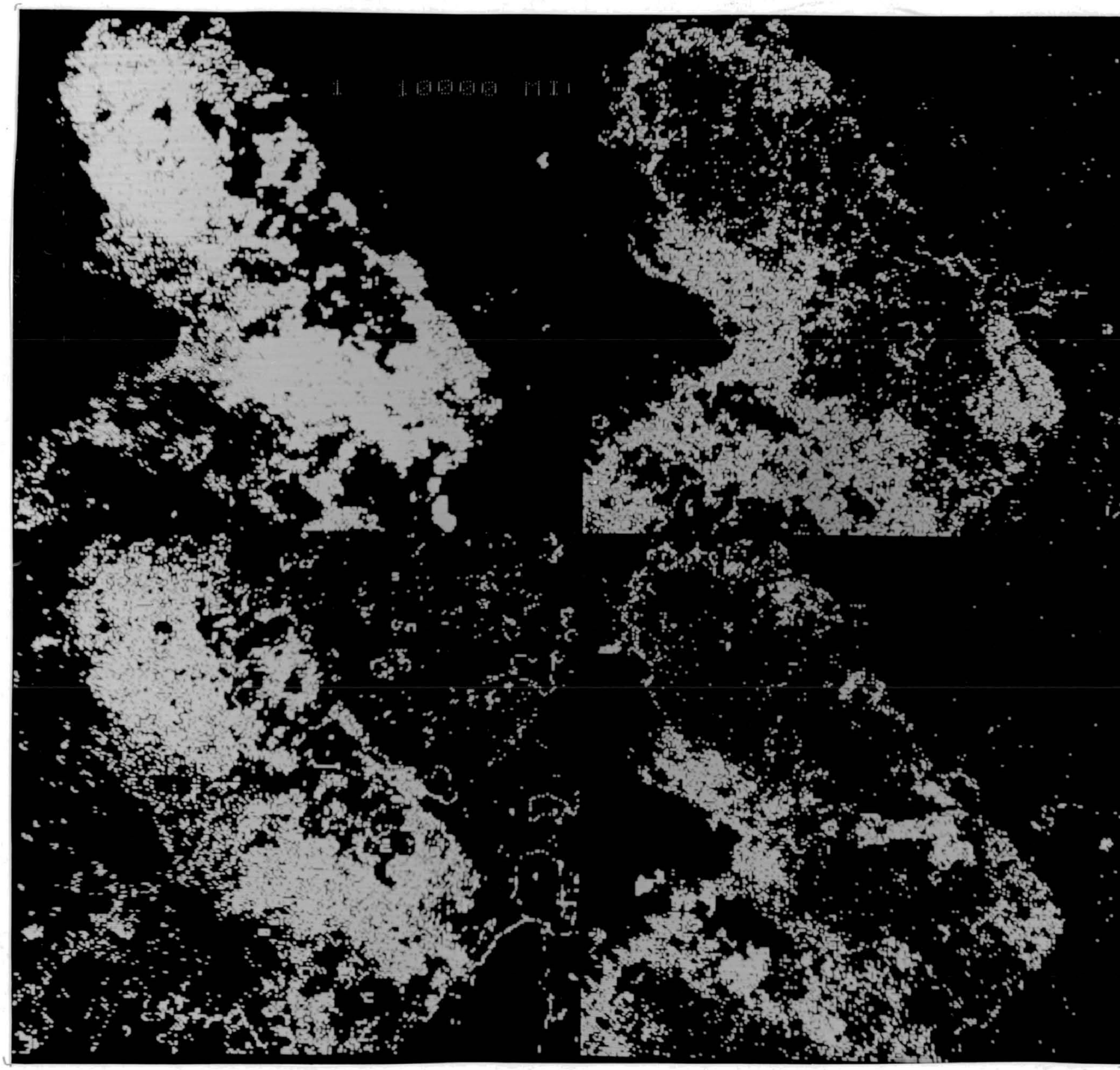
1 10000 MD

Fig 4.3. Fersmite (f), from quartz syenite dyke C1418 is corroded and partially replaced by pyrochlore along margins.

Fig 4.4. Mottled pyrochlore (p) inclusion in perthite is surrounded by an alteration silicate (as) corona. The alteration may result from the breakdown of the feldspar lattice by $\alpha$-particle emission of the actinide bearing pyrochlore.

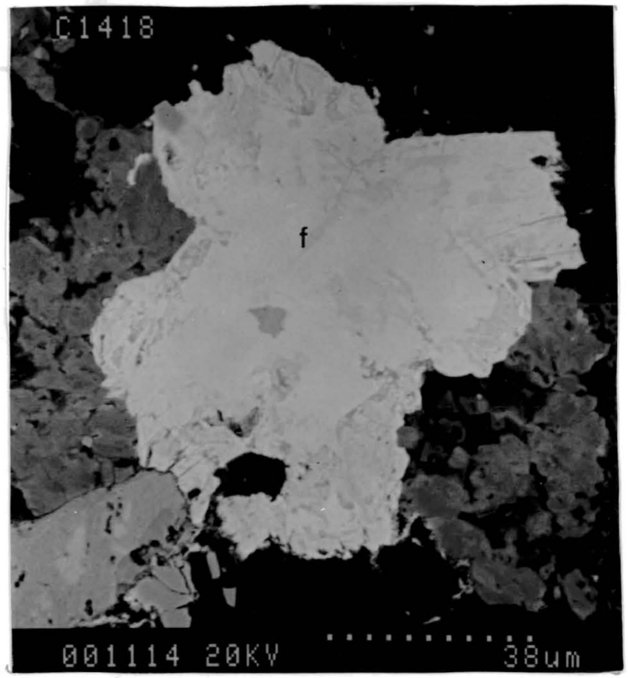
C1418
f
001114 20KV
38um

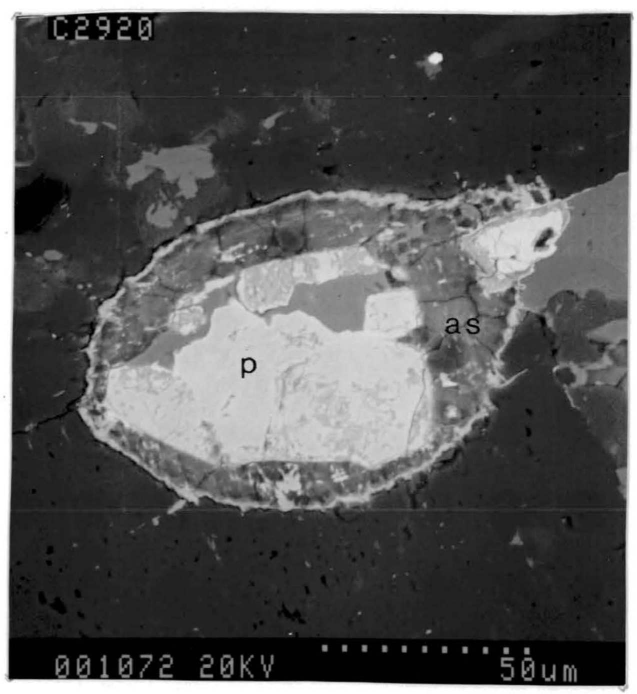
C2920
as
p
001072 20KV
50um

feldspar. Associated rare-metal minerals are fergusonite and zircon.

The southeastern ferroaugite syenites have been found to contain pyrochlores only in the most highly differentiated phases. Here they are associated with the interstitial residual minerals- zircon, calcite, and quartz. Several of grains contain small (<2μm) inclusions of galena.

### 4.1.3 Craddock Cove Syenite

Small (20-30μm) grains of pyrochlore appear to be primary subhedral prisms included in albite or amphiboles. Back scattered imaging shows distinct mottling of the crystal. Grains in albite typically have halos of alteration silicate due to radiation damage from uranium and thorium-bearing pyrochlore (Fig. 4.4).Hematite is commonly associated with the alteration silicate. In C1513 the niobates of variable compositions from Nb- $TiO_2$ (Nb-rutile ?) to pyrochlore, including fluocarbonates are alteration products of a primary mineral, possibly chevkinite.

### 4.1.4 Eastern Contact Pegmatite

The larger crystals in the pegmatite allowed their concentration in a heavy mineral separate for X-ray diffraction. A heated - mineral concentrate produced the powder X-ray diffraction pattern seen in Fig 4.5. This and Table 4.1 confirm the presence of pyrochlore in addition to fersmite. The large (>1mm) dark brown to dark reddish brown grains are translucent-to-opaque with concoidal fractures. In thin section the pyrochlore is dark reddish brown and turbid. Back scattered imagery reveals euhedral heterogenous prisms are altered to Nb-rutile, fluorocarbonate and alteration silicate. Fig 4.6 shows replacement by an alteration silicate and textural features of pyrochlore recrystallization (ie growth zones encroaching on alteration silicate patches.

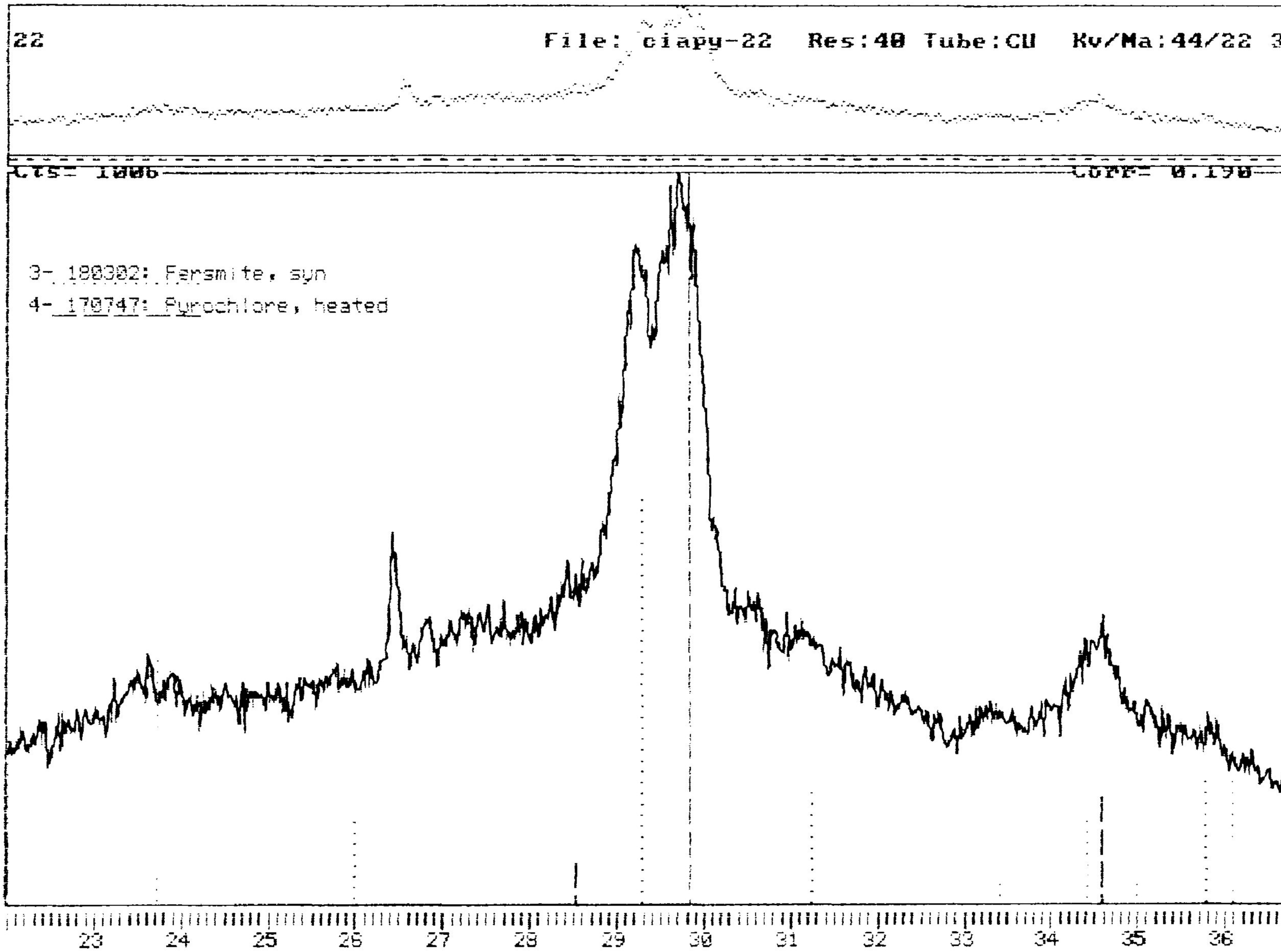


Fig 4.5. X-ray diffractometer scan of an heated heavy mineral separate from the eastern contact ferroaugite pegmatites over the region 22-37°. Peaks 3.05 and 3.792 signify the presence of fersmite, while peaks 3.002 and 2.603 indicate pyrochlore.

| Pyrochlore -heated* | | fersmite-syn | | Pyrochlore-fersmite Ferroaugite pegmatites | |
|---|---|---|---|---|---|
| dA | int | dA | Int | dA | int |
| | | 7.44 | 40 | | |
| 5.99 | 10 | | | 6.063 | F |
| | | 5.35 | 10 | | F |
| | | 3.76 | 30 | 3.792 | P |
| | | 3.74 | 30 | | |
| | | 3.43 | 20 | 3.478 | F |
| 3.13 | 6 | | | 3.375 | F |
| | | | | 3.331 | |
| | | | | 3.147 | |
| | | 3.02 | 100 | 3.052 | F |
| 2.995 | 100 | | | 3.002 | P |
| | | 2.87 | 20 | 2.875 | F |
| | | 2.69 | 10 | | |
| 2.594 | 16 | 2.61 | 20 | 2.603 | P,F |
| | | 2.57 | 10 | | |
| | | 2.515 | 20 | | |
| | | 2.494 | 20 | | |
| | | 2.464 | 10 | | |
| | | 2.384 | 10 | | |
| | | 2.311 | 10 | | |
| | | 2.246 | 10 | 2.235 | F |
| | | 2.145 | 10 | 2.146 | F |
| | | 2.088 | 10 | | F |
| 1.996 | 6 | 2.005 | 10 | 2.029 | F,P |
| | | 1.968 | 10 | | F |
| | | 1.932 | 20 | | F |
| | | 1.915 | 10 | | F |
| | | 1.884 | 20 | | F |
| | | 1.872 | 10 | | F |
| 1.8338 | 40 | | | 1.829 | P |
| | | 1.787 | 20 | 1.727 | F |
| 1.5637 | 30 | | | 1.564 | F |
| | | | | 1.557 | |
| 1.4968 | 8 | | | | |
| 1.3500 | 2 | | | | |
| 1.2961 | 4 | | | | |
| 1.1894 | 12 | | | | |
| 1.1590 | 5 | | | | |
| 1.0580 | 8 | | | | |
| 0.9977 | 8 | | | | |
| 0.9164 | 4 | | | | |
| 0.8764 | 12 | | | | |
| 0.8639 | 10 | | | | |
| 0.8196 | 8 | | | | |
| 0.7904 | 12 | | | | |
| 0.7814 | 14 | | | | |

Table 4.1. X-ray diffraction data for heated heavy mineral separate from the eastern contact ferroaugite pegmatites. Fersmite and pyrochlore d-spacings are designated by (F) and (P) respectively.

## 4.1.5 C III, Quartz Syenite

Ashburton Lookout area pyrochlores are relatively large (approximately 40µm, but can be upto 200µm) euhedral six sided prisms occurring as inclusions in interstial biotite and partially-included in potassium feldspar. They may or may not contain inclusions of K-feldspar and fluorite. Compositions are diverse due to recrystallization and alteration to fluorocarbonate and other unidentified niobates, as well as. Fig 4.7 illustrates recrystallization of hydrated pyrochlore,while Fig 4.8 and corresponding X-ray maps show compositional differences between core and altered rim.

Smaller subhedral-to-euhedral grains in Western Contact quartz syenites (C2040)(<20µm) are included albite, quartz, or K-feldspar. Rare euhedral apatite may be found as inclusions in the pyrochlore. Feldspars surrounding pyrochlores are commonly changed to alteration silicates. Stringers of a secondary niobium-titanium oxide phase permeates the alteration silicate mantles. The stringers are too fine for quantitative analysis but semi-quantitative analysis show the stringers have variable rare metal composition but exhibit no distinct enrichment or depletion in Nb, REE relative to the associated niobate grain. In the Guse Point quartz syenite large (150 µm) altered euhedral prisms appear to be composed of two pyrochlores of differing compostion, one "low" in Si, the other higher in Si.

## 4.1.6 Contaminated Ferro-edenite Syenite

Pyrochlore is found as small (<20µm) irregular inclusions in allanite or as subrounded grains included in plagioclase, alkali-feldspar, biotite and quartz. Surrounding feldspars are transformed to halos of calcite, hematite, and alteration silicate. As in the quartz syenite, Nb-REE-Ti oxides are found permeating alteration silicate and precipitating along biotite and K-feldspar

Fig 4.6. BSE micrograph of altered and recrystallized pyrochlore (p) from eastern contact pegmatites. It is compositionally heterogeneous and extensively replaced by unidentified alteration silicate (as), calcite, and nb-rutile (r). Associated minerals are metamict zircon (zr) and fluorocarbonate (fl)(sample C1C).

Fig 4.7. BSE micrograph of pyrochlore from a quartz syenite pegmatite, Centre III. The fracturing of grain (dark) is evidence for metamictization and hydration. Secondary niobate (bright) replaces the precursor around rim(sample * C2924).

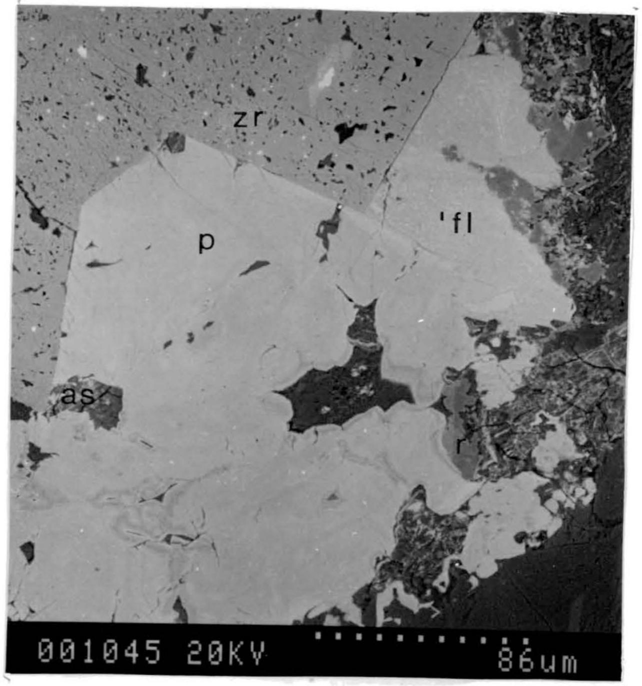
zr
p
'fl
as
r
001045 20KV
86um

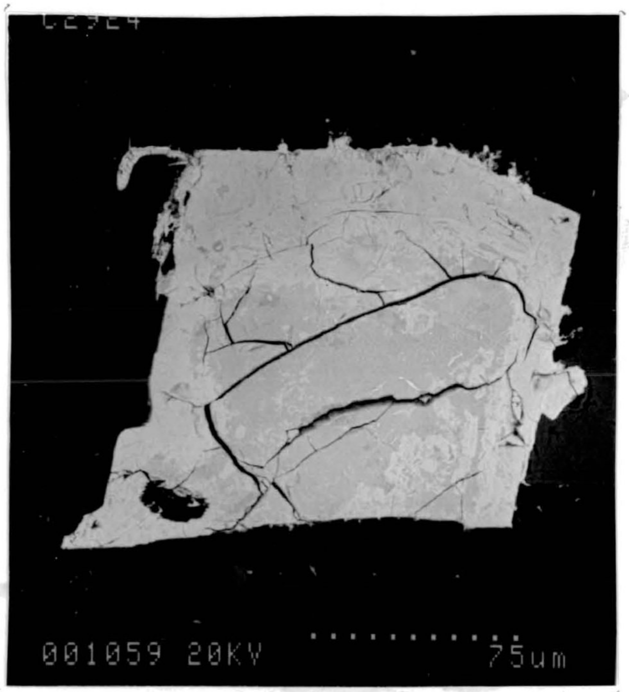
001059 20KV
75um

Fig 4.8. Backscattered micrograph and X-ray maps of a compositionally variable pyrochlore from the quartz syenite. Grain mantle is enriched in Si (3.64 wt % $SiO_2$), Nb(44.85 wt % $Nb_2O_5$), and Fe(3.17 wt % FeO) relative to the core.

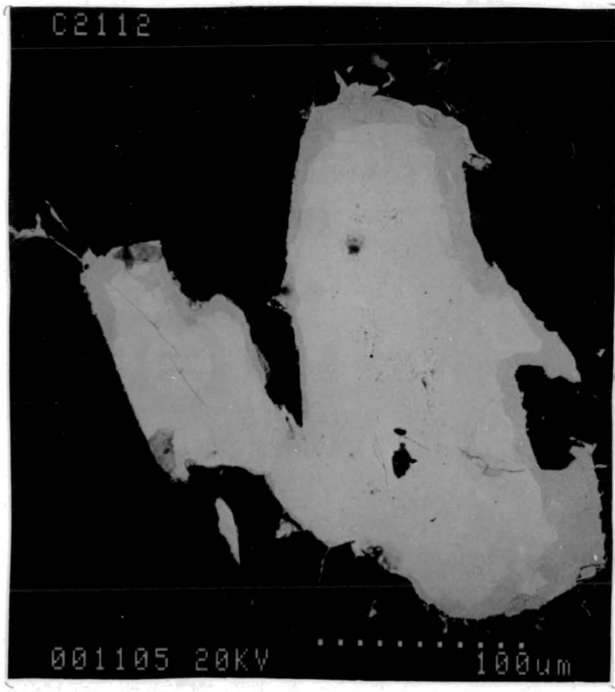
C2112
001105 20KV
100um

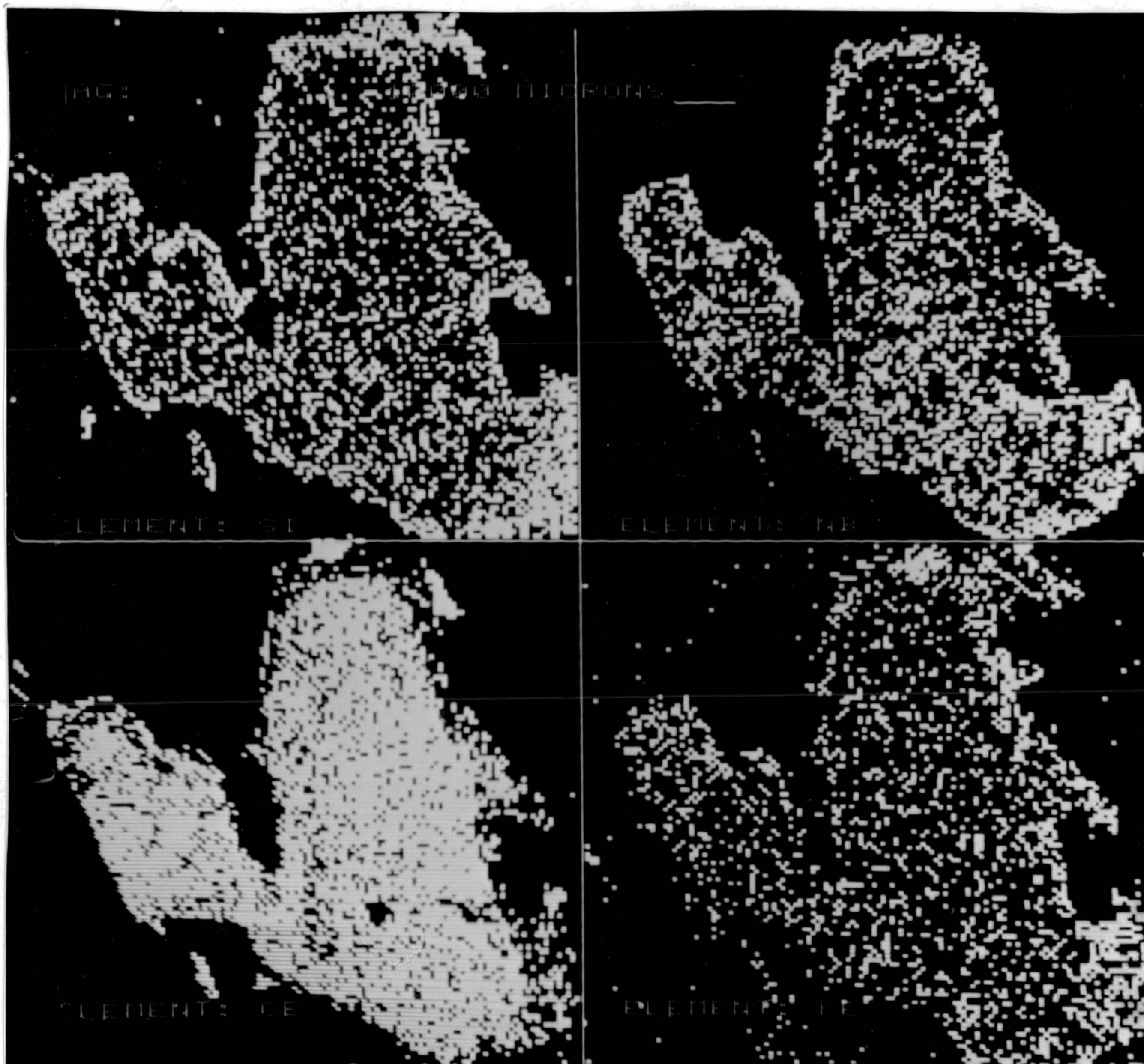
MICRONS
ELEMENT: SI
ELEMENT: NB
ELEMENT: CE

cleavage planes.

### 4.1.7 Ferro-edenite Syenite

Small (<20μm) subhedral-to-euhedral grains of hexagonal pyrochlore are found only in the western contact zone as inclusions in K-feldspar. Slight alteration around rims and along fractures to fluorocarbonate is common.

### 3.3 Compostion

Pyrochlore cannot be identified unambiguously on the basis of composition alone . Numerous complex niobates having the general formula $AB_2O_3$ or $(AB)_2O_4$ (eg. aeschynite - Nb, vigezzite, fersmite, and ashanite) have compositional overlaps with the diverse compositional range of pyrochlore. Additional complications result from the common metamictization of pyrochlore and other minerals. The complex replacement textures exhibited by the Coldwell niobates also make analysis and identification difficult. Two pieces of evidence support the pyrochlore identification: (1) pyrochlore from the ferro-augite pegmatites was identified by X-ray diffraction; (2)the compositionally similar complex niobates, unlike pyrochlore, are not known to incorporated significant amounts of Si. Thus, complex niobates containing Th,U, Ca, Ti, and REE are assumed to be pyrochlore and compared as one mineral. Representative compositions and EDS spectra are given in appendix 2.3 and Fig 4.9 respectively.

The characterstic extreme isomorphic substitution of the niobate is evident in the diversity in composition within one thin section, eg. section C1428 with CaO contents ranging from 8.37 to 23.72 wt %, Nb205 from 40.11 to 69.04 wt %, and Y203 from 0.53 to 8.89 wt%.

Most compositions exhibit low analytical totals (appendix 2.3) indicating the presence of undetermined elements, structural $H_2O$ and F,or possible

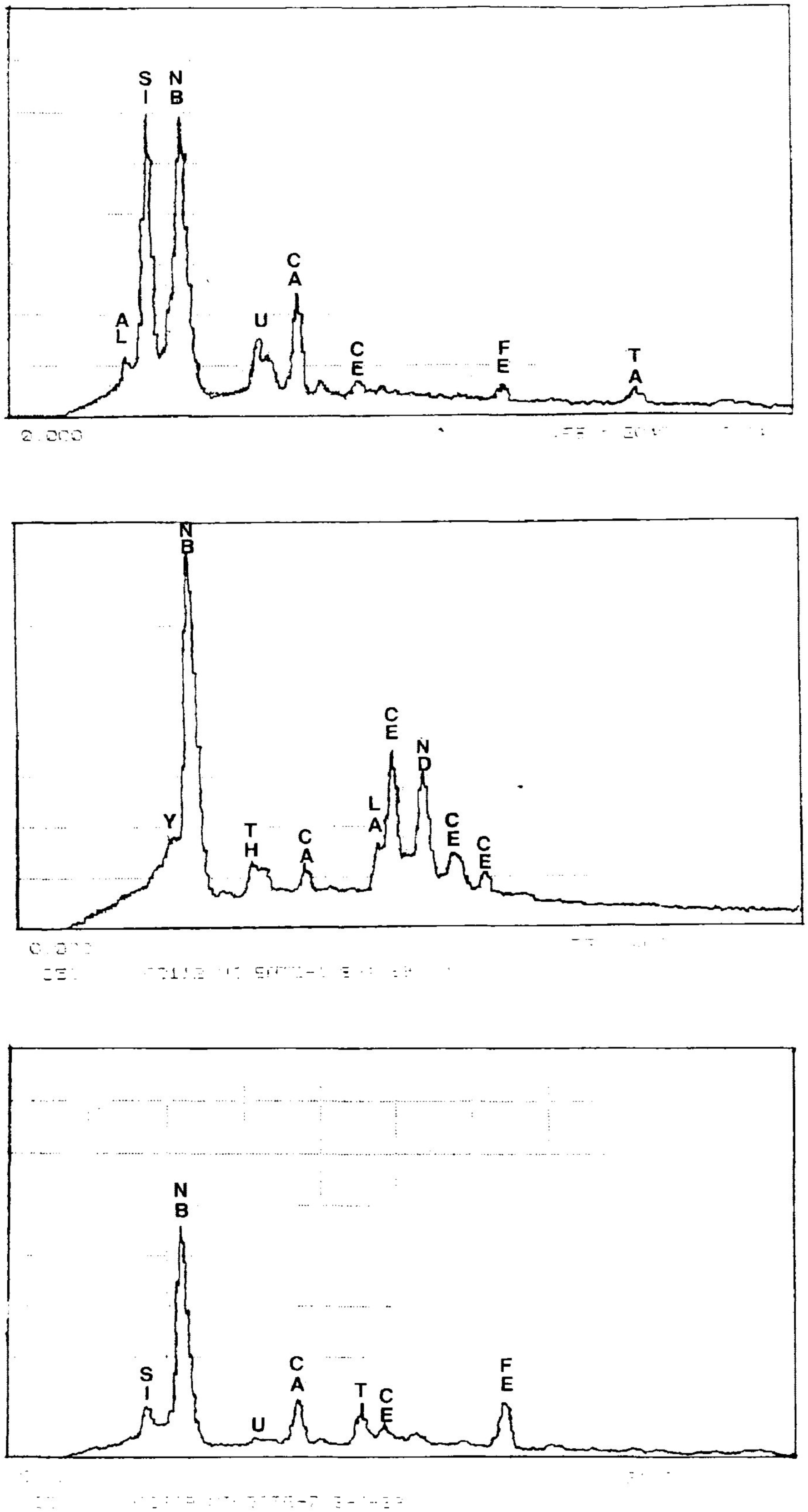


Fig 4.9 Representative spectra illustrate extreme compositional variation of the Coldwell niobates. Spectra 2 (from quartz syenite) and 3 (from Angler Creek ferroaugite syenite) are similar to pyrochlores described in the literature. Spectra 1 (from the quartz syenite) identity is uncertain due to its unusually high Si contents.

metamictization and hydration. Tremendous variation in the totals is apparent in the pyrochlore from different lithologies, the most notable examples being the niobates from the Angler Creek ferroaugite syenite with totals commonly above 95 wt %, and the fluorite-rich quartz syenite dyke C2925 having totals consistently below 94 wt %. Such differences may be related to the stage and conditions of formation. The Angler Creek pyrochlores are primary and are unaltered in appearance. In contrast, those from other units show extensive alteration and recrystallization. In such late-stage (deuteric) conditions, F and $H_2O$ activity is high and therefore, would be expected to be incorporated into the pyrochlore crystal structure.

The Coldwell pyrochlores are unusual in their high $SiO_2$ values, the majority of compositions range between 0.00-7.00 wt % $SiO_2$. Similar values are found in pyrochlores from other alkaline silicate rocks (Payette et al, 1988).However, many grains contain $SiO_2$ in excess of 12.00 wt %. In all grains with high Si content there is a positive correlation between high $SiO_2$ and $UO_2$ in pyrochlore. It is uncertain whether this represents Si and U in a true pyrochlore structure or the presence of a secondary phase.

Almost all pyrochlores can be classified into the pyrochlore subgroup based on Nb/Ta and Nb/Ti ratios. Differences in the B and A site occupation do occur between lithologic units. Pyrochlore from the quartz syenite dykes is the most compostionally distinct in the Coldwell complex. Although all pyrochlores are Nb-dominated minerals (Fig 4.1) the dyke pyrochlores show the greatest Nb-enrichment relative to Ta and Ti compared to pyrochlore from the other units. This is particularly true for dyke C1428 and C2925.Other distinquishing features included the highest $Y_2O_3$ CaO and $ThO_2$ content (Table 4.2). In contrast, the ferro-augite syenite pyrochlores have the lowest $RE_2O_3$, $Y_2O_3$ and $ThO_2$ contents. Those from the pegmatites have similar Nb-Ta-Ti

Table 4.2 Mean composition (wt %) of Pyrochlores from Coldwell Alkali Complex.

| Lithologic Units | Nb205 | Ta205 | Ti02 | RE203 | Y203* | CaO | FeO | U02 | Th02 |
|---|---|---|---|---|---|---|---|---|---|
| Ferroaugite pegmatite Centre I | 53.94 | 2.78 | 4.34 | 6.11 | 1.73 | 6.07 | 6.19 | 3.74 | 1.09 |
| Ferroaugite Syenite Centre I | 53.94 | 2.38 | 5.30 | 3.91 | 0.32 | 6.88 | 15.00 | 3.32 | 0.52 |
| Quartz Syenite Dykes Centre I | 50.45 | 1.13 | 3.39 | 8.42 | 3.86 | 9.56 | 4.59 | 2.8 | 1.58 |
| Craddock Cove Syenite Centre I | 43.41 | 3.113 | 6.84 | 5.40 | 1.91 | 5.45 | 10.10 | 4.13 | 1.22 |
| Ferro-edenite Syenite, Contaminated Ferro-edenite Syenite, and Quartz Syenite. Centre III | 44.61 | 1.84 | 3.7 | 3.70 | 3.07 | 4.81 | 2.19 | 3.03 | 4.54 |

RE203= Total weight % of La+Ce+Pr+Nd+Sm
* = semi - quantitative

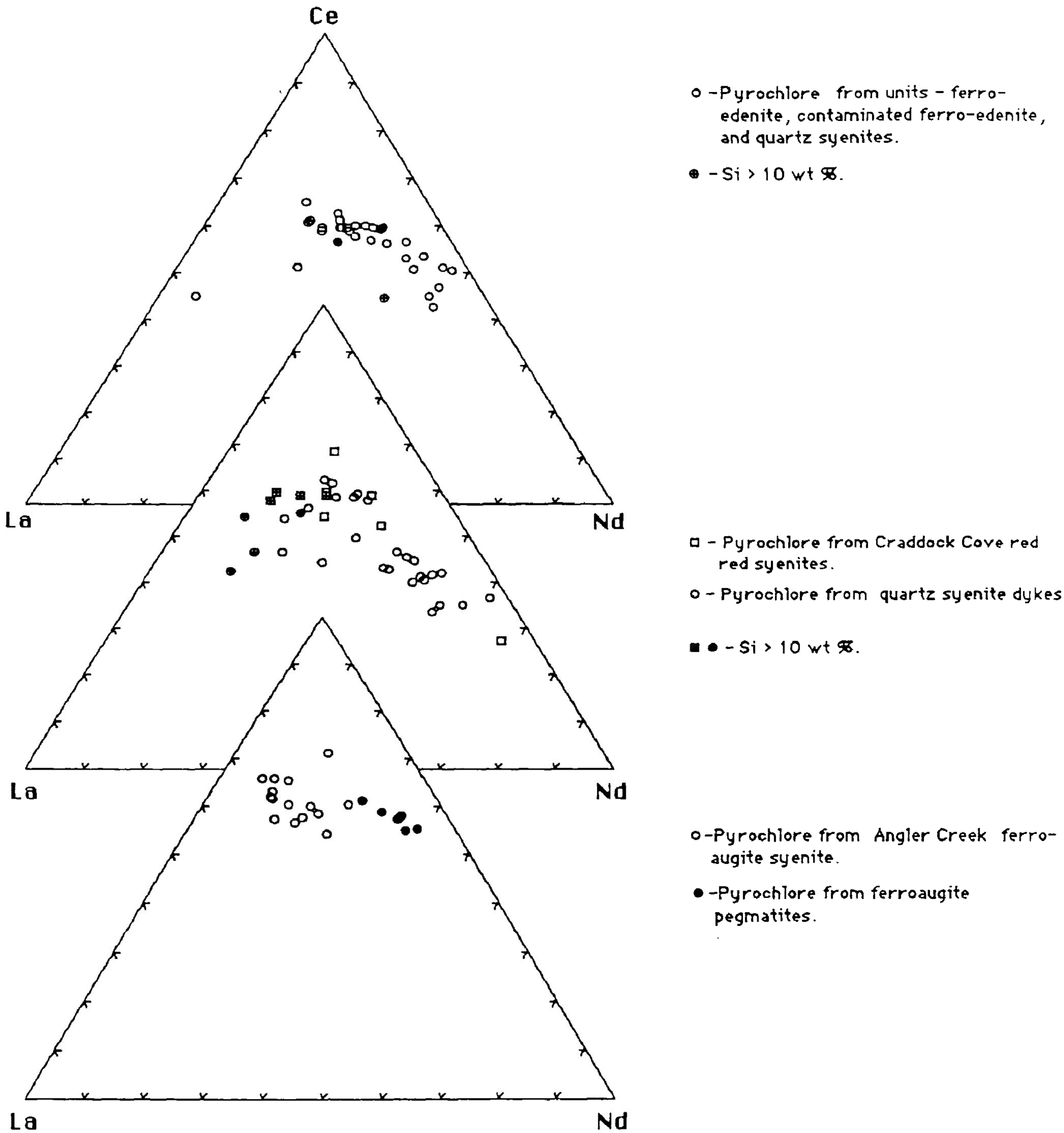


Fig 4.10. La-Ce-Nd composition of pyrochlores from the Coldwell complex. Variable compositions are found in each lithologic unit. Quartz syenite dykes and ferroaugite pegmatites are noticeably enriched in Nd.

content and contain more $ThO_2$ , $Y_2O_3$ and total $RE_2O_3$ than pyrochlores from the related ferroaugite syenite ( Angler Creek ferroaugite syenite). The Craddock Cove red syenites and Angler Creek ferro-augite syenite niobates all have unusually high FeO content, particularly those from section C1513. Pyrochlores in the Centre III units, the ferro-edenite, contaminated ferro-edenite and quartz syenites are similar in composition and have the highest $RE_2O_3$ and a high $ThO_2$ content relative to all other pyrochlore.

Fig 4.10 show Ce-La-Nd atomic ternary plots of pyrochlore composition from the quartz syenite dykes, Craddock Cove red syenites, and the Centre III rocks. Pyrochlore compositions used include only those containing Ce,La, and Nd. The niobates exhibit extreme variability in total rare earth abundances and in their relative proportions and therefore, only general compositional comparisons can be made between units. The dyke pyrochlores have the widest variation in proportions, dykes C2925 and C1428 are HREE-enriched while C1418 and C1432 are distinctly LREE selective. Similarly, the niobates from the Centre III units are variable but, on average, more LREE enriched. The trend in Nd-enrichment in pyrochlores from the ferroaugite pegmatite relative to those from Angler Creek is probably a reflection of differentiation.

## 4.4 Discussion

As a group the Nb- dominated Coldwell pyrochlores are typical of those found in carbonatites and alkali rocks in contrast to the Ta and Ti enriched members from granitic pegmatites (Foord, 1982). The Center III pyrochlores are similar to those of other alkali granites in their enrichment in REE, uranium, yttrium and depletion in Ca. Such pyrochlores are representative of a geochemically primitive paragenesis and are so far known only from non-pegmatitic environments.

The textural relationships and varying compositions imply at least 2 stages of formation. The compositions reflect their position in the paragenetic sequence and the conditions of the mineralizing environment , i.e. they are of primary origin or secondary replacements. It is postulated that pyrochlore with high Nb/Ta ratios and analytical totals , as well as low REE, U, Si contents have been generated directly from a melt. Examples include the euhedral unaltered Angler Creek pyrochlores ( C2905,C2908, and C2909). In contrast, secondary pyrochlore is characterized by increased REE, U, Si and low analytical totals, which may indicate the presence of $H_2O$ and/or F. Ta contents may also distinguish pyrochlore types. Voloshin (1983) advocated a increase in Ta and reduction of Nb/Ta with progressive alteration of Nb, Ta-bearing minerals. In this respect, high Ta contents in the Coldwell niobates may characterize pyrochlore precipitated from a late deuteric fluid. These compositional features would also be influenced by bulk composition of melt, and isolated pockets of deuteric fluid, together with the composition of the precursor mineral(s).

Some of the most common reactions among Nb, Ta- bearing minerals, in granitic pegmatites, involve breakdown of columbite-tantalite to pyrochlore group minerals. Each cation and/or anion active in the fluids may promote precipitation of a different replacement product from the simple precursor. Gross chemical differences in Nb, Ta minerals (primary) assemblages are probably a function of the geochemical features of the parent melts. However, on the small scale of late hydrothermal stages relatively slight variations in P, T-conditions can dramatically, shift the course of low-temperature metasomatism in the same pegmatite (Cerny and Ecrit, 1985). Similar conditions are evident in the Coldwell units, the pyrochlore compostions reflecting increase activity in Ta, Si, LREE in the last stages of mineralization.

The Centre III, the Craddock Cove syenite and quartz syenite dykes pyrochlores have wide ranging REE contents. Earlier subhedral-to-euhedral pyrochlore, crystallizing from (melt?), may represent the HREE-enriched compositions while the LREE-enriched compositions are a result of a later deuteric alteration stage. Evidence for this is the correlation of high Si with high La/Nd ratios for alteration rims around HREE-enriched cores.

Alterations of the pyrochlore group minerals are restricted to relatively F-rich or alkaline environments. The general nature of the replacement process is $AB_2O_6$(precursor) + [Na,Ce, Ca](F,OH) (Burt and London, 1982). In the quartz syenite dykes the proposed alterations are as follows:

$CaNb_2O_6 + CeF_3 \rightarrow$ pyrochlore
(fersmite)

$FeNb_2O_6 + CeF_3 + CaF_2 \rightarrow$ pyrochlore
(columbite)

The complexing of F is supported by the close relationship between pyrochlore and fluorite. The rare replacement of garnet by pyrochlore and calcite and pyrochlore inclusions in calcite suggests that $CO_3$ complexes may also influence the niobate composition.

## 5.0 Columbite

The species columbite belongs to the orthorhombic columbite - tantalite group that is defined by the end members ferrocolumbite ($FeNb_2O_6$), manganocolumbite ($MnNb_2O_6$), ferrotantalite ( $(Fe,Mn)(Ta,Nb)_2O_6$ ) and manganotantalite ($MnTa_2O_6$). Complete isomorphism exists between the end members, with the exception of a substitutional gap between the orthorhombic (Fe,Ta)- rich compositions in the ferrotantalite and the tetragonal tapiolite ($FeTa_2O_6$) fields. Columbite compositions in the $Nb_{2.0}$ to ($Nb_{1.90}$ $Ta_{0.10}$) and $Fe_{1.0}$ to ($Fe_{0.9}$ $Mn_{0.1}$) regions are also rare, but these are due to geochemical parameters, rather than restrictive crystal-chemical features (Cerny and Ercit, 1985).

Most columbite - tantalite specimens described in the literature are from relatively - evolved parental melts, i.e. granitic pegmatites, granites, and alkali granites. Such evolved magmas would evidently be enriched in Nb and Ta allowing for earlier and extended crystallization of Nb-Ta phases in the paragenetic sequence. Protracted crystallization of niobate phases produces the typical fractionation trends towards bulk enrichment in Ta and Mn and therefore the formation of the corresponding end members from the columbite - tantalite group. Few samples have been analysed from more primitive environments, such as syenites or alkali syenites, where bulk Nb-Ta contents should be lower, and thus Nb-Ta saturation and genesis of columbite would be late in the whole rock crystallization sequence. Little fractionation would result, and therefore Fe and Nb-enriched columbite should occur. This hypothesis is supported by the composition of the Coldwell columbites from the ferro-edenite and contaminated ferro-edenite syenite.

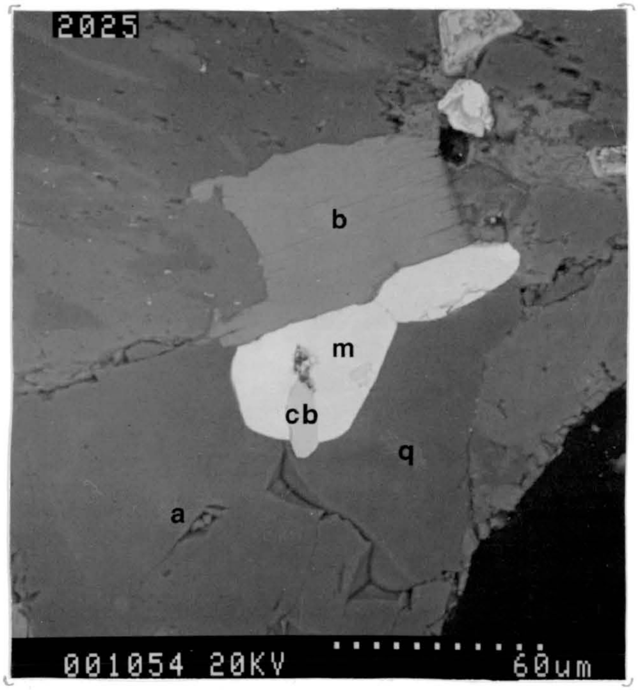


Fig 5.1. Backscattered micrograph showing columbite(cb) partially included in euhedral monazite (m) and quartz (q). Also shown is biotite (b), albite (a) and feldspar (f) (sample # C2025).

## 5.1 Textural Relationships

Ferrocolumbite has been identified in only 2 sections (C2025 and C2028) from the ferro-edenite and contaminated ferro-edenite syenite in the western contact zone. Both samples are from the vicinity of a large metasedimentary xenolith. Ferrocolumbite and manganocolumbite specimens from centre I are found in two quartz syenite dykes (C1432 and C2925) that border and cross-cut the Port Munroe metavolcanic xenolith.

### 5.1.1 Ferro-edenite Syenite

Anhedral-to-subhedral columbite occurs in small (<300μm) aggregates included in, or bordered by late interstitial quartz and albite. Associated aggregate minerals are ilmenite, magnetite, monazite, biotite and less - commonly bastnaesite and a Nb-Ti-REE phase, tentatively identified as pyrochlore. The columbite grains range between 10μm - 40μm in length and may occur as inclusions in the ilmenite, quartz or albite and are infrequently partially-included in monazite (Fig 5.1). Rare subhedral grains may occur as relatively large (<100μm) isolated inclusions in quartz and albite.

### 5.1.2 Contaminated Ferro-edenite Syenite

Small (<30μm) rounded grains of columbite occur as inclusions in interstitial quartz and as small intergrowths with a Nb-Ti-REE phase. Columbite along with flourocarbonate and ilmenite are inclusions in "finger print" textured allanite (see section 6.2).

### 5.1.3 Quartz Syenite Dykes

The largest (20µm-150µm) and most abundant columbite grains from the complex are found in the dykes C1432 and C2925. In sample C1432, interstitial to feldspar, a complex assemblage of rock-forming and accessory rare metal bearing minerals (zircon, quartz, biotite, allanite, fluorocarbonate, and pyrochlore) display intimate intergrowth and replacement textures (Fig 4.2). Subhedral columbite grains are altered to irregular mantles of pyrochlore and quartz and less commonly replaced by calcite, magnetite, and allanite. In C2925 rare small (<30µm) columbite inclusions in quartz and K-feldspar are consistently altered along rims to pyrochlore.

### 5.1.4 Eastern Contact Pegmatites

Columbites appear as micron-sized late-stage metasomatic products occupying interstial cavities between accicular Nb-rutile in the fluorocarbonate-rutile pseudomorphs (Fig 2.2 and 2.3).

### 5.2 Compositions

Representative compositions are given in appendix (2.4 ). The ferrocolumbites from Centre III are characterized by high Fe (16.33-17.78 wt % FeO) and Nb (71.48-74.69 wt % $Nb_2O_5$) contents and low Ti (0.92-3.32 wt % $TiO_2$) contents. Average structural formulas for columbites from the ferro-edenite and contaminated ferro-edenite syenites are $[(Fe_{0.81}, Mn_{0.19})(Nb_{1.88}\ Ta_{0.06})Ti_{0.07}\ O_6]$, and $[(Fe_{0.81}, Mn_{0.22})(Nb_{1.91}\ Ta_{0.06}\ Ti_{0.06})O_6]$ respectively. Columbites in the contaminated ferro-edenite syenite have slightly higher Nb/Ta+Nb and Mn/Fe+Mn ratios than those from the ferro-edenite syenite.

The distinctive Mn - rich columbites from the quartz syenite dykes C2925 and C1432 have average structural formulas ( $Mn_{0.85}$, $Fe_{0.11}$) ($Nb_{1.97}$, $Ti_{0.04}$, $Ta_{0.02}$ )$O_6$ and ($Fe_{0.64}$, $Mn_{0.32}$) ($Nb_{1.87}$, $Ti_{0.14}$, $Ta_{0.03}$)$O_6$. The former composition approaches the pure end member manganocolumbite, the latter being a Mn-rich ferrocolumbite. Due to the small size of the interstial columbite from the ferro-augite pegmatites only one compostion was obtained from a grain that was large enough to preclude the excitation of the surrounding Nb-rutile. It also is Mn enriched relative to the Centre III columbites.

## 5.4 Discussion

The compositions of the Centre III ferrocolumbites appear to be governed by both whole rock chemistry and their late crystallization in the paragenetic sequence. The high Nb/Ta ratios imply the absence of any significant degree of crystallization of previous Nb-Ta bearing phases that would result in the reduction of the Nb/Ta ratio. Although pyrochlore is present in sections C2028 and C2025, its precipitation is contemperanous with, or later than the columbites, and both minerals have similar Nb-Ta contents.

Columbites from the Plex and Huron Claim illustrate the common fractionational trend towards the Mn and Ta end members in granitic pegmatites (Fig 5.2) ( Cerny and Ercit, 1985). However, the Coldwell, and the Thor Lake north-T zone, columbites (de St. Jorre, 1986), both from alkali syenites, exhibit the same unfractionated compositions.

The quartz syenite dyke columbites are unusual in their low Nb/Ta ratios and high Mn content, in particular the manganocolumbite from dyke C2925. The former geochemical characteristic is also found in the associated pyrochlore compositions. The compositions cannot easily be explained by a simple crystal

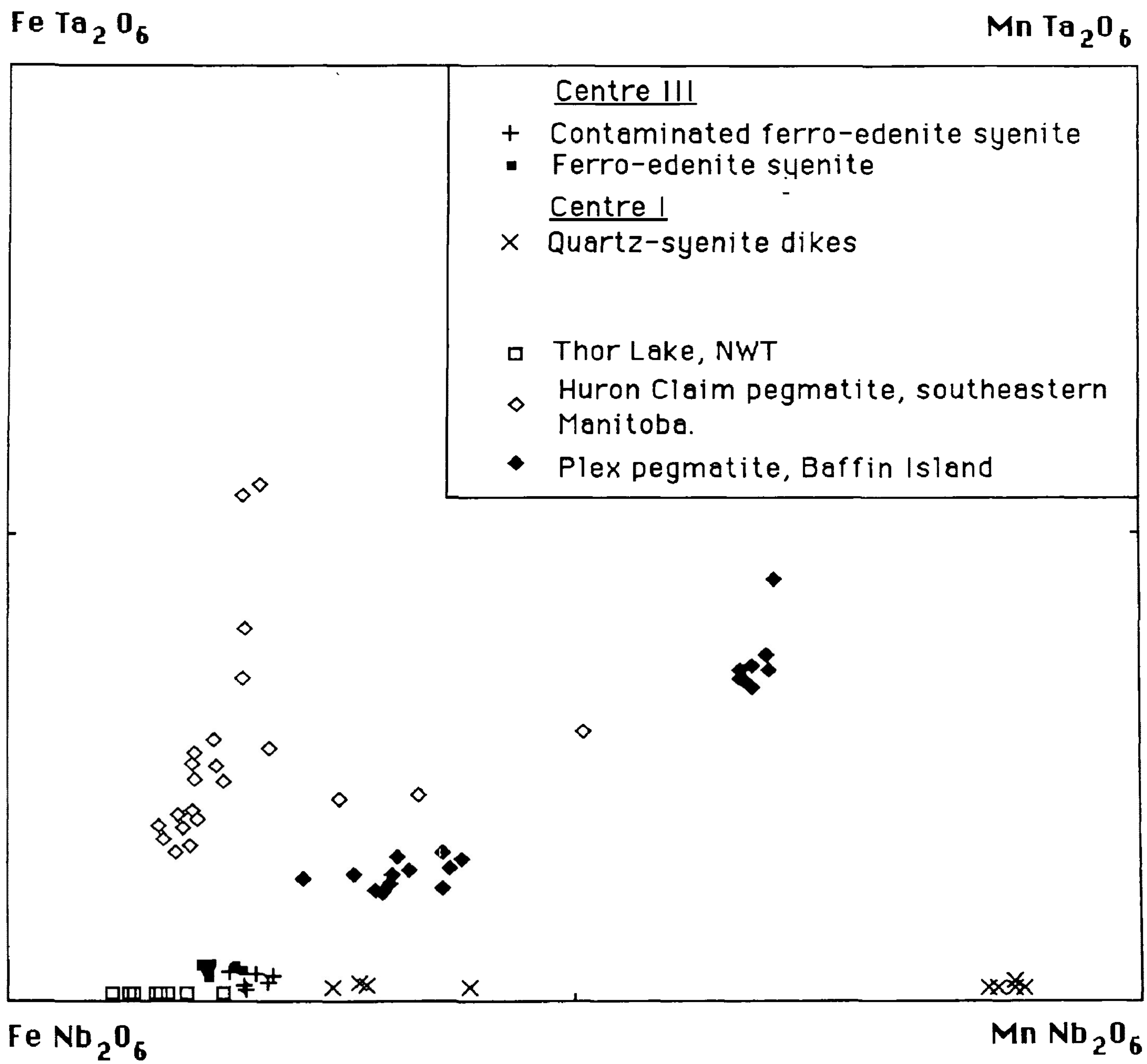


Fig 5.2. Columbite compositional fields showing representative compostions and fractionation trends from the Plex and Huron Claim granitic pegmatites (data from Cerny and Ercit, 1985). Columbites from The north-T zone of the Thor Lake alkaline complex (de St. Jorre, 1986) and Centre III exhibit little Ta and Mn enrichment. Those from the quartz syenite dykes range from Mn rich ferrocolumbite (C1432) to manganocolumbite (C2925).

- liquid fractionation processes. Studies of niobate compostions in granitic pegmatites imply that F-enrichment is conducive to late Nb/Ta fractionation, and may also be responsible for extreme Mn-enrichment (Cerny and Ecrit, 1985). In C2925, the relatively high abundance of fluorite indicates F-enrichment in the dyke. The low Ta abundances may be explained by Mn-enrichment preceding Nb/Ta fractionation, as seen in other mangnocolumbites (Foord, 1976), or by the bulk chemistry of the rock. The trace amounts of the mineral preclude it from contributing significant amounts of Mn to the rock and therefore, the high MnO content (1.01 wt %) of the whole rock composition must be a result of Mn content in other phases, such as the Fe-oxides.

## 6.0 Zirconolite

The $CaZrTi_2O_7$ compound is able to form the monoclinic, orthorhombic, and trigonal polytypes - polygmignite, zirkelite, and zirconolite. Cation substitution is common. REE, actinides and minor Na replace Ca, while Nb, Ta, and Fe are incorporated into the Ti site. In the Zr site minor amounts of Ti may substitute. Due to the similar compositions of the various species, structural information is essential for species identification. As is the case for the Coldwell minerals, this data is commonly absent due to metamictness or small grain size. Following the nomenclature suggested by Bayliss, (1989) for non - crystalline or undetermined polytypoids, the term "zirconolite" will be applied to the (Ca, REE) Zr $(Ti,Nb)_2$ $O_7$ from the Coldwell intrusions.

## 6.1 Textural Relationships

### 6.1.1 Contaminated Ferro-edenite Syenite and Quartz Syenite

Zirconolite is found in ferro-edenite and contaminated ferro-edenite syenite specimens sampled near a large metasedimentary xenolith in the western contact zone (C2025, C2028). The small (<10μm) subhedral to euhedral grains occur as extremely rare laths in the large perthite prisms.

### 6.1.2 Ferroaugite Syenite

Zirconolite has been identified in all sections studied from the southeastern ferroaugite syenite (C35-C68). In the lower series (C35 and C39) of the intrusion, the mineral occurs as small (<30μm) anhedral grains bordering ilmenite and mafic minerals and as relatively large (50μm-70μm in length) acicular inclusions or partial inclusions within the exsolved feldspar mantles

(Fig 6.1). Backscatter images of the largest grains may appear mottled or patchy . Zirconolite and baddelyite are closely associated in the more evolved series of the syenite, occuring as interlocking grains, and rarely with baddelyite rimming and replacing zirconolite. In the most evolved sample (C68), large (<100μm) acicular and opaque crystals are present as partial inclusions in amphibole, magnetite, and ilmenite.

## 6.2 Compositional Variation.

Representive compositions are given in appendix 2.5.

Zirconolites from both centres contain significant amounts of Nb,Th, U, and LREE and MREE and exhibit low total oxide weight percentages. In the southeastern ferroaugite syenite, totals range between 77.97 - 95.60 wt %, and between 82.85 - 90.38 wt % for those zirconolites from the contaminated ferro-edenite syenite. Low totals are probably due to the combination of hydration, the presence of undetectable F, and unanalysed elements,in particular Y, Sm and Gd.

Considering the metamict nature and changing conditions of formation for the zirconolites from the different series of the ferroaugite syenites, the similarity of the compositions is remarkable. Most major oxide abundances vary little between the lower series cumulates and the more peralkaline, Fe-rich upper series. However, niobium increases slightly from the base of the intrusion upwards as reflected in the average $Nb_2O_5$ wt % for C35 (8.22 wt %) and C70 (13.27 wt %).

Similar U, Th, Nb and REE enriched zirconolite in a peralkaline granite from the Chilwa Alkaline Complex have been described by Platt et al, (1987).

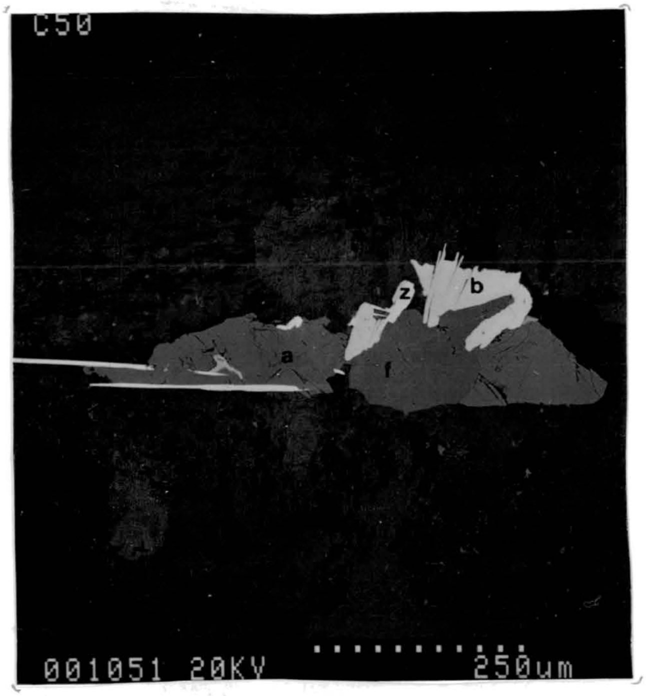


Fig 6.1. Zirconolite (z) from the southeastern ferroaugite syenite are characterized by high abundances in REE and Nb. Mineral clusters, interstitial to feldspars, include zirconolite and associated minerals- acicular baddelyite (b), fluorite (f), and amphibole (a) (sample # C50).

## 7.0 Allanite

Allanite is a monoclinic member of the epidote group with the general formula $A_2M_3Si_3O_{12}(OH)$ where the A site is filled by $Ca^{2+}$, which in allanite, is substituted for by $REE^{3+}$, $Th^{4+}$, $Sr^{2+}$, and possibly $Mn^{2+}$. The M(3) and M(1) sites are occupied by $Al^{3+}$, $Fe^{3+}$,$Fe^{2+}$, $Mn^{3+}$, $Ti^{4+}$, and $Mg^{2+}$, the M(2) is filled by $Al^{3+}$. It appears that allanite and epidote form a complete solid solution series with charge balance maintained by the coupled substitution:

$$Ca^{2+} + Fe^{3+} = REE^{3+} + Fe^{2+}$$

Allanite is one of the most common REE-bearing minerals in silicic igneous rocks and is found mainly in more evolved granodiorites and granites. Allanites form during primary crystallization, and in hydrothermal/metasomatic environments.

### 7.1 Textural Relationships

Allanite has been identified, with the exception of the ferroaugite pegmatites, in all lithologic units studied. It is ubiquitous in the contaminated ferro-edenite syenite, Craddock Cove red syenites and the quartz syenite dykes.

#### 7.1.1 Contaminated Ferro-edenite Syenite

Replacement allanite occurs as a major constituent in large (<0.5 mm) aggregates of amphibole, biotite laths, subhedral ilmenite, magnetite, and small amounts of pyrite, quartz and iddingsite-bowlingite alteration (?). The assemblage appears to be a product of a complicated sequence of multiphase absorbtion, recrystallization, and alteration, giving the aggregate a "xenoblastic"-like appearance. SEM backscatter images of allanite exhibit complex and intricate cuspate bright/dark lineations that produce a "finger print " pattern (Fig 7.1 and 7.2 ). The domains are defined by high and low REE contents and possibly variations in hydration. Inclusions of ilmenite, magnetite and more rarely fluorocarbonates and columbite are found in the allanite. Contaminated ferro-edenite syenite (C2229) from Pic Island contains allanite, biotite, quartz and iddingsite - bowlingite (?) replacing xenolithic material.

In section C2176 isolated biotite laths and biotite in ovoids contain fine grained allanite along cleavage planes and grain boundaries. Other minerals replacing biotite along the cleavage are magnetite and an unidentifed Nb-REE-bearing phase.

### 7.1.2 Ferro-edenite Syenite

One sample from the western contact, on the border between the ferro-edenite and contaminated ferro-edenite syenites, has allanite replacing a xenolith and exhibits similar textures to those in the contaminted ferro-edenite syenite.

### 7.1.3 Magnesio-hornblende Syenite

Rare anhedral-to-subhedral primary grains of allanite range from 10μm to <300 μm form inclusion or partial inclusions in K-feldspar and plagioclase. In transmitted light grains are strongly pleochroic, brown to reddish brown with the larger grains showing distinct zoning as well as patchy pleochroism due to recrystallization. Correlation of optical properties with composition indicates that "hydrous" domains and zones are darker than "non-hydrous" areas. Chlorite replaces allanite along rims.

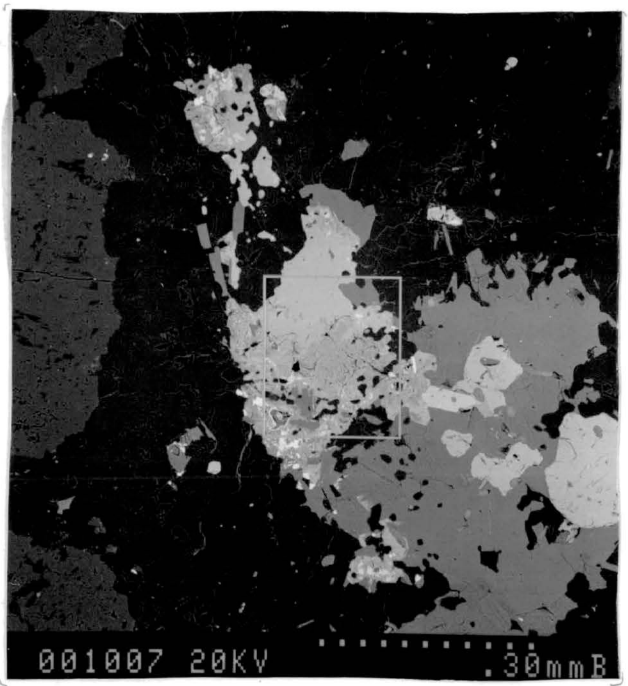


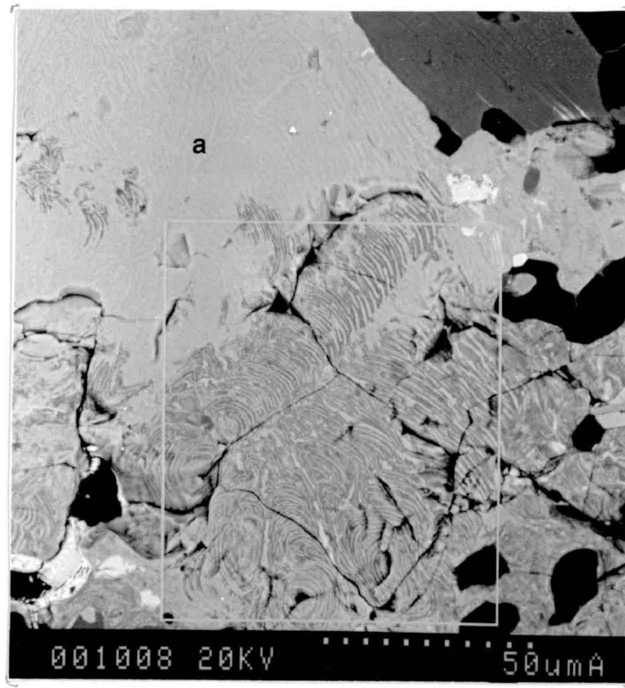


Fig 7.1 and 7.2. Backscatter micrograph (Centre III, contaminated ferro-edenite syenite, western contact zone). Allanite (a) in aggregate of magnetite, ilmenite and recrystallized amphibole interstial to perthite. Alteration of finger print textured allanite. Note continuation of texture in the relatively homogeneous grain (sample # C2028).

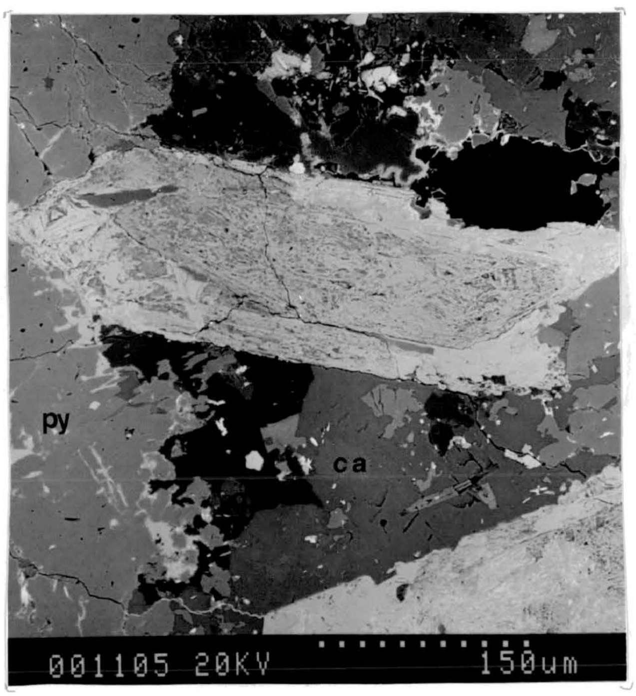


Fig 7.3. Backscatter micrograph of hydrated allanite in assemblage of quartz (q), calcite (ca) and pyroxene (py). Recrystallized allanite occurs as bright domains partially rimming grain ( sample # C2925).

### 7.1.4 Craddock Cove Syenite

Allanite, the dominant REE bearing mineral, is found mainly in the central to eastern rocks (C1522, C1524, C1527, C1528, C2920, C2904) replacing amphibole together with quartz, K-feldspar, ilmenite, magnetite, and biotite and more rarely calcite, chevkinite and fluorocarbonate. Rarely large subhedral allanite grains may be included in amphibole.

### 7.1.5 Quartz Syenite Dykes

The abundance and morphology of allanite grains vary between dykes, although certain textural and mineral relationships are common to all. In dykes C1418,C1428, and C1432 clusters of irregular small (< 20μm) allanite, epidote quartz, and zircon are interstial to and partially replace albite and alkali-feldspar. Individual phases are not resolvable optically and the aggregates appear light brown and turbid to opaque. SEM imaging reveals these to be mainly fine grained aggregates of quartz and epidote with allanite forming partial-to-complete irregular overgrowths around epidote. Rarely the epidote and allanite are bordered or encompassed by pyrochlore.

Two separate allanite parageneses are seen in dyke C2925. Abundant brown-to-reddish brown allanite is mainly found associated with the albite-calcite -quartz-garnet assemblage. Here it occurs as rarely twinned, large (<2 mm) columnar aggregates or isolated prisms in carbonate and quartz. Recrystallization around rims is indicated by a darker hue and stronger pleochroism. SEM micrographs and semi-quantitative analysis show the mineral to be compositionally heterogeneous as a consequence of partial recrystallization of the metamict and hydrated silicate (Fig 7.3 ).

Mottled allanite also occurs as large subhedral grains associated with the albite and alkali-feldspar assemblage and fills rare thin (.05mm) fractures in

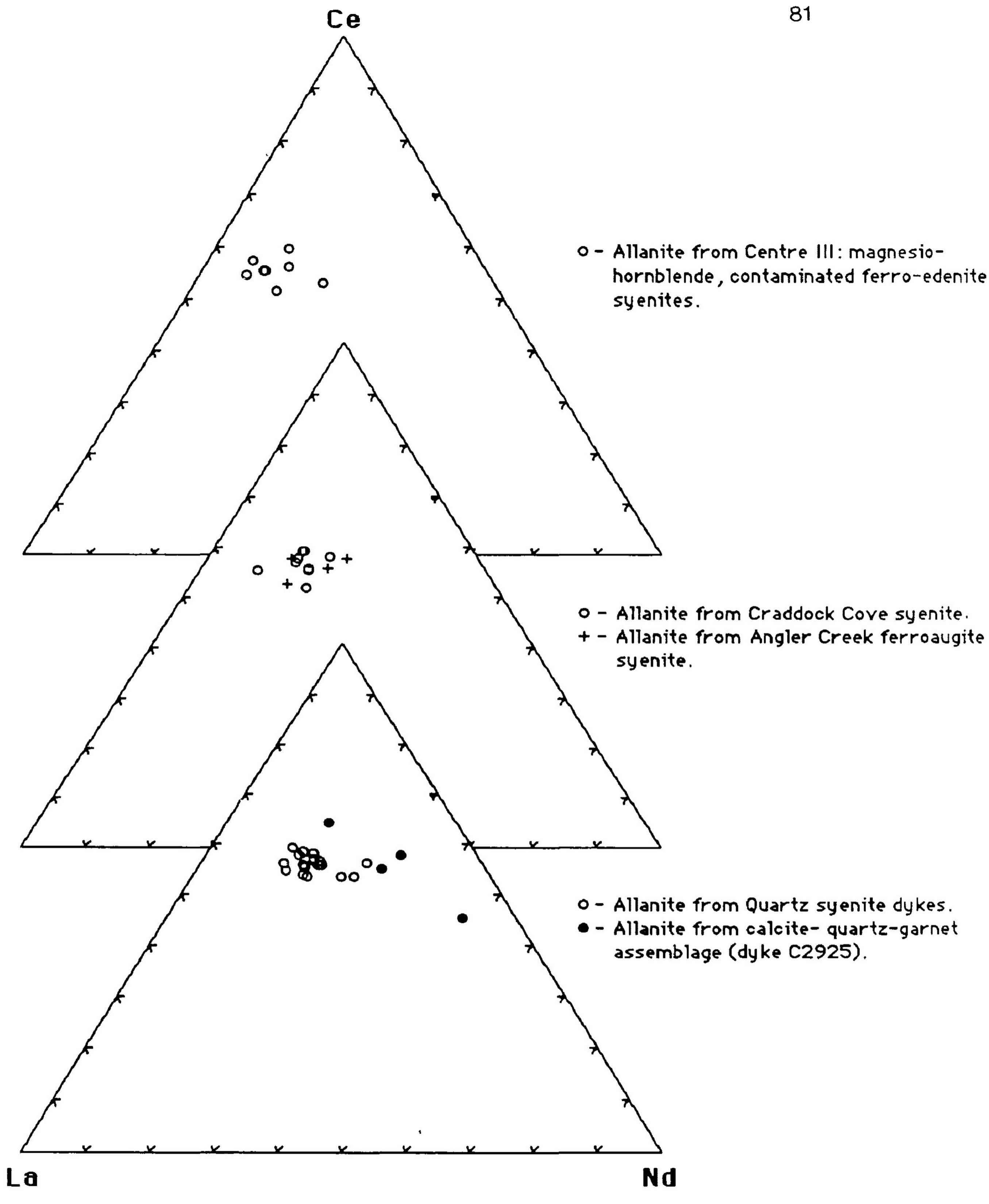


Fig 7.4 Ce-La-Nd ternary diagrams illustrate slight Nd enrichment in Centre I allanites relative to Centre III. The euhedral allanites from the calcite-quartz-garnet assemblages (dyke C2925) are compositionally distinct from other quartz syenite dyke allanites.

the dyke. The small veins suggest the presence and movement of deuteric fluid after the crystallization of the dyke.

## 7.2 Compositional Variation

Representative compostions are given in appendix 2.6. Allanites from plutonic environments show a wide range of compositions, principally because of hydration, alteration, recrystallization, and metamictization. Thus the compositions of allanite may not be representative of the original compositions. Average mean compositions (oxide weight %) of allanite from the lithologic units studied are given in Table 7.1. To minimize the effects of compositional irregularities resulting from hydration and leaching, only allanite with greater than 92.00 wt % oxide have been used in the calculation of the average compositions.

Compositional differences exist between allanites from Centre III and Centre I syenites. The former have significantly higher $Al_2O_3$ (11.81 wt %) and lower FeO and La/Nd ratio relative to those from the ferro-augite and the Craddock Cove red syenites. Allanites in the dykes C1418, C1428, C1432 are distinct from all other allanites in their high CaO and low La/Nd, a feature also characteristic of the pyrochlores (section 4.3). C2925 allanites are on average compositionally-similar to allanite in the other dykes. However, allanites from the calcite-quartz-garnet assemblage are HREE (1.58-4.14 wt% $La_2O_3$ and 3.44-8.7 wt % $Nd_2O_3$) enriched with respect to fracture filling allanites and those found in the plagioclase and alkali-feldspar assemblage (5.87-7.1 wt % $La_2O_3$, 2.55-3.16 wt% $Nd_2O_3$).

REE distribution patterns, as reflected in La-Ce-Nd proportions, are illustrated in Fig 7.4. Allanites from the Craddock Cove and Angler Creek ferroaugite syenites are Nd-enriched relative to the Centre III minerals and in

Table 7.1 Mean Composition (wt %) of Allanites from Coldwell Complex.

| Lithology | SiO2 | TiO2 | Al2O3 | MnO | FeO | CaO | La2O3 | Nd2O3 | RE2O3 |
|---|---|---|---|---|---|---|---|---|---|
| Ferro-augite Syenite *4 | 30.24 | 3.74 | 6.08 | 0.24 | 23.72 | 9.63 | 5.97 | 4.05 | 24.08 |
| Craddock Cover *7 Red Syenite | 30.07 | 2.93 | 6.65 | 0.5 | 22.33 | 9.22 | 6.08 | 3.43 | 21.49 |
| Centre III Syenites *8 | 32.38 | 1.91 | 11.81 | 0.62 | 17.47 | 10.34 | 6.63 | 2.28 | 21.94 |
| Quartz Syenite Dykes *19 | 30.34 | 1.20 | 9.56 | 0.83 | 20.94 | 10.78 | 5.45 | 3.21 | 21.26 |

REE2O3= La+Ce+Pr+Nd+Sm
* number of compositions

Table 7.2 Allanite Analyses

| | Toba Tuff | Skye granite igneous | Skye granite hydrothermal | St. Kilda | Golden Horn |
|---|---|---|---|---|---|
| SiO2 | 31.40 | 30.12 | 33.32 | 31.30 | 30.46 |
| TiO2 | 0.78 | 2.74 | 0.88 | 1.27 | 4.17 |
| Al2O3 | 13.70 | 9.55 | 14.56 | 13.29 | 5.89 |
| Fe2O3 | 2.81 | 4.77 | 7.49 | n.a. | --- |
| FeO | 13.57 | 14.76 | 9.94 | 16.64 | 22.49 |
| MnO | 0.67 | n.d. | n.d. | n.a. | 0.37 |
| MgO | 0.41 | 0.31 | 0.50 | 0.35 | n.a. |
| CaO | 9.13 | 9.05 | 13.04 | 11.21 | 9.32 |
| Y2O3 | 0.43 | 0.32 | 0.31 | 0.23 | --- |
| La2O3 | 4.80 | 7.86 | 5.97 | 6.05 | 6.51 |
| Ce2O3 | 10.81 | 13.73 | 10.58 | 11.24 | 12.89 |
| Pr2O3 | 1.21 | 1.05 | 0.66 | n.a. | 1.01 |
| Nd2O3 | 4.51 | 2.84 | 2.53 | 3.10 | 3.36 |
| Sm2O3 | 0.80 | 0.17 | 0.33 | 0.43 | 0.07 |
| ThO2 | 2.17 | 1.04 | 0.08 | 0.20 | 1.08 |
| | 97.28 | 98.41 | 100.46 | 95.31 | 97.62 |

Toba Tuff- Chesner et al, 1989
Skye Granite- Exley, 1980
St. Kilda- Harding, 1982
Golden Horn- Boggs, 1984

turn those from the quartz syenites show the greatest enrichment. The large euhedral allanite from the C2925 calcite-quartz-garnet assemblage is unusually enriched in HREE relative to compositions from other units.

The Coldwell allanites comprise accessory igneous allanite, as represented by Centre III allanites, and hydrothermal/metasomatic allanites, as represented by the allanites from the Craddock Cove syenites. The accessory igneous allanites are similar to those found in other granitoid intrusions; e.g. the Skye granites (Exley, 1980), St. Kilda granites (Harding et al, 1982) and silicic volcanic flows and tuffs; e.g. from the Toba Tuffs (Chesner et al, 1989) (Table 7.2). However, the postulated hydrothermal/metasomatic allanites and those from the quartz syenite dykes are uncommonly high in $FeO_T$ and low in $Al_2O_3$ relative to the hydrothermal allanites from Skye, in addition to most other allanites. This is probably due to the peralkaline nature of the Centre I rocks as these compositions closely match those of allanites from the peralkaline granite of the Golden Horn batholith (Boggs,1984)

## 8.0 Thorite

Thorite occurs in nature as a mineral in pegmatites (Frondel, 1958), granites (Rimsaite, 1981; Littlejohn, 1981) and as veins or dykes associated with alkalic rocks or carbonatites (Staatz, 1974). Common mineral assemblages include monazite, zircon, allanite, and various niobate - tantalites, such as fergusonite, and betafite. The ideal endmember of thorite is ThSiO4, but most compositions depart widely from this composition due to solid solution and secondary alteration. Th substitution involves the incorporation of U, REE, Ca, Fe, and minor amounts of Mn and Al, while replacement of $(SiO_4)$ by $(OH_4)$ can be expressed in the formula $Th(SiO_4)_{1-x}(OH)_{4x}$. This hydrous isostructural mineral, thorogummite, occurs as a fine grained alteration product of thorite, and other thorium bearing minerals such as thorianite, and yttrialite. Identification between thorogummite and metamict hydrated thorite may be difficult due to their compositional similarity. However, textural relationships and the cation proportions (Si $\approx$ 1.00) imply that the Coldwell Th-silicate is thorite.

### 8.1 Textural Relationships

With the exception of the southeastern ferroaugite syenite, small (<5 µm) thorite inclusions within zircon euhedra occur in virtually all studied Coldwell lithologies. The abundance varies with the host. The more evolved units, such as the Centre III units, Craddock Cove syenite, and quartz syenite dykes, contain thorite as a common accessory phase. Specks and fragments cluster in metamict zones or patches in the zircon and are interpreted to be coeval with the metamict zone. In rare samples, anhedral thorite inclusions may exceed 120 µm in size. These sections are also characterized by thorite occurring as large discrete grains or as aggregates with zircon. Mineralogical and textural relationships are similar to those found in radioactive granites, where inclusions of uraninite, uranothorite, apatite and galena are associated with zircon growth zones (Rimsaite, 1981).

8.1.1 C III, Quartz Syenite and Magnesio-hornblende Syenite

In magnesio-hornblende samples from Ashburton Lookout area (C2150, C2123) thorite, in addition to inclusions in zircon, occurs as separate rare small (15μm-50μm) subhedra included in K-feldspar and more commonly as a grains in thorite-zircon clusters. In the quartz syenite, extremely rare isolated thorite grains are included in perthite prisms or albite.

8.1.2 C I, Quartz Syenite Dykes

Dykes C1428 and C1432 both have trace amounts of thorite as small discrete anhedral to subhedral inclusions in albite, quartz, and more rarely in K-feldspar. Dyke C2925 contains the highest concentrations of thorite in the Coldwell complex. It typically occurs as large inclusions (>120μm) in metamict zircon, as coarse (0.25 mm) intergrowths with zircon or as discrete grains (Fig 8.1). Both minerals are reddish brown, turbid to opaque, thus it is impossible to distinguish one from the other in transmitted light. The isotropic nature of the phases and the radial fracturing of surrounding pyroxenes indicate severe metamictization. Coarse grained thorite-zircon mineralization is undoubtedly related to pyroxene crystallization as all intergrowths are interstial, partly included or included in the outer margins of the pyroxene. The abundance of thorite and the absence of other minerals with thorium or uranium as major constituents makes it the main contributor to the dyke radioactivity.

## 8.2 Composition

Quantitative analyses were obtained from the largest of the thorite and uranothorite grains from the magnesio-hornblende syenite and quartz syenite dyke C2925. Both units have thorite with concentrations of $REE_2O_3$, e. g. 8.75 wt% and 10.31 wt % for the magnesio-hornblende syenite and dyke respectively. In addition compositions from C2925 are significantly enriched in the HREE as evidenced by La/Nd $<1$ and $Y_2O_3$. The uranothorite variety occurs in the magnesio-hornblende syenite, with uranium ranging 10.23- 29.54 wt % $UO_2$. Compared to the Centre III syenite, the dyke thorite is depleted in U (0.00-6.57 wt % $UO_2$).

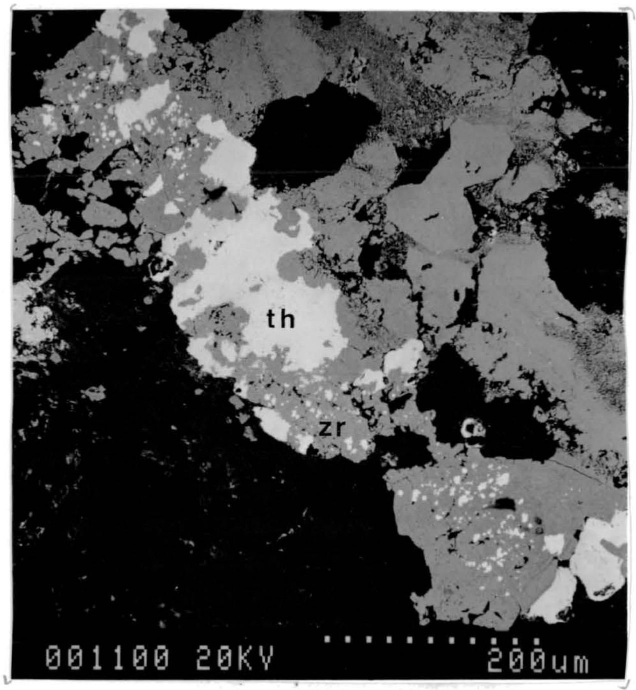


Fig 8.1 BSE micrograph of thorite (th) and zircon (zr) intergrowths in quartz syenite dyke C2925. They are associated with pyroxene crystallization and occur as inclusions within the silicate. The α-particle emission from the thorite has metamictized and hydrated both minerals resulting in the shattering of the enclosing pyroxene.

## 9.0 Zircons

Zircon ($ZrSiO_4$) is a ubiquitous mineral in the Coldwell complex being identified in all lithologies studied. Certain characteristics of the zircons are present in all units, such as its late-stage of formation and association with other rare-metal bearing minerals. Metamict zoning and replacement textures, are unique to certain lithologies. Descriptions of distinct textural and mineral relationships are given below.

### 9.1 Textural Relationships

#### 9.1.1 C I, Eastern Contact Pegmatites

Two different zircon types were extracted from a heavy mineral concentrate from the eastern contact pegmatites. Both have similar crystal habits, being short prisms with pyramidal terminations, but exhibit different optical characteristics. One type is a yellow, vitreous and transparent crystalline zircon, the other a grey, waxy and translucent to opaque metamict variety.

In thin section, zircons range in size between 20 µm - 2.0 mm and are typically situated in perthite interstices or as euhedral-to-subhedral inclusions in amphibole. Metamict zircon is distinguished from the crystalline variety by isotropism or its low first order grey and yellow interference colours. In contast, crystalline or partially-metamict minerals exhibit zoning defined by variations between $3^{rd}$ and $4^{th}$ order interference colours. Backscatter images show the zoning as alternating bands of metamict and "fresh" zircon. The apparent width of the zones seldom exceeds 5µm. Similar zonal features, described by de St. Jorre (1986) from Thor Lake, exhibit birefringent zoning attributed to substantial variations in abundance and relative proportions of the minor and trace elements of Ca, Fe, REE, and $H_2O$. Although optical properties are, in part, governed by composition (Deer et al, 1982), it is postulated that the Coldwell zircon birefringent zoning is a function of the geometry and number of metamict zones. For example, a 30 μm thick non-metamict zircon in polarized light will exhibit interference colours of the 4th order, however light transmitted through alternating metamict and fresh planes will. in effect, be influenced by a crystalline thickness less than 30μm, thus reducing birefingence. Depending on the number and thickness of metamict zones and their orientation, interference colours will be of a 3rd order or lower.

### 9.1.2 Craddock Cove Syenite

Three zircon types have been identified from various locations in the Craddock Cove syenite: euhedral prisms, overgrowths mantling cores of zircon and baddeleyite, anhedral replacement phase.

The most common zircons are colourless, euhedral to subhedral prisms which are found through out the syenite. In western samples (C1513, C1515, C1516, C2920), those situated adjacent to the Redsucker Cove breccia zone, both primary euhedral zircons and overgrowths are present. Overgrowths surround small (<40 μm) euhedral zircon cores in quartz interstitial to perthite grains. Cores and overgrowths are compositionally identical and are defined by a thin (<2μm) layer of quartz rimming the euhedral cores. Rarely zircon forms overgrowths around corroded acicular grains of baddeleyite. In the most westerly sections (C1513 and C1515) stringers of zircon are associated with fluorocarbonate, Nb-rutile (?), quartz, K-feldspar and rarely calcite as a replacement phase for amphibole.

### 9.1.3 C I, Quartz Syenite Dykes

Zircons have variable abundance and form in each dyke studied, however, in all cases the zircon is related and contemporaneous to the other rare metal bearing minerals. In C1418 and C1428, zircon occurs as stringers interstitial to albite or as an anhedral constituent of the complicated calcite, quartz, allanite, niobate assemblages. In dyke C2925 zircons are distinctive in their abundance, size (<1.0 mm) and intergrowths with thorite. This close association with thorite and its emission of $\alpha$-particle has inevitably metamictized the adjoining zircon giving the mineral a mottled and pocked appearance when viewing by BSE microscopy. In transmitted light the grains appear opaque. They are inevitably metamict and occur as subhedral to anhedral fractured grains (Fig 8.1).

### 9.1.4 C III, Magnesio-hornblende Syenite

Zircon is a rare constituent of the magnesio-hornblende syenite. It is a small (<100µm) late forming mineral located at the interstices of feldspar or amphibole. Without exception, they are either completely isotropic or exhibit patchy birefringence. SEM imaging reveals a close association of zircon and thorite with the two minerals forming clusters or thorite included within the zircon. In the biotite oviods zircon fills interstices between biotite laths.

### 9.1.5 C III, Contaminated Ferro-edenite and Ferro-edenite Syenites

The abundance, mineral relationships, and morphological characteristics are similar for zircons from the contaminated ferro-edenite and ferro-edenite syenites. In both units, zircons are subhedral to euhedral prisms averaging 150 µm in size. Metamict zoning is commonly present (Fig 9.1), but the majority of grains have metamict domains surrounding thorite.

### 9.1.6 C III, Quartz Syenite

The greatest abundance of zircon in Centre III is found in the quartz syenite. As occurs in other units, zircon is a relatively late forming subhedral to euhedral inclusion in biotite, quartz, fluorite, amphibole and rarely chevkinite. They are distinguished from other zircons in other Centre III units in their by abundance, large size (upto 2.0 mm) and the development of their metamict-birefringent zonation (Fig 9.2).

## 9.2 Composition

The oscillatory zones and metamict patches are the most distinctive feature found in the Coldwell zircons. The oscillatory metamictization is of particular importance for it must be related to the physio-chemical environment of formation and its evident fluctuation. The dark grey metamict domains contain significant amount Ca (2.33-8.33 wt % CaO) , Fe (0.71-1.54 wt % FeO) along with trace amounts of U, Th, REE (as represented by the $Ce_2O_3$) and upto 17 wt % $H_2O$ (calculated as the difference between the analysed total weight % oxide and the ideal weight of 100 %). Similar metamict zoning in zircon, described by de St. Jorre (1986) from Thor Lake, has been attributed to the minerals extreme variation in U contents between zones and the substitution of (OH,F) for $SiO_4$ in the lattice. The radioactive decay of atoms in the high U zones would have been accompanied by recoil of the nucleii during $\alpha$-particle emission severely damaging the cystal lattice. Experimental studies involving the synthesis of zircon in a fluorinated environment show that the presence of $(OH, F)_4$ tetrahedra weakens the crystalline lattice and hence allows it to be destroyed easily as a result of radioactive disintegration

(Caruba, 1985).

Natural hydroxylated zircons have as general formula Zr $(SiO_4)_{1-x}$ $(OH,F)_{4x}$ · $2H_2O$ (Caruba, 1985). The composition of the metamict zones in the Coldwell zircons indicate that minor amounts of (OH,F) has substituted for $SiO_4$ and therefore, the bulk of the water can be considered non-structural. This excess $H_2O$ has probably been introduced after metamictization.

Those zircons exhibiting metamict zonation (from the ferroaugite pegmatite, ferro-edenite and quartz syenites) are probably a function of both the oscillation of the radioactive elements, U and Th and the change in OH and F activity during zircon growth. However, the absence of significant enrichment in the actinides in the metamict zones relative to the non-metamict suggest that OH and F variations in the melt may be the main factor contributing to the zoning.

Fig 9.1 BSE micrograph of oscillatory metamict zoning in zircon from contaminated ferro-edenite syenite. The metamict zones (dark) contain significant amounts of Ca, Fe, and trace amounts of U and Th.

Fig 9.2 Quartz syenite zircon exhibiting faint birefringent zonation around a metamict core.


2028
001028 20KV
100um

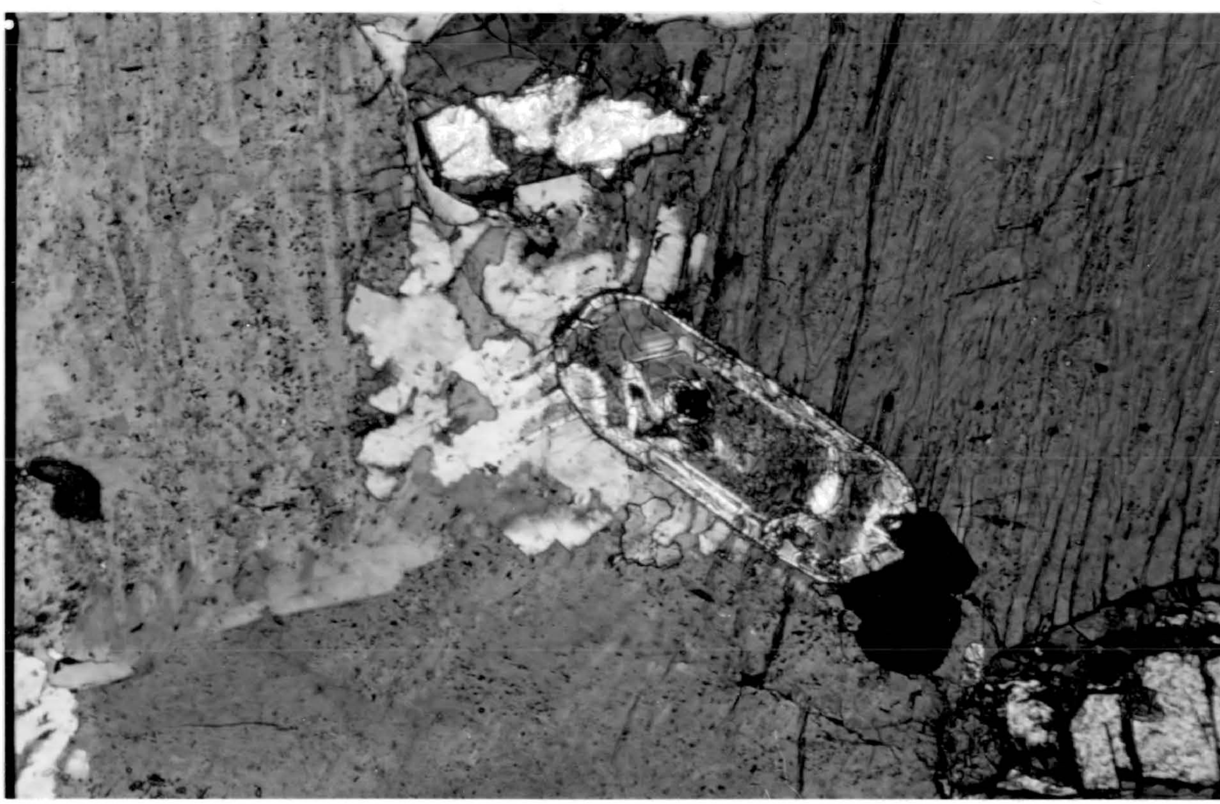

## 10.0 Nb-rutile

Nb-rutile or Ilmenorutile (Ti, Nb, $Fe^{3+})_3O_6$ is essentially a Nb and Fe bearing variety of rutile ($TiO_2$). The Composition can be described as a solid solution of TiO2 with a Tapiolite type phase (Fe, Mn) $(Nb,Ta)_2\ O_6$. Extensive isomorphism leads to variable Nb-Ta absolute abundances and relative proportions.

### 10.1 Textural Relationships

In the Centre I eastern contact pegmatites and Centre III quartz syenite, Nb-rutile forms as a late hypogene mineral replacement. In both units fluorocarbonate and rutile intergrowths pseudomorph an unidentified primary phase or phases. The size and complexity of the intergrowths has made identification and quantitative analysis of the Nb-bearing minerals difficult.

#### 10.1.1 Eastern Contact Pegmatites

Large skeletal pseudomorphs are composed primarily of intimate intergrowths of Nb-rutile, rarely Nb-bearing ilmenite, and fluorocarbonate. The replacement minerals are segregated into clusters of small (upto 50µm in length) interlocking acicular crystals and domains of syntaxial intergrown fluorocarbonate. Within the Nb-rutile aggregates, anhedral Nb-rutile and a Nb, Fe, Ti phase, tentively identified as columbite, fill interstital cavities (Fig 2.3).

#### 10.1.2 Quartz Syenite

Zircon, fluorite, ilmenite, amphibole and a stubby euhedral pseudomorph (<50µm) cluster interstitially to the feldspars in the Guse Point quartz syenite. Complete replacement by Nb-rutile and fluorocarbonate prevents identification of the precursor mineral. Unlike textures present in the eastern contact pegmatites and the Ashburton Lookout quartz syenites, the niobate forms intimate chaotic intergrowths and not distinct acicular crystals. Rare large grains exhibit colloform and zonal replacement textures with the fluorocarbonate and Nb-rutile (?).

### 10.1.3 Craddock Cove

Nb-rutile was only tentatively identified in the Craddock Cove syenite. As is the case of the quartz syenites, Nb and Fe-bearing oxides are intimately intergrown with bastnaesite and Ca-fluorocarbonate (see section 2.1.3). Compositions show low analytical totals and variable FeO.

## 10.2 Compostional Variation

Representative compositions are given in appendix 2.9

Mineral chemistry varies between lithologic units. Compositions from the eastern contact pegmatites have cation proportions close to the ideal structural formula for Nb-rutile. However, the replacement phase of the Guse Point quartz syenite and Craddock Cove syenite typically show low total oxide wt %, which may be due to oxygen deficiencies, the incorporation of hydroxyl anions, or substitutions such as $Ti^{4+} \leftrightarrow 2Fe^{2+}$ and/or $3Ti^{4+} \leftrightarrow 4Fe^{3+}$ (Foord, 1982).

Distinct compostional differences occur between the acicular and interstitial rutile. The earliest Nb-bearing phase, the needle Nb-rutile is depleted in $Nb_2O_5$(4.92-6.06 wt %) and FeO(2.97-3.31 wt %) relative to the later forming interstitial rutile, 15.77-19.96 wt % $Nb_2O_5$ and 5.23-6.19 wt % FeO. The Nb/Ta ratio of the interstial rutile is approximately 3 times that of the acicular rutile. An apparent trend towards niobium-enrichment relative to Ti and Ta in the mineralizing fluids is evidenced by the order of crystallization; needle rutile → interstitial rutile → columbite. $WO_3$ may also be present in concentrations as high as 4.80 wt %.

The quartz syenite "Nb-rutiles" are characterized by high Nb ( 10.93-20.24 wt % $Nb_2O_5$ ) and Fe (5.68-28.81 wt % FeO), the Craddock Cove by low Nb (5.41-7.52 wt % Nb205) and very high Fe (24.64-32.00 wt % FeO).

## 11.0 Monazite

Monazite (Ce, La, Nd, Th) $PO_4$ is typically a rare late-stage primary and replacement mineral, associated with other rare metal bearing phases in the Coldwell complex. It has been identified in both Centre I and Centre III, the greatest abundance being found in ferro-edenite syenite samples from the western contact and Neys Lookout localities. Monazite occurs typically as small (<400μm) anhedral to subhedral grain(s) included in multi-phase aggregates consisting of fluorite, magnetite, ilmenite, biotite, columbite, bastnaesite, and rarely pyrochlore. The mineral clusters seldom exceed 300 μm (Fig 5.1) in size. In other Centre III units, the contaminated ferro-edenite and quartz syenites, monazite is present in only trace amounts as minute inclusions in fluorite.

In the Craddock Cove and ferroaugite syenites of Centre I, rare monazite borders and replaces apatite along grain margins. In the eastern patch pegmatites it occurs as a replacement product after apatite and is rarely intergrown with fluorocarbonate in the rutile - fluorocarbonate pseudomorphs. Only several grains have been identified in one of the quartz syenite dykes (C1432). These are included or intergrown with pyrochlore and allanite.

Representative compositions are given in appendix 2.10. The monazite from the Coldwell complex are typical of other compositions in the literature, being enriched in light REE and containing significant amounts of Th and U. The highest concentrations of thorium are found in the Craddock Cove, quartz, and ferro-edenite syenites, while the quartz syenite dykes and eastern contact pegmatite monazites are relatively depleted in the element. In common with other REE-bearing minerals in the complex, the monazites from Centre III are distinctly LREE dominant relative to the monazite obtained from Centre I. This is clearly seen in average La/Nd ratios for monazite from various units:

| Lithology | |
|---|---|
| **Centre I** | La/Nd |
| Eastern Contact pegmatite (C1A) | 1.621 |
| Quartz syenite dyke (C1432) | 2.002 |
| Angler Creek, ferroaugite syenite (C2909) | 1.449 |
| Craddock Cove red syenite (C2920) | 8.918 |
| **Centre III** | |
| ferro-edenite syenite (C2025) | 2.798 |
| quartz syenite (C2112) | 4.962 |
| quartz syenite pegmatite (C2924) | 7.974 |

The Craddock Cove monazite is unusual in its high La/Nd and abundance of Th. In this respect, it resembles the monazite from the quartz syenite more than those from other Centre I lithologies.

Low analytical totals are characteristic of almost all monazite compositions. Monazite is not known to incorporate substantial amounts of undetectable $H_2O$ or F into its structure and therefore the totals are probably a direct result of metamictization and hydration of the grains.

## 12.0 Fersmite

Fersmite (Ca, REE, Na) (Nb, Ta, Ti)$_2$ (O, OH, F)$_6$ has been identified by composition in the quartz syenite dykes (C1418, C1428, and C2925) and by x-ray diffraction in the eastern contact pegmatites. In the dykes, fersmite occurs as small (<60µm) anhedral grains which are corroded and replaced by mantles of pyrochlore. The niobate may partially-include allanite or fill interstitial cavities within allanite aggregates. Rare small (<5µm)) discrete prisms are found suspended in calcite, and less commonly quartz, in the calcite - quartz - garnet assemblage.

In the eastern contact pegmatites, fersmite has *not* been identified by composition in any of the lithologic sections or microprobe grain mounts studied. However, its presence is supported by x-ray diffraction data from a heated heavy mineral separate (see Fig 3.3 and Table 3.1).

Quantitative compositions have been determined for C1418 fersmite and are given in appendix 2.10. In common with other associated niobates in the quartz dykes, the mineral is Nb ( 74.09 - 76.96 wt % $Nb_2O_5$)dominant relative to Ta (2.19- 3.14 wt % $Ta_2O_5$). Several rare-metal elements, U, Th, and Y, substitute for Ca. Although several wt % $REE_2O_3$ are present in most previously-analysed fersmite compositions (Foord, 1982), the Coldwell minerals contain only trace amounts.

## 13.0 Fergusonite

Fergusonite ($YNbO_4$) is one of the rarest REE bearing minerals in the Coldwell Complex and was identified only in several samples of the Angler Creek ferroaugite syenite and three quartz syenite dykes (C1428, C1432, C2925). In the ferroaugite syenite the mineral is associated with other late-forming minerals, pyrochlore and zircon, as inclusions in fine anhedra of interstitial quartz and rarely in amphibole. The euhedral fergusonite and the associated minerals seldom exceed 40 μm (Fig 13.1). In the quartz syenite dykes small (<10μm) discrete euhedra are suspended in calcite and less commonly in albite, in the calcite-garnet assemblage.

Representative compositions of fergusonite from the ferroaugite syenite have been determined by semi-quantitative methods and are shown in Table 9.1. All compositions exhibit considerable substition of Y by the rare earth elements, in particular HREE, Th, U, Ca, and Fe. The total oxide weight percentages have been normalized to 100 wt %. It is probable that the true values are less due to metamictization and hydration.

Table 13.1. Representive semi-quantitative chemical compositions of fergusonite from the Angler Creek ferroaugite syenites

| | C2909/1 | C2909/2 | C2908/1 | C2905/1 | C2905/2 |
|---|---|---|---|---|---|
| Nb205 | 44.73 | 45.44 | 46.33 | 45.98 | 44.97 |
| Ta205 | 3.03 | 1.99 | 0.33 | na | na |
| Y203 | 28.51 | 28.53 | 27.88 | 18.81 | 15.27 |
| La203 | 0.43 | 0.49 | nd | nd | nd |
| Ce203 | 3.27 | 3.88 | 2.44 | 2.70 | 2.67 |
| Pr203 | 1.36 | 1.22 | 0.60 | 0.65 | 1.28 |
| Nd203 | 4.90 | 4.69 | 4.02 | 9.63 | 12.08 |
| Sm203 | 1.41 | 1.35 | 2.13 | 3.75 | 5.02 |
| Gd203 | 1.78 | 2.26 | 3.47 | 3.56 | 3.93 |
| Tb203 | 0.26 | nd | na | na | na |
| Dy203 | 4.00 | 3.94 | 5.28 | 3.49 | 3.25 |
| Er203 | 3.20 | 3.15 | 2.61 | 2.11 | 2.14 |
| Yb203 | 2.46 | 2.44 | 1.65 | 1.15 | 1.99 |
| Th02 | 0.42 | 0.23 | 1.68 | 3.44 | 3.71 |
| U02 | nd | nd | 0.66 | 2.01 | 1.25 |
| CaO | 0.26 | 0.38 | na | 1.27 | 1.17 |
| FeO | nd | nd | 0.92 | 1.46 | 1.26 |
| Sum | 100.00 | 100.00 | 100.00 | 100.00 | 100.00 |
| | | | | | |
| REE203* | 23.07 | 23.42 | 23.88 | 27.04 | 32.36 |

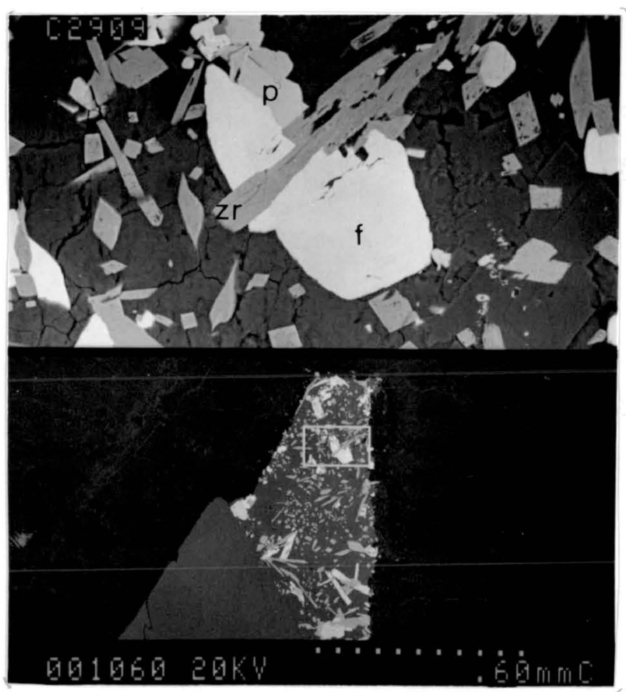


Fig 13.1 BSE micrograph of small (30 mm) fergusonite (f) grain. Associated minerals include acicular zircon (zr), pyrochlore (P), calcite, alteration silicate (chlorite ?), and an unidentified phosphate.

## 14.0 Whole Rock Geochemistry

Sixteen whole rock samples from Centre I and one chevkinite-bearing sample from Centre III have been analysed for major, minor and trace elements. The major oxides $SiO_2$, $TiO_2$, $Al_2O_3$, $Fe_2O_3$, MnO, CaO, MgO, $Na_2O$, $K_2O$, and $P_2O_5$ and trace elements Ni, Cu, Zn, Pb, Zr, Y, Sr, Rb were determined by standard XRF methods using fused glass discs at Laurentian University. Trace elements Ta, Hf, Sc, Cr, Co, and Th were determined by INAA methods. The rare earth elements were obtained by RNAA. Whole rock samples were irradiated at McMaster University and radiochemical separation was performed at Lakehead University. Uranium contents were obtained from Nuclear Activation Services, Hamilton, Ont.

## 14.1 Quartz Syenite Dykes

Each dyke is characterized by a distinct whole rock composition, but similarities in major oxide and trace element contents distinquish the quartz syenite dykes as a separate group from the other Coldwell lithologies. Major oxide proportions vary between the four quartz syenite dykes, but as a group they are characterized by high CaO (2.16-9.16 wt %), $Fe_2O_3$ (9.25-24.15 wt %) and low $Al_2O_3$ (9.03-12.24 wt %) (Fig 14.1)(appendix A.3.1. However, the diversity in major oxide contents can be extreme. Dyke C2925 is unique in its relatively high MnO (1.01 wt %), MgO (1.95 wt %), K20 (7.02 wt %) and low $SiO_2$ (40.45 wt %) and NaO (1.09 wt %). Normative calculations reflect this in the presence of nepheline, leucite, and kalsilite. The low $SiO_2$ and analytical totals of the dyke is apparently caused by the presence of unanalysed volatiles $CO_2$, F, and $H_2O$. Calcite and flourite, which are minor rock constituents, are the main hosts for the volatiles. In Contrast, C1418 is high in $SiO_2$ (71. 959 wt %) and

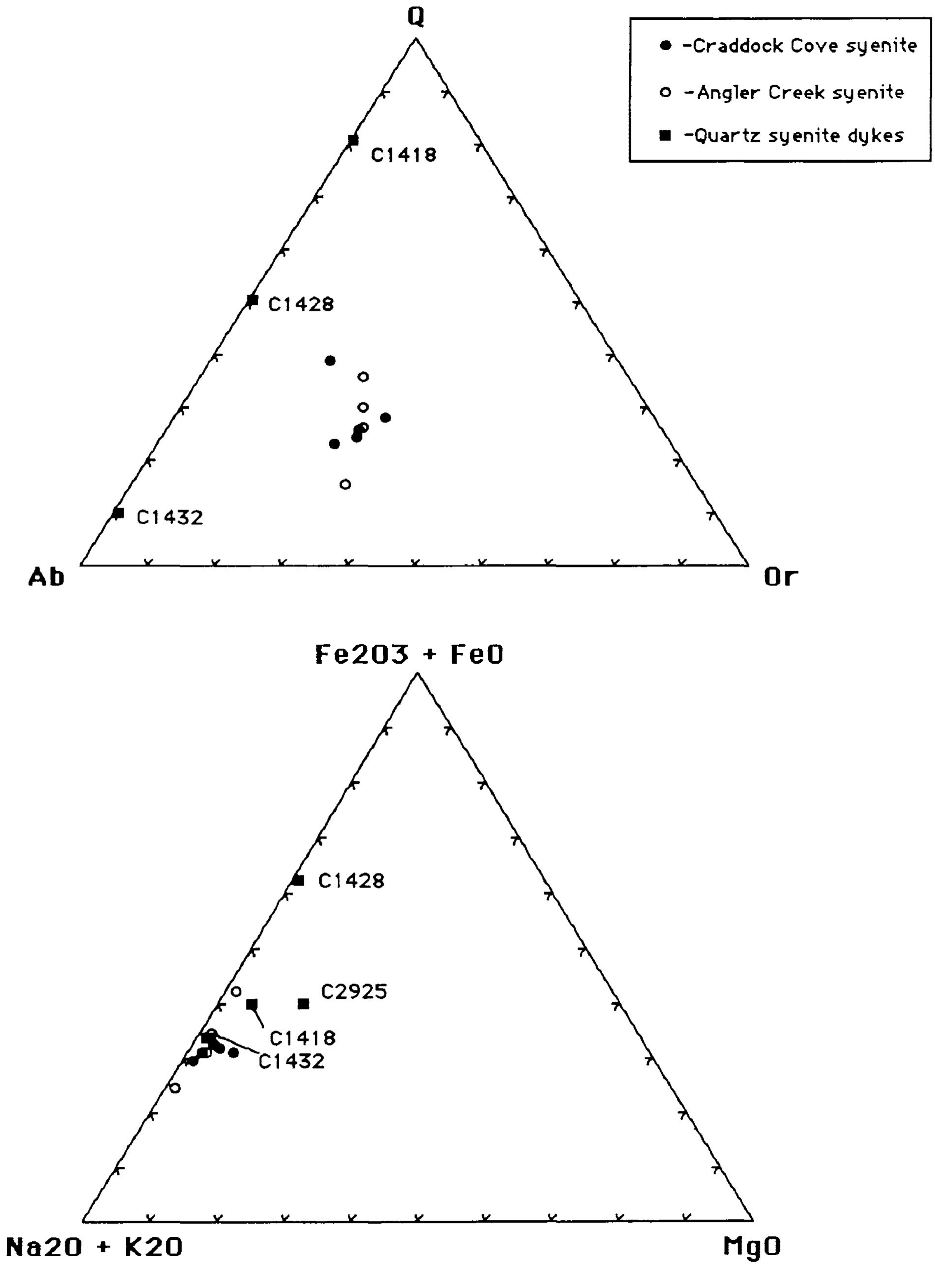


Fig 14.1 Normative and major oxide compositions of the Centre I lithologies are compared on ternary plots. Quartz syenite dykes are distinct from the syenites in their increased saturation and Fe content, with the exception of C1432.

low in $Fe_2O_3$ (9.25 wt %) and CaO (2.16 wt %) relative to the other quartz syenite dykes.

The dykes are uniformly enriched in the incompatible elements (REE, Th, U, Hf, Zr, Ta) and have the highest values yet reported from the Coldwell rocks.

Whole rock REE chondrite normalized plots for the quartz syenite dykes (Fig 14.2) exhibit the flat HREE pattern representative of an A-type granite as described by Collins et al (1982). The slopes are shallow relative to those from other units indicating a reduced LREE/ HREE ratio and the enrichment of the HREE in the dykes (Fig 14.2). Unfortunately only three of the dykes are illustrated. The REE contents of the fourth, C2925, was not determined due to processing difficulties. However, the data obtained, from the REE bearing minerals, would suggest that the dyke is also enriched, if not more so, in the HREE.

The large negative Eu anomaly implies that plagioclase fractionation played a significant role in the evolution of the dykes. The size of the anomaly makes it improbable that such fractionation would occur during or after emplacement. Therefore, the REE signature must resemble the REE composition of the parent melt just prior to injection into the fracture system.

## 14.2 Craddock Cove Syenites and Ferroaugite Syenites.

5 Craddock Cove specimens , sampled from various localities between the Redsucker Cove breccia zone and Wolf Camp Lake, and 7 from the ferroaugite syenite are comparable in their major and minor oxide compositions. This relationship does not appear in the trace element contents of the two suites. The Craddock Cove syenites are enriched in Zn, Pb, Zr, Y, REE, and the actinides, in particular the western samples (C1513, C2920, C1516), relative to the ferroaugite syenite.

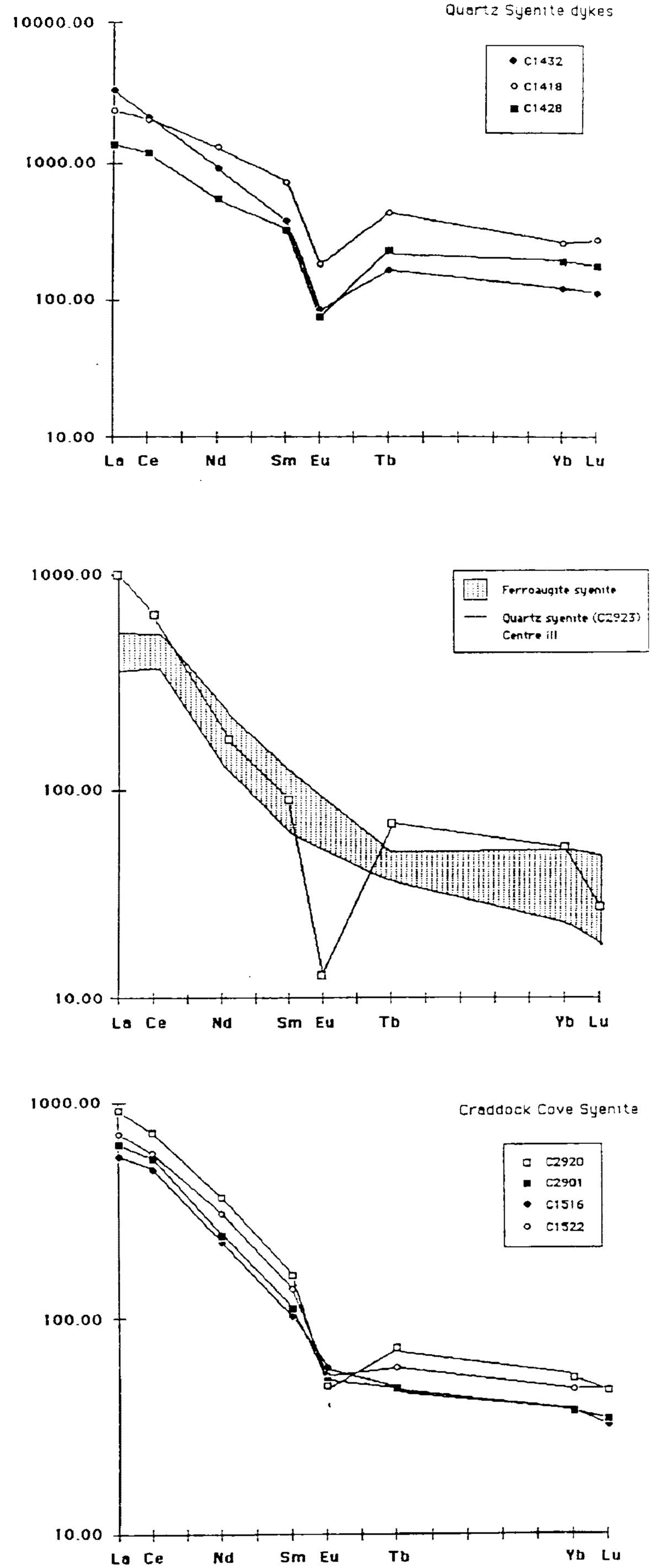


Fig 14.2 Chondrite normalized REE distribution in the quartz syenite dykes, ferroaugite syenite, and Craddock Cove syenite. A trend towards HREE enrichment and larger negative Eu anomalies is evident from the ferroaugite syenite to the Craddock Cove syenite to the quartz syenite dykes (Chondrite values after Boyton, 1984).

Chondrite normalized REE distribution patterns for the ferroaugite syenites exhibit small positive and negative Eu anomalies and smooth and rather steep slopes indicative of LREE enrichment (Fig 14.2). In contrast, the Craddock Cove patterns have shallower slopes with small but distinct negative Eu anomalies (Fig 14.2).

Only one chevkinite bearing sample from the Centre III (C2923) has been analysed for trace element contents. Although chevkinite is present in significant amounts, the whole rock REE abundance is of the same magnitude exhibited by the ferroaugite and Craddock Cove syenites.

## 15.0 T - P - X Conditions of Mineralization in the Quartz Syenite Dykes

All four quartz syenite dykes contain the unusual igneous mineral assemblage, garnet + calcite+ quartz + magnetite + epidote, a suite of minerals more typical of skarns than plutonic rocks. The euhedral garnets of C1428 imply that the assemblage is primary and not a result of re-equilibriation of the dykes due to the intrusion of the nepheline syenites of Centre II. In igneous rocks andradite is generally the Ti variety and has been reported in several granite pegmatites such as the occurrence in a granitic pegmatite cutting skarns in the Aldan Shield (Belyayev,1968). Associated with the assemblage are the rare metal-bearing minerals fergusonite, fersmite, pyrochlore, and allanite occuring as inclusions within the calcite, or as is the case with pyrochlore, a rare replacement phase of garnet. The paragenetic relationships between the garnet assemblage and the rare metal-bearing minerals should indicate the limiting P-T-X conditions of formation.

Semi-quantitative compositional data for garnets from dykes C1432 and C1428 are given in Table 15.1. The Coldwell garnets range in composition from $And_{75}Gro_{25}ss$ to essentially pure andradite and exhibit anisotropy with distinct optical zoning. The birefringent variety of garnet is relatively rare but is characteristic of the andradite - grossular solid solution series (Deer et al, 1982). Experimental studies of anistropic garnets show that they form under certain restrictive conditions. Only grossular - andradite grown at high rates from solutions in which no intermediate metastable phases could develop are doubly refracting (Kalinin, 1967). Experimental work by Hariya and Kimura (1978) showed that the most favourable conditions for the formation of birefringent andradite - grossular garnet appear to be under $CO_2$ pressure with excess water at relatively low P - T conditions (Fig 15.1).

The stability field for natural and synthetic garnets has a broad transition boundary between the anisotropic and isotropic varieties (Fig 15.1). Therefore, the upper limit of the boundary may indicate the highest possible temperature for the formation of birefringent garnet for a given pressure. If shallow dyke emplacement at a pressure of 1-2 Kbar is assumed, the upper temperature limit for the initial crystallization of the Coldwell garnets is approximately 750 °C.

Calcite, Quartz, and rarely magnetite and epidote (also allanite) replace garnet around corroded margins and less-commonly specifc zones. The breakdown of the mineral is a result of the instability of the mineral at low temperatures and relatively high $Xco_2$ conditions.

The molecular proportion of andradite and grossular in the solid solution series is one variable affecting the garnet stability field. The andradite-rich members are stable at lower temperature and higher $Xco_2$ in the fluids than is grossular (Taylor and Liou, 1978). An increase in the mol % grossular will reduce the stability of the garnet as shown in Fig 15.2.

The $And_{75}Gro_{25ss}$ composition contains the greatest grossular content of any garnet analysed in the quartz syenite dykes and thus, represents the maximum amount of grossular in garnet that remained stable during the solidification of the dyke. Garnet containing more than 0.25 mole percent was inherently unstable and broke down by the reaction $Gr_1 + CO_2 \leftrightarrow Gr_2 + An + Qtz + Cc$. In this respect, the preferential replacement of some zones in the garnet may be caused by selective attack on grossular-rich zones while andradite-rich garnet remained unaltered.

The $CO_2$ content in the dykes' parental melt is unknown and must be estimated based on experimental studies of various silicate melts. $CO_2$ generally is second to $H_2O$ in abundance in the magmatic volatile phase and is only slightly soluble in felsic melts at relatively low pressures ($\leq$ 3 Kbar)

(Burnham, 1979). Kadik and Eggler, (1975), from experimental observations of $CO_2$ solubility in albite melts, postulated that an hydrous silicate melt at a pressure of 2 Kbars would have $CO_2/H_2O + CO_2 = 0.1$. Therefore, under low pressure (1-2 Kbar) and temperatures (< 750° C), the $CO_2$ content in Coldwell dykes parental melt is estimated to have ranged between 0.0 to 0.2.

With the the above P and X conditions assumed the oxygen fugacity of the system may also be estimated. The assemblage andratite + magnetite + calcite + quartz under $XCO_2$= 0.0-0.2 can remain stable only if the oxygen fugacity is within the boundaries $fO_2^{-16} \rightarrow fO_2^{-20}$ bars (Taylor and Liou, 1978).

If the estimated values of $fO_2$, P, and $Xco_2$ are assumed to be correct, then the conditions of formation for the Coldwell dykes should be similiar to those hown in Fig 15.2 and 15.3. The latter figure illustrates the relative T- $Xco_2$ stability fields for the system Ca-Fe-Si-Al-C-O-H at $P_f$ = 2.0 Kbars and at a fixed $fO_2$= -18.5. The range in T-$Xco_2$ conditions in the fluid phase present during garnet replacement would be represented by the stippled region in the diagram. Temperature parameters would be 480°C, as defined by the Mt/Hm boundary to 540°C, and the intersection point of the univariant reactions Gr + $CO_2 \leftrightarrow$ Qtz + Cc + An and An + Gr $\leftrightarrow$ Zo (zoisite) + Qtz. The $Xco_2$ parameters are estimated between 0.12, as defined by the invariant point D, and 0.06, the invariant point E.

However, it should be noted that the physico-chemical parameters are difficult to estimate and any significant fluctuations in $fO_2$ and errors in estimating pressure would shift the equilibria shown in Fig 15.2 and 15.3. A decrease in pressure or conversely an increase in $fO_2$ would stabilize the garnet ($And_{75}Gro_{25}$) at lower temperatures. Another consideration when estimating the temperature of formation is the presence $F^-$ and its effect on lowering the crystallization temperature of the melt.

Table 15.1 Semi-quantative composition (wt %) of grandite from quartz syenite dyke C1428

| | C1428/1 | C1428/2 | C1428/3 |
|---|---|---|---|
| TiO2 | 1.32 | 0.02 | 2.01 |
| MnO | 0.34 | 1.87 | 0.26 |
| CaO | 32.83 | 30.55 | 31.76 |
| Fe2O3 | 22.12 | 28.75 | 24.67 |
| Al2O3 | 5.17 | 0.70 | 2.94 |
| SiO2 | 38.02 | 38.09 | 37.12 |
| MgO | 0.19 | nd | 1.23 |
| Total= | 100.00 | 100.00 | 100.00 |

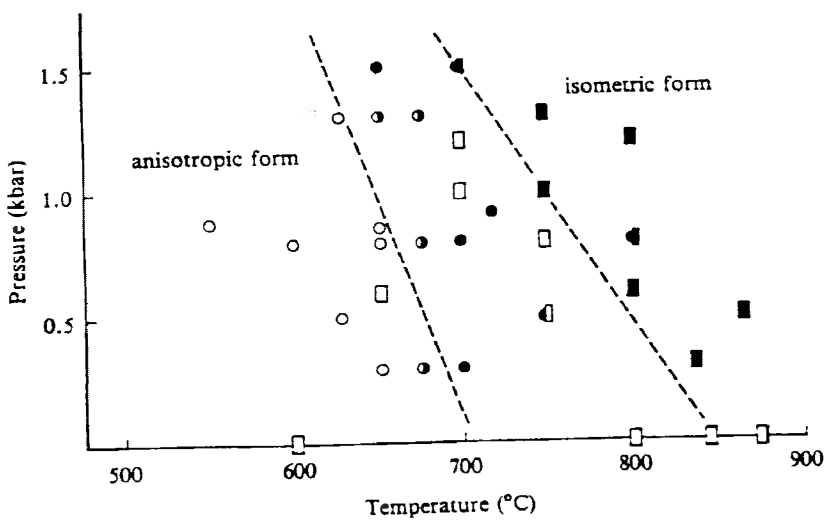


Fig 15.1 Stability field for natural and synthetic garnet showing anisotropic and isometric form. Open circles: synthetic anisotropic garnets. Solid circles: synthetic iostropic garnets. Open rectangle: natural anisotropic garnets. Solid rectangle: natural isotropic garnets (after Hariya and Kimura, 1978; from Deer er al 1982).

Fig 15.2 T-$X_{co_2}$ diagram comparing the stability limits of grossular and andradite. Reactions involving two garnets, illustrated as dashed lines, show the variation in equilibrium temperature with varying garnet composition (from Taylor and Liou, 1978).

Fig 15.3 T-XCO2 diagram for the system Ca-Al-Si-Fe-C-O-H at P=2.0 Kbars for log $fO_2$ = −18.5. Reactions are 4= Hd ↔ Ad + Mt + Qtz, 10=Hd + Cc ↔ Ad + Qtz + $CO_2$, 12=An + Gr ↔ Zo + Qz, 13= Gr + $CO_2$ ↔ Zo + Qtz + Cc, 14 = Zo + $CO_2$ ↔ An + Cc. Reactions 15, 16, and 17 are epidote bearing equilibria which are analogous, respectively to 12, 13, and 14 in the Fe – free portion of the system. The stippled region represents hypothetical T- $X_{co_2}$ environment for garnet replacement and rare-metal crystallization (from Taylor and Liou, 1978).

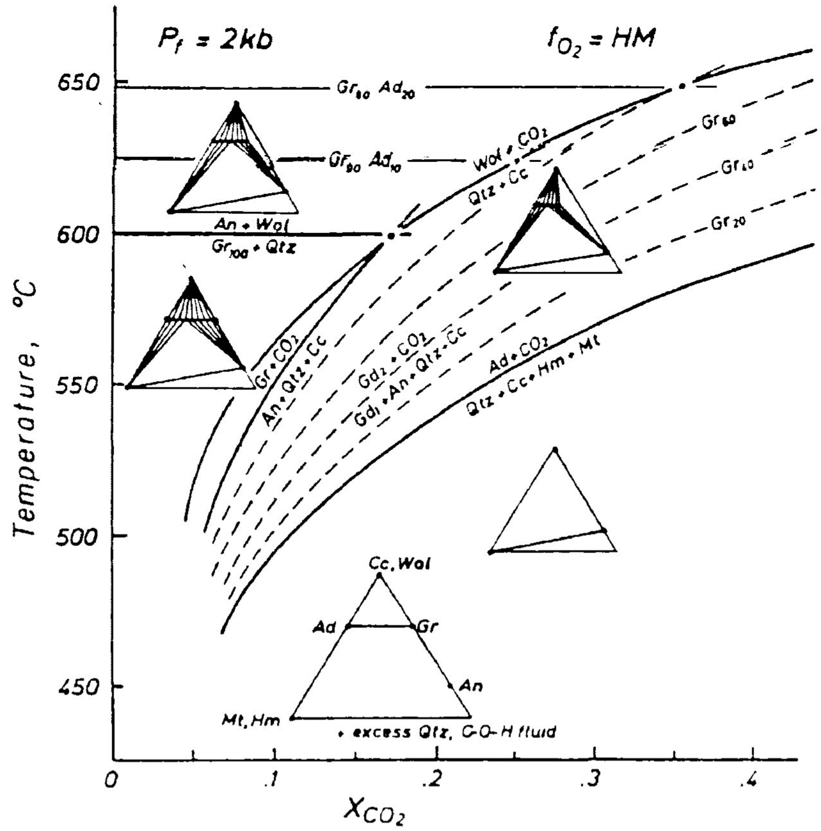
$P_f$ = 2kb
$f_{O_2}$ = HM
Temperature, °C
$X_{CO_2}$
An + Wol
$Gr_{100}$ + Qtz
Wol + $CO_2$
Qtz + Cc
Gr + $CO_2$
An + Qtz + Cc
Ad + $CO_2$
Qtz + Cc + Hm + Mt
Cc, Wol
Ad
Gr
An
Mt, Hm
+ excess Qtz, C-O-H fluid

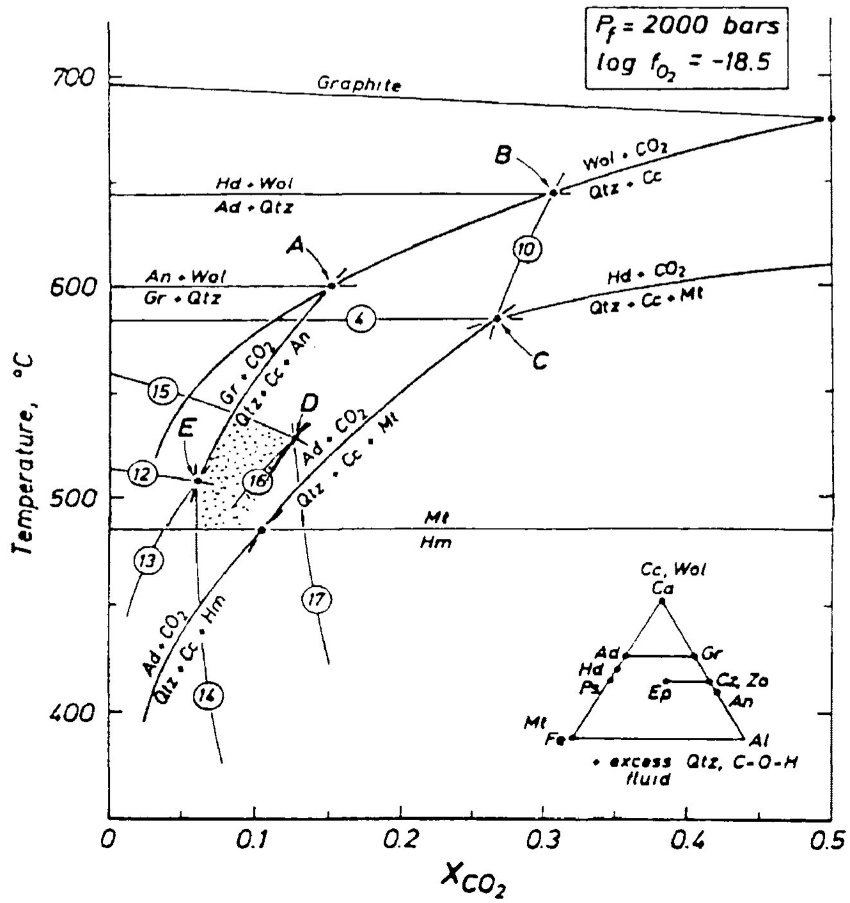
$P_f$ = 2000 bars
log $f_{O_2}$ = -18.5
Graphite
Hd + Wol
Ad + Qtz
An + Wol
Gr + Qtz
Wol + $CO_2$
Qtz + Cc
Hd + $CO_2$
Qtz + Cc + Mt
Gr + $CO_2$
Qtz + Cc + An
Ad + $CO_2$
Qtz + Cc + Mt
Mt
Hm
Ad + $CO_2$
Qtz + Cc + Hm
A
B
C
D
E
Temperature, °C
$X_{CO_2}$
Cc, Wol
Ca
Ad
Hd
Ps
Gr
Cz, Zo
Ep
An
Mt
Fe
Al
+ excess Qtz, C-O-H fluid

## 16.0 Synthesis and Discussion

Microbeam techniques proved to be essential in providing information on both the composition and textural relationships of the Coldwell rare metal-bearing minerals. These relationships have been shown to be complex due to a genesis which involves multiphase intergrowths, deuteric alteration and replacement. The fine grained nature of the assemblages made scanning electron microscopy invaluable in locating and identifying mineral species. In contrast, conventional X-ray diffraction techniques and optical petrography were of limited use.

In Centres I and III, the "incompatible" elements Nb, Zr, REE, Th, U, and Y are minor-to-major components in the accessory rare metal minerals and reflect their enrichment in the bulk composition of the parental magma. A-type granitoids have the geochemical characteristics of high $Na_2O + K_2O$ enrichment and high charge cations such as Nb, Zr, REE, Y, U, Th, and Zn (Whalen et al, 1987; Collins et al, 1982). Whole rock compositions from Centre III (Lukosius-Sanders, 1988) and Centre I, in particular the metaluminous-to-peralkaline quartz syenite dykes, display compositions similar to defined A-type granites. Although the overall composition of the accessory minerals are comparable between Centres, Centre I minerals generally show an enrichment of HREE relative to those from Centre III. Most Centre I rare earth bearing minerals are enriched in the HREE relative to those from Centre III, in particluar pyrochlore, fluorocarbonate, and allanite from the eastern contact pegmatites and the quartz syenite dykes. Compositional analysis of adjacent syntaxial intergrowths of bastnaesite, parisite, and synchysite indicate that REE-distribution in the Ca- bearing members may, in part, have been influenced by the Ca content of the species.

In Centre III, chevkinite, pyrochlore, and monazite have apparently crystallized from late-stage melts or residual pore fluids in the more-evolved quartz and ferro-edenite syenites. These processes have formed subhedral-to-euhedral grains which are invariably altered by later deuteric fluids. The $F^-$ and $CO_3^{2-}$- bearing fluids, as indicated by the predominance of fluorocarbonate replacement, resulted in alteration and recrystallization of the earlier rare metal bearing phases. Precipitation of fluorocarbonates and unidentified niobate phases along grain boundaries and cleavage traces in minerals surrounding altered pyrochlore and chevkinite grains is indicative of remobilization of the elements. Because of the short distance separating the site of removal and that of precipitation, it is believed that transport was not over significant distances

In contrast, large scale movement of Nb, REE, Th, U, and Zr-bearing fluids was fundamental to the enrichment of the Craddock Cove rocks and the formation of the quartz syenite dykes.. The Craddock Cove syenite adjacent to the Redsucker Cove breccia zone is characterized by low grade K-metasomatism with incipient replacement of amphiboles and plagioclase by K-feldspar, fluorocarbonates, Nb-rutile (?), zircon, pyrochlore, calcite, quartz and Fe-oxides. The substantial amounts of Fe-oxides and the enrichment of Fe in the replacement minerals - chevkinite, pyrochlore and allanite imply high Fe contents in the fluids. Further evidence suggests that the metasomatism may have occured in an oxidizing environment. According to the experimental studies of Green and Pearson (1988) elevated Fe contents in chevkinite may be a function of high oxygen fugacity in the parent fluids. Chevkinite compositions with the highest Fe in the Coldwell complex are found in sample C2920 from the Craddock Cove syenite . In addition, the proposed substitution of $Fe^{3+}$ for $REE^{3+}$ in the fluorocarbonate would probably require Fe-rich fluids with high

$Fe_2O_3$/ FeO + $Fe_2O_3$ ratios. It is therefore postulated that rare-metal mineralization in the Craddock Cove syenites is a result of the influx of K and Fe metasomatizing fluids under conditions of high $fO_2$.

The quartz syenite dykes contain the highest concentrations of the rare metal elements than any other Coldwell litholigic unit. They are compositionally variable but are generally Fe-rich, and poor in Al and K (with the exception of dyke C2925). The origin of the dykes and their relation to other magmatic activity in the complex is unclear. However, on the basis of the following obervations, dyke formation appears to be a result of late-stage Centre I magmatism; (1) Dyke contacts in the red syenites are undulatory and suggest that intrusion occurred into a hot plastic syenite (Kent, 1981), (2)The metaluminous-to-peralkaline oversaturated dykes are geochemically similar to the oversaturated peralkaline ferroaugite syenite of Centre I, (3) There is an apparent similarity in chondrite normalized REE distribution patterns between the Craddock Cove syenites and the quartz syenite dykes. The three REE patterns exhibit progressive fractionation (increasingly larger negative Eu anomalies) and the enrichment in REE from the ferroaugite syenite to the Craddock Cove syenite to the quartz syenite dykes.

The HREE enrichment of the dykes, though, is distinctly different from the other lithologic units and is not easily explainable by crystal-liquid fractionation. The enrichment may be analogous to that of the Jabal Sa'id aplite-pegmatite rare metal deposit associated with a peralkaline granite in the Arabian Shield (Drysdall et al, 1984). The geochemical characteristics of the deposit include low Al, high Fe, Fe/alkali, $Fe_2O_3$/FeO and enrichment in all rare earths. Of particular note is the HREE enrichment of the deposit relative to its parent granite. The increase of HREE is explained by the dominant role of $F^-$ and $CO_3^{2-}$ in partitioning the HREE into the residual fluids (Drysdall et al, 1984). Carbonate complexes of HREE and uranyl ions are stable under relatively alkaline and oxidizing conditions and would allow for the transport of the HREE and U in late stage fluids (Taylor et al, 1981). Such a model could be applicable to the calcite and fluorite bearing quartz syenite dykes of Coldwell.

It is possible that both metasomatism of the Craddock Cove syenite and the emplacement of the quartz syenite dykes may be temporally related to the differentiation of residual fluid in the apical zone of the Centre I magma chamber. The presence of cap lava xenoliths and complex pegmatites in the syenite is evidence for its high stratigraphic level in the intrusion (Kent, 1981; Mitchell and Platt, 1982). In this repect, the syenite may represent rocks proximal to the apical zone.

The differentiated $F^-$ and $CO_3^{2-}$ bearing fluid may have subsequently permeated and metasomatized the previously-crystallized and still hot Craddock Cove syenite and were contemporaneously-injected into fractures forming the dykes. The formation of stable complexes of $F^-$ and $CO_3^{2-}$ with the rare metals would allow for their transportation in the fluids and would account for the significant HREE enrichment in the quartz syenite dykes' whole rock and accessory rare metal mineraL compositions.

From evidence collected in the southern portion of the Craddock Cove syenite, it has been shown that enrichment of rare elements in residual fluids and their migration have occured in Centre I. Other occurrences of enriched dykes and metasomatized rocks are conceivably present in the northern portion iof the Craddock Cove syenite. One pegmatite dyke intruding a megaxenolith has been identified north of highway 17 in the locality of Johnston and Craddock Lakes (Pye, 1954). However, the most northerly regions of the intrusion have not fully been investigated for mineralization due to difficulties in accessiblity.

It is concluded that the megaxenoliths should be considered primary targets for rare metal mineralization due to their proximity to the apex of the chamber and their apparent susceptiblity to brittle fracture and intrusion of residual fluids. The red syenites are possible secondary targets, particularly those adjacent to the megaxenoliths. Although it to represents rock at a high stratigraphic level in the intrusion, its high temperature may have made it less prone to fracturing and therefore not as favourable for dyke emplacement.

## References


Andersen, T., 1986. Compositional Variation of Some Rare Earth Minerals from the Fen Complex (Telemark, SE Norway): Implications for the Mobility of Rare Earths in a Carbonatite System. Mineralogical Magazine, 50, 503-9.

Bayliss, P., Mazzi, F., Munno, R., White, T. J., 1989. Mineral Nomenclature: Zirconolite. Mineralogical Magazine, 53, 565 - 569.

Belyayev, G. M., 1968. More Information about Andradite Bearing Pegmatite of the Aldan Shield. Akademiia Nauk SSSR Doklady Earth Science Section, 177, 188-190.

Boggs, R. C., 1984. Mineralogy and Geochemistry of the Golden Horn Batholith, Northern Cascades, Washington. *Unpub. Ph.d. Thesis. Univ. of California, Santa Barbara.*

Boynton, W. V., 1984. Cosmochemistry of the Rare Earth Elements: Meteorite studies. In *Rare Earth Element Geochemistry* (P. Henderson, Ed). Elsevier, New York. 63-114

Brooks, C. K., 1973. Rifting and Domaining in Southern East Greenland. Nature Physical Science, 244, 23-5.

Brooks, C. K., Engell. J., Larsen, L. M., Pedersen, A. K., 1982. Mineralogy of the Werner Bjerge Alkaline Complex, East Greenland. Meddelelser om Grønland, Geoscience. 1.

Burnham, C. W., 1979. The Importance of Volatile Constituents, In *The Evolution of the Igneous Rocks* (H. S. Yoder, Jr. Ed). Princeton University Press, Princeton. 439-482.

Burt, D. M., Londen, D., 1982, Subsolidus Equilibrium. In MAC Short Course Handbook 8. (P. Cerny, Ed). 329-346.

Caruba, R., Baumer, A. Ganteaume, M., Lacconi, P., 1985. An Experimental study of hydroxyl groups and water in Synthetic and natural Zircons: a model for the metamict State. American Mineralogist, 70, 1224-1231.

Cerny, P., Cerna, I., 1972. Bastnaesite after Allanite from Rough Rock Lake, Ont, Canadian Mineralogist, 11, 541 - 543.

Cerny, P., Ercit. T. S., 1985. Some recent advances in the mineralogy and geochemistry of Nb and Ta in rare-element granitic pegmatites. Bull. Mineral, 108, 499-532.

Chesner, C. A., Ettlinger, A. D., 1989. Composition of Volcanic allanite from the Toba Tuffs, Sumatra, Indonesia, American Mineralogist. 74, 750-758.

Collins, W. J., Beamsm S. D., White, A. J., Chappell, B. W., 1982, Nature and origin of A-type Granites with Particular Reference to Southeastern Australia: Contributions to Mineralogy and Petrology, 80, 189-250.

Currie, K. L., 1980. A Contribution to the Petrology of the Coldwell Alkaline Complex, Northern Ontario. Geological Survey of Canada Bulletin 287, 43 p.

Donnay, G., Donnay, J. D. H., 1953. The Crystallography of Bastnaesite, Parisite, Roentgenite, and Synchisite. American Mineralogist, 38, 932-963.

Deer, W. A., Howie, R. A., Zussman, J., 1982. Rock-Forming Minerals, Volume 1A, Orthosilicates. Longman, London, 919 p.

De St. Jorre, L., 1986. Economic Mineralogy of the North T- Zone Deposit, Thor Lake. Northwest Territories. *Unpub. M.Sc. Thesis. Univ. of Alberta, Calgary, Alberta.*

Droop, E., 1987. A General equation for Estimating Fe3+ Concentration in Ferromagnesian Silicates and Oxides from Microprobe Analysis, using Stoichiometric Criteria. Mineralogical Magazine, 51, 431-435.

Drysdall, A. R., Jackson, N. J., Ramsay, C. R., Douch, C. J., Hackett, D., 1984. Rare Element Mineralization related to Precambrian Alkali Granites in the Arabian Shield.

Ewing, R. C., Chakoumakos, B. C., 1982, Lanthanide, Y, Th, U, Zr and Hf Minerals: Selected Structure Descriptions. In MAC Short Course Handbook 8 ( P. Cerny, Ed). 239-346.

Exley, R. A., 1980, Microprobe studies of REE-Rich Accessory Minerals: Implications for Skye Granite petrogenesis and REE Mobility in Hydrothermal Systems. Earth and Planetary Science Letters. 48, 97-110.

Fleischer, M., 1965. Some Aspects of the Geochemistry of Ytrrium and the Lanthanides. Geochimica et Cosmochimica Acta, 29, 755-772.

Fleischer, M., 1978. Relative proportions of the Lanthanides in minerals of the Bastnaesite group, Canadian Mineralogist. 16, 361-363.

Frondel, C., 1958. Systematic Mineralogy of Uranium and Thorium. United Stated Geological Survey Bulletin 1064, 400 p.

Foord, E. E., 1982. Minerals of Tin, Titanium, Niobium, and Tantalum in Granitic Pegmatites. In: MAC Short Course Handbook 8, (P. Cerny, Ed.) 187-238.

Green, T. H., Pearson, N. J., 1988. Experimental Crystallization of Chevkinite/Perrierite from REE-enriched Silicate Liquids at High Pressure and Temperature, Mineralogical Magazine, 52, 113-20.

Harding, R. R., Merrimen, R. J., Nancarrow, P. H., 1982. A note on the Occurrence of Chevkinite, Allanite, and Zirkelite on St. Kilda, Scotland. Mineralogical Magazine, 46, 445-448.

Hariya, Y., Kimura, M., 1978. Optical Anomaly Garnet and its Stability field at High Pressures and Temperatures. J. Fac. Sci. Hokkaido.Univ . Ser IV, 18, 611-624.

Haggerty, S. E., Mariano, A. N., 1983. Strontian - loparite and Strontio - Chevkinite: Two New Minerals in Rheomorphic Fenites from the Parana Basin Carbonatites, South America. Contributions to Mineralogy and Petrology, 84, 365-381.

Hogarth, D. D., 1977. Classification and nomenclature of the pyrochlore group. American Mineralogist, 62, 403-410.

Hogarth, D. D., 1989. Pyrochlore, Apatite and Amphibole : Distinctive Minerals in Carbonatite. In: *Carbonatites, Genesis and Evolution* ,(ed) Bell, K., Unwin Hyman Ltd, London, U.K.

Ito, J., 1967. A study of chevkinite and perrierite. American Mineralogist, 52, 1094-104.

Kadik, A. A., Eggler, D. H., 1975, Melt-vapour relations on the $NaAlSi_3O_8$-$H_2O$-$CO_2$. Carnegie Institute of Washington, Year Book 74, 479-484.

Kalinin, D. V.,1967. Anisotropism in Garnets in Relation to Composition and Chemical Background of their synthesis. Akademiia Nauk SSSR Doklady Earth Science Section, 172,128-130.

Kent, A. E., 1981. Geology of the Craddock Cove Area: Coldwell Alkaline Complex, Northwestern Ontario. *Unpub. HB.Sc. Thesis. Lakehead Univ.*

Lahti, S. I., Suominen, V.,1988. Occurence, crystallography and chemistry of the Fluocerite-Bastnaesite-Cerianite intergrowths from the Fjalskar Granite, Southwestern Finland. Bulleten of the Geological Society of Finland, 60, 1, 45-53.

Littlejohn, A. C., 1981, Alteration Products of Accessory Allanite in Radioactive Granites from the Canadian Shield, Current Research, Part B, Geological Survey of Canada, Paper 81-1B, 95-104.

Lukosius-Sanders, J., 1988, Petrology of Syenites from Centre III of the Coldwell Alkaline Complex, Northwest Ontario. *Unpub. M.Sc. Thesis. Lakeheao Univ. Thunderbay, Ont.*

McDowell, S. D., 1979. Chevkinite from the Little Chief Granite Porphyry Stock, California. American Mineralogist 64, 721-727.

Mitchell, R. H., Platt, R. G., 1977. Field Guide to aspects of the Coldwell Alkaline Complex. 23rd Annual Institute on Lake Superior Geology, Thunder Bay, Ont. 34 pp.

Mitchell, R. H., Platt, R. G., 1978. Mafic Mineralogy of Ferroaugite Syenite from the Coldwell Alkaline Complex, Ontario, Canada. Journal of Petrology, 19, 4, 627-651.

Mitchell, R. H., Platt, R. G., 1982. Mineralogy and Petrology of Nepheline Syenites from the Coldwell Complex, Ontario, Canada. Journal of Petrology. 23, 186-214.

Novak, S. W., Mahood, G. A., 1986. Rise and Fall of a Basalt - Trachyte - Rhyolite Magma System at the Kane Springs Wash Caldera, Nevada. Contribution to Mineralogy and Petrology, 94, 352 - 373.

Payette, C., Martin R. F., 1988. The Welsford Anorogenic Igneous Complex, Southwestern New Brunswick: Rift-Related Acadian Magmatism, Final Report. Mineral Exploration Institute and Department of Geological Sciences, McGill University.

Platt, R. G., Wall, F., Williams, C. T., Woolley, A. R., 1987. Zirconolite, Chevkinite and other Rare Earth Minerals from Nepheline Syenites and Peralkaline Granites and Syenites of the Chilwa Alkaline Prov, Malawi, Mineralogical Magazine, 51, 253-263.

Pye, 1954. Resident Geologist's Files, Ontario Ministry of Northern Development and Mines, Thunder Bay.

Rimsaite, J., 1981. Isotope, Scanning Electron Microscopy, and energy dispesive spectrometer studies of Heterogeneous Zircons from Radioactive Granites in the Grenville Structural Province, Quebec and Ontario. Current Research, Part B, Geological Survey of Canada, Paper 81-1B, 25-35.

Segalstad, T. V., Larsen, A. O., 1978. Chevkinite and Perrierite from the Oslo Region, Norway. American Mineralogist, 63, 499-505.

Shannon, R. D., Prewitt, C. T., 1969. Effective Ionic Radii in Oxides and Fluorides. Acta Crystallographica. B25, 925-946.

Staatz, M. H., 1974. Thorium Veins in the United States, Economic Geology, 69, 494-507.

Taylor R. P., Strong, D. F., Fryer, B. J., 1981, Volatile Control of Contrasting Trace Element Distributions in Peralkaline Granitic and Volcanic Rocks. Contribution to Mineralogy and Petrology, 77, 267 - 271.

Taylor, B. E. and Liou, J. G., 1978. The Low-temperature Stability of Andradite in C-O-H fluids. American Mineralogist, 63, 378-393.

Van Landuyt, J., Amelinckx, S., 1975. Multiple Beam Direct Lattice Imaging of New Mixed-Layer Compounds of the Bastnaesite-Synchysite Series, American Mineralogist, 60, 351-358.

Vlasov, K. A. (ed.), 1966. Geochemistry and Mineralogy of Rare Elements and Genetic Types of their Deposits: V III, Genetic Types of Rare Element Deposits. Israel Program for Scientific Translations, Jerusalem.

Whalen, J. B., Currie, K. L., Chappell, B. W., 1987, A-type Granites: Geochemical characteristics, Discrimination, and Petrogenesis. Contribution to Mineralogy and Petrology. 95, 407-419.

Yefimov, A. F., Yes'kova, Y. M., Lebedera, S. I., Levin, V. Y., 1985. Type Compositions of Accessory Pyrochlore in a Ural Alkali Complex, Geokhimiya, 2, 201 - 208.

Zhang, R., Fan, L., 1976. Iron Chevkinite in Quartz Syenite from a certain district in Hubei. Geochimica, 244 - 250.

# APPENDIX 1

An Energy Dispersive X-ray Spectrometer (EDS) attached to an Hitachi 570 SEM at Lakehead University was used in analysing all mineral compositions. The operating conditions were: accelerating voltage of 20 KV, a beam current of 0.38 nA, and counting times ranging between 80 to 350 seconds. The analytical data was obtained using the Tracor Northern ZAF computer programmes. The accuracy and precision of the rare earths, CaO, TiO2, FeO, and SiO2 are shown in Table A.1

Table A.1 Accuracy and precision of REE2O3, TiO2, FeO, CaO, and SiO2 analyses by EDS.

Bastnaesite: Lincoln County

| Analyses | La2O3 | Ce2O3 | Pr2O3 | Nd2O3 | Total |
|---|---|---|---|---|---|
| Standard | 25.59 | 35.01 | 2.71 | 6.87 | 70.18 |
| 1 | 25.17 | 35.06 | 2.44 | 5.97 | 67.89 |
| 2 | 24.03 | 35.32 | 2.12 | 5.67 | 67.14 |
| 3 | 24.86 | 35.47 | 3.29 | 6.06 | 69.91 |
| 4 | 25.89 | 35.50 | 2.48 | 6.25 | 70.12 |
| 5 | 24.73 | 35.32 | 2.65 | 6.55 | 69.25 |
| 6 | 25.03 | 35.10 | 3.66 | 6.15 | 69.92 |
| 7 | 26.48 | 35.90 | 1.90 | 5.80 | 70.76 |
| 8 | 24.27 | 35.21 | 3.69 | 6.09 | 69.35 |
| 9 | 24.36 | 34.96 | 3.34 | 6.70 | 69.36 |
| 10 | 25.07 | 35.40 | 2.46 | 5.87 | 68.8 |
| 11 | 25.47 | 35.38 | 2.52 | 6.87 | 70.23 |
| 12 | 25.95 | 35.40 | 2.64 | 6.68 | 70.79 |
| 13 | 25.60 | 36.20 | 3.04 | 6.37 | 71.21 |
| 14 | 25.58 | 35.25 | 3.04 | 6.68 | 70.54 |
| 15 | 25.16 | 35.76 | 2.97 | 6.38 | 70.28 |
| 16 | 24.74 | 35.18 | 2.91 | 7.73 | 70.85 |
| 17 | 25.81 | 34.99 | 2.70 | 6.75 | 70.65 |
| 18 | 25.02 | 35.43 | 2.48 | 6.38 | 69.5 |
| 19 | 25.26 | 35.05 | 2.92 | 7.89 | 71.12 |
| 20 | 25.63 | 35.08 | 2.46 | 6.35 | 69.52 |
| 21 | 25.69 | 35.36 | 1.80 | 6.10 | 69.39 |
| Average | 25.23 | 35.35 | 2.74 | 6.44 | 69.84 |
| STD | 0.59 | 0.30 | 0.49 | 0.55 | 1.01 |
| Accuracy | -0.36 | 0.34 | 0.03 | -0.43 | |
| Precision | 1.19 | 0.60 | 0.99 | 1.10 | |

Ilmenite G1 (MgO and MnO fixed)

| Analyses | TiO2 | FeO | Total |
|---|---|---|---|
| Standard | 49.92 | 47.47 | 97.39 |
| 1 | 49.63 | 47.47 | 97.10 |
| 2 | 49.30 | 47.65 | 96.95 |
| 3 | 50.03 | 47.60 | 97.63 |
| 4 | 49.38 | 47.43 | 96.81 |
| 5 | 49.51 | 47.05 | 96.56 |
| 6 | 50.29 | 47.49 | 97.78 |
| 7 | 50.25 | 47.10 | 97.35 |
| 8 | 50.18 | 47.27 | 97.45 |
| 9 | 49.95 | 47.35 | 97.30 |
| 10 | 49.82 | 47.36 | 97.18 |
| 11 | 49.95 | 47.35 | 97.30 |
| 12 | 49.75 | 47.94 | 97.69 |
| Average | 49.84 | 47.42 | |
| STD | 0.33 | 0.18 | |
| Accuracy | -0.08 | -0.10 | |
| Precision | 0.66 | 0.35 | |

Diopside DI2

| Analyses | fixed MgO | SiO2 | CaO | TiO2 | Total |
|---|---|---|---|---|---|
| Standard | 18.25 | 54.37 | 25.38 | 2 | 100.00 |
| 1 | 18.26 | 54.88 | 25.44 | 1.85 | 97.36 |
| 2 | 18.26 | 54.43 | 25.85 | 1.85 | 100.4 |
| 3 | 18.26 | 54.14 | 25.6 | 1.91 | 99.91 |
| 4 | 18.26 | 54.33 | 26.15 | 1.91 | 100.6 |
| 5 | 18.26 | 54.21 | 25.12 | 1.65 | 99.24 |
| Average | --- | 54.4 | 25.63 | 1.83 | 99.66 |
| STD | --- | 0.26 | 0.35 | 0.1 | |
| Accuracy | --- | 0.03 | 0.25 | -0.17 | |
| Precision | --- | 0.52 | 0.7 | 0 | |

APPENDIX 2.1

Centre I — B = bastnaesite
Fluorocarbonates — P = parisite
Craddock Cove — S = synchysite

| | S | S | S | S | S | S | S | S |
|---|---|---|---|---|---|---|---|---|
| | C1513/1 | C1513/2 | C1513/3 | C1513/5 | C1513/6 | C1513/7 | C1513/8 | C1513/9 |
| CaO | 17.99 | 17.86 | 16.13 | 16.50 | 18.23 | 16.37 | 15.19 | 18.51 |
| FeO | 7.78 | 7.59 | 10.98 | 10.79 | 3.29 | 7.54 | 12.87 | 7.67 |
| La2O3 | 7.23 | 7.11 | 6.14 | 7.43 | 8.81 | 7.19 | 7.49 | 7.28 |
| Ce2O3 | 16.90 | 17.71 | 15.28 | 17.28 | 19.40 | 18.60 | 16.72 | 18.11 |
| Pr2O3 | 2.48 | 1.54 | 1.85 | 1.72 | 1.72 | 2.43 | 0.98 | 2.67 |
| Nd2O3 | 7.56 | 5.95 | 6.90 | 7.45 | 5.59 | 7.25 | 5.62 | 6.97 |
| Sm2O3 | 0.82 | 0.00 | 0.83 | nd | 0.90 | 0.52 | 0.58 | 0.99 |
| UO2 | nd | nd | nd | nd | nd | nd | nd | nd |
| ThO2 | nd | 0.89 | nd | 0.89 | nd | nd | 0.83 | nd |
| TOTAL= | 60.81 | 58.70 | 58.16 | 62.09 | 57.98 | 59.94 | 60.30 | 62.26 |
| La/Nd | 0.98 | 1.23 | 0.92 | 1.03 | 1.62 | 1.03 | 1.37 | 1.07 |

| | P | B | B | B | P | P | P | P |
|---|---|---|---|---|---|---|---|---|
| | C1513/10 | C1513/11 | C1513/2 | C1513/3 | C1515/1 | C1515/2 | C1515/3 | C1515/4 |
| CaO | 8.90 | 0.25 | 0.77 | 0.87 | 10.36 | 10.27 | 10.29 | 10.53 |
| FeO | nd | 0.36 | nd | 0.98 | 2.65 | 3.11 | 2.55 | 9.13 |
| La2O3 | 14.10 | 17.16 | 18.83 | 17.14 | 13.63 | 11.78 | 12.13 | 11.08 |
| Ce2O3 | 32.29 | 36.84 | 36.87 | 35.93 | 27.69 | 26.37 | 27.70 | 23.96 |
| Pr2O3 | 3.31 | 2.91 | 3.07 | 3.82 | 2.55 | 2.65 | 3.29 | 2.28 |
| Nd2O3 | 8.74 | 9.05 | 8.28 | 9.80 | 8.28 | 8.49 | 10.39 | 7.51 |
| Sm2O3 | 0.46 | nd | nd | 0.83 | 0.69 | 0.54 | 0.97 | 0.31 |
| UO2 | nd | nd | nd | nd | na | na | na | na |
| ThO2 | nd | nd | nd | 0.84 | nd | 0.67 | 0.93 | 0.88 |
| TOTAL= | 67.86 | 66.64 | 67.92 | 70.25 | 65.85 | 63.88 | 68.25 | 65.68 |
| La/Nd | 1.67 | 1.96 | 2.35 | 1.8 | 1.7 | 1.43 | 1.2 | 1.52 |

| | P | P | B | B | B | B | B | B |
|---|---|---|---|---|---|---|---|---|
| | C1515/5 | C1515/6 | C1515/1 | C1515/2 | C1515/3 | C1515/4 | C1515/5 | C1515/6 |
| CaO | 10.92 | 10.58 | 0.86 | 0.30 | 0.30 | 0.49 | 0.54 | 0.66 |
| FeO | na | 2.81 | 1.40 | 0.36 | 0.61 | 0.71 | 0.73 | na |
| La2O3 | 13.64 | 15.01 | 16.83 | 18.67 | 17.39 | 17.33 | 16.82 | 17.20 |
| Ce2O3 | 28.14 | 28.45 | 34.65 | 34.89 | 35.21 | 36.33 | 36.96 | 35.50 |
| Pr2O3 | 2.39 | 3.20 | 3.04 | 3.05 | 2.99 | 2.95 | 3.91 | 2.93 |
| Nd2O3 | 8.68 | 7.17 | 9.08 | 9.08 | 9.69 | 9.72 | 10.92 | 10.37 |
| Sm2O3 | 0.38 | 0.25 | nd | 0.38 | nd | nd | nd | nd |
| UO2 | na | na | na | na | na | na | na | na |
| ThO2 | na | 1.00 | 0.79 | nd | 1.40 | 0.52 | 0.84 | na |
| TOTAL= | 64.15 | 68.47 | 66.65 | 66.73 | 67.59 | 68.05 | 70.72 | 66.66 |
| La/Nd | 1.63 | 2.15 | 1.92 | 2.12 | 1.85 | 1.85 | 1.59 | |

eastern contact pegmatites
Ca-fluorocarbonates

| | P | B | B | S | | | | S |
|---|---|---|---|---|---|---|---|---|
| | C1449/1 | C1449/2 | C1449/3 | C1A/1 | C1A/2 | C1A/4 | C1A/5 | C1A/6 |
| CaO | 10.72 | 0.36 | 0.52 | 14.24 | 17.20 | 11.27 | 14.81 | 17.18 |
| FeO | 0.00 | 0.65 | 1.11 | 1.66 | nd | 0.63 | nd | nd |
| La2O3 | 17.40 | 23.73 | 15.73 | 6.76 | 12.38 | 14.02 | 11.75 | 12.05 |
| Ce2O3 | 27.33 | 35.75 | 35.36 | 22.17 | 24.56 | 29.36 | 25.05 | 25.80 |
| Pr2O3 | 1.89 | 3.00 | 3.06 | 2.32 | 2.52 | 2.30 | 2.71 | 2.60 |
| Nd2O3 | 9.06 | 7.53 | 12.00 | 11.00 | 7.63 | 8.33 | 7.97 | 7.56 |
| Sm2O3 | nd | nd | nd | 1.44 | nd | 0.92 | 0.64 | 0.38 |
| UO2 | nd | nd | nd | nd | 0.61 | nd | nd | na |
| ThO2 | 0.00 | nd | 0.68 | 0.97 | 2.17 | 1.54 | 3.82 | 0.34 |
| TOTAL= | 66.92 | 71.04 | 68.46 | 60.56 | 67.07 | 68.37 | 66.75 | 65.91 |
| La/Nd | 1.99 | 3.25 | 1.35 | 0.64 | 4.68 | 1.74 | 1.52 | 1.64 |

| | | | P | B | B | B | B | B |
|---|---|---|---|---|---|---|---|---|
| | C1A/7 | C1A/8 | C1A/9 | C1A/1 | C1A/2 | C1A/3 | C1A/4 | C1A/5 |
| CaO | 8.35 | 7.38 | 9.32 | 0.22 | 0.24 | 0.45 | 0.35 | 0.48 |
| FeO | 2.06 | 3.14 | 0.83 | 0.66 | nd | nd | 0.26 | nd |
| La2O3 | 14.86 | 16.31 | 14.88 | 18.38 | 18.84 | 18.48 | 18.71 | 18.78 |
| Ce2O3 | 28.29 | 29.53 | 28.06 | 33.93 | 35.82 | 35.84 | 35.25 | 33.12 |
| Pr2O3 | 2.92 | 2.46 | 2.15 | 2.59 | 3.09 | 2.43 | 3.85 | 3.36 |
| Nd2O3 | 7.82 | 7.33 | 6.11 | 9.43 | 9.47 | 7.93 | 9.85 | 8.72 |
| Sm2O3 | nd | nd | 0.41 | 0.85 | nd | nd | 1.31 | nd |
| UO2 | na | na | na | nd | nd | nd | nd | nd |
| ThO2 | 0.77 | 1.41 | 0.49 | 1.60 | 1.36 | 1.75 | 1.84 | 2.27 |
| TOTAL= | 65.07 | 67.56 | 62.25 | 67.66 | 68.82 | 66.88 | 71.42 | 66.73 |
| La/Nd | 1.96 | 2.30 | 2.51 | 2.00 | 2.05 | 2.40 | 1.96 | 2.22 |

| | B | B | B |
|---|---|---|---|
| | C1A/6 | C1A/7 | C1A/8 |
| CaO | nd | 0.30 | 0.35 |
| FeO | nd | nd | 0.23 |
| La2O3 | 19.70 | 20.32 | 17.64 |
| Ce2O3 | 36.80 | 34.75 | 35.18 |
| Pr2O3 | 3.02 | 3.34 | 3.87 |
| Nd2O3 | 9.02 | 8.56 | 9.79 |
| Sm2O3 | 0.48 | 0.46 | 0.39 |
| UO2 | na | na | na |
| ThO2 | 0.81 | 2.02 | 0.74 |
| TOTAL= | 69.83 | 69.75 | 68.19 |
| La/Nd | 2.26 | 2.44 | 1.86 |

quartz syenite dykes

| | B | B | B | B | B | B | B | B |
|---|---|---|---|---|---|---|---|---|
| | C1432/1 | C1432/2 | C1432/3 | C1432/4 | C1432/5 | C1432/6 | C1432/7 | C1432/8 |
| CaO | 0.14 | 0.17 | 0.42 | 0.60 | 0.39 | 0.11 | nd | nd |
| FeO | nd | 0.48 | 0.22 | 0.24 | nd | 0.24 | nd | nd |
| La2O3 | 22.63 | 19.53 | 19.06 | 20.92 | 21.77 | 19.35 | 18.98 | 21.86 |
| Ce2O3 | 36.60 | 38.43 | 37.54 | 35.12 | 38.14 | 36.68 | 37.88 | 35.38 |
| Pr2O3 | 3.33 | 3.69 | 3.27 | 1.96 | 3.45 | 2.94 | 2.69 | 2.81 |
| Nd2O3 | 7.96 | 9.41 | 9.95 | 8.90 | 8.70 | 9.89 | 10.24 | 8.09 |
| Sm2O3 | 0.54 | 0.62 | 0.66 | 0.57 | nd | 0.80 | 1.05 | 0.51 |
| UO2 | nd | nd | nd | nd | nd | nd | nd | nd |
| ThO2 | 0.00 | 0.41 | 0.34 | 1.32 | nd | nd | nd | 0.57 |
| TOTAL= | 71.20 | 72.75 | 71.47 | 69.62 | 72.45 | 70.02 | 70.84 | 69.22 |
| La/Nd | 2.93 | 2.15 | 1.98 | 2.43 | 2.59 | 2.02 | 1.91 | 2.78 |

| | B | P | P | P | P | P | P | P |
|---|---|---|---|---|---|---|---|---|
| | C1432/9 | C1432/1 | C1432/2 | C1432/3 | C1432/4 | C1432/5 | C1432/6 | C1432/7 |
| CaO | nd | 10.65 | 9.22 | 10.23 | 10.74 | 10.45 | 10.89 | 10.51 |
| FeO | 0.35 | nd | 12.63 | nd | 1.00 | 0.25 | nd | 0.54 |
| La2O3 | 17.97 | 15.19 | 18.54 | 16.54 | 15.18 | 16.08 | 14.91 | 15.62 |
| Ce2O3 | 37.24 | 29.46 | 22.67 | 29.54 | 30.04 | 28.30 | 30.63 | 29.44 |
| Pr2O3 | 4.47 | 2.64 | 1.65 | 2.60 | 2.54 | 2.40 | 2.30 | 2.33 |
| Nd2O3 | 10.84 | 9.18 | 4.30 | 9.20 | 8.78 | 8.08 | 7.98 | 8.91 |
| Sm2O3 | 0.95 | 0.79 | nd | nd | nd | 0.45 | nd | 1.01 |
| UO2 | nd | nd | nd | nd | nd | nd | nd | nd |
| ThO2 | 0.45 | nd | 0.42 | nd | nd | nd | nd | nd |
| TOTAL= | 72.27 | 67.92 | 69.42 | 68.11 | 68.29 | 66.02 | 66.71 | 68.35 |
| La/Nd | 1.71 | 1.70 | 4.45 | 1.86 | 1.78 | 2.05 | 1.93 | 1.82 |

| | P | P | P | S | S | S | S |
|---|---|---|---|---|---|---|---|
| | C1432/8 | C1432/9 | C1432/10 | C1432/1 | C1432/2 | C1432/3 | C1432/4 |
| CaO | 10.59 | 10.65 | 10.83 | 17.56 | 19.00 | 17.63 | 18.20 |
| FeO | nd | nd | 0.34 | nd | 0.32 | nd | 0.18 |
| La2O3 | 16.42 | 15.91 | 14.16 | 12.11 | 12.68 | 12.72 | 12.70 |
| Ce2O3 | 28.00 | 30.76 | 30.59 | 25.17 | 24.12 | 26.08 | 25.37 |
| Pr2O3 | 3.06 | 2.23 | 2.66 | 2.98 | 1.27 | 2.87 | 1.99 |
| Nd2O3 | 9.75 | 8.52 | 9.37 | 8.28 | 8.26 | 8.97 | 7.39 |
| Sm2O3 | 1.11 | nd | 0.62 | 0.74 | 0.82 | 0.74 | 0.39 |
| UO2 | nd | nd | nd | nd | nd | nd | nd |
| ThO2 | nd | nd | nd | 0.34 | nd | nd | nd |
| TOTAL= | 66.21 | 68.94 | 68.07 | 68.57 | 67.18 | 66.48 | 69.01 |
| La/Nd | 1.74 | 1.93 | 1.56 | 1.52 | 1.59 | 1.46 | 1.77 |

| | south eastern ferro-augite syenite | | | | CENTRE III fluorocarbonates ferro-edenite syenites | | | |
|---|---|---|---|---|---|---|---|---|
| | B | P | | | B | B | B | B |
| | C68/2 | C68/3 | C68/4 | C68/5 | C2025/1 | C2025/2 | C2025/3 | C2025/4 |
| CaO | 1.36 | 10.40 | 12.14 | 2.10 | 0.09 | 0.22 | nd | 0.38 |
| FeO | nd | 2.14 | 0.35 | 0.73 | nd | nd | nd | nd |
| La2O3 | 15.04 | 9.69 | 8.70 | 14.67 | 18.63 | 9.48 | 19.94 | 20.70 |
| Ce2O3 | 31.26 | 24.43 | 22.56 | 33.16 | 37.47 | 35.31 | 34.95 | 36.56 |
| Pr2O3 | 2.00 | 2.07 | 2.35 | 3.15 | 3.14 | 5.00 | 3.44 | 3.48 |
| Nd2O3 | 10.29 | 9.97 | 11.26 | 10.43 | 8.54 | 19.21 | 11.05 | 7.73 |
| Sm2O3 | 0.52 | 0.88 | 0.77 | 0.51 | 0.02 | 1.40 | 0.61 | nd |
| UO2 | na | na | na | na | nd | nd | nd | 0.51 |
| ThO2 | 1.67 | 1.07 | 1.41 | 0.79 | nd | nd | nd | nd |
| TOTAL= | 62.14 | 60.65 | 59.54 | 65.53 | 67.97 | 70.62 | 69.99 | 69.36 |
| La/Nd | | | | | 2.24 | 0.50 | 1.86 | 2.77 |

| | B | B | B | | | | | |
|---|---|---|---|---|---|---|---|---|
| | C2025/5 | C2025/6 | C2025/7 | C2122/1 | C2122/2 | C2122/3 | C2122/4 | C2129/1 |
| CaO | nd | nd | nd | 2.57 | 4.80 | 4.32 | 7.77 | 6.30 |
| FeO | 0.24 | 0.29 | nd | 0.44 | 3.95 | 1.74 | 0.66 | 2.03 |
| La2O3 | 20.16 | 8.82 | 22.36 | 17.63 | 8.55 | 31.48 | 18.06 | 17.28 |
| Ce2O3 | 38.10 | 36.28 | 36.10 | 31.71 | 39.39 | 8.91 | 29.00 | 29.66 |
| Pr2O3 | 3.57 | 5.01 | 2.99 | 2.27 | 2.39 | 5.32 | 2.76 | 3.50 |
| Nd2O3 | 6.99 | 17.95 | 6.76 | 9.25 | 5.99 | 13.61 | 7.20 | 7.10 |
| Sm2O3 | 1.00 | 0.92 | nd | nd | nd | 1.19 | 1.03 | 0.87 |
| UO2 | nd | nd | nd | nd | nd | nd | nd | nd |
| ThO2 | nd | 0.68 | nd | nd | 1.11 | 0.93 | 0.76 | nd |
| TOTAL= | 70.06 | 69.95 | 68.21 | 63.87 | 66.18 | 67.5 | 67.24 | 66.74 |
| La/Nd | 2.99 | 0.51 | 3.41 | 1.98 | 1.47 | 2.39 | 2.60 | 2.52 |

| | | P | B | B | S | S | S | B |
|---|---|---|---|---|---|---|---|---|
| | C2211/1 | C2211/2 | C2211/3 | C2211/4 | C2217/1 | C2217/2 | C2217/3 | C2217/4 |
| CaO | 3.09 | 10.35 | 0.17 | 0.95 | 17.42 | 18.75 | 15.78 | 0.31 |
| FeO | 0.74 | 4.39 | nd | nd | 2.20 | 2.38 | 2.75 | nd |
| La2O3 | 14.48 | 11.63 | 16.76 | 18.73 | 9.63 | 8.80 | 11.05 | 17.11 |
| Ce2O3 | 31.70 | 25.85 | 35.73 | 35.12 | 21.79 | 21.44 | 23.84 | 36.40 |
| Pr2O3 | 3.44 | 3.20 | 3.92 | 2.49 | 3.11 | 2.42 | 2.35 | 3.80 |
| Nd2O3 | 8.73 | 8.77 | 10.21 | 8.64 | 7.52 | 7.32 | 7.63 | 10.53 |
| Sm2O3 | 0.79 | 0.64 | 0.40 | 0.33 | 0.67 | 0.77 | 0.60 | 0.50 |
| UO2 | na | na | na | na | na | na | na | na |
| ThO2 | 3.30 | nd | 1.09 | 2.32 | 1.77 | 1.84 | 1.34 | 0.74 |
| TOTAL= | 66.27 | 64.83 | 68.29 | 68.59 | 64.11 | 63.72 | 65.34 | 69.39 |
| La/Nd | 1.72 | 1.37 | 1.69 | 2.23 | 1.32 | 1.24 | 1.50 | 1.68 |

| | quartz syenite B | | | | B | | B | |
|---|---|---|---|---|---|---|---|---|
| | C2217/5 | C2040/1 | C2040/2 | C2040/3 | C2040/4 | C2040/5 | C2112/1 | C2112/2 |
| CaO | 1.26 | 5.61 | 15.47 | 5.57 | 1.36 | 2.63 | 1.71 | 2.38 |
| FeO | 0.95 | 1.05 | 4.85 | 0.47 | nd | 0.76 | 1.38 | 1.01 |
| La2O3 | 17.03 | 13.78 | 12.82 | 15.10 | 20.70 | 20.81 | 16.72 | 18.11 |
| Ce2O3 | 35.58 | 33.55 | 26.12 | 32.22 | 36.47 | 32.72 | 36.70 | 33.42 |
| Pr2O3 | 3.97 | 3.63 | 2.52 | 2.47 | 2.93 | 2.60 | 3.06 | 2.16 |
| Nd2O3 | 10.33 | 6.95 | 5.93 | 7.79 | 7.96 | 7.39 | 8.24 | 8.23 |
| Sm2O3 | 0.60 | nd | nd | 0.47 | nd | nd | nd | nd |
| UO2 | na | nd | nd | 0.64 | nd | nd | na | na |
| ThO2 | 0.60 | 3.45 | 1.55 | 3.86 | 0.63 | 0.53 | 0.88 | nd |
| TOTAL= | 70.32 | 68.02 | 69.26 | 68.59 | 70.05 | 67.44 | 68.69 | 65.31 |
| La/Nd | 1.70 | 2.05 | 2.24 | 2.01 | 2.68 | 2.91 | 2.09 | 2.27 |

| | | B | B | B | B | B | B |
|---|---|---|---|---|---|---|---|
| | C2112/3 | C2116/1 | C2116/2 | C2454/1 | C2454/2 | C2454/3 | C2454/4 |
| CaO | 2.63 | 1.16 | 1.36 | nd | 0.52 | 1.03 | nd |
| FeO | 0.80 | nd | nd | nd | nd | 0.29 | 1.59 |
| La2O3 | 16.89 | 15.67 | 17.97 | 18.41 | 17.97 | 14.78 | 18.82 |
| Ce2O3 | 33.05 | 34.82 | 34.93 | 36.67 | 34.09 | 32.98 | 35.39 |
| Pr2O3 | 2.58 | 2.45 | 3.61 | 3.53 | 3.04 | 2.73 | 4.13 |
| Nd2O3 | 7.72 | 10.01 | 9.65 | 9.91 | 10.42 | 10.85 | 9.04 |
| Sm2O3 | 0.46 | nd | 0.66 | 0.39 | 0.45 | 0.58 | 0.59 |
| UO2 | na | na | na | na | na | na | na |
| ThO2 | 1.12 | 0.73 | 1.36 | 0.65 | 0.88 | 2.62 | 1.86 |
| TOTAL= | 65.25 | 64.88 | 68.34 | 69.56 | 67.37 | 65.86 | 71.42 |
| La/Nd | 2.26 | 1.61 | 1.93 | 1.92 | 1.78 | 1.40 | 2.15 |

contaminated ferro-edenite syenite

| | | | | | | B | B | B |
|---|---|---|---|---|---|---|---|---|
| | C2028/1 | C2028/2 | C2028/3 | C2028/4 | C2028/5 | C2028/6 | C2028/7 | C2028/8 |
| CaO | 4.25 | 4.36 | 4.30 | 4.26 | 1.23 | nd | nd | 1.10 |
| FeO | 0.69 | 2.67 | 0.62 | 0.57 | 0.55 | nd | 0.73 | 0.57 |
| La2O3 | 16.84 | 16.07 | 21.98 | 22.70 | 19.35 | 20.55 | 18.99 | 21.81 |
| Ce2O3 | 30.76 | 27.56 | 27.98 | 30.00 | 37.44 | 35.89 | 36.28 | 34.96 |
| Pr2O3 | 2.81 | 2.64 | 1.66 | 2.23 | 3.41 | 1.93 | 2.99 | 3.15 |
| Nd2O3 | 7.61 | 7.05 | 5.66 | 5.61 | 7.66 | 8.17 | 7.65 | 7.41 |
| Sm2O3 | nd | nd | 0.54 | nd | nd | nd | nd | nd |
| UO2 | nd | nd | nd | nd | nd | nd | nd | nd |
| ThO2 | 1.33 | 4.22 | 2.51 | 1.11 | nd | nd | 0.55 | nd |
| SiO2 | 2.03 | 4.06 | na | na | 1.69 | na | na | na |
| Cl | 0.64 | 0.20 | na | na | nd | na | na | na |
| TOTAL= | 66.96 | 68.83 | 65.25 | 66.48 | 71.33 | 66.54 | 67.19 | 69.00 |
| La/Nd | 2.29 | 2.36 | 4.03 | 4.19 | 2.61 | 2.60 | 2.56 | 3.04 |

syntaxial intergrowths

| | B | | S | B | P | B | P | B |
|---|---|---|---|---|---|---|---|---|
| | C1A/9 | C1A/9 | C1A/9 | C1A/10 | C1A/10 | C1A/11 | C1A/11 | C1A/12 |
| CaO | 0.34 | 13.40 | 17.21 | 0.36 | 11.51 | 0.22 | 8.77 | 1.11 |
| FeO | nd | 0.34 | 1.91 | 0.41 | 1.60 | nd | 2.2 | nd |
| La2O3 | 20.99 | 14.36 | 10.03 | 17.92 | 11.90 | 19.35 | 13.01 | 18.44 |
| Ce2O3 | 36.05 | 25.69 | 20.64 | 35.05 | 28.43 | 37.09 | 29 | 36.72 |
| Pr2O3 | 2.38 | 2.30 | 1.16 | 3.12 | 2.44 | 2.91 | 1.68 | 2.77 |
| Nd2O3 | 8.46 | 8.02 | 7.28 | 10.06 | 8.66 | 8.53 | 8.09 | 10.14 |
| Sm2O3 | 0.60 | nd | 1.21 | 0.83 | 0.52 | 0.63 | 0.94 | nd |
| UO2 | na | na | na | na | na | na | na | na |
| ThO2 | 1.67 | 1.66 | nd | 2.04 | nd | 1.07 | 1.78 | 0.44 |
| TOTAL= | 70.49 | 65.77 | 59.44 | 69.79 | 65.07 | 69.8 | 65.46 | 69.61 |
| La/Nd | 2.57 | 1.84 | 1.43 | 1.84 | 1.42 | 2.34 | 1.66 | 1.88 |

| | P | B | P | B | P | P | S | B |
|---|---|---|---|---|---|---|---|---|
| | C1A/12 | C1A/13 | C1A/13 | C1A/14 | C1A/14 | C1432/11 | C1432/11 | C1432/12 |
| CaO | 10.68 | 0.22 | 10.79 | 0.37 | 10.20 | 10.67 | 17.10 | nd |
| FeO | 2.79 | 0.29 | nd | 0.35 | 2.73 | 0.46 | nd | nd |
| La2O3 | 12.74 | 20.01 | 14.42 | 20.67 | 13.33 | 16.95 | 12.08 | 19.17 |
| Ce2O3 | 25.83 | 35.59 | 29.55 | 35.16 | 25.11 | 27.36 | 24.45 | 37.14 |
| Pr2O3 | 0.51 | 2.96 | 2.1 | 2.66 | 2.67 | 1.60 | 2.49 | 2.04 |
| Nd2O3 | 8.05 | 8.94 | 8.21 | 9.07 | 6.82 | 8.58 | 8.64 | 9.21 |
| Sm2O3 | nd | 0.79 | 0.59 | nd | 0.52 | 0.40 | 0.59 | nd |
| UO2 | na | na | na | na | na | na | na | na |
| ThO2 | nd | 0.77 | 0.46 | 1.97 | 1.99 | nd | nd | 0.42 |
| TOTAL= | 60.6 | 69.57 | 66.1 | 70.26 | 63.38 | 66.01 | 65.35 | 67.98 |
| La/Nd | 1.63 | 2.313 | 1.815 | 2.353 | 2.03 | 2.04 | 1.45 | 2.18 |

| | P | P | S | B | P | B | P |
|---|---|---|---|---|---|---|---|
| | C1432/13 | C1432/14 | C1432/14 | C1432/15 | C1432/15 | C1432/16 | C1432/16 |
| CaO | 10.81 | nd | 18.16 | nd | 10.66 | 0.21 | 10.38 |
| FeO | 0.42 | nd | 0.36 | nd | nd | nd | 0.36 |
| La2O3 | 17.30 | 21.87 | 12.53 | 22.70 | 16.61 | 22.98 | 14.70 |
| Ce2O3 | 26.96 | 36.95 | 25.30 | 37.38 | 30.24 | 36.88 | 29.20 |
| Pr2O3 | 2.23 | 2.96 | 1.45 | 3.03 | 2.62 | 1.98 | 3.76 |
| Nd2O3 | 9.90 | 7.14 | 7.67 | 8.39 | 7.96 | 7.72 | 9.06 |
| Sm2O3 | 1.50 | nd | 0.62 | nd | nd | nd | 1.57 |
| UO2 | na | na | na | na | na | na | na |
| ThO2 | nd | 1.00 | nd | 0.44 | nd | nd | nd |
| TOTAL= | 69.13 | 69.92 | 66.09 | 71.94 | 68.09 | 69.78 | 69.02 |
| La/Nd | 1.80 | 3.17 | 1.69 | 2.80 | 2.15 | 3.08 | 1.68 |

CHEYKINITES APPENDIX 2.2

Centre I: Contaminated Ferro-edenite Syenite Quartz syenite

| | C2028/1 | C2028/2 | C2036/1 | C2036/2 | C2454/1 | C2454/2 | C2454/3 | 2454/4 | 2454/5 |
|---|---|---|---|---|---|---|---|---|---|
| FEO | 11.96 | 11.93 | 11.75 | 11.78 | 11.25 | 12.02 | 11.55 | 11.62 | 11.44 |
| UO2 | na | na | na | na | na | na | na | na | na |
| THO2 | 0.84 | 2.10 | 3.82 | 2.69 | 0.76 | 0.97 | 0.80 | 0.87 | 1.22 |
| ZRO2 | 2.11 | 0.00 | nd | 0.00 | 0.00 | 0.63 | 0.76 | 1.10 | 1.79 |
| NB2O5 | 4.55 | 3.10 | 2.32 | 1.81 | 2.89 | 2.77 | 2.00 | 2.75 | 3.14 |
| LA2O3 | 11.47 | 11.73 | 12.53 | 12.62 | 11.40 | 10.60 | 10.97 | 11.36 | 11.08 |
| CE2O3 | 19.11 | 22.70 | 20.54 | 21.10 | 22.09 | 21.00 | 21.49 | 22.85 | 20.32 |
| PR2O3 | 1.24 | 1.74 | 1.89 | 0.91 | 2.41 | 1.89 | 2.59 | 1.99 | 1.21 |
| ND2O3 | 4.21 | 4.40 | 3.86 | 3.97 | 5.56 | 5.35 | 5.95 | 4.91 | 3.92 |
| SM2O3 | 0.00 | 0.62 | nd | 0.00 | 0.00 | 0.72 | 0.00 | 0.00 | 0.00 |
| GD2O3 | 0.00 | 0.00 | nd | 0.27 | 0.00 | 0.00 | 0.00 | 0.00 | 0.00 |
| CAO | 4.40 | 2.63 | 3.32 | 3.66 | 4.17 | 3.73 | 3.82 | 3.52 | 5.01 |
| TIO2 | 14.25 | 14.58 | 16.62 | 16.58 | 16.75 | 16.10 | 16.90 | 16.50 | 16.66 |
| SIO2 | 19.94 | 19.42 | 20.83 | 19.89 | 20.67 | 19.69 | 20.08 | 19.68 | 20.42 |
| Al2O3 | na | na | na | na | na | na | na | na | na |
| MnO | na | na | na | na | na | na | na | na | na |
| TOTAL= | 94.08 | 94.98 | 97.50 | 95.33 | 98.03 | 95.51 | 96.96 | 97.20 | 96.26 |
| RE2O3= | 36.03 | 41.19 | 38.82 | 38.6 | 41.46 | 39.56 | 41.00 | 41.11 | 36.53 |
| Ca | 1.003 | 0.616 | 0.740 | 0.837 | 0.921 | 0.849 | 0.856 | 0.792 | 1.106 |
| La | 0.900 | 0.946 | 0.962 | 0.993 | 0.866 | 0.831 | 0.846 | 0.880 | 0.842 |
| Ce | 1.489 | 1.817 | 1.565 | 1.649 | 1.667 | 1.636 | 1.646 | 1.756 | 1.533 |
| Pr | 0.096 | 0.139 | 0.143 | 0.071 | 0.181 | 0.146 | 0.197 | 0.152 | 0.091 |
| Nd | 0.320 | 0.344 | 0.288 | 0.303 | 0.409 | 0.406 | 0.445 | 0.368 | 0.289 |
| Sm | ---- | 0.047 | --- | ---- | ---- | 0.053 | ---- | --- | --- |
| Gd | ---- | ---- | --- | 0.019 | ---- | ---- | ---- | --- | --- |
| Mn | ---- | ---- | ---- | ---- | ---- | ---- | ---- | 0.042 | 0.057 |
| Th | 0.041 | 0.105 | 0.181 | 0.131 | 0.036 | 0.047 | 0.038 | ---- | ---- |
| U | ---- | ---- | ---- | ---- | ---- | ---- | ---- | ---- | ---- |
| | 3.849 | 4.014 | 3.879 | 4.003 | 4.080 | 3.968 | 4.028 | 3.99 | 3.918 |
| Ti | 2.280 | 2.398 | 2.601 | 2.661 | 2.596 | 2.573 | 2.659 | 2.605 | 2.583 |
| Nb | 0.438 | 0.306 | 0.218 | 0.175 | 0.269 | 0.266 | 0.189 | 0.261 | 0.293 |
| Fe | 2.128 | 2.182 | 2.045 | 2.102 | 1.939 | 2.137 | 2.021 | 2.040 | 1.972 |
| Zr | 0.219 | ---- | nd | ---- | nd | 0.065 | 0.078 | 0.113 | 0.180 |
| | 5.065 | 4.886 | 4.864 | 4.938 | 4.804 | 5.041 | 4.947 | 5.019 | 5.028 |
| Si | 4.243 | 4.247 | 4.334 | 4.245 | 4.260 | 4.185 | 4.200 | 4.131 | 4.209 |
| Al | ---- | ---- | ---- | ---- | ---- | ---- | ---- | ---- | ---- |
| | 4.243 | 4.247 | 4.334 | 4.245 | 4.260 | 4.185 | 4.200 | 4.131 | 4.209 |
| TOTAL= | 13.157 | 13.147 | 13.077 | 13.186 | 13.140 | 13.194 | 13.175 | 13.140 | 13.155 |

| | 2454/6 | C2454/7 | C2923/1 | C2923/2 | C2923/3 | C2923/4 | C2923/5 | C2923/6 | C2923/7 |
|---|---|---|---|---|---|---|---|---|---|
| FEO | 11.42 | 10.87 | 11.29 | 11.42 | 12.18 | 12.02 | 11.65 | 11.62 | 11.59 |
| UO2 | na | na | nd | 1.08 | 0.71 | nd | nd | nd | 0.95 |
| THO2 | 1.13 | 0.98 | 1.13 | 0.52 | 1.93 | 0.82 | 0.44 | 1.34 | 0.52 |
| ZRO2 | 1.07 | 0.88 | 0.85 | 1.29 | 0.50 | nd | 0.75 | nd | 1.09 |
| NB2O5 | 3.43 | 2.61 | 2.86 | 2.88 | 4.23 | 3.53 | 2.09 | 4.08 | 3.04 |
| LA2O3 | 10.79 | 11.09 | 9.87 | 10.01 | 10.90 | 10.20 | 10.98 | 10.57 | 11.32 |
| CE2O3 | 20.94 | 21.45 | 20.39 | 19.93 | 22.10 | 21.29 | 20.13 | 20.84 | 21.56 |
| PR2O3 | 2.36 | 1.88 | 1.75 | 1.61 | 1.82 | 1.92 | 0.53 | 0.54 | 1.86 |
| ND2O3 | 5.48 | 5.04 | 5.83 | 5.23 | 5.98 | 6.67 | 4.14 | 4.32 | 4.75 |
| SM2O3 | 0.90 | nd | nd | nd | tr | nd | tr | nd | nd |
| GD2O3 | 0.00 | nd | na | na | na | na | na | na | na |
| CAO | 4.09 | 4.08 | 3.48 | 4.46 | 2.93 | 2.89 | 4.04 | 3.36 | 4.45 |
| TIO2 | 16.76 | 17.32 | 15.98 | 16.60 | 15.29 | 15.69 | 17.07 | 15.50 | 17.42 |
| SIO2 | 20.85 | 20.54 | 20.32 | 19.83 | 20.70 | 20.37 | 20.07 | 20.28 | 21.18 |
| Al2O3 | na | na | nd | 0.60 | 0.27 | 0.41 | 0.86 | 0.47 | 0.54 |
| MnO | na | na | nd | nd | tr | tr | nd | nd | nd |
| TOTAL= | 99.25 | 96.74 | 93.81 | 95.46 | 99.54 | 95.81 | 92.75 | 92.92 | 100.27 |
| RE2O3= | 40.47 | 39.46 | 37.84 | 36.78 | 40.8 | 40.08 | 35.78 | 36.27 | 39.49 |
| Ca | 0.889 | 0.903 | 0.795 | 0.997 | 0.645 | 0.652 | 0.913 | 0.768 | 0.947 |
| La | 0.807 | 0.845 | 0.776 | 0.771 | 0.826 | 0.792 | 0.854 | 0.832 | 0.829 |
| Ce | 1.555 | 1.622 | 1.592 | 1.523 | 1.663 | 1.640 | 1.554 | 1.627 | 1.567 |
| Pr | 0.174 | 0.142 | 0.136 | 0.122 | 0.136 | 0.147 | 0.041 | 0.042 | 0.135 |
| Nd | 0.397 | 0.372 | 0.444 | 0.390 | 0.439 | 0.501 | 0.312 | 0.329 | 0.337 |
| Sm | 0.063 | ---- | ---- | ---- | ---- | ---- | ---- | ---- | ---- |
| Gd | --- | ---- | ---- | ---- | ---- | ---- | ---- | ---- | ---- |
| Mn | 0.052 | ---- | ---- | ---- | ---- | ---- | ---- | ---- | ---- |
| Th | ---- | 0.046 | 0.055 | 0.025 | 0.090 | 0.039 | 0.021 | 0.065 | 0.023 |
| U | ---- | ---- | ---- | 0.050 | 0.032 | ---- | ---- | ---- | 0.042 |
| | 3.937 | 3.930 | 3.798 | 3.878 | 3.831 | 3.771 | 3.695 | 3.663 | 3.880 |
| Ti | 2.557 | 2.691 | 2.563 | 2.605 | 2.364 | 2.483 | 2.707 | 2.486 | 2.601 |
| Nb | 0.315 | 0.244 | 0.276 | 0.272 | 0.393 | 0.336 | 0.199 | 0.393 | 0.273 |
| Fe | 1.938 | 1.878 | 2.014 | 1.993 | 2.094 | 2.116 | 2.054 | 2.073 | 1.925 |
| Zr | 0.106 | 0.089 | 0.088 | 0.131 | 0.050 | ---- | 0.077 | ---- | 0.106 |
| | 4.916 | 4.902 | 4.941 | 5.001 | 4.901 | 4.935 | 5.037 | 4.952 | 4.905 |
| Si | 4.23 | 4.243 | 4.333 | 4.139 | 4.255 | 4.287 | 4.232 | 4.325 | 4.205 |
| Al | ---- | ---- | ---- | 0.148 | 0.065 | 0.102 | 0.214 | 0.118 | 0.126 |
| | 4.23 | 4.243 | 4.333 | 4.287 | 4.320 | 4.389 | 4.446 | 4.443 | 4.331 |
| TOTAL= | 13.083 | 13.075 | 13.072 | 13.166 | 13.052 | 13.095 | 13.178 | 13.058 | 13.116 |

| | C2923/8 | C2923/9 | 2923/10 | 2923/11 | 2116/1 | 2116/2 | 2116/3 | 2116/4 | 2116/5 |
|---|---|---|---|---|---|---|---|---|---|
| FEO | 12.61 | 11.52 | 11.22 | 11.98 | 10.93 | 11.19 | 11.35 | 11.73 | 12.97 |
| UO2 | nd | nd | 0.99 | nd | na | na | na | na | na |
| THO2 | 0.92 | 1.28 | 1.67 | 0.81 | 0.79 | 0.71 | 1.28 | 1.53 | 2.01 |
| ZRO2 | nd | 1.66 | 1.02 | 0.76 | 1.50 | 1.10 | 0.91 | 0.50 | nd |
| NB2O5 | 3.73 | 2.27 | 2.89 | 2.92 | 2.75 | 2.55 | 2.56 | 2.38 | 4.81 |
| LA2O3 | 10.74 | 11.10 | 12.34 | 10.94 | 10.21 | 11.10 | 11.44 | 10.91 | 10.45 |
| CE2O3 | 22.94 | 21.00 | 21.38 | 21.32 | 20.32 | 19.98 | 21.12 | 21.21 | 21.54 |
| PR2O3 | 2.31 | 1.49 | 1.03 | 1.86 | 2.76 | 2.28 | 1.74 | 1.34 | 1.69 |
| ND2O3 | 6.29 | 5.08 | 5.41 | 5.86 | 5.29 | 5.32 | 4.81 | 6.58 | 5.71 |
| SM2O3 | nd | nd | nd | nd | na | na | na | na | na |
| GD2O3 | na | na | na | na | na | na | na | na | na |
| CAO | 2.90 | 4.13 | 3.73 | 3.04 | 3.52 | 4.10 | 3.87 | 2.74 | 2.26 |
| TIO2 | 16.02 | 16.67 | 17.50 | 15.43 | 16.31 | 16.97 | 17.26 | 16.71 | 13.91 |
| SIO2 | 20.85 | 19.59 | 20.07 | 19.28 | 19.26 | 19.89 | 20.24 | 20.50 | 20.43 |
| Al2O3 | 0.41 | 0.27 | 0.61 | 0.61 | 0.47 | 0.53 | 0.54 | 0.61 | 0.54 |
| MnO | tr | nd | nd | nd | 0.21 | 0.22 | nd | nd | 0.19 |
| TOTAL= | 99.72 | 96.06 | 99.86 | 94.81 | 94.32 | 95.95 | 97.12 | 96.74 | 96.51 |
| RE2O3= | 42.28 | 38.67 | 40.16 | 39.98 | 38.58 | 38.68 | 39.11 | 40.04 | 39.39 |
| Ca | 0.633 | 0.929 | 0.811 | 0.699 | 0.805 | 0.915 | 0.854 | 0.611 | 0.512 |
| La | 0.807 | 0.860 | 0.924 | 0.866 | 0.804 | 0.852 | 0.869 | 0.837 | 0.814 |
| Ce | 1.711 | 1.614 | 1.588 | 1.676 | 1.588 | 1.523 | 1.592 | 1.615 | 1.666 |
| Pr | 0.171 | 0.114 | 0.076 | 0.146 | 0.215 | 0.173 | 0.131 | 0.102 | 0.130 |
| Nd | 0.458 | 0.381 | 0.392 | 0.449 | 0.403 | 0.396 | 0.354 | 0.489 | 0.431 |
| Sm | ---- | ---- | ---- | ---- | --- | --- | --- | --- | --- |
| Gd | ---- | ---- | ---- | ---- | --- | --- | --- | --- | --- |
| Mn | ---- | ---- | ---- | ---- | 0.038 | 0.039 | --- | --- | 0.034 |
| Th | 0.043 | 0.061 | 0.077 | 0.040 | 0.038 | 0.034 | 0.060 | 0.072 | 0.097 |
| U | ---- | ---- | 0.045 | ---- | ---- | ---- | ---- | ---- | ---- |
| | 3.823 | 3.959 | 3.913 | 3.876 | 3.891 | 3.932 | 3.860 | 3.726 | 3.684 |
| Ti | 2.455 | 2.633 | 2.671 | 2.492 | 2.619 | 2.657 | 2.673 | 2.614 | 2.211 |
| Nb | 0.344 | 0.216 | 0.265 | 0.283 | 0.265 | 0.240 | 0.238 | 0.224 | 0.460 |
| Fe | 2.149 | 2.023 | 1.904 | 2.151 | 1.951 | 1.948 | 1.954 | 2.040 | 2.292 |
| Zr | ---- | 0.170 | 0.101 | 0.080 | 0.156 | 0.112 | 0.091 | 0.051 | --- |
| | 4.948 | 5.042 | 4.941 | 5.006 | 4.991 | 4.957 | 4.956 | 4.929 | 4.963 |
| Si | 4.248 | 4.114 | 4.073 | 4.140 | 4.112 | 4.141 | 4.167 | 4.264 | 4.317 |
| Al | 0.098 | 0.067 | 0.146 | 0.154 | 0.118 | 0.130 | 0.131 | 0.150 | 0.135 |
| | 4.346 | 4.181 | 4.219 | 4.294 | 4.230 | 4.271 | 4.298 | 4.414 | 4.452 |
| TOTAL= | 13.117 | 13.182 | 13.073 | 13.176 | 13.112 | 13.160 | 13.114 | 13.069 | 13.099 |

Craddock Cove Red Syenites　　　　　Ferro-augite Syenites

| | C2920/1 | C2920/2 | C2920/3 | C2905/1 | C2905/2 | C2908/1 | C2909/1 | C2909/2 |
|---|---|---|---|---|---|---|---|---|
| FEO | 13.39 | 13.07 | 13.25 | 11.35 | 13.94 | 11.97 | 12.13 | 11.33 |
| UO2 | nd | nd | nd | na | na | nd | na | na |
| THO2 | nd | nd | nd | na | na | nd | na | na |
| ZRO2 | nd | nd | nd | nd | nd | nd | 1.61 | 1.54 |
| NB2O5 | 1.67 | 1.70 | 0.57 | nd | 7.21 | 0.44 | 5.01 | 3.41 |
| LA2O3 | 13.66 | 12.62 | 14.53 | 10.86 | 12.05 | 11.89 | 13.18 | 12.31 |
| CE2O3 | 24.96 | 23.61 | 24.78 | 21.56 | 25.35 | 24.44 | 21.97 | 20.40 |
| PR2O3 | 1.71 | 2.06 | 1.79 | 1.81 | 2.28 | 1.71 | 1.96 | 1.21 |
| ND2O3 | 5.09 | 6.30 | 5.11 | 6.53 | 6.06 | 6.73 | 4.23 | 4.24 |
| SM2O3 | nd | 0.47 | nd | nd | nd | 1.02 | nd | nd |
| GD2O3 | na | na | na | na | na | na | na | na |
| CAO | 1.03 | 0.95 | 1.05 | 2.24 | 1.09 | 1.24 | 2.31 | 3.13 |
| TIO2 | 16.47 | 16.31 | 16.25 | 18.52 | 9.51 | 18.48 | 14.31 | 16.77 |
| SIO2 | 19.16 | 18.68 | 18.02 | 19.52 | 20.07 | 19.86 | 18.79 | 19.75 |
| Al2O3 | 0.29 | nd | 0.43 | 0.62 | 0.77 | nd | nd | 0.20 |
| MnO | 0.40 | 0.35 | 0.35 | 0.29 | 0.38 | 0.59 | 0.42 | nd |
| TOTAL= | 97.83 | 96.12 | 96.13 | 93.3 | 98.71 | 98.37 | 95.92 | 94.29 |
| RE2O3= | 45.42 | 45.06 | 46.21 | 40.76 | 45.74 | 45.79 | 41.34 | 38.16 |
| | 0.236 | 0.222 | 0.248 | 0.515 | 0.251 | 0.279 | 0.534 | 0.708 |
| La | 1.075 | 1.016 | 1.182 | 0.860 | 0.957 | 0.920 | 1.048 | 0.959 |
| Ce | 1.951 | 1.887 | 2.001 | 1.695 | 1.998 | 1.876 | 1.735 | 1.577 |
| Pr | 0.133 | 0.164 | 0.144 | 0.142 | 0.179 | 0.131 | 0.154 | 0.093 |
| Nd | 0.388 | 0.491 | 0.403 | 0.501 | 0.466 | 0.504 | 0.326 | 0.320 |
| Sm | ---- | ---- | ---- | ---- | ---- | 0.074 | ---- | ---- |
| Gd | ---- | ---- | ---- | ---- | ---- | ---- | ---- | ---- |
| Mn | 0.072 | 0.065 | 0.065 | 0.053 | 0.069 | 0.105 | 0.077 | ---- |
| Th | ---- | ---- | ---- | ---- | ---- | ---- | ---- | ---- |
| U | ---- | ---- | ---- | ---- | ---- | ---- | ---- | ---- |
| | 3.855 | 3.845 | 4.043 | 3.766 | 3.920 | 3.889 | 3.874 | 3.657 |
| Ti | 2.644 | 2.678 | 2.695 | 2.990 | 1.540 | 2.914 | 2.321 | 2.663 |
| Nb | 0.161 | 0.168 | 0.057 | ---- | 0.702 | 0.042 | 0.489 | 0.325 |
| Fe | 2.390 | 2.387 | 2.444 | 2.038 | 2.510 | 2.099 | 2.188 | 2.000 |
| Zr | ---- | ---- | ---- | ---- | ---- | ---- | 0.169 | 0.159 |
| | 5.195 | 5.233 | 5.196 | 5.028 | 4.752 | 5.055 | 5.167 | 5.147 |
| Si | 4.090 | 4.079 | 3.974 | 4.191 | 4.321 | 4.164 | 4.052 | 4.169 |
| Al | 0.073 | ---- | 0.112 | 0.157 | 0.195 | ---- | ---- | 0.050 |
| | 4.163 | 4.079 | 4.086 | 4.348 | 4.516 | 4.164 | 4.052 | 4.219 |
| TOTAL= | 13.213 | 13.157 | 13.325 | 13.142 | 13.188 | 13.108 | 13.093 | 13.023 |

PYROCHLORE : Centre III APPENDIX Z.3

| | Ferro-edenite | Contaminated ferro-edenite syenite | | | | | | |
|---|---|---|---|---|---|---|---|---|
| | 2025/1 | 2028/1 | 2028/3 | 2028/4 | 2028/5 | 2028/6 | 2028/7 | 2028/9 |
| SiO2 | 5.74 | 4.36 | 4.21 | 7.93 | 6.23 | 4.15 | 6.64 | 6.66 |
| CaO | 3.95 | 5.74 | 5.49 | 3.44 | 8.40 | 5.28 | 2.80 | 8.50 |
| TiO2 | 12.30 | 0.67 | 0.90 | 8.51 | 9.23 | 1.25 | 0.82 | 8.59 |
| MnO | nd | 0.14 | 0.25 | 0.13 | 0.38 | 0.14 | nd | 0.53 |
| FeO | 3.25 | 4.12 | 4.05 | 2.32 | 3.15 | 4.50 | 1.66 | 2.46 |
| Ta2O5 | nd | 0.44 | 0.52 | 3.10 | 2.85 | nd | 0.66 | 2.52 |
| Nb2O5 | 41.65 | 47.66 | 49.96 | 36.76 | 45.82 | 48.82 | 38.16 | 45.87 |
| La2O3 | 0.40 | 1.29 | 1.24 | 2.01 | 1.59 | 1.25 | 0.95 | 1.55 |
| Ce2O3 | 9.93 | 5.44 | 6.75 | 9.94 | 4.48 | 7.05 | 4.13 | 4.59 |
| Pr2O3 | 1.60 | 0.92 | 0.97 | 1.60 | 0.67 | 1.40 | 0.65 | 0.67 |
| Nd2O3 | 6.29 | 3.94 | 4.59 | 5.94 | 1.58 | 5.08 | 4.72 | 1.54 |
| Sm2O3 | 1.02 | 0.90 | 0.79 | 0.54 | 0.18 | 1.04 | 1.23 | 0.20 |
| ThO2 | nd | 10.63 | 10.00 | 3.12 | 2.60 | 7.80 | 13.35 | 2.28 |
| UO2 | 1.16 | 0.31 | 0.45 | 5.85 | 7.71 | 0.39 | 2.28 | 7.54 |
| Y2O3 | 1.15 | 2.25 | 2.37 | 1.34 | 1.68 | 2.31 | 10.20 | 0.96 |
| PbO | 0.51 | 0.60 | 0.64 | 0.71 | 0.72 | 0.47 | 0.51 | 0.54 |
| WO3 | nd | na | na | na | na | na | na | na |
| SrO | na | na | na | na | na | na | na | na |
| BaO | 0.36 | nd | nd | nd | 0.41 | nd | nd | nd |
| TOTAL= | 89.31 | 89.41 | 93.18 | 93.24 | 97.68 | 90.93 | 88.76 | 95.00 |
| RE2O3= | 19.24 | 12.49 | 14.34 | 20.03 | 8.50 | 15.82 | 11.68 | 8.55 |
| | | | | | | | | |
| Ca | 0.264 | 0.423 | 0.389 | 0.235 | 0.524 | 0.381 | 0.214 | 0.539 |
| La | 0.009 | 0.033 | 0.030 | 0.047 | 0.034 | 0.031 | 0.025 | 0.034 |
| Ce | 0.227 | 0.137 | 0.164 | 0.232 | 0.096 | 0.174 | 0.108 | 0.099 |
| Pr | 0.036 | 0.023 | 0.023 | 0.037 | 0.014 | 0.034 | 0.017 | 0.014 |
| Nd | 0.140 | 0.097 | 0.108 | 0.135 | 0.033 | 0.122 | 0.120 | 0.033 |
| Sm | 0.022 | 0.021 | 0.018 | 0.012 | 0.004 | 0.024 | 0.030 | 0.004 |
| Y | 0.038 | 0.082 | 0.083 | 0.045 | 0.052 | 0.083 | 0.387 | 0.030 |
| U | 0.016 | 0.005 | 0.007 | 0.083 | 0.100 | 0.006 | 0.036 | 0.099 |
| Th | ---- | 0.166 | 0.151 | 0.045 | 0.034 | 0.119 | 0.217 | 0.031 |
| Mn | ---- | 0.008 | 0.014 | 0.007 | 0.019 | 0.008 | ---- | 0.027 |
| Fe | 0.170 | 0.237 | 0.224 | 0.124 | 0.153 | 0.253 | 0.099 | 0.122 |
| Sr | ---- | ---- | ---- | ---- | ---- | ---- | ---- | ---- |
| Pb | 0.009 | 0.011 | 0.011 | 0.012 | 0.011 | 0.009 | 0.010 | 0.009 |
| | 0.931 | 1.243 | 1.211 | 1.014 | 1.074 | 1.244 | 1.263 | 1.041 |
| | | | | | | | | |
| Ti | 0.577 | 0.035 | 0.045 | 0.407 | 0.404 | 0.063 | 0.044 | 0.382 |
| Nb | 1.175 | 1.481 | 1.494 | 1.058 | 1.207 | 1.485 | 1.230 | 1.227 |
| Ta | ---- | 0.008 | 0.009 | 0.054 | 0.045 | ---- | 0.013 | 0.041 |
| W | ---- | ---- | ---- | ---- | ---- | ---- | ---- | ---- |
| Si | 0.358 | 0.300 | 0.279 | 0.505 | 0.363 | 0.279 | 0.473 | 0.394 |
| Ba | ---- | ---- | ---- | ---- | 0.009 | ---- | ---- | ---- |
| | 2.110 | 1.82 | 1.83 | 2.02 | 2.03 | 1.83 | 1.76 | 2.04 |
| | | | | | | | | |
| Total= | 3.041 | 3.07 | 3.04 | 3.04 | 3.10 | 3.07 | 3.02 | 3.09 |

| Quartz syenite | | | | | | rim | core | | |
|---|---|---|---|---|---|---|---|---|---|
| | 2040/1 | 2040/2 | 2040/3 | 2040/4 | 2040/5 | 2112/1 | 2112/1 | 2112/2 | 2112/3 |
| SiO2 | 15.87 | 2.38 | 10.76 | 2.63 | 12.58 | 3.65 | nd | 1.65 | 5.57 |
| CaO | 3.73 | 5.08 | 4.85 | 4.16 | 2.33 | 2.83 | 1.54 | 1.30 | 4.25 |
| TiO2 | 8.52 | 11.04 | 9.82 | 0.30 | 0.90 | 0.26 | nd | 0.32 | 0.20 |
| MnO | nd | 0.45 | 0.35 | nd | nd | 0.99 | nd | 0.33 | 0.70 |
| FeO | 2.07 | 0.79 | 0.74 | 0.74 | 1.33 | 3.17 | nd | 0.37 | 2.64 |
| Ta205 | 4.87 | 5.48 | 6.50 | 0.41 | nd | 2.10 | 0.59 | 2.26 | 2.80 |
| Nb205 | 26.74 | 48.70 | 45.40 | 38.26 | 35.15 | 44.85 | 43.17 | 41.93 | 50.28 |
| La203 | 0.97 | 0.74 | 1.07 | 0.97 | 1.89 | 1.13 | 5.17 | 5.43 | 0.30 |
| Ce203 | 5.63 | 3.05 | 3.15 | 4.72 | 4.82 | 10.30 | 19.19 | 20.08 | 5.79 |
| Pr203 | 0.75 | 0.44 | 0.70 | 0.43 | 0.64 | 2.08 | 2.25 | 2.20 | 1.18 |
| Nd203 | 2.92 | 1.61 | 1.34 | 4.86 | 4.20 | 7.93 | 8.33 | 8.35 | 5.53 |
| Sm203 | 0.44 | nd | nd | 1.36 | 0.74 | 1.40 | 0.77 | 0.93 | 1.32 |
| ThO2 | 1.52 | 2.91 | 2.92 | 9.18 | 11.80 | 4.25 | 6.61 | 4.07 | 6.08 |
| UO2 | 4.42 | 10.46 | 6.59 | 2.58 | 1.13 | 0.61 | 0.89 | 1.73 | 2.17 |
| Y203 | 2.43 | 1.49 | nd | 12.38 | 6.67 | 3.72 | 5.18 | 4.94 | 3.54 |
| PbO | 13.54 | 0.83 | 0.69 | 0.68 | nd | nd | 0.51 | 0.69 | 0.36 |
| WO3 | na | nd | nd | na | na | nd | 1.65 | nd | nd |
| SrO | na | na | | na | na | na | na | na | na |
| BaO | nd | 5.76 | 5.05 | 0.56 | nd | na | na | na | na |
| TOTAL= | 94.42 | 100.38 | 99.93 | 84.22 | 84.18 | 89.27 | 95.85 | 96.58 | 92.71 |
| RE2O3= | 10.71 | 5.84 | 6.26 | 12.34 | 12.29 | 22.84 | 35.71 | 36.99 | 14.12 |
| | | | | | | | | | |
| Ca | 0.245 | 0.328 | 0.289 | 0.349 | 0.171 | 0.217 | 0.125 | 0.102 | 0.298 |
| La | 0.022 | 0.016 | 0.022 | 0.028 | 0.048 | 0.030 | 0.144 | 0.147 | 0.007 |
| Ce | 0.126 | 0.067 | 0.064 | 0.135 | 0.121 | 0.270 | 0.532 | 0.540 | 0.139 |
| Pr | 0.017 | 0.010 | 0.014 | 0.012 | 0.016 | 0.054 | 0.062 | 0.059 | 0.028 |
| Nd | 0.064 | 0.035 | 0.027 | 0.136 | 0.103 | 0.203 | 0.225 | 0.219 | 0.129 |
| Sm | 0.009 | ---- | ---- | 0.037 | 0.017 | 0.035 | 0.020 | 0.024 | 0.030 |
| Y | 0.079 | 0.048 | ---- | 0.516 | 0.243 | 0.142 | 0.209 | 0.193 | 0.123 |
| U | 0.060 | 0.140 | 0.081 | 0.045 | 0.017 | 0.010 | 0.015 | 0.028 | 0.032 |
| Th | 0.021 | 0.040 | 0.037 | 0.164 | 0.184 | 0.069 | 0.114 | 0.068 | 0.090 |
| Mn | ---- | 0.023 | 0.016 | ---- | ---- | 0.060 | --- | 0.021 | 0.039 |
| Fe | 0.106 | 0.040 | 0.034 | 0.048 | 0.076 | 0.190 | --- | 0.023 | 0.144 |
| Sr | ---- | ---- | ---- | ---- | ---- | --- | --- | --- | --- |
| Pb | 0.223 | 0.013 | 0.010 | 0.014 | ---- | --- | 0.010 | 0.014 | 0.006 |
| | 0.972 | 0.760 | 0.594 | 1.484 | 0.996 | 1.280 | 1.456 | 1.438 | 1.065 |
| | | | | | | | | | |
| Ti | 0.393 | 0.501 | 0.410 | 0.018 | 0.046 | 0.014 | --- | 0.018 | 0.010 |
| Nb | 0.741 | 1.328 | 1.140 | 1.355 | 1.087 | 1.450 | 1.477 | 1.393 | 1.485 |
| Ta | 0.081 | 0.090 | 0.098 | 0.009 | ---- | 0.041 | 0.012 | 0.045 | 0.050 |
| W | ---- | ---- | ---- | ---- | ---- | --- | 0.032 | --- | --- |
| Si | 0.973 | 0.144 | 0.598 | 0.206 | 0.860 | 0.261 | --- | 0.121 | 0.364 |
| Ba | ---- | 0.136 | 0.110 | 0.017 | ---- | ---- | ---- | ---- | ---- |
| | 2.188 | 2.199 | 2.356 | 1.605 | 1.993 | 1.766 | 1.521 | 1.577 | 1.909 |
| | | | | | | | | | |
| | 3.160 | 2.959 | 2.950 | 3.089 | 2.989 | 3.046 | 2.977 | 3.015 | 2.974 |

| | | core | rim | | | | | | core |
|---|---|---|---|---|---|---|---|---|---|
| | 2112/4 | 2112/5 | 2112/5 | 2112/6 | 2112/7 | 2112/8 | 2112/9 | 2112/10 | 2217/1 |
| SiO2 | 3.91 | 1.71 | 4.14 | 3.93 | 1.23 | 1.28 | nd | nd | 4.15 |
| CaO | 4.85 | 1.17 | 1.58 | 5.12 | 1.63 | 1.44 | 2.00 | 1.85 | 7.00 |
| TiO2 | 0.20 | 0.23 | 0.17 | 0.13 | 0.17 | nd | 0.25 | 0.13 | 17.28 |
| MnO | 1.15 | nd | 0.52 | 1.29 | nd | 0.19 | nd | 0.14 | 0.14 |
| FeO | 2.33 | 0.14 | 0.20 | 1.83 | 0.37 | nd | 0.28 | 0.48 | 1.36 |
| Ta2O5 | 1.32 | 0.78 | 1.21 | 1.33 | 0.69 | 1.16 | 0.89 | 1.41 | 2.93 |
| Nb2O5 | 50.62 | 39.51 | 43.44 | 50.00 | 40.92 | 40.29 | 41.16 | 41.29 | 49.74 |
| La2O3 | 0.47 | 5.27 | 2.45 | 0.46 | 5.69 | 4.14 | 4.92 | 5.71 | nd |
| Ce2O3 | 6.16 | 18.07 | 12.61 | 6.24 | 19.46 | 19.07 | 17.94 | 20.84 | 0.52 |
| Pr2O3 | 1.04 | 1.80 | 1.46 | 1.28 | 2.11 | 2.35 | 2.34 | 2.79 | nd |
| Nd2O3 | 5.55 | 7.19 | 6.19 | 5.60 | 7.65 | 8.75 | 8.41 | 7.73 | 0.29 |
| Sm2O3 | 1.07 | 0.63 | 0.43 | 1.06 | 0.85 | 0.70 | 1.02 | 1.15 | nd |
| ThO2 | 5.89 | 8.97 | 7.30 | 5.15 | 6.20 | 3.48 | 7.62 | 4.80 | 2.58 |
| UO2 | 1.28 | 0.93 | 1.82 | 1.49 | 1.17 | 1.79 | 0.56 | 0.95 | 1.89 |
| Y2O3 | 3.81 | 3.36 | 3.40 | 3.40 | 4.29 | 5.32 | 3.16 | 4.40 | 0.33 |
| PbO | 0.89 | nd | 0.64 | 0.66 | 0.54 | 0.78 | 0.78 | 0.30 | 0.55 |
| WO3 | nd | nd | nd | nd | nd | nd | nd | 1.81 | na |
| SrO | na | na | na | na | na | na | na | na | na |
| BaO | na | na | na | na | na | na | na | na | 0.79 |
| TOTAL= | 90.54 | 89.76 | 87.56 | 88.97 | 92.97 | 90.74 | 91.33 | 95.78 | 89.55 |
| RE2O3= | 14.29 | 32.96 | 23.14 | 14.64 | 35.76 | 35.01 | 34.63 | 38.22 | 0.81 |
| | | | | | | | | | |
| Ca | 0.352 | 0.100 | 0.126 | 0.377 | 0.134 | 0.121 | 0.171 | 0.151 | 0.431 |
| La | 0.012 | 0.154 | 0.067 | 0.012 | 0.162 | 0.120 | 0.145 | 0.160 | ---- |
| Ce | 0.153 | 0.526 | 0.345 | 0.157 | 0.549 | 0.547 | 0.524 | 0.581 | 0.011 |
| Pr | 0.026 | 0.052 | 0.040 | 0.032 | 0.059 | 0.067 | 0.068 | 0.077 | ---- |
| Nd | 0.134 | 0.204 | 0.165 | 0.137 | 0.210 | 0.245 | 0.240 | 0.210 | 0.006 |
| Sm | 0.025 | 0.017 | 0.011 | 0.025 | 0.023 | 0.019 | 0.028 | 0.030 | ---- |
| Y | 0.137 | 0.142 | 0.135 | 0.124 | 0.176 | 0.222 | 0.134 | 0.178 | 0.010 |
| U | 0.019 | 0.016 | 0.030 | 0.023 | 0.020 | 0.031 | 0.010 | 0.016 | 0.024 |
| Th | 0.091 | 0.162 | 0.124 | 0.080 | 0.109 | 0.062 | 0.138 | 0.083 | 0.034 |
| Mn | 0.066 | --- | 0.033 | 0.075 | ---- | 0.013 | ---- | 0.009 | 0.007 |
| Fe | 0.132 | 0.009 | 0.012 | 0.105 | 0.024 | ---- | 0.019 | 0.031 | 0.065 |
| Sr | --- | --- | ---- | ---- | ---- | ---- | ---- | ---- | ---- |
| Pb | 0.016 | --- | 0.013 | 0.012 | 0.011 | 0.016 | 0.017 | 0.006 | 0.009 |
| | 1.163 | 1.382 | 1.101 | 1.159 | 1.477 | 1.463 | 1.494 | 1.532 | 0.597 |
| | | | | | | | | | |
| Ti | 0.010 | 0.014 | 0.010 | 0.007 | 0.010 | ---- | 0.015 | 0.007 | 0.747 |
| Nb | 1.549 | 1.420 | 1.466 | 1.552 | 1.424 | 1.428 | 1.484 | 1.421 | 1.292 |
| Ta | 0.024 | 0.017 | 0.025 | 0.025 | 0.014 | 0.025 | 0.019 | 0.029 | 0.046 |
| W | --- | --- | ---- | ---- | ---- | ---- | ---- | 0.036 | ---- |
| Si | 0.265 | 0.136 | 0.309 | 0.270 | 0.095 | 0.100 | ---- | ---- | 0.238 |
| Ba | ---- | ---- | ---- | ---- | ---- | ---- | ---- | ---- | 0.018 |
| | 1.848 | 1.587 | 1.810 | 1.854 | 1.543 | 1.553 | 1.518 | 1.493 | 2.341 |
| | | | | | | | | | |
| | 3.011 | 2.969 | 2.911 | 3.013 | 3.020 | 3.016 | 3.012 | 3.025 | 2.938 |

| | rim | core | rim | | | | | | |
|---|---|---|---|---|---|---|---|---|---|
| | 2217/1 | 2217/2 | 2217/2 | 2217/3 | 2217/4 | 2924/1 | 2924/2 | 2924/3 | 2924/4 |
| SiO2 | 15.05 | 4.18 | 4.01 | 3.14 | 4.52 | 6.07 | 7.10 | 5.04 | 21.14 |
| CaO | 8.14 | 6.71 | 5.37 | 5.51 | 12.33 | 7.14 | 5.19 | 8.99 | 6.58 |
| TiO2 | 2.14 | 7.79 | 6.83 | 6.75 | 6.09 | 1.32 | 4.11 | 1.44 | 0.87 |
| MnO | 0.21 | nd | 1.15 | 0.27 | 1.76 | 0.35 | 0.55 | 4.56 | 0.27 |
| FeO | 2.04 | 4.76 | 7.32 | 6.39 | 0.41 | 4.93 | 1.24 | 3.41 | 1.74 |
| Ta2O5 | 6.36 | 2.56 | 2.57 | 0.30 | 1.55 | 3.50 | 2.44 | 3.55 | 5.86 |
| Nb2O5 | 40.43 | 48.75 | 50.05 | 46.76 | 54.71 | 51.29 | 53.63 | 50.57 | 34.80 |
| La2O3 | 0.42 | 0.57 | 0.33 | 1.38 | 1.33 | 1.92 | 2.37 | 2.91 | 1.13 |
| Ce2O3 | 1.15 | 3.19 | 2.13 | 9.99 | 2.36 | 7.92 | 9.14 | 9.16 | 1.02 |
| Pr2O3 | 0.26 | 0.53 | 0.29 | 1.24 | nd | 1.07 | 1.10 | 1.14 | nd |
| Nd2O3 | 0.32 | 2.59 | 2.16 | 6.43 | 0.96 | 3.46 | 3.14 | 2.08 | 0.16 |
| Sm2O3 | nd | 1.11 | 0.63 | 1.06 | nd | 0.57 | 0.28 | nd | nd |
| ThO2 | nd | 0.96 | 0.99 | 0.26 | 3.42 | 0.70 | 0.25 | 0.61 | 0.69 |
| UO2 | 9.90 | 6.78 | 5.74 | nd | 1.21 | 0.39 | 2.91 | nd | 10.91 |
| Y2O3 | nd | 3.11 | 2.48 | 2.79 | nd | 2.00 | 2.90 | nd | nd |
| PbO | 0.60 | 0.80 | 0.60 | 0.76 | 0.46 | 0.23 | 1.12 | 0.22 | 0.51 |
| WO3 | na | na | na | na | na | nd | nd | nd | nd |
| SrO | na | na | na | na | na | na | na | na | na |
| BaO | 2.03 | nd | nd | nd | 0.28 | 0.49 | 0.27 | nd | 0.85 |
| TOTAL= | 89.05 | 96.39 | 92.65 | 93.03 | 91.39 | 93.35 | 97.74 | 93.68 | 86.53 |
| RE2O3= | 2.15 | 7.99 | 5.54 | 20.10 | 4.65 | 14.94 | 16.03 | 15.29 | 2.31 |
| | | | | | | | | | |
| Ca | 0.521 | 0.556 | 0.354 | 0.375 | 0.785 | 0.473 | 0.325 | 0.597 | 0.413 |
| La | 0.009 | 0.013 | 0.007 | 0.032 | 0.029 | 0.044 | 0.051 | 0.066 | 0.024 |
| Ce | 0.025 | 0.070 | 0.048 | 0.232 | 0.051 | 0.179 | 0.196 | 0.208 | 0.022 |
| Pr | 0.006 | 0.012 | 0.006 | 0.029 | ---- | 0.024 | 0.023 | 0.026 | ---- |
| Nd | 0.007 | 0.055 | 0.047 | 0.146 | 0.020 | 0.076 | 0.066 | 0.046 | 0.003 |
| Sm | ---- | 0.023 | 0.013 | 0.023 | ---- | 0.012 | 0.006 | ---- | ---- |
| Y | ---- | 0.099 | 0.081 | 0.094 | ---- | 0.066 | 0.090 | ---- | ---- |
| U | 0.132 | 0.090 | 0.079 | ---- | 0.016 | 0.005 | 0.038 | ---- | 0.142 |
| Th | ---- | 0.013 | 0.014 | 0.004 | 0.046 | 0.010 | 0.003 | 0.009 | 0.009 |
| Mn | 0.011 | ---- | 0.060 | 0.015 | 0.089 | 0.018 | 0.027 | 0.239 | 0.013 |
| Fe | 0.102 | 0.237 | 0.376 | 0.340 | 0.020 | 0.255 | 0.061 | 0.177 | 0.085 |
| Sr | ---- | ---- | ---- | ---- | ---- | ---- | ---- | ---- | ---- |
| Pb | 0.010 | 0.013 | 0.010 | 0.013 | 0.007 | 0.004 | 0.018 | 0.004 | 0.008 |
| | 0.823 | 1.181 | 1.095 | 1.303 | 1.063 | 1.166 | 0.904 | 1.372 | 0.719 |
| | | | | | | | | | |
| Ti | 0.096 | 0.349 | 0.316 | 0.323 | 0.272 | 0.061 | 0.181 | 0.067 | 0.038 |
| Nb | 1.091 | 1.313 | 1.391 | 1.343 | 1.469 | 1.434 | 1.418 | 1.416 | 0.921 |
| Ta | 0.103 | 0.041 | 0.043 | 0.005 | 0.025 | 0.059 | 0.039 | 0.060 | 0.093 |
| W | ---- | ---- | ---- | ---- | ---- | ---- | ---- | ---- | ---- |
| Si | 0.899 | 0.249 | 0.247 | 0.200 | 0.268 | 0.375 | 0.415 | 0.312 | 1.237 |
| Ba | 0.047 | ---- | ---- | ---- | 0.007 | 0.012 | 0.006 | ---- | 0.019 |
| | 2.236 | 1.95 | 2.00 | 1.87 | 2.04 | 1.94 | 2.06 | 1.855 | 2.308 |
| | | | | | | | | | |
| | 3.059 | 3.13 | 3.09 | 3.17 | 3.10 | 3.107 | 2.963 | 3.227 | 3.027 |

| | Centre I | Craddock Cove syenite | | | | | | | |
|---|---|---|---|---|---|---|---|---|---|
| | | intergrowths ? | | | | alteration | | | |
| | 1513/1 | 1513/1 | 1513/1 | 1513/2 | 1513/3 | 1513/3 | 1513/4 | 1513/5 | 2904/1 |
| SiO2 | 1.78 | 5.53 | 12.56 | 1.92 | 1.80 | 19.17 | 6.12 | 20.33 | nd |
| CaO | 0.30 | 2.71 | 4.76 | 0.33 | 0.56 | 6.00 | 3.35 | 7.02 | 19.54 |
| TiO2 | 17.30 | 9.95 | 5.10 | 7.71 | 12.44 | 2.02 | 7.98 | 3.71 | 7.45 |
| MnO | 0.60 | 0.22 | 0.35 | 1.13 | 0.85 | 0.14 | 0.67 | 0.24 | 1.21 |
| FeO | 29.61 | 13.10 | 11.83 | 32.37 | 28.93 | 3.31 | 7.27 | 3.05 | 1.77 |
| Ta2O5 | 0.35 | 1.76 | 5.07 | 1.24 | 2.45 | 7.47 | 2.58 | 5.73 | 3.09 |
| Nb2O5 | 43.45 | 38.66 | 33.05 | 53.33 | 51.41 | 31.77 | 49.41 | 31.57 | 57.03 |
| La2O3 | 0.32 | 0.54 | 0.61 | nd | nd | 0.85 | 0.53 | 0.96 | nd |
| Ce2O3 | 0.25 | 2.05 | 1.25 | 0.20 | nd | 1.65 | 2.58 | 2.04 | 1.91 |
| Pr2O3 | nd | 0.18 | nd | nd | nd | nd | 0.23 | nd | 0.47 |
| Nd2O3 | nd | 1.33 | nd | nd | nd | 0.36 | 1.27 | 0.44 | 0.97 |
| Sm2O3 | nd | 0.37 | nd | nd | nd | nd | 0.39 | nd | 0.37 |
| ThO2 | 1.05 | 1.78 | 0.60 | 0.98 | 1.48 | 0.67 | 0.65 | nd | 1.40 |
| UO2 | 1.20 | 2.84 | 7.96 | 1.14 | 1.83 | 9.22 | 5.57 | 11.14 | 1.44 |
| Y2O3 | 0.81 | 4.30 | nd | 0.79 | nd | nd | nd | nd | 1.46 |
| PbO | 0.75 | 0.52 | nd | 1.10 | nd | nd | 0.82 | nd | 1.17 |
| WO3 | 0.42 | nd | 0.55 | nd | nd | nd | nd | nd | 2.14 |
| SrO | na | na | na | na | na | na | na | na | na |
| BaO | 0.65 | 0.57 | 1.30 | nd | nd | 1.87 | 2.12 | 1.80 | nd |
| TOTAL= | 98.84 | 86.41 | 84.99 | 102.24 | 101.75 | 84.50 | 91.54 | 88.03 | 101.42 |
| RE2O3= | 0.57 | 4.47 | 1.86 | 0.20 | 0.00 | 2.86 | 5.00 | 3.44 | 3.72 |
| | | | | | | | | | |
| Ca | 0.018 | 0.187 | 0.323 | 0.020 | 0.033 | 0.392 | 0.218 | 0.435 | 1.167 |
| La | 0.007 | 0.013 | 0.014 | ---- | ---- | 0.019 | 0.012 | 0.020 | ---- |
| Ce | 0.005 | 0.048 | 0.029 | 0.004 | ---- | 0.037 | 0.057 | 0.043 | 0.039 |
| Pr | ---- | 0.004 | ---- | ---- | ---- | ---- | 0.005 | ---- | 0.010 |
| Nd | ---- | 0.031 | ---- | ---- | ---- | 0.008 | 0.028 | 0.009 | 0.019 |
| Sm | ---- | 0.008 | ---- | ---- | ---- | ---- | 0.008 | ---- | 0.007 |
| Y | 0.024 | 0.147 | ---- | 0.024 | ---- | ---- | ---- | ---- | 0.043 |
| U | 0.015 | 0.041 | 0.112 | 0.014 | 0.022 | 0.125 | 0.075 | 0.143 | 0.018 |
| Th | 0.013 | 0.026 | 0.009 | 0.013 | 0.019 | 0.009 | 0.009 | ---- | 0.018 |
| Mn | 0.028 | 0.012 | 0.019 | 0.054 | 0.040 | 0.007 | 0.035 | 0.012 | 0.057 |
| Fe | 1.385 | 0.705 | 0.627 | 1.519 | 1.331 | 0.169 | 0.370 | 0.148 | 0.083 |
| Sr | ---- | ---- | ---- | ---- | ---- | ---- | ---- | ---- | ---- |
| Pb | 0.011 | 0.009 | ---- | 0.017 | ---- | ---- | 0.013 | ---- | 0.031 |
| | 1.506 | 1.231 | 1.133 | 1.665 | 1.445 | 0.766 | 0.830 | 0.810 | 1.492 |
| | | | | | | | | | |
| Ti | 0.728 | 0.481 | 0.243 | 0.325 | 0.515 | 0.093 | 0.365 | 0.162 | 0.312 |
| Nb | 1.099 | 1.124 | 0.947 | 1.353 | 1.278 | 0.876 | 1.359 | 0.826 | 1.437 |
| Ta | 0.005 | 0.031 | 0.087 | 0.019 | 0.037 | 0.124 | 0.043 | 0.090 | 0.047 |
| W | 0.006 | ---- | 0.009 | ---- | ---- | ---- | ---- | ---- | 0.031 |
| Si | 0.100 | 0.356 | 0.796 | 0.108 | 0.099 | 1.169 | 0.372 | 1.177 | ---- |
| Ba | 0.014 | 0.014 | 0.032 | ---- | ---- | 0.045 | 0.051 | 0.041 | ---- |
| | 1.952 | 2.006 | 2.114 | 1.805 | 1.929 | 2.307 | 2.190 | 2.296 | 1.83 |
| | | | | | | | | | |
| | 3.458 | 3.237 | 3.247 | 3.470 | 3.374 | 3.073 | 3.020 | 3.106 | 3.319 |

| | alteration | | alteration | | | alteration | |
|---|---|---|---|---|---|---|---|
| | 2904/1 | 2904/2 | 2904/2 | 2904/3 | 2920/1 | 2920/1 | 2920/2 |
| SiO2 | 15.65 | nd | 13.30 | 4.73 | 7.74 | 4.58 | 3.93 |
| CaO | 4.05 | 15.86 | 4.73 | 7.70 | 3.92 | 3.21 | 3.10 |
| TiO2 | 5.54 | 8.69 | 7.64 | 6.97 | 6.37 | 0.49 | 0.15 |
| MnO | 0.34 | 0.75 | 0.30 | 0.75 | 0.78 | nd | nd |
| FeO | 1.03 | 4.98 | 1.56 | 1.30 | 8.21 | 4.97 | 8.29 |
| Ta2O5 | 4.16 | 2.95 | 5.20 | 2.62 | 2.92 | 1.35 | 0.87 |
| Nb2O5 | 35.35 | 51.86 | 23.46 | 58.67 | 45.17 | 44.15 | 46.25 |
| La2O3 | 3.73 | 0.54 | 2.27 | 1.08 | 1.19 | 0.59 | 0.38 |
| Ce2O3 | 9.03 | 2.55 | 6.90 | 2.67 | 3.59 | 3.45 | 1.90 |
| Pr2O3 | 0.98 | 0.42 | 0.31 | 0.38 | 0.46 | 0.57 | 0.32 |
| Nd2O3 | 2.65 | 0.69 | 2.45 | 1.15 | 1.33 | 3.58 | 4.74 |
| Sm2O3 | 0.19 | nd | 0.41 | nd | 0.53 | 1.25 | 2.03 |
| ThO2 | 1.16 | 1.14 | 1.26 | 1.61 | 1.47 | 2.84 | 1.51 |
| UO2 | 7.66 | 5.82 | 2.83 | 3.87 | 1.31 | 1.60 | 0.74 |
| Y2O3 | nd | 1.50 | nd | 0.34 | 2.05 | 8.90 | 10.40 |
| PbO | nd | 0.89 | 0.40 | 0.36 | 0.3 | 0.55 | 0.57 |
| WO3 | 0.40 | 2.25 | nd | nd | 0.93 | nd | 1.06 |
| SrO | na | na | na | na | na | na | na |
| BaO | 0.85 | nd | 0.44 | 0.92 | 3.24 | nd | nd |
| TOTAL= | 92.77 | 100.89 | 73.46 | 95.12 | 91.51 | 82.08 | 86.24 |
| RE2O3= | 16.58 | 4.20 | 12.34 | 5.28 | 7.10 | 9.44 | 9.37 |
| | | | | | | | |
| Ca | 0.256 | 0.980 | 0.364 | 0.476 | 0.255 | 0.250 | 0.230 |
| La | 0.081 | 0.011 | 0.060 | 0.023 | 0.027 | 0.016 | 0.010 |
| Ce | 0.195 | 0.054 | 0.181 | 0.056 | 0.080 | 0.092 | 0.048 |
| Pr | 0.021 | 0.009 | 0.008 | 0.008 | 0.010 | 0.015 | 0.008 |
| Nd | 0.056 | 0.014 | 0.063 | 0.024 | 0.029 | 0.093 | 0.117 |
| Sm | 0.004 | ---- | 0.010 | ---- | 0.011 | 0.031 | 0.049 |
| Y | ---- | 0.046 | ---- | 0.010 | 0.066 | 0.344 | 0.384 |
| U | 0.101 | 0.075 | 0.045 | 0.050 | 0.018 | 0.026 | 0.011 |
| Th | 0.016 | 0.015 | 0.021 | 0.021 | 0.020 | 0.047 | 0.024 |
| Mn | 0.017 | 0.037 | 0.018 | 0.037 | 0.040 | ---- | ---- |
| Fe | 0.051 | 0.240 | 0.094 | 0.063 | 0.418 | 0.302 | 0.481 |
| Sr | ---- | ---- | ---- | ---- | ---- | ---- | ---- |
| Pb | ---- | 0.014 | 0.008 | 0.006 | 0.005 | 0.011 | 0.011 |
| | 0.798 | 1.495 | 0.872 | 0.774 | 0.979 | 1.216 | 1.373 |
| | | | | | | | |
| Ti | 0.246 | 0.377 | 0.412 | 0.302 | 0.291 | 0.027 | 0.008 |
| Nb | 0.944 | 1.352 | 0.761 | 1.529 | 1.242 | 1.449 | 1.450 |
| Ta | 0.067 | 0.046 | 0.101 | 0.041 | 0.048 | 0.027 | 0.016 |
| W | 0.006 | 0.034 | ---- | ---- | 0.015 | ---- | 0.019 |
| Si | 0.925 | ---- | 0.954 | 0.273 | 0.471 | 0.332 | 0.273 |
| Ba | 0.020 | ---- | 0.012 | 0.021 | 0.077 | ---- | ---- |
| | 2.21 | 1.81 | 2.24 | 2.17 | 2.144 | 1.835 | 1.77 |
| | | | | | | | |
| | 3.006 | 3.304 | 3.112 | 2.94 | 3.123 | 3.051 | 3.139 |

Craddock Cove Ferro-augite syenite

| | 2905/1 | 2905/2 | 2905/3 | 2909/1 | 2909/2 | 2909/3 | 2909/4 | 2909/5 | 2909/6 |
|---|---|---|---|---|---|---|---|---|---|
| SiO2 | nd | 2.12 | nd | 3.42 | 3.91 | 3.59 | 3.59 | 4.13 | 2.76 |
| CaO | 18.26 | 14.83 | 16.51 | 7.14 | 8.05 | 3.24 | 8.78 | 6.56 | 2.50 |
| TiO2 | 3.60 | 5.94 | 6.06 | 1.21 | 6.46 | 7.46 | 7.02 | 7.03 | 6.44 |
| MnO | 0.71 | 0.61 | 0.71 | 1.32 | 0.91 | 1.80 | 0.85 | 1.30 | 1.21 |
| FeO | 4.09 | 6.16 | 6.41 | 12.87 | 13.76 | 17.88 | 13.91 | 16.08 | 23.30 |
| Ta2O5 | 3.39 | 2.48 | 2.23 | 2.09 | 2.41 | 2.41 | 2.93 | 1.49 | 1.74 |
| Nb2O5 | 62.15 | 53.53 | 56.90 | 57.53 | 51.20 | 51.74 | 51.53 | 50.86 | 49.97 |
| La2O3 | 0.26 | nd | 0.41 | 1.43 | 1.53 | 1.06 | 1.18 | 0.77 | 0.82 |
| Ce2O3 | 1.51 | 0.60 | 1.61 | 3.37 | 3.48 | 2.63 | 3.14 | 2.08 | 2.30 |
| Pr2O3 | nd | nd | nd | 0.22 | 0.33 | 0.22 | nd | nd | nd |
| Nd2O3 | 0.36 | 0.42 | 0.66 | 0.57 | 0.64 | 0.31 | 0.43 | 0.72 | 0.43 |
| Sm2O3 | na | nd | nd | nd | nd | nd | nd | nd | nd |
| ThO2 | 1.24 | 0.70 | 1.01 | 0.74 | 0.13 | 0.42 | nd | 0.51 | 0.88 |
| UO2 | 0.35 | 3.50 | 2.71 | 4.98 | 3.24 | 4.74 | 4.28 | 5.16 | 2.74 |
| Y2O3 | na | 0.69 | 0.68 | 0.26 | nd | nd | 0.94 | nd | nd |
| PbO | 0.63 | 0.78 | 0.52 | 0.85 | 0.47 | 0.72 | nd | 0.85 | 0.71 |
| WO3 | na | na | na | na | na | na | na | na | na |
| SrO | na | na | na | na | na | na | na | na | na |
| BaO | na | na | na | na | na | na | na | na | na |
| TOTAL= | 96.55 | 92.36 | 96.42 | 98.00 | 96.52 | 98.22 | 98.58 | 97.54 | 95.80 |
| RE2O3= | 2.13 | 1.02 | 2.68 | 5.59 | 5.98 | 4.22 | 4.75 | 3.57 | 3.55 |
| | | | | | | | | | |
| Ca | 1.133 | 0.952 | 1.036 | 0.456 | 0.503 | 0.202 | 0.538 | 0.407 | 0.161 |
| La | 0.006 | ---- | 0.009 | 0.031 | 0.033 | 0.023 | 0.025 | 0.016 | 0.018 |
| Ce | 0.032 | 0.013 | 0.035 | 0.074 | 0.074 | 0.056 | 0.066 | 0.044 | 0.051 |
| Pr | ---- | ---- | ---- | 0.005 | 0.007 | 0.005 | --- | --- | --- |
| Nd | 0.007 | 0.009 | 0.014 | 0.012 | 0.013 | 0.006 | 0.009 | 0.015 | 0.009 |
| Sm | ---- | ---- | ---- | --- | --- | --- | --- | --- | --- |
| Y | ---- | 0.022 | 0.021 | 0.008 | --- | --- | 0.029 | --- | --- |
| U | 0.005 | 0.047 | 0.035 | 0.066 | 0.042 | 0.061 | 0.054 | 0.066 | 0.037 |
| Th | 0.016 | 0.010 | 0.013 | 0.010 | 0.002 | 0.006 | --- | 0.007 | 0.012 |
| Mn | 0.035 | 0.031 | 0.035 | 0.067 | 0.045 | 0.089 | 0.041 | 0.064 | 0.062 |
| Fe | 0.198 | 0.309 | 0.314 | 0.641 | 0.671 | 0.869 | 0.665 | 0.779 | 1.171 |
| Sr | ---- | ---- | ---- | --- | --- | --- | --- | --- | --- |
| Pb | 0.010 | 0.013 | 0.008 | 0.014 | 0.007 | 0.011 | --- | 0.013 | 0.011 |
| | 1.442 | 1.406 | 1.520 | 1.384 | 1.397 | 1.328 | 1.427 | 1.411 | 1.532 |
| | | | | | | | | | |
| Ti | 0.157 | 0.268 | 0.267 | 0.054 | 0.283 | 0.326 | 0.302 | 0.306 | 0.291 |
| Nb | 1.627 | 1.450 | 1.507 | 1.550 | 1.350 | 1.359 | 1.331 | 1.331 | 1.358 |
| Ta | 0.053 | 0.040 | 0.036 | 0.034 | 0.038 | 0.038 | 0.046 | 0.023 | 0.028 |
| W | ---- | ---- | ---- | --- | --- | --- | --- | --- | --- |
| Si | ---- | 0.127 | ---- | 0.204 | 0.228 | 0.209 | 0.205 | 0.239 | 0.166 |
| Ba | ---- | ---- | ---- | ---- | ---- | --- | --- | --- | --- |
| | 1.837 | 1.885 | 1.810 | 1.842 | 1.899 | 1.932 | 1.884 | 1.899 | 1.843 |
| | | | | | | | | | |
| | 3.279 | 3.291 | 3.330 | 3.226 | 3.296 | 3.260 | 3.311 | 3.310 | 3.375 |

| | 2909/7 | 2909/8 | 2909/9 | 2908/1 | 2908/2 | 2908/3 | 2908/4 | 2908/5 |
|---|---|---|---|---|---|---|---|---|
| SiO2 | 5.03 | 4.57 | 4.54 | 3.27 | 3.14 | 3.09 | 2.80 | 3.02 |
| CaO | 5.52 | 4.60 | 5.30 | 6.29 | 2.30 | 4.53 | 4.19 | 4.36 |
| TiO2 | 5.59 | 3.55 | 7.13 | 4.56 | 4.68 | 4.45 | 4.18 | 5.29 |
| MnO | 1.40 | 1.49 | 1.72 | 0.79 | 4.82 | 1.38 | 1.05 | 1.34 |
| FeO | 9.76 | 19.97 | 16.55 | 12.71 | 19.61 | 13.81 | 22.07 | 15.04 |
| Ta2O5 | 2.02 | 2.46 | 3.00 | 2.20 | 1.59 | 2.22 | 2.86 | 2.49 |
| Nb2O5 | 52.29 | 54.71 | 52.62 | 52.18 | 54.35 | 55.40 | 54.61 | 56.12 |
| La2O3 | 2.52 | 1.33 | 0.74 | 1.62 | 1.35 | 1.46 | nd | 1.62 |
| Ce2O3 | 6.03 | 2.88 | 1.79 | 4.48 | 3.04 | 3.55 | 0.74 | 3.19 |
| Pr2O3 | 0.21 | 0.41 | nd | 0.26 | 0.22 | 0.31 | 0.13 | nd |
| Nd2O3 | 1.44 | 0.89 | 0.82 | 1.38 | 0.51 | 1.13 | 0.17 | 0.78 |
| Sm2O3 | 0.36 | 0.18 | nd | na | na | na | na | na |
| ThO2 | 0.26 | 0.17 | 0.55 | 0.35 | 0.51 | nd | 0.77 | 0.49 |
| UO2 | 3.21 | 2.44 | 4.42 | 3.17 | 2.76 | 2.44 | 3.86 | 2.74 |
| Y2O3 | 0.39 | nd | 0.56 | na | na | na | na | na |
| PbO | 0.67 | 0.44 | 0.95 | 0.31 | 0.36 | 0.63 | 0.29 | 0.70 |
| WO3 | na | na | na | na | na | na | na | na |
| SrO | na | na | na | na | na | na | na | na |
| BaO | na | na | na | na | na | na | na | na |
| TOTAL= | 96.70 | 100.09 | 100.69 | 93.57 | 99.24 | 94.40 | 97.72 | 97.18 |
| RE2O3= | 10.56 | 5.69 | 3.35 | 7.74 | 5.12 | 6.45 | 1.04 | 5.59 |
| | | | | | | | | |
| Ca | 0.348 | 0.281 | 0.318 | 0.413 | 0.143 | 0.293 | 0.264 | 0.274 |
| La | 0.055 | 0.028 | 0.015 | 0.037 | 0.029 | 0.033 | ---- | 0.035 |
| Ce | 0.130 | 0.060 | 0.037 | 0.101 | 0.065 | 0.078 | 0.016 | 0.069 |
| Pr | 0.005 | 0.009 | --- | 0.006 | 0.005 | 0.007 | 0.003 | ---- |
| Nd | 0.030 | 0.018 | 0.016 | 0.030 | 0.011 | 0.024 | 0.004 | 0.016 |
| Sm | 0.007 | 0.004 | --- | ---- | ---- | ---- | ---- | ---- |
| Y | 0.012 | --- | 0.017 | ---- | ---- | ---- | ---- | ---- |
| U | 0.042 | 0.031 | 0.055 | 0.043 | 0.036 | 0.033 | 0.050 | 0.036 |
| Th | 0.003 | 0.002 | 0.007 | 0.005 | 0.007 | ---- | 0.010 | 0.007 |
| Mn | 0.070 | 0.072 | 0.082 | 0.041 | 0.237 | 0.071 | 0.052 | 0.067 |
| Fe | 0.480 | 0.952 | 0.776 | 0.652 | 0.954 | 0.697 | 1.085 | 0.738 |
| Sr | --- | --- | --- | ---- | ---- | ---- | ---- | ---- |
| Pb | 0.011 | 0.007 | 0.014 | 0.005 | 0.006 | 0.010 | 0.005 | 0.011 |
| | 1.193 | 1.464 | 1.337 | 1.328 | 1.493 | 1.246 | 1.489 | 1.253 |
| | | | | | | | | |
| Ti | 0.247 | 0.152 | 0.301 | 0.210 | 0.205 | 0.202 | 0.185 | 0.234 |
| Nb | 1.390 | 1.410 | 1.333 | 1.447 | 1.429 | 1.512 | 1.451 | 1.490 |
| Ta | 0.032 | 0.038 | 0.046 | 0.037 | 0.025 | 0.036 | 0.046 | 0.040 |
| W | --- | --- | --- | ---- | ---- | ---- | ---- | ---- |
| Si | 0.296 | 0.261 | 0.254 | 0.201 | 0.183 | 0.187 | 0.165 | 0.177 |
| Ba | --- | --- | --- | ---- | ---- | ---- | ---- | ---- |
| | 1.965 | 1.861 | 1.934 | 1.895 | 1.842 | 1.937 | 1.847 | 1.94 |
| | | | | | | | | |
| | 3.158 | 3.325 | 3.271 | 3.223 | 3.335 | 3.183 | 3.336 | 3.19 |

Quartz syenite dykes

| | 1418/1 | 1418/2 | 1418/3 | 1418/4 | 1428/1 | 1428/2 | 1428/3 | 1428/4 | 1428/5 |
|---|---|---|---|---|---|---|---|---|---|
| SiO2 | 8.98 | 2.87 | 2.58 | 5.47 | 1.91 | 0.96 | 2.70 | 5.13 | 14.08 |
| CaO | 8.34 | 13.75 | 12.58 | 9.68 | 21.25 | 12.42 | 12.09 | 8.58 | 14.76 |
| TiO2 | 2.39 | 1.66 | 1.80 | 2.78 | 5.01 | 5.45 | 1.44 | 2.25 | 5.67 |
| MnO | nd | 0.11 | 0.60 | nd | 1.59 | 0.20 | nd | 0.12 | 0.39 |
| FeO | 2.23 | 1.66 | 0.97 | 5.83 | 3.34 | 1.44 | 3.14 | 7.95 | 1.82 |
| Ta2O5 | 1.06 | 1.55 | 2.11 | 0.92 | 3.99 | nd | 1.04 | nd | 2.34 |
| Nb2O5 | 45.39 | 70.21 | 68.63 | 49.80 | 50.27 | 69.04 | 66.79 | 50.22 | 42.17 |
| La2O3 | 1.23 | 0.52 | 0.78 | 0.55 | nd | 0.39 | 0.96 | 1.22 | 1.81 |
| Ce2O3 | 3.21 | 0.80 | 1.40 | 1.81 | nd | 0.90 | 3.65 | 3.09 | 2.76 |
| Pr2O3 | 0.38 | nd | nd | 0.31 | nd | nd | 0.78 | 0.39 | 0.39 |
| Nd2O3 | 2.02 | 0.56 | 0.45 | 2.20 | nd | 1.45 | 3.64 | 2.95 | 0.54 |
| Sm2O3 | 0.33 | nd | 0.13 | 0.58 | nd | 0.26 | 0.78 | 1.31 | nd |
| ThO2 | 0.32 | 0.43 | 0.33 | 0.22 | 0.49 | 0.33 | 0.24 | nd | 0.26 |
| UO2 | 1.49 | nd | 0.49 | 1.21 | 5.56 | nd | 0.23 | 0.25 | 7.09 |
| Y2O3 | 4.70 | 3.54 | 2.74 | 5.33 | 0.53 | 6.54 | 3.60 | 8.03 | 1.21 |
| PbO | 0.38 | 3.82 | 3.52 | 0.85 | 0.69 | 0.60 | 0.47 | 0.59 | 0.74 |
| WO3 | 0.72 | na | na | na | na | na | na | na | na |
| SrO | na | na | na | na | na | na | na | na | na |
| BaO | 3.71 | nd | 0.30 | nd | na | na | na | na | na |
| TOTAL= | 86.88 | 101.48 | 99.41 | 87.54 | 94.63 | 99.98 | 101.55 | 92.08 | 96.03 |
| RE2O3= | 7.17 | 1.88 | 2.76 | 5.45 | 0.00 | 3.00 | 9.81 | 8.96 | 5.50 |
| | | | | | | | | | |
| Ca | 0.565 | 0.804 | 0.757 | 0.653 | 1.351 | 0.726 | 0.701 | 0.564 | 0.854 |
| La | 0.029 | 0.010 | 0.016 | 0.013 | --- | 0.008 | 0.019 | 0.028 | 0.036 |
| Ce | 0.074 | 0.016 | 0.029 | 0.042 | --- | 0.018 | 0.072 | 0.069 | 0.055 |
| Pr | 0.009 | ---- | ---- | 0.007 | --- | --- | 0.015 | 0.009 | 0.008 |
| Nd | 0.046 | 0.011 | 0.009 | 0.049 | --- | 0.028 | 0.070 | 0.065 | 0.010 |
| Sm | 0.007 | ---- | 0.003 | 0.013 | --- | 0.005 | 0.015 | 0.028 | ---- |
| Y | 0.158 | 0.103 | 0.082 | 0.178 | 0.017 | 0.190 | 0.104 | 0.262 | 0.035 |
| U | 0.021 | ---- | 0.006 | 0.017 | 0.073 | --- | 0.003 | 0.003 | 0.085 |
| Th | 0.005 | 0.005 | 0.004 | 0.003 | 0.007 | 0.004 | 0.003 | ---- | 0.003 |
| Mn | ---- | 0.005 | 0.029 | ---- | 0.080 | 0.009 | --- | 0.006 | 0.018 |
| Fe | 0.118 | 0.076 | 0.046 | 0.307 | 0.166 | 0.066 | 0.142 | 0.408 | 0.082 |
| Sr | ---- | ---- | ---- | ---- | --- | --- | --- | ---- | ---- |
| Pb | 0.006 | 0.056 | 0.053 | 0.014 | 0.011 | 0.009 | 0.007 | 0.010 | 0.011 |
| | 1.038 | 1.086 | 1.034 | 1.296 | 1.705 | 1.063 | 1.151 | 1.452 | 1.197 |
| | | | | | | | | | |
| Ti | 0.114 | 0.068 | 0.076 | 0.132 | 0.224 | 0.224 | 0.059 | 0.104 | 0.230 |
| Nb | 1.297 | 1.732 | 1.743 | 1.417 | 1.349 | 1.703 | 1.700 | 1.392 | 1.030 |
| Ta | 0.018 | 0.023 | 0.032 | 0.016 | 0.064 | --- | 0.015 | ---- | 0.034 |
| W | 0.012 | ---- | ---- | ---- | | | | ---- | ---- |
| Si | 0.567 | 0.157 | 0.145 | 0.344 | 0.113 | 0.052 | 0.146 | 0.314 | 0.761 |
| Ba | 0.092 | ---- | 0.007 | ---- | ---- | ---- | ---- | ---- | ---- |
| | 2.10 | 1.98 | 2.00 | 1.91 | 1.761 | 1.979 | 1.92 | 1.81 | 2.055 |
| | | | | | | | | | |
| | 3.14 | 3.07 | 3.04 | 3.21 | 3.466 | 3.042 | 3.071 | 3.262 | 3.252 |

| | alteration | core | rim | | domain 1 | domain 2 | | | |
|---|---|---|---|---|---|---|---|---|---|
| | 1428/5 | 1428/6 | 1428/6 | 1428/7 | 1428/8 | 1428/8 | 1432/1 | 1432/2 | 1432/3 |
| SiO2 | 6.44 | nd | 5.72 | 4.66 | 24.52 | 6.17 | 6.70 | 7.27 | 5.64 |
| CaO | 8.37 | 23.72 | 8.61 | 8.39 | 9.67 | 8.49 | 8.11 | 10.99 | 7.05 |
| TiO2 | 5.98 | 6.99 | 5.29 | 3.87 | 4.39 | 5.45 | 2.95 | 5.12 | 5.96 |
| MnO | 0.44 | 0.19 | 0.20 | 0.25 | 0.24 | 0.22 | 0.13 | 0.15 | nd |
| FeO | 6.54 | 0.90 | 5.73 | 5.02 | 1.15 | 6.12 | 5.51 | 2.48 | 7.20 |
| Ta2O5 | 1.29 | 0.63 | 1.07 | 1.02 | 3.61 | 1.24 | 1.82 | 0.90 | 1.80 |
| Nb2O5 | 44.73 | 63.08 | 49.84 | 52.59 | 40.11 | 46.83 | 48.83 | 45.45 | 38.21 |
| La2O3 | 1.16 | 0.25 | 0.93 | 1.12 | 1.50 | 1.18 | 3.15 | nd | nd |
| Ce2O3 | 3.86 | 0.35 | 2.59 | 3.96 | 1.84 | 2.85 | 7.36 | 0.36 | 0.41 |
| Pr2O3 | 0.38 | nd | 0.32 | 0.50 | nd | 0.28 | 0.86 | nd | nd |
| Nd2O3 | 3.34 | 0.14 | 2.97 | 3.70 | 0.64 | 2.64 | 2.64 | nd | 1.20 |
| Sm2O3 | 1.06 | nd | 1.00 | 1.21 | nd | 0.80 | 0.26 | nd | 0.47 |
| ThO2 | 1.01 | 0.84 | 0.49 | nd | nd | 0.71 | 0.68 | nd | 0.28 |
| UO2 | nd | 1.20 | 0.39 | 0.33 | 9.39 | 0.88 | 2.09 | 20.29 | 3.24 |
| Y2O3 | 7.25 | 1.62 | 8.89 | 6.31 | 1.05 | 8.56 | 0.95 | 0.42 | 11.29 |
| PbO | nd | 0.44 | 1.10 | 0.62 | 1.19 | 0.81 | 0.52 | 0.56 | nd |
| WO3 | na | 1.28 | na | na | na | na | na | na | na |
| SrO | na | na | na | na | na | na | na | na | na |
| BaO | na | na | na | na | na | na | na | na | na |
| TOTAL= | 91.85 | 101.63 | 95.14 | 93.55 | 99.30 | 93.23 | 92.56 | 93.99 | 82.75 |
| RE2O3= | 9.80 | 0.74 | 7.81 | 10.49 | 3.90 | 7.75 | 14.27 | 0.36 | 2.08 |
| Ca | 0.540 | 1.358 | 0.539 | 0.541 | 0.508 | 0.542 | 0.534 | 0.722 | 0.504 |
| La | 0.026 | 0.005 | 0.020 | 0.025 | 0.027 | 0.026 | 0.071 | ---- | ---- |
| Ce | 0.085 | 0.007 | 0.055 | 0.087 | 0.033 | 0.062 | 0.166 | 0.008 | 0.010 |
| Pr | 0.008 | ---- | 0.007 | 0.011 | ---- | 0.006 | 0.019 | ---- | ---- |
| Nd | 0.072 | 0.003 | 0.062 | 0.080 | 0.011 | 0.056 | 0.058 | ---- | 0.029 |
| Sm | 0.022 | ---- | 0.020 | 0.025 | ---- | 0.016 | 0.006 | ---- | 0.011 |
| Y | 0.232 | 0.046 | 0.277 | 0.202 | 0.027 | 0.271 | 0.031 | 0.014 | 0.401 |
| U | ---- | 0.014 | 0.005 | 0.004 | 0.102 | 0.012 | 0.029 | 0.277 | 0.048 |
| Th | 0.014 | 0.010 | 0.007 | ---- | ---- | 0.010 | 0.010 | ---- | 0.004 |
| Mn | 0.022 | 0.009 | 0.010 | 0.013 | 0.010 | 0.011 | 0.007 | 0.008 | ---- |
| Fe | 0.329 | 0.040 | 0.280 | 0.253 | 0.047 | 0.305 | 0.283 | 0.127 | 0.402 |
| Sr | ---- | ---- | ---- | ---- | ---- | ---- | ---- | ---- | ---- |
| Pb | ---- | 0.006 | 0.017 | 0.010 | 0.016 | 0.013 | 0.009 | 0.009 | ---- |
| | 1.350 | 1.498 | 1.299 | 1.251 | 0.781 | 1.330 | 1.214 | 1.165 | 1.409 |
| Ti | 0.271 | 0.281 | 0.233 | 0.175 | 0.162 | 0.244 | 0.136 | 0.236 | 0.299 |
| Nb | 1.217 | 1.524 | 1.317 | 1.431 | 0.888 | 1.262 | 1.357 | 1.259 | 1.153 |
| Ta | 0.021 | 0.009 | 0.017 | 0.017 | 0.048 | 0.020 | 0.030 | 0.015 | 0.033 |
| W | ---- | 0.018 | ---- | ---- | ---- | ---- | ---- | ---- | ---- |
| Si | 0.388 | ---- | 0.334 | 0.280 | 1.201 | 0.368 | 0.412 | 0.445 | 0.376 |
| Ba | ---- | ---- | | | ---- | ---- | ---- | ---- | ---- |
| | 1.897 | 1.832 | 1.901 | 1.903 | 2.299 | 1.894 | 1.935 | 1.955 | 1.861 |
| | 3.247 | 3.330 | 3.200 | 3.154 | 3.080 | 3.224 | 3.149 | 3.120 | 3.270 |

| | 1432/4 | alt of col 1432/5 | 1432/6 | core 1432/7 | rim 1432/7 | 1432/8 | 1432/9 | alt of col 1432/10 | 1432/11 |
|---|---|---|---|---|---|---|---|---|---|
| SiO2 | 2.78 | 5.91 | nd | 7.06 | 12.49 | 7.97 | 6.69 | 6.35 | 3.82 |
| CaO | 6.26 | 8.76 | 15.02 | 6.93 | 7.51 | 6.25 | 6.57 | 5.90 | 6.04 |
| TiO2 | 3.10 | 2.92 | 2.79 | 4.22 | 1.73 | 4.95 | 1.41 | 6.56 | 4.68 |
| MnO | 2.85 | 0.24 | nd | nd | nd | nd | nd | nd | 2.35 |
| FeO | 9.02 | 5.20 | 0.40 | 6.16 | 2.31 | 5.65 | 3.51 | 4.68 | 11.03 |
| Ta2O5 | 1.45 | 1.35 | 1.05 | 1.44 | 1.10 | 0.92 | 1.43 | 1.20 | 2.05 |
| Nb2O5 | 62.90 | 51.27 | 74.07 | 45.95 | 41.73 | 43.54 | 46.04 | 39.16 | 58.32 |
| La2O3 | 1.15 | 1.94 | nd | 3.58 | 5.07 | 4.11 | 0.22 | 3.10 | 1.48 |
| Ce2O3 | 3.82 | 7.97 | 0.30 | 12.82 | 10.81 | 13.92 | 0.57 | 12.03 | 6.23 |
| Pr2O3 | 0.46 | 1.16 | nd | 1.42 | 1.14 | 1.66 | nd | 1.56 | 0.84 |
| Nd2O3 | 1.57 | 3.64 | 0.80 | 4.44 | 3.76 | 4.41 | 0.92 | 5.45 | 3.15 |
| Sm2O3 | nd | 1.57 | 0.40 | 0.21 | 0.40 | 0.69 | 0.76 | 0.71 | 0.60 |
| ThO2 | nd | nd | 0.58 | 0.86 | nd | nd | 3.08 | 1.56 | 0.59 |
| UO2 | 0.56 | 1.57 | nd | 0.87 | 3.15 | 0.74 | 4.92 | 0.98 | 0.49 |
| Y2O3 | 0.53 | 1.16 | 4.16 | nd | 0.80 | nd | 11.07 | 0.62 | 0.65 |
| PbO | 0.51 | 0.59 | 0.59 | 0.27 | 0.25 | 0.31 | 0.82 | 0.35 | 0.33 |
| WO3 | na | na | na | na | na | na | na | na | na |
| SrO | na | na | na | na | na | na | na | na | na |
| BaO | na | na | na | na | na | na | na | na | na |
| TOTAL= | 96.96 | 95.25 | 100.16 | 96.23 | 92.25 | 95.12 | 88.01 | 90.21 | 102.65 |
| RE2O3= | 7.00 | 16.28 | 1.50 | 22.47 | 21.18 | 24.79 | 1.71 | 22.85 | 12.30 |
| | | | | | | | | | |
| Ca | 0.388 | 0.565 | 0.881 | 0.450 | 0.487 | 0.408 | 0.457 | 0.412 | 0.361 |
| La | 0.025 | 0.043 | ---- | 0.080 | 0.113 | 0.092 | 0.005 | 0.075 | 0.030 |
| Ce | 0.081 | 0.176 | 0.006 | 0.284 | 0.239 | 0.310 | 0.014 | 0.287 | 0.127 |
| Pr | 0.010 | 0.025 | ---- | 0.031 | 0.025 | 0.037 | ---- | 0.037 | 0.017 |
| Nd | 0.032 | 0.078 | 0.016 | 0.096 | 0.081 | 0.096 | 0.021 | 0.127 | 0.063 |
| Sm | ---- | 0.033 | 0.008 | 0.004 | 0.008 | 0.014 | 0.017 | 0.016 | 0.012 |
| Y | 0.016 | 0.037 | 0.121 | ---- | 0.026 | ---- | 0.382 | 0.021 | 0.019 |
| U | 0.007 | 0.021 | ---- | 0.012 | 0.042 | 0.010 | 0.071 | 0.014 | 0.006 |
| Th | ---- | ---- | 0.007 | 0.012 | ---- | ---- | 0.045 | 0.023 | 0.007 |
| Mn | 0.140 | 0.012 | ---- | ---- | ---- | ---- | ---- | ---- | 0.111 |
| Fe | 0.437 | 0.262 | 0.018 | 0.312 | 0.117 | 0.288 | 0.191 | 0.255 | 0.515 |
| Sr | ---- | ---- | ---- | ---- | ---- | ---- | ---- | ---- | ---- |
| Pb | 0.008 | 0.010 | 0.009 | 0.004 | 0.004 | 0.005 | 0.014 | 0.006 | 0.005 |
| | 1.144 | 1.262 | 1.066 | 1.285 | 1.138 | 1.260 | 1.217 | 1.273 | 1.273 |
| | | | | | | | | | |
| Ti | 0.135 | 0.132 | 0.115 | 0.192 | 0.079 | 0.227 | 0.069 | 0.321 | 0.197 |
| Nb | 1.647 | 1.396 | 1.833 | 1.258 | 1.141 | 1.198 | 1.351 | 1.154 | 1.472 |
| Ta | 0.023 | 0.022 | 0.016 | 0.024 | 0.018 | 0.015 | 0.025 | 0.021 | 0.031 |
| W | ---- | ---- | ---- | ---- | ---- | ---- | ---- | ---- | ---- |
| Si | 0.161 | 0.356 | ---- | 0.427 | 0.756 | 0.485 | 0.434 | 0.414 | 0.213 |
| Ba | ---- | ---- | ---- | ---- | ---- | ---- | ---- | ---- | ---- |
| | 1.966 | 1.906 | 1.964 | 1.901 | 1.994 | 1.925 | 1.879 | 1.910 | 1.913 |
| | | | | | | | | | |
| | 3.110 | 3.168 | 3.030 | 3.186 | 3.132 | 3.185 | 3.096 | 3.183 | 3.186 |

| | 2925/1 | 2925/2 | 2925/3 | 2925/4 | 2925/5 | 2925/6 | 2925/7 | 2925/8 |
|---|---|---|---|---|---|---|---|---|
| Si02 | 3.45 | 5.09 | 4.40 | 3.83 | 3.18 | 3.62 | 18.00 | 21.30 |
| Ca0 | 8.84 | 7.82 | 8.74 | 9.99 | 7.65 | 3.91 | 5.14 | 6.50 |
| Ti02 | 0.33 | 0.24 | 0.40 | 0.55 | 0.28 | 0.48 | 5.85 | 3.82 |
| Mn0 | nd | 0.10 | 0.11 | 0.17 | nd | 0.22 | 0.25 | nd |
| Fe0 | 6.65 | 6.61 | 6.84 | 7.95 | 8.84 | 2.89 | 1.22 | 1.26 |
| Ta205 | nd | 0.44 | nd | nd | nd | 0.66 | 5.26 | 5.93 |
| Nb205 | 49.87 | 46.92 | 48.93 | 53.64 | 49.45 | 40.16 | 26.26 | 21.19 |
| La203 | 0.69 | 0.46 | 0.95 | 0.52 | nd | 0.21 | 1.46 | 4.79 |
| Ce203 | 2.63 | 2.01 | 3.03 | 2.49 | 1.71 | 2.64 | 1.41 | 4.65 |
| Pr203 | 0.47 | nd | 0.40 | 0.91 | 0.54 | 0.43 | nd | 0.56 |
| Nd203 | 3.08 | 3.33 | 3.51 | 3.03 | 4.72 | 4.47 | nd | 1.52 |
| Sm203 | 0.70 | 0.82 | 0.81 | 1.04 | 1.94 | 0.81 | nd | nd |
| Th02 | 5.07 | 9.18 | 8.73 | 5.60 | nd | 11.25 | 0.61 | 0.68 |
| U02 | nd | nd | nd | nd | nd | 2.85 | 16.32 | 9.62 |
| Y203 | 3.90 | 3.50 | 3.35 | 3.46 | 4.85 | 10.68 | 1.74 | 2.18 |
| Pb0 | 0.36 | 0.39 | 0.22 | 0.37 | nd | 0.73 | tr | nd |
| W03 | na | tr | na | nd | na | nd | 2.57 | 0.96 |
| Sr0 | na | na | na | na | na | na | na | na |
| Ba0 | nd | nd | nd | nd | nd | nd | 0.77 | 1.04 |
| TOTAL= | 86.04 | 86.91 | 90.42 | 93.55 | 83.16 | 86.01 | 86.86 | 86.00 |
| RE203= | 7.57 | 6.62 | 8.70 | 7.99 | 8.91 | 8.56 | 2.87 | 11.52 |
| | | | | | | | | |
| Ca | 0.643 | 0.568 | 0.615 | 0.667 | 0.566 | 0.313 | 0.339 | 0.426 |
| La | 0.017 | 0.012 | 0.023 | 0.012 | ---- | 0.006 | 0.033 | 0.108 |
| Ce | 0.065 | 0.050 | 0.073 | 0.057 | 0.043 | 0.072 | 0.032 | 0.104 |
| Pr | 0.012 | ---- | 0.010 | 0.021 | 0.014 | 0.012 | ---- | 0.012 |
| Nd | 0.075 | 0.081 | 0.082 | 0.067 | 0.116 | 0.119 | ---- | 0.033 |
| Sm | 0.016 | 0.019 | 0.018 | 0.022 | 0.046 | 0.021 | ---- | ---- |
| Y | 0.141 | 0.126 | 0.117 | 0.115 | 0.178 | 0.425 | 0.057 | 0.071 |
| U | ---- | ---- | ---- | ---- | ---- | 0.047 | 0.223 | 0.131 |
| Th | 0.078 | 0.142 | 0.131 | 0.079 | ---- | 0.191 | 0.009 | 0.009 |
| Mn | ---- | 0.006 | 0.006 | 0.009 | ---- | 0.014 | 0.013 | ---- |
| Fe | 0.377 | 0.375 | 0.376 | 0.414 | 0.510 | 0.181 | 0.063 | 0.064 |
| Sr | ---- | ---- | ---- | ---- | ---- | ---- | ---- | ---- |
| Pb | 0.007 | 0.007 | 0.004 | 0.006 | ---- | 0.015 | ---- | ---- |
| | 1.431 | 1.386 | 1.455 | 1.469 | 1.473 | 1.401 | 0.769 | 0.958 |
| | | | | | | | | |
| Ti | 0.017 | 0.012 | 0.020 | 0.026 | 0.015 | 0.027 | 0.270 | 0.176 |
| Nb | 1.530 | 1.438 | 1.454 | 1.510 | 1.544 | 1.356 | 0.730 | 0.586 |
| Ta | ---- | 0.008 | ---- | ---- | ---- | 0.013 | 0.088 | 0.099 |
| W | ---- | ---- | ---- | ---- | ---- | ---- | 0.041 | 0.015 |
| Si | 0.234 | 0.345 | 0.289 | 0.239 | 0.220 | 0.270 | 1.106 | 1.302 |
| Ba | ---- | ---- | ---- | ---- | ---- | ---- | 0.019 | 0.025 |
| | 1.781 | 1.803 | 1.763 | 1.775 | 1.779 | 1.666 | 2.254 | 2.203 |
| | | | | | | | | |
| Total= | 3.212 | 3.189 | 3.218 | 3.244 | 3.252 | 3.067 | 3.023 | 3.161 |

Eastern contact pegmatites

| | | domain A | domain B | A | B | A | B | |
|---|---|---|---|---|---|---|---|---|
| | C1C/1 | C1C/2 | C1C /2 | C1C/3 | C1C-3 | C1C/4 | C1C/4 | C1C/5 |
| SiO2 | 4.96 | 5.32 | 15.72 | 5.10 | 15.85 | 4.78 | 15.60 | 4.74 |
| CaO | 6.69 | 6.36 | 6.42 | 8.41 | 6.48 | 6.90 | 6.42 | 6.59 |
| TiO2 | 6.50 | 8.07 | 4.81 | 6.10 | 4.66 | 5.91 | 5.17 | 6.65 |
| MnO | 0.14 | 0.20 | 0.30 | 0.25 | 0.48 | 0.19 | 0.49 | 0.13 |
| FeO | 3.37 | 2.83 | 2.14 | 4.28 | 2.48 | 3.86 | 1.48 | 4.06 |
| Ta2O5 | 1.68 | 1.72 | 5.64 | 1.82 | 4.88 | 1.83 | 4.75 | 2.07 |
| Nb2O5 | 42.80 | 46.47 | 41.66 | 48.01 | 45.43 | 46.15 | 42.98 | 43.16 |
| La2O3 | nd | 0.68 | nd | 0.81 | nd | 0.56 | nd | nd |
| Ce2O3 | 4.13 | 4.98 | 1.48 | 5.10 | 1.39 | 4.85 | 1.75 | 4.17 |
| Pr2O3 | 0.58 | 0.87 | nd | 1.07 | nd | 0.67 | nd | 0.33 |
| Nd2O3 | 3.13 | 3.03 | nd | 3.11 | nd | 3.42 | nd | 3.41 |
| Sm2O3 | 0.69 | na | na | na | na | na | na | na |
| ThO2 | 0.40 | 0.94 | nd | 0.85 | 0.21 | 0.65 | 5.80 | 0.72 |
| UO2 | 3.94 | 4.78 | 6.01 | 3.35 | 5.31 | 2.48 | 5.58 | 4.34 |
| Y2O3 | 3.00 | 4.04 | nd | 3.10 | nd | 4.01 | nd | 3.92 |
| PbO | 0.44 | 0.61 | 0.64 | 0.80 | 0.52 | 0.45 | nd | 0.26 |
| WO3 | nd | na | na | na | na | na | na | na |
| SrO | na | 0.41 | 1.47 | nd | 1.31 | nd | 1.19 | nd |
| TOTAL= | 82.45 | 91.31 | 86.29 | 92.16 | 89.00 | 86.71 | 91.21 | 84.55 |
| RE2O3= | 8.53 | 9.56 | 1.48 | 10.09 | 1.39 | 9.50 | 1.75 | 7.91 |
| Ca | 0.487 | 0.421 | 0.401 | 0.553 | 0.390 | 0.479 | 0.389 | 0.471 |
| La | 0.000 | 0.015 | 0.000 | 0.018 | ---- | 0.013 | ---- | ---- |
| Ce | 0.103 | 0.113 | 0.032 | 0.115 | 0.029 | 0.115 | 0.036 | 0.102 |
| Pr | 0.014 | 0.020 | ---- | 0.024 | ---- | 0.016 | ---- | 0.008 |
| Nd | 0.076 | 0.067 | ---- | 0.068 | ---- | 0.079 | ---- | 0.081 |
| Sm | 0.016 | 0.000 | ---- | ---- | ---- | ---- | ---- | ---- |
| Y | 0.108 | 0.133 | ---- | 0.101 | ---- | 0.138 | ---- | 0.139 |
| U | 0.060 | 0.066 | 0.078 | 0.046 | 0.066 | 0.036 | 0.070 | 0.064 |
| Th | 0.006 | 0.013 | ---- | 0.012 | 0.003 | 0.010 | 0.075 | 0.011 |
| Mn | 0.008 | 0.010 | 0.015 | 0.013 | 0.023 | 0.010 | 0.023 | 0.007 |
| Fe | 0.191 | 0.146 | 0.104 | 0.220 | 0.116 | 0.209 | 0.070 | 0.226 |
| Sr | ---- | 0.015 | 0.050 | ---- | 0.043 | ---- | 0.039 | ---- |
| Pb | 0.008 | 0.010 | 0.010 | 0.013 | 0.008 | 0.008 | ---- | 0.005 |
| | 1.077 | 1.029 | 0.690 | 1.183 | 0.678 | 1.113 | 0.702 | 1.114 |
| Ti | 0.332 | 0.375 | 0.211 | 0.282 | 0.197 | 0.288 | 0.220 | 0.333 |
| Nb | 1.314 | 1.297 | 1.097 | 1.332 | 1.153 | 1.353 | 1.099 | 1.301 |
| Ta | 0.031 | 0.029 | 0.089 | 0.030 | 0.074 | 0.013 | 0.073 | 0.038 |
| W | ---- | ---- | ---- | ---- | ---- | ---- | ---- | ---- |
| Si | 0.337 | 0.328 | 0.915 | 0.313 | 0.889 | 0.310 | 0.882 | 0.316 |
| | 2.014 | 2.029 | 2.312 | 1.957 | 2.313 | 1.964 | 2.274 | 1.988 |
| TOTAL | 3.091 | 3.058 | 3.002 | 3.140 | 2.991 | 3.077 | 2.976 | 3.102 |

| | C1C/6 | C1C/7 | A C1A/1 | B C1A/1 | A C1A/2 | B C1A/2 |
|---|---|---|---|---|---|---|
| SiO2 | 5.49 | 4.51 | 3.85 | 4.71 | 7.42 | 4.37 |
| CaO | 8.50 | 6.35 | 2.74 | 6.81 | 1.32 | 5.03 |
| TiO2 | 7.27 | 7.49 | 5.41 | 4.85 | 4.65 | 4.70 |
| MnO | 0.38 | 0.55 | 0.51 | 0.14 | 0.83 | 0.23 |
| FeO | 3.74 | 2.61 | 18.22 | 5.01 | 26.81 | 5.74 |
| Ta2O5 | 1.69 | 3.62 | 2.13 | 2.67 | 2.31 | 2.15 |
| Nb2O5 | 48.35 | 54.11 | 52.54 | 51.23 | 47.71 | 49.39 |
| La2O3 | 0.80 | nd | nd | 1.04 | nd | 0.84 |
| Ce2O3 | 3.84 | 2.15 | 2.07 | 5.96 | 0.20 | 5.36 |
| Pr2O3 | 0.32 | nd | 0.43 | 0.83 | nd | 1.20 |
| Nd2O3 | 1.70 | 0.62 | 1.10 | 3.19 | nd | 3.62 |
| Sm2O3 | na | na | na | na | na | na |
| ThO2 | 0.58 | 1.28 | 0.85 | 1.13 | 0.79 | 1.05 |
| UO2 | 3.70 | 3.17 | 2.20 | 2.80 | 1.76 | 2.95 |
| Y2O3 | 1.89 | 1.24 | nd | 1.57 | nd | 1.51 |
| PbO | 0.59 | 0.82 | 0.43 | 0.58 | 0.78 | 0.46 |
| WO3 | na | na | na | na | na | na |
| SrO | nd | 1.95 | nd | nd | nd | nd |
| BaO | na | na | na | na | na | na |
| TOTAL= | 88.84 | 90.47 | 92.48 | 92.52 | 94.58 | 88.60 |
| RE2O3= | 6.66 | 2.77 | 3.60 | 11.02 | 0.20 | 11.02 |
| Ca | 0.561 | 0.412 | 0.178 | 0.450 | 0.082 | 0.349 |
| La | 0.018 | ---- | ---- | 0.024 | ---- | 0.020 |
| Ce | 0.087 | 0.048 | 0.046 | 0.135 | 0.004 | 0.127 |
| Pr | 0.007 | ---- | 0.010 | 0.019 | ---- | 0.028 |
| Nd | 0.037 | 0.013 | 0.024 | 0.070 | ---- | 0.084 |
| Sm | ---- | ---- | ---- | ---- | ---- | ---- |
| Y | 0.062 | 0.040 | ---- | 0.052 | ---- | 0.052 |
| U | 0.051 | 0.043 | 0.030 | 0.038 | 0.023 | 0.043 |
| Th | 0.008 | 0.018 | 0.012 | 0.016 | 0.010 | 0.015 |
| Mn | 0.020 | 0.028 | 0.026 | 0.007 | 0.041 | 0.013 |
| Fe | 0.193 | 0.132 | 0.926 | 0.259 | 1.302 | 0.311 |
| Sr | ---- | 0.068 | ---- | ---- | ---- | ---- |
| Pb | 0.010 | 0.013 | 0.007 | 0.010 | 0.012 | 0.008 |
| | 1.054 | 0.815 | 1.259 | 1.080 | 1.474 | 1.050 |
| Ti | 0.337 | 0.341 | 0.247 | 0.225 | 0.203 | 0.229 |
| Nb | 1.345 | 1.480 | 1.444 | 1.429 | 1.252 | 1.447 |
| Ta | 0.028 | 0.060 | 0.035 | 0.045 | 0.036 | 0.038 |
| W | ---- | ---- | ---- | ---- | ---- | ---- |
| Si | 0.338 | 0.273 | 0.234 | 0.291 | 0.431 | 0.283 |
| | 2.048 | 2.154 | 1.960 | 1.990 | 1.922 | 1.997 |
| TOTAL | 3.102 | 2.969 | 3.219 | 3.070 | 3.396 | 3.047 |

COLUMBITE

APPENDIX 2.4

| | Ferro-edenite syenite | | | | | Contaminated ferro-edenite syenite | | | |
|---|---|---|---|---|---|---|---|---|---|
| | 2025/1 | 2025/2 | 2025/3 | 2025/4 | 2025/6 | 2028/1 | 2028/2 | 2028/3 | 2028/4 |
| TiO2 | 3.32 | 1.17 | 1.43 | 1.36 | 1.03 | 1.27 | 1.78 | 2.04 | 0.92 |
| FeO | 16.99 | 17.11 | 17.38 | 17.5 | 16.75 | 16.33 | 16.52 | 16.48 | 17.06 |
| MnO | 3.54 | 4.35 | 3.65 | 3.41 | 4.27 | 4.78 | 4.91 | 4.42 | 4.5 |
| MgO | nd | nd | nd | nd | nd | nd | nd | nd | nd |
| Nb2O5 | 73.85 | 73.04 | 73.17 | 73.03 | 71.61 | 75.14 | 74.56 | 74.69 | 73.73 |
| Ta2O5 | 2.89 | 3.64 | 4.73 | 4.76 | 4.59 | 2.73 | 3.04 | 1.48 | 2.53 |
| SnO | na | na | na | na | na | na | na | na | na |
| TOTAL= | 100.59 | 99.32 | 100.35 | 100.06 | 98.25 | 100.25 | 100.8 | 99.12 | 98.74 |
| | | | | | | | | | |
| Fe | 0.792 | 0.819 | 0.825 | | 0.814 | 0.770 | 0.775 | 0.803 | 0.819 |
| Mn | 0.167 | 0.211 | 0.176 | | 0.210 | 0.228 | 0.233 | 0.218 | 0.219 |
| Mg | ---- | ---- | ---- | | ---- | ---- | ---- | ---- | ---- |
| | 0.959 | 1.030 | 1.001 | | 1.024 | 0.998 | 1.008 | 1.021 | 1.038 |
| | | | | | | | | | |
| Nb | 1.861 | 1.891 | 1.878 | | 1.882 | 1.916 | 1.890 | 1.968 | 1.914 |
| Ta | 0.044 | 0.057 | 0.073 | | 0.073 | 0.042 | 0.046 | 0.023 | 0.04 |
| Ti | 0.139 | 0.050 | 0.061 | | 0.045 | 0.054 | 0.075 | 0.09 | 0.04 |
| Sn | ---- | ---- | ---- | | ---- | ---- | ---- | ---- | ---- |
| | 2.044 | 1.998 | 2.012 | | 2.000 | 2.012 | 2.011 | 2.081 | 1.994 |
| | | | | | | | | | |
| TOTAL | 3.003 | 3.028 | 3.013 | | 3.024 | 3.010 | 3.020 | 3.103 | 3.031 |

| | | | Quartz syenite dykes | | | | | | |
|---|---|---|---|---|---|---|---|---|---|
| | 2028/5 | 2028/6 | 2925/1 | 2925/2 | 2925/3 | 2925/4 | 2925/5 | 1432/31 | 432/3b |
| TiO2 | 1.29 | 1.72 | 0.96 | 0.76 | 1.46 | 0.92 | 0.45 | 3.88 | 3.97 |
| FeO | 16.98 | 17.78 | 2.24 | 2.09 | 2.55 | 2.29 | 2.23 | 14.07 | 13.94 |
| MnO | 4.74 | 4.28 | 17.45 | 17.85 | 17.71 | 18.09 | 18.16 | 6.71 | 6.38 |
| MgO | nd | nd | na | na | na | na | na | na | na |
| Nb2O5 | 73.17 | 71.48 | 78.16 | 78.12 | 77.7 | 76.1 | 77.49 | 75.15 | 73.11 |
| Ta2O5 | 3.39 | 3.94 | 1.54 | 0.46 | 1.03 | 1.14 | 2.05 | 1.74 | 2.64 |
| SnO | na | na | na | na | na | na | na | na | na |
| TOTAL= | 99.57 | 99.19 | 100.35 | 99.28 | 100.45 | 98.54 | 100.38 | 101.55 | 100.04 |
| | | | | | | | | | |
| Fe | 0.81 | 0.854 | 0.105 | 0.098 | 0.119 | 0.109 | 0.105 | 0.645 | 0.651 |
| Mn | 0.229 | 0.208 | 0.825 | 0.851 | 0.835 | 0.872 | 0.863 | 0.312 | 0.302 |
| Mg | ---- | ---- | ---- | ---- | ---- | ---- | ---- | ---- | ---- |
| | 1.039 | 1.062 | 0.93 | 0.949 | 0.954 | 0.981 | 0.968 | 0.957 | 0.953 |
| | | | | | | | | | |
| Nb | 1.887 | 1.855 | 1.973 | 1.988 | 1.954 | 1.958 | 1.966 | 1.863 | 1.845 |
| Ta | 0.053 | 0.062 | 0.023 | 0.007 | 0.016 | 0.018 | 0.031 | 0.026 | 0.040 |
| Ti | 0.055 | 0.074 | 0.04 | 0.032 | 0.061 | 0.039 | 0.019 | 0.160 | 0.167 |
| Sn | ---- | ---- | ---- | ---- | ---- | ---- | ---- | ---- | ---- |
| | 1.995 | 1.991 | 2.036 | 2.027 | 2.031 | 2.015 | 2.016 | 2.049 | 2.052 |
| | | | | | | | | | |
| TOTAL | 3.035 | 3.052 | 2.966 | 2.976 | 2.985 | 2.996 | 2.984 | 3.006 | 3.005 |

| | 1432/5 |
|---|---|
| TiO2 | 1.47 |
| FeO | 12.02 |
| MnO | 8.11 |
| MgO | na |
| Nb2O5 | 75.41 |
| Ta2O5 | 1.73 |
| SnO | na |
| TOTAL= | 98.74 |
| | |
| Fe | 0.571 |
| Mn | 0.391 |
| Mg | ---- |
| | 0.962 |
| | |
| Nb | 1.938 |
| Ta | 0.027 |
| Ti | 0.063 |
| Sn | ---- |
| | 2.028 |
| | |
| TOTAL | 2.990 |

ZIRCONOLITES

APPENDIX 2.5

Centre I: Southeastern ferroaugite syenite

| | C48/1 | C48/2b | C48/2d | C48/3 | C48/4 | C48/5 | C48/6 | C68/1 | C68/2 |
|---|---|---|---|---|---|---|---|---|---|
| Al2O3 | 0.55 | nd | 0.45 | nd | nd | 0.31 | nd | 0.62 | nd |
| SiO2 | 0.00 | 1.05 | nd | nd | nd | nd | nd | nd | nd |
| TiO2 | 18.97 | 24.18 | 25.13 | 20.49 | 19.36 | 18.75 | 17.87 | 18.00 | 20.40 |
| FeO | 8.70 | 8.89 | 7.50 | 9.25 | 10.33 | 9.27 | 8.23 | 9.33 | 10.54 |
| ZrO2 | 28.10 | 25.74 | 27.55 | 27.43 | 27.12 | 29.72 | 26.10 | 23.96 | 26.89 |
| Nb2O5 | 17.43 | 11.72 | 8.71 | 11.84 | 14.73 | 14.87 | 13.55 | 11.54 | 10.16 |
| La2O3 | 1.83 | nd | 0.74 | 2.20 | 1.61 | 1.91 | 1.33 | 1.11 | 1.27 |
| Ce2O3 | 6.76 | 3.61 | 4.61 | 6.97 | 6.30 | 6.62 | 4.31 | 4.96 | 5.52 |
| Pr2O3 | 0.73 | 0.94 | 0.51 | 0.84 | 1.35 | 0.91 | 0.57 | 0.71 | 1.12 |
| Nd2O3 | 2.16 | 3.32 | 2.75 | 2.13 | 3.13 | 1.92 | 2.64 | 1.81 | 2.06 |
| ThO2 | 1.00 | 1.70 | 0.77 | 1.54 | 2.14 | 2.17 | 1.80 | 5.18 | 6.50 |
| UO2 | nd | 1.98 | nd | 1.20 | 2.82 | 1.25 | 2.49 | 0.49 | nd |
| CaO | 7.44 | 7.77 | 7.60 | 6.36 | 6.71 | 7.48 | 6.74 | 5.03 | 5.36 |
| Total= | 93.67 | 90.90 | 86.32 | 90.25 | 95.60 | 95.18 | 85.63 | 82.74 | 89.82 |
| | | | | | | | | | |
| Ree total | 11.48 | 7.87 | 8.61 | 12.14 | 12.39 | 11.36 | 8.85 | 8.59 | 9.97 |

calculated to 7 oxygen

| | | | | | | | | | |
|---|---|---|---|---|---|---|---|---|---|
| Ca | 0.566 | 0.592 | 0.602 | 0.511 | 0.519 | 0.572 | 0.571 | 0.444 | 0.440 |
| La | 0.048 | ---- | 0.020 | 0.061 | 0.043 | 0.050 | 0.039 | 0.034 | 0.036 |
| Ce | 0.176 | 0.094 | 0.125 | 0.191 | 0.166 | 0.173 | 0.125 | 0.149 | 0.155 |
| Pr | 0.019 | 0.024 | 0.014 | 0.023 | 0.035 | 0.024 | 0.016 | 0.021 | 0.031 |
| Nd | 0.055 | 0.084 | 0.073 | 0.057 | 0.081 | 0.049 | 0.075 | 0.053 | 0.056 |
| Th | 0.016 | 0.027 | 0.013 | 0.026 | 0.035 | 0.035 | 0.032 | 0.097 | 0.113 |
| U | ---- | 0.031 | ---- | 0.020 | 0.045 | 0.020 | 0.044 | 0.009 | ---- |
| | | | | | | | | | |
| Σ Ca | 0.880 | 0.852 | 0.847 | 0.889 | 0.924 | 0.923 | 0.902 | 0.807 | 0.831 |
| | | | | | | | | | |
| Zr | 0.973 | 0.892 | 0.992 | 1.003 | 0.954 | 1.034 | 1.007 | 0.962 | 1.005 |
| | | | | | | | | | |
| Al | 0.046 | 0.000 | 0.039 | ---- | ---- | 0.026 | ---- | 0.060 | ---- |
| Si | ---- | 0.075 | ---- | ---- | ---- | ---- | ---- | ---- | ---- |
| Ti | 1.013 | 1.292 | 1.396 | 1.155 | 1.050 | 1.006 | 1.063 | 1.114 | 1.176 |
| Mn | ---- | ---- | ---- | ---- | ---- | ---- | ---- | ---- | ---- |
| Fe | 0.517 | 0.528 | 0.463 | 0.580 | 0.623 | 0.553 | 0.544 | 0.642 | 0.675 |
| Nb | 0.559 | 0.377 | 0.291 | 0.401 | 0.480 | 0.480 | 0.484 | 0.429 | 0.352 |
| | | | | | | | | | |
| Σ Ti | 2.135 | 2.272 | 2.189 | 2.136 | 2.153 | 2.065 | 2.091 | 2.245 | 2.203 |
| | | | | | | | | | |
| Total= | 3.988 | 4.016 | 4.028 | 4.028 | 4.031 | 4.022 | 4.000 | 4.014 | 4.039 |

| | C68/3 | C68/4 | C68/5 | C50/1 | C50/2 | C50/3 | C50/4 | C50/5 | C50/7 |
|---|---|---|---|---|---|---|---|---|---|
| Al2O3 | nd | nd | nd | 0.57 | nd | nd | nd | nd | 0.57 |
| SiO2 | nd | nd | nd | nd | nd | nd | nd | nd | nd |
| TiO2 | 18.24 | 19.42 | 19.20 | 20.12 | 19.62 | 19.91 | 20.99 | 21.81 | 22.05 |
| FeO | 9.73 | 10.17 | 6.76 | 9.37 | 9.38 | 9.81 | 9.18 | 8.61 | 3.10 |
| ZrO2 | 24.69 | 26.90 | 24.05 | 26.09 | 26.74 | 27.99 | 28.66 | 29.31 | 27.64 |
| Nb2O5 | 12.51 | 10.28 | 9.47 | 10.83 | 14.97 | 15.13 | 12.51 | 12.87 | 11.92 |
| La2O3 | 0.62 | 2.08 | 1.60 | 2.33 | 0.88 | 1.75 | 2.50 | 3.15 | 1.88 |
| Ce2O3 | 3.45 | 4.53 | 4.97 | 5.99 | 5.30 | 7.10 | 7.74 | 7.51 | 7.72 |
| Pr2O3 | 0.76 | nd | nd | nd | 0.39 | 0.92 | 0.81 | nd | 1.52 |
| Nd2O3 | 1.91 | 1.12 | 1.53 | 1.29 | 2.43 | 2.83 | 2.59 | 1.50 | 2.50 |
| ThO2 | 8.80 | 6.29 | 5.41 | 2.84 | 1.82 | 1.99 | 1.27 | 1.54 | 1.70 |
| UO2 | 0.57 | 1.60 | nd | 2.83 | 1.68 | 1.44 | nd | nd | 1.29 |
| CaO | 6.08 | 5.51 | 4.98 | 6.44 | 7.44 | 7.46 | 6.88 | 7.51 | 3.71 |
| Total= | 87.36 | 87.92 | 77.97 | 88.70 | 90.65 | 96.33 | 93.13 | 93.81 | 85.60 |
| Ree total | 6.74 | 7.73 | 8.10 | 9.61 | 9.00 | 12.60 | 13.64 | 12.16 | 12.14 |

| | | | | | | | | | |
|---|---|---|---|---|---|---|---|---|---|
| Ca | 0.517 | 0.463 | 0.462 | 0.528 | 0.589 | 0.565 | 0.533 | 0.572 | 0.309 |
| La | 0.018 | 0.060 | 0.051 | 0.066 | 0.024 | 0.046 | 0.067 | 0.083 | 0.054 |
| Ce | 0.100 | 0.130 | 0.157 | 0.168 | 0.143 | 0.184 | 0.205 | 0.195 | 0.220 |
| Pr | 0.022 | ---- | ---- | ---- | 0.010 | 0.024 | 0.021 | ---- | 0.043 |
| Nd | 0.054 | 0.031 | 0.047 | 0.035 | 0.064 | 0.071 | 0.067 | 0.038 | 0.069 |
| Th | 0.159 | 0.112 | 0.106 | 0.049 | 0.031 | 0.032 | 0.021 | 0.025 | 0.030 |
| U | 0.010 | 0.028 | ---- | 0.048 | 0.028 | 0.023 | ---- | ---- | 0.022 |
| Σ Ca | 0.880 | 0.824 | 0.823 | 0.894 | 0.889 | 0.945 | 0.914 | 0.913 | 0.747 |
| Zr | 0.955 | 1.028 | 1.014 | 0.973 | 0.963 | 0.965 | 1.011 | 1.015 | 1.049 |
| Al | ---- | ---- | ---- | 0.051 | ---- | ---- | ---- | ---- | 0.052 |
| Si | ---- | ---- | ---- | ---- | ---- | ---- | ---- | ---- | ---- |
| Ti | 1.088 | 1.145 | 1.249 | 1.157 | 1.089 | 1.059 | 1.142 | 1.165 | 1.290 |
| Mn | ---- | ---- | ---- | ---- | ---- | ---- | ---- | ---- | ---- |
| Fe | 0.646 | 0.667 | 0.489 | 0.599 | 0.579 | 0.580 | 0.555 | 0.511 | 0.202 |
| Nb | 0.449 | 0.364 | 0.370 | 0.375 | 0.500 | 0.484 | 0.409 | 0.413 | 0.419 |
| Σ Ti | 2.183 | 2.176 | 2.108 | 2.182 | 2.168 | 2.123 | 2.106 | 2.089 | 1.963 |
| Total= | 4.018 | 4.028 | 3.945 | 4.049 | 4.020 | 4.033 | 4.031 | 4.017 | 3.759 |

| | C39/1 | C39/2 | C39/3 | C39/4 | C39/5 | C39/6 | C35/1 | C35/2 | C35/3 |
|---|---|---|---|---|---|---|---|---|---|
| Al203 | nd | nd | nd | 0.31 | nd | nd | 0.45 | 0.47 | 1.13 |
| Si02 | nd | 0.39 | nd | nd | nd | 0.95 | nd | nd | nd |
| Ti02 | 21.62 | 19.72 | 18.38 | 17.97 | 19.38 | 20.26 | 27.33 | 22.00 | 14.97 |
| Fe0 | 9.05 | 7.19 | 9.00 | 8.93 | 9.03 | 8.88 | 7.98 | 9.06 | 9.65 |
| Zr02 | 29.76 | 25.50 | 26.53 | 29.08 | 27.35 | 26.94 | 28.61 | 27.70 | 24.24 |
| Nb205 | 9.32 | 11.63 | 12.20 | 13.08 | 11.98 | 13.97 | 6.37 | 8.27 | 16.41 |
| La203 | 1.79 | 2.01 | 1.59 | 1.50 | 1.15 | 1.95 | nd | 0.85 | 1.18 |
| Ce203 | 6.31 | 6.37 | 6.85 | 5.24 | 5.67 | 6.74 | 3.31 | 5.42 | 5.07 |
| Pr203 | 0.55 | 0.62 | 1.48 | 0.97 | 0.67 | 1.17 | 0.59 | 0.55 | 0.48 |
| Nd203 | 2.59 | 3.15 | 2.86 | 2.38 | 2.52 | 2.95 | 2.76 | 2.74 | 1.70 |
| Th02 | 1.28 | 1.74 | 2.52 | 2.15 | 2.14 | 0.87 | 2.95 | 2.70 | 3.82 |
| U02 | nd | 0.53 | 1.02 | 2.31 | 1.38 | 0.46 | 1.91 | 1.82 | 2.71 |
| Ca0 | 6.53 | 6.37 | 6.08 | 6.91 | 6.57 | 7.39 | 7.96 | 6.20 | 6.45 |
| Total = | 88.80 | 85.22 | 88.51 | 90.83 | 87.84 | 92.53 | 90.22 | 87.78 | 87.81 |
| | | | | | | | | | |
| Ree total | 11.24 | 12.15 | 12.78 | 10.09 | 10.01 | 12.81 | 6.66 | 9.56 | 8.43 |

| | | | | | | | | | |
|---|---|---|---|---|---|---|---|---|---|
| Ca | 0.525 | 0.537 | 0.507 | 0.557 | 0.541 | 0.569 | 0.609 | 0.507 | 0.542 |
| La | 0.049 | 0.058 | 0.046 | 0.042 | 0.033 | 0.052 | ---- | 0.024 | 0.034 |
| Ce | 0.173 | 0.184 | 0.195 | 0.144 | 0.160 | 0.177 | 0.087 | 0.151 | 0.146 |
| Pr | 0.015 | 0.018 | 0.042 | 0.027 | 0.019 | 0.031 | 0.015 | 0.015 | 0.014 |
| Nd | 0.069 | 0.089 | 0.080 | 0.064 | 0.069 | 0.076 | 0.070 | 0.075 | 0.048 |
| Th | 0.022 | 0.031 | 0.045 | 0.037 | 0.037 | 0.014 | 0.048 | 0.047 | 0.068 |
| U | ---- | 0.009 | 0.018 | 0.039 | 0.024 | 0.007 | 0.030 | 0.031 | 0.047 |
| | | | | | | | | | |
| Σ Ca | 0.853 | 0.926 | 0.933 | 0.910 | 0.883 | 0.926 | 0.859 | 0.850 | 0.899 |
| | | | | | | | | | |
| Zr | 1.088 | 0.979 | 1.007 | 1.066 | 1.026 | 0.944 | 0.996 | 1.030 | 0.927 |
| | | | | | | | | | |
| Al | ---- | ---- | ---- | 0.027 | ---- | ---- | 0.038 | 0.042 | 0.104 |
| Si | ---- | 0.031 | ---- | ---- | ---- | 0.068 | ---- | ---- | ---- |
| Ti | 1.219 | 1.167 | 1.076 | 1.016 | 1.121 | 1.095 | 1.468 | 1.262 | 0.883 |
| Mn | ---- | ---- | ---- | ---- | ---- | ---- | ---- | ---- | ---- |
| Fe | 0.567 | 0.473 | 0.586 | 0.561 | 0.581 | 0.534 | 0.477 | 0.578 | 0.633 |
| Nb | 0.316 | 0.414 | 0.429 | 0.445 | 0.417 | 0.454 | 0.206 | 0.285 | 0.582 |
| | | | | | | | | | |
| Σ Ti | 2.102 | 2.085 | 2.091 | 2.049 | 2.119 | 2.151 | 2.189 | 2.167 | 2.202 |
| | | | | | | | | | |
| Total = | 4.043 | 3.990 | 4.031 | 4.025 | 4.028 | 4.021 | 4.044 | 4.047 | 4.028 |

| | C35/4 | C35/5 | C35/6 | C2028/1 | C2028/2 | C2028/3 | C2028/4 |
|---|---|---|---|---|---|---|---|
| Al2O3 | nd | nd | nd | na | na | na | na |
| SiO2 | nd | nd | nd | nd | nd | na | nd |
| TiO2 | 31.41 | 20.50 | 22.77 | 21.51 | 14.60 | 21.83 | 21.45 |
| FeO | 7.19 | 8.99 | 8.44 | 8.69 | 8.46 | 8.64 | 8.29 |
| ZrO2 | 34.23 | 26.57 | 27.91 | 23.34 | 24.52 | 24.96 | 28.34 |
| Nb2O5 | 2.48 | 9.04 | 6.76 | 10.79 | 17.16 | 11.25 | 7.08 |
| Ta2O5 | na | na | na | na | 1.16 | na | 1.28 |
| La2O3 | 1.13 | 1.04 | 0.90 | 0.78 | 1.82 | 0.62 | 2.70 |
| Ce2O3 | 5.30 | 4.23 | 4.54 | 4.87 | 6.57 | 5.02 | 9.40 |
| Pr2O3 | 0.68 | 0.62 | 0.68 | nd | nd | 1.02 | 0.69 |
| Nd2O3 | 1.83 | 2.73 | 3.20 | 2.75 | 2.34 | 3.44 | 3.30 |
| ThO2 | 0.54 | 3.74 | 5.42 | 2.49 | 3.86 | 3.21 | 1.41 |
| UO2 | nd | 5.57 | 3.28 | 0.96 | 0.57 | 1.26 | 1.00 |
| CaO | 8.31 | 5.79 | 5.77 | 6.63 | 5.53 | 6.59 | 5.40 |
| Total= | 93.10 | 88.82 | 89.67 | 82.81 | 86.59 | 87.84 | 90.34 |
| Ree total | 8.94 | 8.62 | 9.32 | 8.40 | 10.73 | 10.10 | 16.09 |

| | | | | | | | |
|---|---|---|---|---|---|---|---|
| Ca | 0.602 | 0.485 | 0.474 | 0.569 | 0.479 | 0.543 | 0.446 |
| La | 0.028 | 0.030 | 0.025 | 0.023 | 0.054 | 0.018 | 0.077 |
| Ce | 0.131 | 0.121 | 0.127 | 0.143 | 0.195 | 0.141 | 0.265 |
| Pr | 0.017 | 0.018 | 0.019 | ---- | ---- | 0.029 | 0.019 |
| Nd | 0.044 | 0.076 | 0.088 | 0.079 | 0.068 | 0.094 | 0.091 |
| Th | 0.008 | 0.067 | 0.095 | 0.045 | 0.071 | 0.056 | 0.025 |
| U | ---- | 0.097 | 0.056 | 0.017 | 0.010 | 0.022 | 0.017 |
| Σ Ca | 0.830 | 0.894 | 0.884 | 0.876 | 0.877 | 0.903 | 0.940 |
| Zr | 1.129 | 1.013 | 1.043 | 0.912 | 0.967 | 0.935 | 1.066 |
| Al | ---- | ---- | ---- | ---- | ---- | ---- | ---- |
| Si | ---- | ---- | ---- | ---- | ---- | ---- | ---- |
| Ti | 1.598 | 1.205 | 1.312 | 1.297 | 0.888 | 1.262 | 1.244 |
| Mn | ---- | ---- | ---- | ---- | ---- | ---- | ---- |
| Fe | 0.407 | 0.588 | 0.541 | 0.583 | 0.572 | 0.555 | 0.535 |
| Nb | 0.076 | 0.319 | 0.234 | 0.391 | 0.628 | 0.391 | 0.247 |
| Σ Ti | 2.081 | 2.112 | 2.087 | 2.271 | 2.088 | 2.208 | 2.026 |
| Total= | 4.040 | 4.019 | 4.014 | 4.059 | 3.932 | 4.046 | 4.032 |

ALLANITES

APPENDIX 2.6

Centre I: Angler Creek Ferroaugite Syenites | Craddock Cove syenite

| | C2905/1 | C2905/2 | C2905/3 | C2905/4 | C2920/2 | C2920/4 | C2920/5 | C2920/7 |
|---|---|---|---|---|---|---|---|---|
| SiO2 | 29.03 | 29.25 | 30.59 | 32.09 | 28.24 | 26.88 | 27.28 | 29.02 |
| TiO2 | 6.45 | 4.63 | 1.81 | 2.09 | 5.83 | 5.78 | 3.48 | 3.91 |
| Al2O3 | 3.11 | 4.60 | 8.26 | 8.36 | 3.46 | 2.98 | 5.90 | 6.00 |
| MnO | 0.17 | 0.41 | 0.19 | 0.20 | 0.91 | 0.66 | 0.33 | 0.78 |
| FeO | 24.92 | 24.05 | 23.04 | 22.87 | 22.93 | 21.53 | 23.02 | 22.09 |
| Nb2O3 | 0.56 | nd | 0.23 | nd | nd | 0.84 | nd | nd |
| CaO | 9.03 | 9.61 | 9.84 | 10.05 | 8.62 | 7.92 | 8.78 | 8.82 |
| La2O3 | 6.83 | 6.75 | 5.46 | 4.84 | 5.88 | 5.93 | 5.97 | 5.41 |
| Ce2O3 | 13.56 | 11.16 | 12.60 | 13.67 | 11.65 | 11.50 | 12.23 | 12.05 |
| Pr2O3 | 1.03 | 0.75 | 1.49 | 1.97 | 0.71 | nd | 0.75 | 0.98 |
| Nd2O3 | 3.16 | 3.20 | 4.60 | 5.26 | 2.95 | 1.47 | 3.06 | 2.96 |
| Sm2O3 | nd | nd | nd | nd | nd | nd | nd | nd |
| ThO2 | nd | nd | nd | nd | nd | nd | nd | nd |
| UO2 | nd | nd | nd | nd | nd | nd | nd | nd |
| Total= | 97.85 | 94.41 | 98.11 | 101.40 | 91.18 | 85.49 | 90.80 | 92.02 |
| REE2O3= | 24.58 | 21.86 | 24.15 | 25.74 | 21.19 | 18.9 | 22.01 | 21.40 |

| | | | | | | | | |
|---|---|---|---|---|---|---|---|---|
| Ca | 0.984 | 1.062 | 1.037 | 1.024 | 0.988 | 0.960 | 1.015 | 0.987 |
| La | 0.256 | 0.257 | 0.198 | 0.170 | 0.232 | 0.247 | 0.238 | 0.207 |
| Ce | 0.505 | 0.421 | 0.454 | 0.476 | 0.456 | 0.476 | 0.483 | 0.464 |
| Pr | 0.038 | 0.028 | 0.053 | 0.068 | 0.028 | ---- | 0.029 | 0.037 |
| Nd | 0.115 | 0.118 | 0.162 | 0.179 | 0.113 | 0.059 | 0.118 | 0.110 |
| Sm | ---- | ---- | ---- | ---- | ---- | ---- | ---- | ---- |
| Th | ---- | ---- | ---- | ---- | ---- | ---- | ---- | ---- |
| | 1.898 | 1.886 | 1.904 | 1.917 | 1.817 | 1.742 | 1.883 | 1.805 |
| Fe | 2.119 | 2.075 | 1.896 | 1.818 | 2.052 | 2.036 | 2.077 | 1.930 |
| Al | 0.373 | 0.559 | 0.958 | 0.937 | 0.436 | 0.397 | 0.750 | 0.739 |
| Mn | 0.015 | 0.036 | 0.016 | 0.016 | 0.032 | 0.063 | 0.032 | 0.069 |
| Mg | ---- | ---- | ---- | ---- | ---- | ---- | ---- | ---- |
| Nb | 0.026 | ---- | 0.010 | ---- | ---- | 0.043 | ---- | ---- |
| Ti | 0.493 | 0.359 | 0.134 | 0.149 | 0.469 | 0.492 | 0.282 | 0.307 |
| | 3.026 | 3.029 | 3.014 | 2.920 | 2.989 | 3.031 | 3.141 | 3.045 |
| Si | 2.951 | 3.017 | 3.010 | 3.050 | 3.021 | 3.040 | 2.943 | 3.031 |
| Total= | 7.875 | 7.932 | 7.928 | 7.887 | 7.827 | 7.813 | 7.967 | 7.881 |

| | C1524/1 | C1524/2 | C1524/3 | C1524/3 | 1524/4 | 1522/1 | 1418/2 | 1418/3 |
|---|---|---|---|---|---|---|---|---|
| SiO2 | 31.13 | 30.01 | 30.99 | 30.13 | 30.11 | 29.13 | 32.81 | 31.50 |
| TiO2 | 2.80 | 4.42 | 4.68 | 2.96 | 1.25 | 0.51 | nd | 0.15 |
| Al2O3 | 7.70 | 6.83 | 5.81 | 6.66 | 7.39 | 6.15 | 14.37 | 12.54 |
| MnO | 0.25 | 0.53 | 0.30 | 0.61 | 0.21 | 0.79 | nd | 0.25 |
| MgO | na | na | na | na | na | na | na | na |
| PbO | na | na | na | na | na | na | na | na |
| FeO | 21.90 | 19.50 | 22.70 | 21.07 | 23.71 | 25.31 | 20.11 | 19.02 |
| Nb2O3 | nd | 0.38 | nd | 1.95 | nd | 0.32 | na | na |
| CaO | 8.96 | 9.59 | 9.32 | 9.26 | 9.73 | 8.83 | 16.54 | 15.09 |
| Ce2O3 | 12.57 | 11.40 | 12.35 | 13.43 | 12.18 | 1.51 | 4.90 | 6.34 |
| La2O3 | 8.00 | 4.45 | 6.13 | 6.00 | 5.93 | 6.63 | 1.58 | 2.74 |
| Pr2O3 | 0.67 | 1.74 | 1.11 | 1.24 | 0.68 | 1.51 | nd | 0.74 |
| Nd2O3 | 2.11 | 3.79 | 3.84 | 3.32 | 3.75 | 4.26 | 2.33 | 2.83 |
| Sm2O3 | nd | nd | nd | nd | 0.21 | 0.22 | 0.67 | nd |
| ThO2 | nd | nd | nd | nd | 0.37 | nd | nd | 0.50 |
| UO2 | na | na | na | na | na | 11.75 | nd | na |
| Total= | 96.09 | 92.64 | 97.23 | 96.63 | 95.76 | 95.41 | 93.31 | 91.70 |
| REE2O3= | 23.35 | 21.38 | 23.43 | 23.99 | 22.75 | 14.13 | 9.48 | 12.65 |

| | | | | | | | | |
|---|---|---|---|---|---|---|---|---|
| Ca | 0.952 | 1.046 | 0.987 | 0.993 | 1.056 | 0.988 | 1.627 | 1.554 |
| La | 0.293 | 0.167 | 0.224 | 0.221 | 0.222 | 0.255 | 0.053 | 0.097 |
| Ce | 0.456 | 0.425 | 0.447 | 0.492 | 0.452 | 0.449 | 0.165 | 0.223 |
| Pr | 0.024 | 0.065 | 0.040 | 0.045 | 0.025 | 0.057 | ---- | 0.026 |
| Nd | 0.075 | 0.138 | 0.136 | 0.119 | 0.136 | 0.159 | 0.076 | 0.097 |
| Sm | ---- | ---- | ---- | ---- | 0.007 | 0.008 | 0.021 | ---- |
| Th | ---- | ---- | ---- | ---- | 0.009 | ---- | ---- | 0.011 |
| | 1.800 | 1.841 | 1.834 | 1.870 | 1.907 | 1.916 | 1.942 | 2.008 |
| Fe | 1.816 | 1.660 | 1.877 | 1.764 | 2.009 | 2.211 | 1.544 | 1.529 |
| Al | 0.900 | 0.819 | 0.677 | 0.786 | 0.883 | 0.757 | 1.555 | 1.421 |
| Mn | 0.021 | 0.046 | 0.025 | 0.052 | 0.039 | 0.070 | ---- | 0.020 |
| Mg | ---- | ---- | ---- | ---- | ---- | ---- | ---- | ---- |
| Nb | ---- | 0.017 | ---- | 0.088 | ---- | 0.015 | ---- | ---- |
| Ti | 0.209 | 0.338 | 0.348 | 0.223 | 0.095 | 0.040 | ---- | 0.011 |
| | 2.946 | 2.880 | 2.927 | 2.913 | 3.026 | 3.093 | 3.099 | 2.981 |
| Si | 3.086 | 3.054 | 3.064 | 3.015 | 3.051 | 3.042 | 3.012 | 3.028 |
| Total= | 7.832 | 7.775 | 7.825 | 7.798 | 7.984 | 8.051 | 8.053 | 8.017 |

| | 1418/5 | 1418/6 | 1418/7 | 1418/9 | 1428/1a | 1428/1b | 1428/3 | 1428/4 | 1428/5 |
|---|---|---|---|---|---|---|---|---|---|
| SiO2 | 31.34 | 31.95 | 32.68 | 31.93 | 31.22 | 27.45 | 28.86 | 29.16 | 29.24 |
| TiO2 | 0.23 | 0.46 | 0.38 | 0.19 | 1.37 | 0.73 | 1.10 | 1.00 | 1.06 |
| Al2O3 | 12.24 | 13.33 | 12.23 | 13.22 | 10.00 | 7.49 | 6.78 | 6.59 | 6.96 |
| MnO | 0.19 | 0.59 | 0.20 | 0.45 | 0.83 | 0.97 | 1.73 | 1.48 | 1.18 |
| MgO | na | na | na | na | na | na | na | na | na |
| PbO | 1.51 | 0.78 | 2.76 | nd | na | na | na | na | na |
| FeO | 16.71 | 18.00 | 17.67 | 18.28 | 21.71 | 17.55 | 22.14 | 24.36 | 24.35 |
| Nb2O3 | na | na | na | na | na | na | na | na | na |
| CaO | 12.76 | 14.09 | 14.01 | 15.37 | 10.95 | 10.02 | 10.25 | 10.08 | 9.95 |
| Ce2O3 | 6.58 | 6.38 | 6.39 | 5.97 | 13.12 | 8.99 | 12.28 | 12.71 | 11.59 |
| La2O3 | 2.37 | 2.88 | 2.86 | 2.35 | 5.68 | 3.98 | 5.85 | 6.11 | 4.94 |
| Pr2O3 | nd | 0.89 | 0.41 | 0.52 | 1.66 | nd | 1.31 | 1.33 | 1.07 |
| Nd2O3 | 2.60 | 2.17 | 1.98 | 2.86 | 4.08 | 2.51 | 3.15 | 3.61 | 3.40 |
| Sm2O3 | nd | 0.44 | 0.40 | 0.36 | nd | nd | nd | nd | nd |
| ThO2 | nd | 0.38 | 0.77 | 0.43 | nd | 0.62 | nd | nd | nd |
| UO2 | na | na | na | na | na | na | na | na | na |
| Total= | 86.53 | 92.34 | 92.74 | 91.93 | 100.62 | 80.31 | 93.45 | 96.43 | 93.74 |
| | | | | | | | | | |
| REE2O3= | 11.55 | 12.76 | 12.04 | 12.06 | 24.54 | 15.48 | 22.59 | 23.76 | 21.00 |

| | | | | | | | | | |
|---|---|---|---|---|---|---|---|---|---|
| Ca | 1.376 | 1.436 | 1.439 | 1.563 | 1.115 | 1.236 | 1.149 | 1.108 | 1.104 |
| La | 0.088 | 0.101 | 0.101 | 0.082 | 0.199 | 0.169 | 0.226 | 0.231 | 0.189 |
| Ce | 0.243 | 0.222 | 0.224 | 0.207 | 0.457 | 0.379 | 0.470 | 0.478 | 0.439 |
| Pr | ---- | 0.031 | 0.014 | 0.018 | 0.058 | ---- | 0.050 | 0.050 | 0.040 |
| Nd | 0.093 | 0.074 | 0.068 | 0.097 | 0.139 | 0.103 | 0.118 | 0.132 | 0.126 |
| Sm | ---- | 0.014 | 0.013 | 0.012 | ---- | ---- | ---- | ---- | ---- |
| Th | ---- | 0.008 | 0.017 | 0.009 | ---- | 0.016 | ---- | ---- | ---- |
| | 1.800 | 1.886 | 1.876 | 1.988 | 1.968 | 1.903 | 2.013 | 1.999 | 1.898 |
| | | | | | | | | | |
| Fe | 1.407 | 1.432 | 1.416 | 1.451 | 1.726 | 1.690 | 1.937 | 2.091 | 2.108 |
| Al | 1.453 | 1.495 | 1.382 | 1.479 | 1.121 | 1.016 | 0.836 | 0.797 | 0.849 |
| Mn | 0.016 | 0.048 | 0.016 | 0.036 | 0.067 | 0.095 | 0.153 | 0.129 | 0.103 |
| Mg | ---- | ---- | ---- | ---- | ---- | ---- | ---- | ---- | ---- |
| Nb | ---- | ---- | ---- | ---- | ---- | ---- | ---- | ---- | ---- |
| Ti | 0.017 | 0.033 | 0.027 | 0.014 | 0.098 | 0.063 | 0.087 | 0.077 | 0.083 |
| | 2.893 | 3.008 | 2.841 | 2.980 | 3.012 | 2.864 | 3.013 | 3.094 | 3.143 |
| | | | | | | | | | |
| Si | 3.155 | 3.039 | 3.132 | 3.030 | 2.968 | 3.160 | 3.019 | 2.993 | 3.027 |
| | | | | | | | | | |
| Total= | 7.848 | 7.933 | 7.849 | 7.998 | 7.948 | 7.927 | 8.045 | 8.086 | 8.068 |

| | 1428/6 | 1428/9 | 1428/12 | 1428/13 | 1428/14 | 1432/2 | 1432/5 | 1432/7 | 1432/8 |
|---|---|---|---|---|---|---|---|---|---|
| SiO2 | 28.09 | 29.92 | 30.32 | 30.29 | 30.35 | 29.42 | 29.01 | 32.07 | 30.09 |
| TiO2 | 0.90 | 0.38 | 1.17 | 0.70 | 0.58 | 0.71 | 0.45 | 0.45 | 0.18 |
| Al2O3 | 6.57 | 7.75 | 8.16 | 8.48 | 7.83 | 8.74 | 15.52 | 9.75 | 15.07 |
| MnO | 1.41 | 1.37 | 0.95 | 0.59 | 1.39 | 1.80 | 0.50 | 0.87 | 0.50 |
| MgO | na | na | na | na | na | na | na | na | na |
| PbO | na | na | na | na | na | na | na | na | na |
| FeO | 24.73 | 19.53 | 23.22 | 23.00 | 23.56 | 23.01 | 15.14 | 19.99 | 16.90 |
| Nb2O3 | na | na | na | na | na | na | na | na | na |
| CaO | 9.54 | 10.12 | 10.81 | 9.51 | 9.69 | 10.06 | 9.33 | 11.59 | 9.41 |
| Ce2O3 | 12.37 | 10.21 | 11.54 | 13.06 | 12.23 | 11.30 | 13.70 | 10.19 | 13.26 |
| La2O3 | 6.16 | 4.42 | 6.52 | 5.72 | 5.49 | 5.18 | 6.51 | 4.49 | 6.98 |
| Pr2O3 | 1.34 | 0.95 | 1.37 | 1.59 | 1.35 | 0.56 | 0.89 | 1.03 | 1.49 |
| Nd2O3 | 3.69 | 3.93 | 3.01 | 4.35 | 4.26 | 3.82 | 3.00 | 3.59 | 4.57 |
| Sm2O3 | 0.67 | 0.35 | nd | nd | 0.79 | 0.39 | nd | nd | 0.35 |
| ThO2 | nd | 0.41 | 0.54 | nd | nd | nd | nd | 1.19 | nd |
| UO2 | na | 0.33 | nd | nd | nd | na | na | na | na |
| Total= | 95.47 | 89.67 | 97.61 | 97.29 | 97.52 | 94.99 | 94.05 | 95.21 | 98.80 |
| REE2O3= | 24.23 | 19.86 | 22.44 | 24.72 | 24.12 | 21.25 | 24.1 | 19.3 | 26.65 |

| | | | | | | | | | |
|---|---|---|---|---|---|---|---|---|---|
| Ca | 1.071 | 1.145 | 1.153 | 1.018 | 1.039 | 1.091 | 0.980 | 1.211 | 0.958 |
| La | 0.238 | 0.172 | 0.239 | 0.211 | 0.203 | 0.193 | 0.235 | 0.162 | 0.245 |
| Ce | 0.475 | 0.395 | 0.420 | 0.478 | 0.448 | 0.419 | 0.492 | 0.364 | 0.461 |
| Pr | 0.051 | 0.037 | 0.050 | 0.058 | 0.049 | 0.021 | 0.032 | 0.037 | 0.052 |
| Nd | 0.138 | 0.148 | 0.107 | 0.155 | 0.152 | 0.138 | 0.105 | 0.125 | 0.155 |
| Sm | 0.024 | 0.013 | ---- | ---- | 0.027 | 0.014 | ---- | ---- | 0.011 |
| Th | ---- | 0.010 | 0.012 | ---- | ---- | ---- | ---- | 0.026 | ---- |
| | 1.997 | 1.920 | 1.981 | 1.920 | 1.918 | 1.876 | 1.844 | 1.925 | 1.882 |
| Fe | 2.167 | 1.725 | 1.932 | 1.922 | 1.973 | 1.948 | 1.241 | 1.631 | 1.343 |
| Al | 0.812 | 0.965 | 0.957 | 0.999 | 0.924 | 1.043 | 1.793 | 1.121 | 1.688 |
| Mn | 0.125 | 0.123 | 0.080 | 0.050 | 0.118 | 0.154 | 0.042 | 0.072 | 0.040 |
| Mg | ---- | ---- | ---- | ---- | ---- | ---- | ---- | ---- | ---- |
| Nb | ---- | ---- | ---- | ---- | ---- | ---- | ---- | ---- | ---- |
| Ti | 0.071 | 0.030 | 0.088 | 0.053 | 0.044 | 0.054 | 0.033 | 0.033 | 0.013 |
| | 3.175 | 2.843 | 3.057 | 3.024 | 3.059 | 3.199 | 3.109 | 2.857 | 3.084 |
| Si | 2.944 | 3.159 | 2.987 | 3.027 | 3.038 | 2.978 | 2.843 | 3.128 | 2.858 |
| Total= | 8.116 | 7.922 | 8.025 | 7.971 | 8.015 | 8.053 | 7.796 | 7.910 | 7.824 |

| | v | v | | c | c | | | | |
|---|---|---|---|---|---|---|---|---|---|
| | 1432/9 | 1432/11 | 1432/13 | 1432/15 | 2925/3 | 2925/5 | 2925/4 | 2925/2 | 2925/6 |
| SiO2 | 30.63 | 30.99 | 30.57 | 30.75 | 30.68 | 30.71 | 29.97 | 31.24 | 31.62 |
| TiO2 | nd | nd | 0.18 | 0.78 | 2.07 | 2.02 | 1.38 | 0.54 | 1.26 |
| Al2O3 | 14.07 | 12.49 | 14.90 | 7.73 | 10.13 | 9.89 | 9.27 | 8.09 | 7.75 |
| MnO | 0.45 | 0.34 | 0.41 | 2.72 | 0.21 | 0.32 | 0.50 | 1.04 | 0.87 |
| MgO | na | na | na | na | nd | 0.35 | nd | nd | nd |
| PbO | na | na | na | na | na | na | na | na | na |
| FeO | 17.27 | 19.29 | 15.55 | 23.14 | 20.33 | 19.35 | 21.47 | 20.93 | 20.24 |
| Nb2O3 | na | na | na | na | na | na | na | na | na |
| CaO | 10.00 | 11.94 | 9.58 | 10.03 | 9.71 | 9.70 | 10.27 | 10.35 | 10.17 |
| Ce2O3 | 13.04 | 11.12 | 13.04 | 11.45 | 13.84 | 14.21 | 12.55 | 10.84 | 13.54 |
| La2O3 | 7.05 | 5.07 | 6.56 | 6.14 | 7.07 | 6.92 | 7.10 | 3.32 | 4.14 |
| Pr2O3 | 1.16 | 0.70 | 1.46 | 1.63 | 0.92 | 1.70 | 1.25 | 1.84 | 2.33 |
| Nd2O3 | 3.06 | 2.90 | 4.05 | 3.67 | 2.99 | 3.16 | 2.87 | 6.45 | 3.44 |
| Sm2O3 | nd | nd | nd | nd | nd | nd | nd | nd | nd |
| ThO2 | nd | nd | 0.43 | nd | nd | nd | 0.45 | nd | nd |
| UO2 | na | nd | 0.37 | nd | nd | na | na | na | nd |
| Total= | 96.73 | 94.84 | 97.10 | 98.04 | 97.95 | 98.33 | 97.08 | 94.64 | 95.36 |
| | | | | | | | | | |
| REE2O3= | 24.31 | 19.79 | 25.11 | 22.89 | 24.82 | 25.99 | 23.77 | 22.45 | 23.45 |

v=allanite from vien
c= allanite from calcite assemblage

| | | | | | | | | | |
|---|---|---|---|---|---|---|---|---|---|
| Ca | 1.029 | 1.237 | 0.982 | 1.063 | 1.010 | 1.009 | 1.091 | 1.115 | 1.088 |
| La | 0.250 | 0.181 | 0.231 | 0.224 | 0.253 | 0.246 | 0.260 | 0.123 | 0.152 |
| Ce | 0.458 | 0.394 | 0.457 | 0.415 | 0.492 | 0.505 | 0.456 | 0.399 | 0.495 |
| Pr | 0.041 | 0.025 | 0.051 | 0.059 | 0.033 | 0.060 | 0.045 | 0.067 | 0.085 |
| Nd | 0.105 | 0.100 | 0.138 | 0.130 | 0.104 | 0.110 | 0.102 | 0.232 | 0.123 |
| Sm | ---- | ---- | ---- | ---- | ---- | ---- | ---- | ---- | ---- |
| Th | ---- | ---- | 0.009 | ---- | ---- | ---- | 0.010 | ---- | ---- |
| | 1.883 | 1.937 | 1.868 | 1.891 | 1.892 | 1.932 | 1.964 | 1.936 | 1.943 |
| | | | | | | | | | |
| Fe | 1.386 | 1.560 | 1.244 | 1.915 | 1.651 | 1.572 | 1.780 | 1.760 | 1.689 |
| Al | 1.592 | 1.423 | 1.680 | 0.902 | 1.160 | 1.132 | 1.083 | 0.959 | 0.912 |
| Mn | 0.037 | 0.028 | 0.033 | 0.228 | 0.017 | 0.026 | 0.042 | 0.089 | 0.074 |
| Mg | ---- | ---- | ---- | ---- | ---- | 0.051 | ---- | ---- | ---- |
| Nb | ---- | ---- | ---- | ---- | ---- | ---- | ---- | ---- | ---- |
| Ti | ---- | ---- | 0.013 | 0.058 | 0.151 | 0.148 | 0.103 | 0.041 | 0.095 |
| | 3.015 | 3.011 | 2.970 | 3.103 | 2.979 | 2.929 | 3.008 | 2.849 | 2.770 |
| | | | | | | | | | |
| Si | 2.940 | 2.996 | 2.923 | 3.042 | 2.979 | 2.982 | 2.971 | 3.142 | 3.156 |
| | | | | | | | | | |
| Total= | 7.838 | 7.944 | 7.761 | 8.036 | 7.850 | 7.843 | 7.943 | 7.927 | 7.869 |

Centre III: Contaminated ferro-
edenite syenite

| | c<br>2925/8 | c<br>2925/9 | 2229/1 | 2229/2 | 2229/3 | C2150/1 | C2150/2 | C2150/3 | C2150/4 |
|---|---|---|---|---|---|---|---|---|---|
| SiO2 | 31.42 | 32.12 | 33.09 | 33.32 | 36.01 | 30.01 | 31.06 | 31.80 | 30.86 |
| TiO2 | 0.24 | 0.70 | 1.22 | 0.67 | 0.89 | 2.41 | 2.72 | 2.48 | 2.44 |
| Al2O3 | 8.21 | 9.88 | 12.95 | 11.83 | 10.39 | 11.27 | 11.36 | 11.30 | 11.02 |
| MnO | 0.96 | 1.68 | 0.28 | 0.66 | 0.56 | 0.98 | 0.25 | 0.25 | 0.90 |
| MgO | 0.66 | 0.44 | na | na | na | na | na | na | 0.86 |
| PbO | na | na | na | na | na | na | na | na | na |
| FeO | 20.75 | 20.09 | 17.73 | 20.67 | 21.56 | 13.19 | 16.48 | 12.21 | 13.99 |
| Nb2O3 | na | na | nd | 0.47 | nd | nd | nd | nd | nd |
| CaO | 11.02 | 1.58 | 11.21 | 10.14 | 9.76 | 10.03 | 10.25 | 12.21 | 10.34 |
| Ce2O3 | 10.61 | 8.30 | 11.54 | 10.37 | 10.22 | 11.51 | 12.24 | 10.56 | 12.37 |
| La2O3 | 2.15 | 1.58 | 6.22 | 6.92 | 5.11 | 6.52 | 8.38 | 6.48 | 7.79 |
| Pr2O3 | 1.47 | 1.52 | 0.84 | 1.16 | 1.14 | nd | 0.82 | 1.57 | 1.58 |
| Nd2O3 | 5.72 | 8.70 | 2.76 | 2.79 | 3.94 | 1.46 | 1.67 | 1.96 | 2.19 |
| Sm2O3 | nd | 0.60 | 0.24 | nd | nd | nd | nd | nd | na |
| ThO2 | nd | nd | nd | nd | nd | nd | 0.38 | 0.97 | nd |
| UO2 | nd | na | na | na | na | na | na | na | na |
| Total= | 93.21 | 96.38 | 98.08 | 99.00 | 99.58 | 87.39 | 95.61 | 91.78 | 94.34 |
| | | | | | | | | | |
| REE2O3= | 19.95 | 20.70 | 21.60 | 21.24 | 20.41 | 19.49 | 23.11 | 20.57 | 23.93 |

| | | | | | | | | | |
|---|---|---|---|---|---|---|---|---|---|
| Ca | 1.185 | 1.113 | 1.110 | 1.007 | 0.952 | 1.103 | 1.062 | 1.281 | 1.082 |
| La | 0.080 | 0.056 | 0.212 | 0.237 | 0.172 | 0.247 | 0.299 | 0.234 | 0.281 |
| Ce | 0.390 | 0.293 | 0.390 | 0.352 | 0.340 | 0.433 | 0.433 | 0.379 | 0.442 |
| Pr | 0.054 | 0.053 | 0.028 | 0.039 | 0.038 | ---- | 0.029 | 0.056 | 0.056 |
| Nd | 0.205 | 0.300 | 0.091 | 0.092 | 0.128 | 0.054 | 0.058 | 0.069 | 0.076 |
| Sm | ---- | 0.020 | 0.008 | ---- | ---- | ---- | ---- | ---- | ---- |
| Th | ---- | ---- | ---- | ---- | ---- | ---- | 0.008 | 0.022 | ---- |
| | 1.914 | 1.835 | 1.839 | 1.727 | 1.630 | 1.837 | 1.889 | 2.041 | 1.937 |
| | | | | | | | | | |
| Fe | 1.742 | 1.620 | 1.370 | 1.602 | 1.641 | 1.132 | 1.332 | 0.999 | 1.143 |
| Al | 0.971 | 1.123 | 1.411 | 1.293 | 1.115 | 1.364 | 1.294 | 1.305 | 1.269 |
| Mn | 0.082 | 0.137 | 0.022 | 0.052 | 0.043 | 0.085 | 0.020 | 0.021 | 0.074 |
| Mg | 0.099 | 0.063 | ---- | ---- | ---- | ---- | ---- | ---- | 0.125 |
| Nb | ---- | ---- | ---- | 0.020 | ---- | ---- | ---- | ---- | ---- |
| Ti | 0.018 | 0.051 | 0.085 | 0.047 | 0.061 | 0.186 | 0.198 | 0.183 | 0.179 |
| | 2.912 | 2.994 | 2.888 | 3.014 | 2.860 | 2.767 | 2.844 | 2.508 | 2.790 |
| | | | | | | | | | |
| Si | 3.154 | 3.098 | 3.058 | 3.088 | 3.277 | 3.081 | 3.002 | 3.114 | 3.015 |

| Total= | 7.980 | 7.927 | 7.785 | 7.829 | 7.767 | 7.685 | 7.735 | 7.663 | 7.742 |
|---|---|---|---|---|---|---|---|---|---|

Quartz syenite

| | C2150/5 | C2123/1 | C2123/1 | C2123/1 | neys-1 | neys-2 | neys-7 | neys-8 | neys-9 |
|---|---|---|---|---|---|---|---|---|---|
| SiO2 | 33.17 | 32.12 | 35.01 | 31.53 | 29.53 | 29.77 | 30.12 | 31.53 | 32.14 |
| TiO2 | 2.83 | 2.16 | 2.83 | 2.72 | 3.86 | 3.61 | 2.74 | 3.40 | 2.43 |
| Al2O3 | 11.66 | 10.24 | 11.81 | 11.08 | 7.64 | 7.00 | 9.18 | 9.79 | 10.71 |
| MnO | 0.56 | 0.96 | 0.99 | 0.97 | 0.35 | 0.58 | 0.71 | 1.04 | 0.43 |
| MgO | 1.11 | 7.40 | 5.32 | 2.88 | na | na | na | na | na |
| PbO | na | na | na | na | na | na | na | na | na |
| FeO | 11.51 | 7.89 | 9.39 | 6.53 | 15.69 | 15.48 | 14.71 | 13.92 | 12.30 |
| Nb2O3 | nd | nd | nd | nd | nd | 0.70 | 0.39 | nd | nd |
| CaO | 11.20 | 4.45 | 7.13 | 6.28 | 10.06 | 9.75 | 9.35 | 10.48 | 10.03 |
| Ce2O3 | 10.68 | 4.01 | 6.54 | 5.66 | 12.13 | 12.39 | 12.81 | 11.45 | 11.86 |
| La2O3 | 6.65 | 2.09 | 3.15 | 2.99 | 6.22 | 6.59 | 6.52 | 5.43 | 5.39 |
| Pr2O3 | 0.71 | 0.26 | 1.01 | 0.31 | 0.76 | 1.39 | 1.55 | 0.67 | 0.94 |
| Nd2O3 | 1.31 | 0.71 | 1.29 | 0.95 | 2.71 | 3.02 | 3.28 | 3.35 | 3.14 |
| Sm2O3 | na | na | na | na | nd | nd | 0.39 | nd | nd |
| ThO2 | 0.74 | 1.37 | 1.30 | 1.55 | 0.70 | 0.98 | 0.56 | 0.99 | 0.31 |
| UO2 | na | na | na | na | na | na | na | na | na |
| Total= | 92.13 | 73.66 | 84.77 | 73.45 | 89.65 | 91.26 | 92.31 | 92.05 | 89.68 |
| REE2O3= | 19.35 | 7.07 | 11.99 | 9.91 | 21.82 | 23.39 | 24.55 | 20.90 | 21.33 |

| | | | | | | | | | |
|---|---|---|---|---|---|---|---|---|---|
| Ca | 1.143 | 0.733 | 0.729 | 0.733 | 1.126 | 1.087 | 1.022 | 1.112 | 1.074 |
| La | 0.234 | 0.120 | 0.111 | 0.120 | 0.240 | 0.253 | 0.245 | 0.198 | 0.199 |
| Ce | 0.373 | 0.226 | 0.228 | 0.226 | 0.464 | 0.472 | 0.478 | 0.415 | 0.434 |
| Pr | 0.025 | 0.012 | 0.035 | 0.012 | 0.029 | 0.053 | 0.058 | 0.024 | 0.034 |
| Nd | 0.045 | 0.037 | 0.044 | 0.037 | 0.101 | 0.112 | 0.119 | 0.119 | 0.112 |
| Sm | ---- | ---- | ---- | ---- | ---- | ---- | 0.014 | ---- | ---- |
| Th | 0.016 | 0.038 | 0.028 | 0.038 | 0.017 | 0.023 | 0.013 | 0.022 | 0.007 |
| | 1.836 | 1.166 | 1.175 | 1.166 | 1.977 | 2.000 | 1.949 | 1.890 | 1.860 |
| Fe | 0.917 | 0.595 | 0.670 | 0.595 | 1.371 | 1.347 | 1.255 | 1.153 | 1.028 |
| Al | 1.310 | 1.422 | 1.329 | 1.422 | 0.941 | 0.859 | 1.104 | 1.143 | 1.262 |
| Mn | 0.045 | 0.089 | 0.080 | 0.089 | 0.031 | 0.051 | 0.061 | 0.087 | 0.036 |
| Mg | 0.158 | 0.467 | 0.757 | 0.467 | ---- | ---- | ---- | ---- | ---- |
| Nb | ---- | ---- | ---- | ---- | ---- | 0.033 | 0.018 | ---- | ---- |
| Ti | 0.203 | 0.223 | 0.203 | 0.223 | 0.303 | 0.283 | 0.210 | 0.253 | 0.183 |
| | 2.633 | 2.796 | 3.039 | 2.796 | 2.646 | 2.573 | 2.648 | 2.636 | 2.509 |
| Si | 3.160 | 3.434 | 3.341 | 3.434 | 3.085 | 3.098 | 3.072 | 3.123 | 3.211 |
| Total= | 7.629 | 7.396 | 7.555 | 7.396 | 7.708 | 7.671 | 7.669 | 7.649 | 7.580 |

APPENDIX 2.7

THORITE

Centrel: Magnesio-hornblende Syenite | Centre III: Quartz Syenite Dyke

| | 2123/1 | 2123/2 | C2150/1 | C2150/2 | C2150/3 | C2925/1 | C2925/2 | C2925/3 | C2925/4 |
|---|---|---|---|---|---|---|---|---|---|
| SiO2 | 22.73 | 20.22 | 20.81 | 22.25 | 23.39 | 18.00 | 22.10 | 22.89 | 21.27 |
| Al2O3 | 1.51 | nd | nd | 0.89 | 2.71 | 0.69 | nd | nd | nd |
| ThO2 | 40.75 | 43.81 | 48.18 | 60.03 | 40.65 | 57.66 | 52.79 | 48.14 | 58.42 |
| UO2 | 20.09 | 12.71 | 21.61 | 10.23 | 29.54 | nd | 3.32 | 2.02 | nd |
| La2O3 | nd | nd | 2.15 | 0.43 | nd | 1.58 | nd | 0.57 | 1.18 |
| Ce2O3 | 5.54 | 2.33 | 3.24 | nd | 0.40 | 3.38 | 2.39 | 1.11 | 3.00 |
| Pr2O3 | nd | nd | nd | nd | nd | nd | 1.09 | 0.97 | 0.78 |
| Nd2O3 | 2.84 | 4.51 | 0.62 | 0.53 | nd | 1.96 | 4.80 | 3.03 | 2.68 |
| Sm2O3 | na | *1.91 | na | na | na | nd | 0.70 | 0.63 | nd |
| Y2O3* | na | 5.37 | na | na | na | 1.26 | 2.29 | 10.33 | 1.50 |
| CaO | 0.96 | 0.86 | 1.37 | 1.90 | 2.00 | 3.39 | 2.14 | 1.69 | 3.49 |
| FeO | 0.20 | 0.60 | 0.18 | nd | 0.95 | 1.72 | 0.33 | 1.00 | 2.47 |
| Total | 94.62 | 92.32 | 98.16 | 96.26 | 99.64 | 89.64 | 91.95 | 92.38 | 94.79 |
| | | | | | | | | | |
| RE2O3 | 8.38 | 8.75 | 6.01 | 0.96 | 0.4 | 6.92 | 8.98 | 6.31 | 7.64 |

* - semi-quantitative

calculated to 4 oxygen

| | 2123/1 | 2123/2 | C2150/1 | C2150/2 | C2150/3 | C2925/1 | C2925/2 | C2925/3 | C2925/4 |
|---|---|---|---|---|---|---|---|---|---|
| Ca | 0.051 | 0.048 | 0.075 | 0.101 | 0.099 | 0.198 | 0.116 | 0.087 | 0.186 |
| Fe | 0.008 | 0.026 | 0.008 | ---- | 0.037 | 0.078 | 0.014 | 0.040 | 0.103 |
| Th | 0.456 | 0.522 | 0.562 | 0.679 | 0.428 | 0.716 | 0.609 | 0.529 | 0.662 |
| U | 0.220 | 0.148 | 0.246 | 0.113 | 0.304 | ---- | 0.037 | 0.022 | ---- |
| La | ---- | ---- | 0.041 | 0.008 | ---- | 0.032 | ---- | 0.010 | 0.022 |
| Ce | 0.100 | 0.045 | 0.061 | ---- | 0.007 | 0.068 | 0.044 | 0.020 | 0.055 |
| Pr | ---- | ---- | ---- | ---- | ---- | ---- | 0.020 | 0.017 | 0.014 |
| Nd | 0.050 | 0.084 | 0.011 | 0.009 | ---- | 0.038 | 0.087 | 0.052 | 0.048 |
| Sm | ---- | 0.034 | ---- | ---- | ---- | ---- | 0.012 | 0.010 | ---- |
| Y | ---- | 0.150 | ---- | ---- | ---- | 0.037 | 0.062 | 0.265 | 0.040 |
| | 0.885 | 1.057 | 1.004 | 0.910 | 0.875 | 1.167 | 1.001 | 1.052 | 1.130 |
| | | | | | | | | | |
| Si | 1.117 | 1.058 | 1.066 | 1.106 | 1.083 | 0.982 | 1.120 | 1.105 | 1.060 |
| Al | 0.088 | ---- | --- | 0.052 | 0.148 | 0.044 | ---- | ---- | ---- |
| | 1.205 | 1.058 | 1.066 | 1.158 | 1.231 | 1.026 | 1.120 | 1.105 | 1.060 |
| | | | | | | | | | |
| Sum | 2.090 | 2.115 | 2.070 | 2.068 | 2.106 | 2.193 | 2.121 | 2.157 | 2.190 |

| | C2925/5 |
|---|---|
| SiO2 | 22.71 |
| Al2O3 | nd |
| ThO2 | 46.75 |
| UO2 | 6.57 |
| La2O3 | nd |
| Ce2O3 | 1.08 |
| Pr2O3 | nd |
| Nd2O3 | 2.38 |
| Sm2O3 | 1.13 |
| Y2O3* | 7.90 |
| CaO | 1.87 |
| FeO | 0.34 |
| Total | 90.73 |
| | |
| RE2O3 | 4.59 |

APPENDIX 2.8

ZIRCON

| | F | M | M | M | M | F | F | M | M |
|---|---|---|---|---|---|---|---|---|---|
| | C2155/1 | C2155/1 | C2155/2 | C2155/3 | C2025/1 | C2025/1 | C2025/2 | C2025/2 | C2125/1 |
| SiO2 | 33.61 | 30.03 | 29.05 | 29.27 | 30.50 | 33.23 | 33.42 | 28.49 | 27.98 |
| ZrO2 | 65.47 | 56.24 | 46.18 | 44.74 | 55.82 | 65.68 | 65.64 | 49.40 | 54.05 |
| HfO2 | 1.51 | 1.87 | 1.33 | 0.87 | 1.05 | nd | 1.22 | 0.94 | nd |
| Ce2O3 | na | na | na | 2.74 | na | na | na | na | na |
| ThO2 | nd | nd | 1.33 | na | 0.45 | nd | nd | nd | nd |
| UO2 | nd | 0.44 | 1.00 | 0.38 | nd | 0.66 | nd | nd | nd |
| CaO | nd | 6.02 | 2.39 | 2.33 | 8.33 | nd | 0.27 | 6.82 | 2.84 |
| FeO | 0.27 | 1.54 | 0.86 | 0.78 | 1.33 | 0.21 | 0.27 | 1.03 | 0.71 |
| MnO | nd | 0.50 | 0.42 | 0.28 | 0.77 | nd | nd | 0.30 | 0.71 |
| Total= | 100.86 | 96.64 | 83.43 | 81.39 | 98.24 | 99.78 | 100.82 | 86.98 | 85.58 |

| | | | | | | | | | |
|---|---|---|---|---|---|---|---|---|---|
| Si | 1.017 | 0.966 | 1.070 | 1.087 | 0.961 | 1.015 | 1.012 | 0.999 | 0.991 |
| Zr | 0.966 | 0.882 | 0.830 | 0.810 | 0.858 | 0.978 | 0.969 | 0.844 | 0.934 |
| Hf | 0.013 | 0.017 | 0.014 | 0.009 | 0.009 | ---- | 0.011 | 0.009 | ---- |
| Ce | ---- | ---- | ---- | 0.037 | ---- | ---- | ---- | ---- | ---- |
| Th | ---- | ---- | 0.011 | ---- | 0.003 | ---- | ---- | ---- | ---- |
| U | ---- | 0.003 | 0.008 | 0.003 | ---- | 0.004 | ---- | ---- | ---- |
| Ca | ---- | 0.208 | 0.094 | 0.093 | 0.281 | ---- | 0.009 | 0.256 | 0.108 |
| Fe | 0.007 | 0.041 | 0.026 | 0.024 | 0.035 | 0.005 | 0.007 | 0.030 | 0.021 |
| Mn | ---- | 0.014 | 0.013 | 0.009 | 0.021 | ---- | ---- | 0.009 | 0.021 |
| Total= | 2.003 | 2.131 | 2.066 | 2.072 | 2.168 | 2.002 | 2.008 | 2.147 | 2.075 |

F= "Fresh"
M= metamict
C= core
O= overgrowth

| | C | O | C | O | F | M | M | F |
|---|---|---|---|---|---|---|---|---|
| | C1513/1 | C1513/1 | C1513/2 | C1513/2 | C2028/1 | C2028/1 | C2040/1 | C2040/1 |
| $SiO_2$ | 33.71 | 33.38 | 31.63 | 34.12 | 32.54 | 29.88 | 29.25 | 33.93 |
| $ZrO_2$ | 61.80 | 63.94 | 58.96 | 60.10 | 66.00 | 56.79 | 57.94 | 65.13 |
| $HfO_2$ | 0.87 | 1.29 | 1.23 | 0.48 | 1.73 | 1.27 | 0.86 | 0.95 |
| $Ce_2O_3$ | na | na | na | na | na | na | na | na |
| $ThO_2$ | 0.64 | 0.44 | nd | 0.69 | nd | na | na | na |
| $UO_2$ | nd | 0.45 | 0.47 | nd | na | 0.39 | 0.43 | 0.60 |
| CaO | 0.44 | nd | 0.69 | 0.41 | nd | 3.69 | 2.46 | nd |
| FeO | 0.62 | 0.40 | 2.88 | 1.14 | nd | 1.07 | 1.44 | nd |
| MnO | nd | 0.19 | 0.14 | 0.17 | nd | nd | 0.72 | nd |
| Total = | 98.07 | 100.09 | 96.00 | 97.11 | 100.27 | 93.08 | 93.11 | 100.61 |

| | | | | | | | | |
|---|---|---|---|---|---|---|---|---|
| Si | 1.041 | 1.021 | 1.013 | 1.058 | 0.998 | 0.989 | 0.974 | 1.027 |
| Zr | 0.931 | 0.954 | 0.921 | 0.909 | 0.987 | 0.916 | 0.941 | 0.961 |
| Hf | 0.008 | 0.011 | 0.011 | 0.004 | 0.015 | 0.012 | 0.008 | 0.008 |
| Ce | ---- | ---- | ---- | ---- | ---- | ---- | ---- | ---- |
| Th | 0.004 | 0.003 | ---- | 0.005 | ---- | ---- | ---- | ---- |
| U | ---- | 0.003 | 0.003 | ---- | ---- | 0.003 | 0.003 | 0.004 |
| Ca | 0.015 | ---- | 0.024 | 0.014 | ---- | 0.131 | 0.088 | ---- |
| Fe | 0.016 | 0.010 | 0.077 | 0.030 | ---- | 0.030 | 0.040 | ---- |
| Mn | ---- | 0.005 | 0.004 | 0.004 | ---- | ---- | 0.020 | ---- |
| Total = | 2.015 | 2.007 | 2.053 | 2.024 | 2.000 | 2.081 | 2.074 | 2.000 |

NB-RUTILE
Centre I: Eastern Contact Pegmatites

APPENDIX 2.9

a= acicular Nb-rutile
i= interstial Nb-rutile

| | | | | a | a | i | i | | i |
|---|---|---|---|---|---|---|---|---|---|
| | C1C/1 | C1C/2 | C1A/1 | C1A/2 | C1A/3 | C1A/3 | C1A/4 | C1A/5 | C1A/6 |
| TiO2 | 85.58 | 86.17 | 81.41 | 89.73 | 87.84 | 71.73 | 75.07 | 83.45 | 76.85 |
| Nb2O5 | 6.76 | 8.30 | 10.50 | 4.92 | 6.06 | 19.96 | 17.44 | 4.50 | 15.77 |
| Ta2O5 | 1.54 | 2.15 | 1.46 | 1.69 | 2.02 | 2.52 | 1.88 | 4.25 | 1.42 |
| WO3 | 1.88 | 1.06 | 1.17 | na | na | na | na | 4.80 | na |
| FeO | 3.90 | 2.57 | 5.04 | 2.97 | 3.31 | 6.19 | 5.38 | 3.52 | 5.23 |
| MnO | nd | 0.22 | 0.13 | nd | nd | nd | nd | nd | nd |
| Total= | 99.66 | 100.46 | 99.69 | 99.31 | 99.23 | 100.40 | 99.78 | 100.52 | 99.27 |
| | | | | | | | | | |
| Ti | 2.717 | 2.707 | 2.614 | 2.809 | 2.770 | 2.357 | 2.447 | 2.686 | 2.499 |
| Nb | 0.129 | 0.157 | 0.203 | 0.093 | 0.115 | 0.394 | 0.342 | 0.087 | 0.308 |
| Ta | 0.018 | 0.024 | 0.017 | 0.019 | 0.023 | 0.030 | 0.022 | 0.049 | 0.017 |
| W | 0.021 | 0.011 | 0.013 | ---- | ---- | ---- | ---- | 0.053 | ---- |
| Sn | ---- | ---- | ---- | ---- | ---- | ---- | ---- | ---- | ---- |
| Fe | 0.136 | 0.090 | 0.180 | 0.103 | 0.116 | 0.226 | 0.195 | 0.126 | 0.189 |
| Mn | ---- | 0.008 | 0.005 | ---- | ---- | ---- | ---- | ---- | ---- |
| | | | | | | | | | |
| total | 3.021 | 2.997 | 3.032 | 3.024 | 3.024 | 3.007 | 3.006 | 3.001 | 3.013 |

Centre III: Quartz Syenite

| | C2217/2 | C2217/3 | C2211/3 | C2211/4 |
|---|---|---|---|---|
| TiO2 | 67.03 | 66.18 | 45.95 | 69.13 |
| Nb2O5 | 20.24 | 19.53 | 10.93 | 14.65 |
| Ta2O5 | 2.66 | 2.71 | 3.34 | 3.91 |
| WO3 | na | na | na | na |
| SnO2 | 0.29 | 1.61 | nd | nd |
| FeO | 7.57 | 7.99 | 28.81 | 5.68 |
| MnO | nd | nd | nd | 0.15 |
| Total= | 97.79 | 98.02 | 89.03 | 93.52 |
| | | | | |
| Ti | 2.292 | 2.282 | 1.923 | 2.436 |
| Nb | 0.416 | 0.405 | 0.275 | 0.310 |
| Ta | 0.033 | 0.034 | 0.051 | 0.050 |
| W | ---- | ---- | ---- | ---- |
| Sn | 0.006 | 0.033 | ---- | ---- |
| Fe | 0.288 | 0.306 | 1.341 | 0.223 |
| Mn | ---- | ---- | ---- | 0.006 |
| | | | | |
| total | 3.035 | 3.060 | 3.590 | 3.025 |

MONAZITE

APPENDIX 2.10

Centre I: Eastern contact pegmatite

Craddock Cove red syenites

| | C1A/2 | C1A/3 | C1A/4 | C1A/5 | C1A/6 | C1A/8 | C2920/1 | C2920/2 | C2920/3 |
|---|---|---|---|---|---|---|---|---|---|
| CaO | 0.2 | 0.16 | nd | nd | 0.14 | 0.36 | nd | 0.08 | nd |
| FeO | 0.7 | nd | 0.19 | nd | nd | 0.69 | nd | 0.33 | nd |
| ThO2 | 1.56 | 4.18 | 1.57 | 2.17 | 4.46 | 1.3 | 5.99 | 7.53 | 9.80 |
| UO2 | na | na | na | na | na | na | nd | 0.69 | nd |
| La2O3 | 14.75 | 18.54 | 18.49 | 14.31 | 16.2 | 12.97 | 26.29 | 25.88 | 24.03 |
| Ce2O3 | 33.42 | 33.32 | 34.56 | 33.56 | 32.71 | 33.7 | 29.66 | 29.61 | 28.08 |
| Pr2O3 | 3.07 | 3.36 | 3.97 | 4.15 | 3.45 | 5.42 | 1.21 | 1.81 | 0.82 |
| Nd2O3 | 11.65 | 8.13 | 8.9 | 11.81 | 9.83 | 13.86 | 2.78 | 3.31 | 2.72 |
| Sm2O3 | 0.6 | nd | nd | 0.74 | 0.32 | 0.88 | nd | nd | nd |
| P2O5 | 29.84 | 28.08 | 29.45 | 29.75 | 27.08 | 29.05 | 27.28 | 27.01 | 23.81 |
| SiO2 | 0.95 | 0.82 | 0.71 | 0.6 | 1.09 | 0.48 | 1.99 | 2.39 | 2.79 |
| Total | 96.73 | 96.59 | 97.85 | 97.08 | 95.29 | 98.7 | 95.20 | 98.64 | 92.06 |
| La/Nd | 1.311 | 2.345 | 2.151 | 1.250 | 1.705 | 0.964 | 9.707 | 8.000 | 9.047 |

calculated to 4 oxygen

| | | | | | | | | | |
|---|---|---|---|---|---|---|---|---|---|
| Ca | 0.008 | 0.007 | ---- | ---- | 0.006 | 0.015 | ---- | 0.003 | ---- |
| Fe | 0.023 | ---- | 0.006 | ---- | ---- | 0.023 | ---- | 0.011 | ---- |
| Th | 0.014 | 0.039 | 0.014 | 0.020 | 0.042 | 0.012 | 0.056 | 0.069 | 0.098 |
| U | ---- | ---- | ---- | ---- | ---- | ---- | ---- | 0.006 | ---- |
| La | 0.215 | 0.279 | 0.271 | 0.210 | 0.249 | 0.190 | 0.398 | 0.384 | 0.389 |
| Ce | 0.483 | 0.498 | 0.502 | 0.489 | 0.499 | 0.491 | 0.446 | 0.436 | 0.452 |
| Pr | 0.044 | 0.050 | 0.057 | 0.060 | 0.052 | 0.079 | 0.018 | 0.027 | 0.013 |
| Nd | 0.164 | 0.119 | 0.126 | 0.168 | 0.146 | 0.197 | 0.041 | 0.048 | 0.043 |
| Sm | 0.008 | ---- | ---- | 0.010 | 0.005 | 0.012 | ---- | ---- | ---- |
| | 0.959 | 0.992 | 0.976 | 0.957 | 0.999 | 1.019 | 0.959 | 0.984 | 0.995 |
| P | 0.997 | 0.971 | 0.990 | 1.003 | 0.956 | 0.979 | 0.948 | 0.92 | 0.886 |
| Si | 0.038 | 0.034 | 0.028 | 0.024 | 0.045 | 0.019 | 0.082 | 0.096 | 0.123 |
| | 1.035 | 1.005 | 1.018 | 1.027 | 1.001 | 0.998 | 1.030 | 1.016 | 1.009 |
| Sum | 1.994 | 1.997 | 1.994 | 1.984 | 2.000 | 2.017 | 1.989 | 2.000 | 2.004 |

| | Angler Creek ferroaugite syenite | | | Quartz syenite dyke | | | Centre III, Quartz syenite | | |
|---|---|---|---|---|---|---|---|---|---|
| | C1449/1 | C2909/1 | C2909/2 | C1432/1 | C1432/2 | C1432/3 | C2112/1 | C2112/2 | C2112/3 |
| CaO | 0.10 | nd | nd | 0.16 | 0.16 | 0.28 | 0.09 | nd | 0.17 |
| FeO | nd | 0.26 | nd | nd | 0.69 | nd | nd | 0.22 | 0.35 |
| ThO2 | nd | 0.85 | 0.58 | nd | 2.68 | nd | 7.47 | 10.34 | 4.44 |
| UO2 | na | na | na | na | nd | nd | na | na | na |
| La2O3 | 12.16 | 15.58 | 15.19 | 18.48 | 18.73 | 17.57 | 21.62 | 21.54 | 21.34 |
| Ce2O3 | 32.52 | 34.37 | 34.54 | 35.42 | 35.04 | 35.32 | 30.04 | 30.33 | 33.66 |
| Pr2O3 | 2.45 | 3.19 | 3.45 | 3.25 | 3.08 | 3.15 | 2.57 | 3.1 | 3.74 |
| Nd2O3 | 11.77 | 10.65 | 11.25 | 9.30 | 8.83 | 10.29 | 5.36 | 4.43 | 4.6 |
| Sm2O3 | 1.32 | 0.51 | 1.07 | 0.66 | 0.73 | nd | nd | nd | 0.48 |
| P2O5 | 26.51 | 29.41 | 29.41 | 29.88 | 28.96 | 29.85 | 25.85 | 24.99 | 27.37 |
| SiO2 | 0.66 | 0.80 | 0.53 | 0.45 | 1.48 | 0.46 | 2.57 | 2.85 | 1.27 |
| Total | 87.49 | 95.62 | 96.02 | 97.60 | 100.38 | 96.92 | 95.58 | 97.79 | 97.42 |
| La/Nd | 1.065 | 1.510 | 1.389 | 2.061 | 2.187 | 1.760 | 4.150 | 5.015 | 4.791 |

| | | | | | | | | | |
|---|---|---|---|---|---|---|---|---|---|
| Ca | 0.005 | ---- | ---- | 0.007 | 0.007 | 0.012 | 0.004 | ---- | 0.007 |
| Fe | ---- | 0.009 | ---- | ---- | 0.022 | ---- | ---- | 0.008 | 0.012 |
| Th | ---- | 0.008 | 0.005 | ---- | 0.024 | ---- | 0.071 | 0.098 | 0.041 |
| U | ---- | ---- | ---- | ---- | ---- | ---- | ---- | ---- | ---- |
| La | 0.198 | 0.231 | 0.225 | 0.270 | 0.269 | 0.257 | 0.332 | 0.331 | 0.321 |
| Ce | 0.527 | 0.505 | 0.509 | 0.513 | 0.500 | 0.513 | 0.458 | 0.462 | 0.503 |
| Pr | 0.039 | 0.047 | 0.051 | 0.047 | 0.044 | 0.046 | 0.039 | 0.047 | 0.056 |
| Nd | 0.186 | 0.153 | 0.162 | 0.131 | 0.123 | 0.146 | 0.080 | 0.066 | 0.067 |
| Sm | 0.020 | 0.007 | 0.015 | 0.009 | 0.010 | ---- | ---- | ---- | 0.007 |
| | 0.975 | 0.960 | 0.967 | 0.977 | 0.999 | 0.974 | 0.984 | 1.012 | 1.014 |
| P | 0.993 | 0.999 | 1.002 | 1.001 | 0.956 | 1.003 | 0.911 | 0.880 | 0.946 |
| Si | 0.029 | 0.032 | 0.021 | 0.018 | 0.058 | 0.018 | 0.107 | 0.199 | 0.052 |
| | 1.022 | 1.031 | 1.023 | 1.019 | 1.014 | 1.021 | 1.018 | 1.079 | 0.998 |
| Sum | 1.997 | 1.991 | 1.990 | 1.996 | 2.013 | 1.995 | 2.002 | 2.091 | 2.012 |

ferro-edenite syenite

| | C2112/4 | C2112/5 | 2112/6 | C2924/2 | C2924/3 | C2924/4 | C2025/1 | C2025/2 | C2025/3 |
|---|---|---|---|---|---|---|---|---|---|
| CaO | nd | 0.11 | nd | 0.08 | nd | 0.08 | nd | nd | nd |
| FeO | 0 | nd | nd | 0.25 | nd | 0.33 | nd | 0.6 | 0.45 |
| ThO2 | 3.6 | 11.22 | 13.19 | 6.11 | 5.99 | 7.53 | 14.52 | 8.68 | 10.4 |
| UO2 | na | na | nd | nd | na | na | na | na | na |
| La2O3 | 19.71 | 18.03 | 23.48 | 26.60 | 26.29 | 25.88 | 16.19 | 17.73 | 16.64 |
| Ce2O3 | 33.9 | 31.45 | 28.28 | 30.26 | 29.66 | 29.61 | 30.29 | 31.39 | 32.73 |
| Pr2O3 | 4.03 | 2.51 | 1.20 | 1.86 | 1.21 | 1.81 | 2.12 | 1.97 | 3.21 |
| Nd2O3 | 5.6 | 4.57 | 3.02 | 4.44 | 2.78 | 3.31 | 6.19 | 6.09 | 6.62 |
| Sm2O3 | nd | nd | nd | nd | na | nd | nd | 0.43 | nd |
| P2O5 | 28.18 | 25.86 | 24.94 | 28.64 | 27.28 | 27.01 | 25.98 | 26.63 | 27.94 |
| SiO2 | 1.31 | 3.45 | 3.73 | 1.94 | 1.99 | 2.39 | 3.8 | 1.61 | 2.91 |
| Total | 96.34 | 97.2 | 97.84 | 100.18 | 95.20 | 97.95 | 99.09 | 95.13 | 100.89 |
| La/Nd | 3.642 | 4.060 | 8.114 | 6.194 | 9.707 | 8.021 | 2.708 | 3.000 | 2.598 |

| | | | | | | | | | |
|---|---|---|---|---|---|---|---|---|---|
| Ca | ---- | 0.005 | ---- | 0.003 | ---- | 0.003 | ---- | ---- | ---- |
| Fe | ---- | ---- | ---- | 0.008 | ---- | 0.011 | ---- | 0.021 | 0.015 |
| Th | 0.033 | 0.104 | 0.124 | 0.054 | 0.056 | 0.069 | 0.133 | 0.083 | 0.092 |
| U | ---- | ---- | ---- | ---- | ---- | ---- | ---- | ---- | ---- |
| La | 0.295 | 0.272 | 0.357 | 0.384 | 0.398 | 0.385 | 0.241 | 0.273 | 0.239 |
| Ce | 0.503 | 0.470 | 0.427 | 0.433 | 0.446 | 0.438 | 0.447 | 0.481 | 0.467 |
| Pr | 0.060 | 0.037 | 0.018 | 0.027 | 0.018 | 0.027 | 0.031 | 0.030 | 0.046 |
| Nd | 0.081 | 0.067 | 0.044 | 0.062 | 0.041 | 0.048 | 0.089 | 0.091 | 0.092 |
| Sm | ---- | ---- | ---- | ---- | ---- | ---- | ---- | 0.006 | ---- |
| | 0.972 | 0.955 | 0.970 | 0.971 | 0.959 | 0.981 | 0.941 | 0.985 | 0.951 |
| P | 0.968 | 0.894 | 0.870 | 0.948 | 0.948 | 0.923 | 0.886 | 0.943 | 0.923 |
| Si | 0.053 | 0.141 | 0.154 | 0.076 | 0.082 | 0.096 | 0.153 | 0.067 | 0.114 |
| | 1.021 | 1.035 | 1.024 | 1.024 | 1.030 | 1.019 | 1.039 | 1.010 | 1.037 |
| Sum | 1.993 | 1.990 | 1.994 | 1.995 | 1.989 | 2.000 | 1.980 | 1.995 | 1.988 |

| | C2025/5 | C2025/6 | C2025/7 |
|---|---|---|---|
| CaO | 0.21 | 0.5 | 0.09 |
| FeO | 0.39 | nd | na |
| ThO2 | 10.64 | 5.42 | 8.32 |
| UO2 | na | na | na |
| La2O3 | 15.45 | 17.43 | 19.63 |
| Ce2O3 | 31.22 | 31.07 | 29.81 |
| Pr2O3 | 2.49 | 2.41 | 2.84 |
| Nd2O3 | 7.85 | 6.17 | 5.74 |
| Sm2O3 | nd | 0.32 | nd |
| P2O5 | 25.69 | 29.45 | 27.73 |
| SiO2 | 3.06 | 1.31 | 2.28 |
| TOTAL | 96.99 | 94.09 | 96.44 |
| La/Nd | 2.043 | 2.910 | 3.530 |

| | | | |
|---|---|---|---|
| Ca | 0.009 | 0.022 | 0.004 |
| Fe | 0.013 | ---- | ---- |
| Th | 0.100 | 0.050 | 0.077 |
| U | ---- | ---- | ---- |
| La | 0.235 | 0.259 | 0.293 |
| Ce | 0.471 | 0.458 | 0.441 |
| Pr | 0.037 | 0.035 | 0.042 |
| Nd | 0.115 | 0.089 | 0.083 |
| Sm | ---- | 0.004 | ---- |
| | 0.980 | 0.917 | 0.94 |
| P | 0.896 | 1.003 | 0.949 |
| Si | 0.126 | 0.053 | 0.092 |
| | 1.022 | 1.056 | 1.041 |
| Sum | 2.002 | 1.973 | 1.981 |

APPENDIX 2.11

FERSMITE
Centre I, Quartz syenite dyke.

| | C1418/1 | C1418/2 | C1418/3 | C1418/4 | C1418/5 | C1418/6 |
|---|---|---|---|---|---|---|
| Nb205 | 74.91 | 74.70 | 74.63 | 74.09 | 76.96 | 75.28 |
| Ta205 | 2.43 | 2.46 | 3.11 | 3.14 | 2.35 | 2.19 |
| CaO | 15.72 | 15.58 | 15.32 | 15.13 | 15.73 | 15.43 |
| ThO2 | nd | 0.58 | nd | nd | nd | 0.90 |
| UO2 | 0.91 | 0.41 | nd | 0.59 | 0.41 | 0.76 |
| TiO2 | 2.12 | 2.29 | 2.44 | 2.16 | 2.11 | 1.59 |
| FeO | 0.86 | 0.37 | 0.43 | 0.20 | nd | 0.81 |
| MnO | 0.12 | 0.09 | 0.21 | nd | 0.13 | 0.15 |
| Y2O3* | 3.23 | 3.18 | 4.00 | 4.83 | 2.18 | 3.13 |
| Total | 100.30 | 99.66 | 100.14 | 100.14 | 99.87 | 100.24 |

* - semi-quantitative
calculated to 6 oxygen

| | | | | | | |
|---|---|---|---|---|---|---|
| Ca | 0.917 | 0.914 | 0.893 | 0.887 | 0.914 | 0.906 |
| Th | ---- | 0.007 | nd | nd | nd | 0.011 |
| U | 0.011 | 0.005 | nd | 0.007 | 0.005 | 0.009 |
| Y | 0.094 | 0.093 | 0.116 | 0.141 | 0.063 | 0.091 |
| Mn | 0.006 | 0.004 | 0.010 | nd | 0.006 | 0.007 |
| Fe | 0.039 | 0.017 | 0.020 | 0.009 | nd | 0.037 |
| | 1.067 | 1.040 | 1.039 | 1.044 | 0.988 | 1.061 |
| Nb | 1.845 | 1.849 | 1.836 | 1.833 | 1.887 | 1.864 |
| Ta | 0.036 | 0.037 | 0.046 | 0.047 | 0.035 | 0.033 |
| Ti | 0.087 | 0.094 | 0.100 | 0.089 | 0.086 | 0.065 |
| | 1.968 | 1.980 | 1.982 | 1.969 | 2.008 | 1.962 |
| Sum | 3.035 | 3.020 | 3.021 | 3.013 | 2.996 | 3.023 |

# APPENDIX 3.0

WHOLE ROCK

| | Quartz syenite dykes | | | | Craddock Cove syenite | | | | |
|---|---|---|---|---|---|---|---|---|---|
| | C1418 | C1428 | C1432 | C2925 | C1513 | C1516 | C1522 | C2901 | C2920 |
| SiO2 | 71.96 | 50.72 | 56.84 | 40.45 | 59.61 | 58.70 | 59.00 | 60.27 | 59.66 |
| TiO2 | 0.22 | 0.47 | 0.32 | 0.69 | 0.54 | 0.72 | 0.72 | 0.97 | 0.67 |
| Al2O3 | 9.03 | 9.04 | 12.24 | 10.56 | 14.18 | 15.34 | 14.66 | 14.92 | 14.50 |
| Fe2O3 a | 9.25 | 24.15 | 11.10 | 12.34 | 9.63 | 10.46 | 11.12 | 10.14 | 10.50 |
| MnO | 0.08 | 0.14 | 0.36 | 1.01 | 0.41 | 0.33 | 0.32 | 0.20 | 0.30 |
| MgO | 0.59 | 0.15 | 0.26 | 1.95 | 0.25 | 1.13 | 0.49 | 0.72 | 0.36 |
| CaO | 2.16 | 6.83 | 8.14 | 9.16 | 2.79 | 2.65 | 3.22 | 2.50 | 2.80 |
| Na2O | 4.87 | 5.54 | 8.12 | 1.09 | 5.38 | 4.53 | 5.18 | 5.59 | 5.77 |
| K2O | 0.04 | 0.06 | 0.08 | 7.02 | 5.06 | 5.41 | 4.99 | 3.52 | 4.59 |
| P2O5 | 0.00 | 0.00 | 0.00 | 0.07 | 0.00 | 0.13 | 0.11 | 0.23 | 0.06 |
| Total= | 98.21 | 97.10 | 97.46 | 84.35 | 97.84 | 99.40 | 99.80 | 99.06 | 99.19 |

a = all Fe as Fe2O3

Trace elements

| | C1418 | C1428 | C1432 | C2925 | C1513 | C1516 | C1522 | C2901 | C2920 |
|---|---|---|---|---|---|---|---|---|---|
| La | 743 | 423 | 1038 | *2598 | 618 | 173 | 221 | 196 | 286 |
| Ce | 1639 | 954 | 1721 | *4193 | ---- | 392 | 465 | 436 | 579 |
| Nd | 776 | 327 | 552 | ---- | ---- | 135 | 181 | 144 | 214 |
| Sm | 142 | 63 | 73 | ---- | ---- | 20 | 27 | 22 | 31 |
| Eu | 13 | 5 | 6 | ---- | 5 | 4 | 4 | 4 | 4 |
| Tb | 20 | 11 | 8 | ---- | ---- | 2 | 3 | 2 | 4 |
| Yb | 54 | 40 | 25 | ---- | ---- | 8 | 10 | 8 | 11 |
| Lu | 9 | 6 | 4 | ---- | ---- | 1 | 2 | 1 | 2 |
| Ta | 139 | 54 | 43 | ---- | 38 | 10 | 13 | 12 | 17 |
| Hf | 99 | 81 | 49 | ---- | 42 | 10 | 15 | 13 | 20 |
| Sc | ---- | 2 | 1 | ---- | 1 | 5 | 5 | 12 | 4 |
| Cr | ---- | ---- | ---- | ---- | ----- | ---- | ---- | ---- | ---- |
| Co | 138 | 35 | 23 | 49 | 87 | 17 | 25 | 43 | 70 |
| Th | 223 | 154 | 139 | ---- | 112 | 28 | 36 | 30 | 47 |
| U | 428 | 216 | 93 | ---- | 182 | 43 | 44 | 38 | 77 |
| Ni | 98 | 45 | 45 | 140 | 44 | 15 | 16 | 12 | 27 |
| Cu | 2381 | 993 | 14 | 0 | 6 | 20 | 20 | 12 | 20 |
| Zn | 1767 | 30 | 34 | 15568 | 903 | 323 | 208 | 127 | 760 |
| Pb | 257 | 61 | 7 | 66 | 109 | 53 | 38 | 33 | 0 |
| Zr | 2980 | 2820 | 1613 | 8150 | 1484 | 467 | 641 | 553 | 841 |
| Y | 498 | 264 | 229 | 650 | 182 | 61 | 80 | 60 | 119 |
| Sr | 141 | 77 | 89 | 217 | 65 | 202 | 122 | 202 | 81 |
| Rb | 0 | 1 | 5 | 305 | 280 | 188 | 196 | 109 | 257 |
| Ba | 553 | 304 | 246 | 6477 | 246 | 1528 | 980 | 699 | 409 |

* determined by XRF

| | ferroaugite syenite | | | | | | | Quartz sye |
|---|---|---|---|---|---|---|---|---|
| | C2905 | C2908 | C2909 | C2910 | C2911 | C2912 | C2914 | C2923 |
| SiO2 | 58.862 | 57.358 | 59.033 | 60.892 | 60.7 | 59.523 | 56.242 | 64.503 |
| TiO2 | 0.966 | 1.133 | 0.723 | 0.542 | 0.574 | 0.729 | 1.26 | 0.398 |
| Al2O3 | 15.202 | 12.517 | 14.507 | 15.771 | 15.318 | 14.909 | 14.111 | 15.938 |
| Fe2O3 a | 10.042 | 14.743 | 11.493 | 8.074 | 9.106 | 10.042 | 13.414 | 5.163 |
| MnO | 0.256 | 0.358 | 0.301 | 0.203 | 0.236 | 0.257 | 0.343 | 0.135 |
| MgO | 0.434 | 0.246 | 0.299 | 0.225 | 0.237 | 0.236 | 0.64 | 0.18 |
| CaO | 3.44 | 4.284 | 3.568 | 2.567 | 2.93 | 3.068 | 4.149 | 1.377 |
| Na2O | 4.989 | 4.711 | 4.94 | 5.81 | 5.46 | 5.21 | 3.914 | 5.407 |
| K2O | 4.985 | 4.408 | 4.876 | 5.354 | 5.098 | 4.942 | 4.886 | 6.011 |
| P2O5 | 0.115 | 0.115 | 0.087 | 0.035 | 0.024 | 0.116 | 0.192 | 0.001 |
| Total= | 99.291 | 99.87 | 99.828 | 99.473 | 99.683 | 99.031 | 99.149 | 99.113 |

a = all Fe as Fe2O3

Trace elements

| | | | | | | | | |
|---|---|---|---|---|---|---|---|---|
| La | 134 | 166 | 116 | 111 | 129 | 137 | 94 | 308 |
| Ce | 291 | 424 | 376 | 303 | 387 | 299 | 417 | 521 |
| Nd | 112 | 146 | 91 | 78 | 101 | 89 | 59 | 108 |
| Sm | 18 | 24 | 15 | 12 | 16 | 14 | 8 | 16 |
| Eu | 6 | 4 | 4 | 4 | 4 | 4 | 6 | 1 |
| Tb | 2 | 3 | 2 | 2 | 2 | 2 | 3 | 3 |
| Yb | 6 | 9 | 8 | 6 | 7 | 5 | 8 | 11 |
| Lu | 1 | 2 | 1 | 1 | 1 | 1 | 0 | 1 |
| Ta | 8 | 18 | 7 | 6 | 7 | 7 | 5 | 10 |
| Hf | 7 | 10 | 8 | 6 | 9 | 8 | 5 | 21 |
| Sc | 9 | 4 | 6 | 4 | 5 | 5 | 17 | 3 |
| Cr | ---- | ---- | ---- | ---- | ---- | ---- | ---- | ---- |
| Co | 15 | 17 | 18 | 21 | 15 | 16 | 21 | 53 |
| Th | 15 | 18 | 15 | 12 | 22 | 20 | 11 | 46 |
| U | 22 | 31 | 24 | 20 | 28 | 25 | 18 | 38 |
| Ni | 11 | 17 | 8 | 9 | 10 | 11 | 2 | 15 |
| Cu | 14 | 27 | 22 | 16 | 17 | 22 | 24 | 10 |
| Zn | 171 | 271 | 169 | 131 | 145 | 161 | 142 | 117 |
| Pb | 46 | 38 | 31 | 35 | 37 | 35 | 34 | 35 |
| Zr | 289 | 489 | 309 | 233 | 315 | 365 | 219 | 910 |
| Y | 46 | 72 | 46 | 36 | 45 | 56 | 38 | 58 |
| Sr | 156 | 39 | 86 | 80 | 76 | 74 | 71 | 15 |
| Rb | 136 | 152 | 137 | 175 | 153 | 173 | 91 | 197 |
| Ba | 1433 | 272 | 769 | 699 | 691 | 664 | 685 | 161 |

* determined by XRF